Xenobiotics interfering with corticosteroid action: from adrenal steroid synthesis to peripheral receptor activity

Inauguraldissertation
zur
Erlangung der Würde eines Doktors der Philosophie
vorgelegt der
Philosophisch-Naturwissenschaftlichen Fakultät
der Universität Basel
von

Melanie Patt

Basel, 2020

Genehmigt von der Philosophisch-Naturwissenschaftlichen Fakultät

auf Antrag von Prof. Dr. Alex Odermatt, Prof. Dr. Jörg Huwyler und Prof. Dr. Michael Arand

Basel, den 17. Dezember 2019

Dekan

Prof. Dr. Martin Spiess

Table of content

1. Summary

Corticosteroids are steroid hormones synthesized by the adrenal gland and regulating a variety of physiological processes to maintain whole-body homeostasis by acting through their corresponding receptors. Although the adrenal gland is considered one of the most toxin-vulnerable organs and steroid receptor regulation is recognized to have a considerable impact on tissue- and cell-specific steroid signaling, only few studies are currently exploring and characterizing the effects of xenobiotics on corticosteroid hormone action.

The first part of this thesis aimed to establish optimized steroid profile analysis in cell culture supernatants and apply it in combination with further biological assessments and molecular modeling for the identification and characterization of exogenous chemicals potentially disrupting corticosteroid hormone production.

A widely used *in vitro* model for studying effects of chemicals on adrenal steroid hormone synthesis constitutes the human H295R adrenocarcinoma cell line. Since the OECD test guideline No. 456 based on H295R cells has several limitations, this thesis refined the H295R steroidogenesis assay by simultaneously analyzing the most important adrenal steroid metabolites using a mass spectrometry-based method. A medium control at the beginning of the experiment as well as reference compounds with known mechanisms were introduced and, additionally, gene expression analyses were performed, in order to not only detect chemical-induced disturbances but also providing initial mechanistic insights into the mode-of-action of a given chemical. The newly established improved version of the H295R steroidogenesis assay was then further evolved by activating the cells either with torcetrapib, a potent inducer of corticosteroid synthesis, or with forskolin, a general inducer of steroidogenesis, allowing to assess the inhibitory potential of various test chemicals.

The modified torcetrapib-stimulated H295R assay was then used to evaluate three selected hits from an *in silico* screening of environmental chemical databases using ligand-based pharmacophore models of 11β-hydroxylase (CYP11B1) and aldosterone synthase (CYP11B2). This proof-of-concept for the application of pharmacophore-based virtual screening followed by biological assessment has proven suitable for assessing substances potentially interfering with corticosteroid synthesis.

In another study within this thesis, the adapted version of the H295R steroidogenesis assay using forskolin-stimulated cells was applied to investigate the inhibitory effects of 19 anabolic androgenic steroids (AAS) and 3 selective androgen receptor modulators (SARMs). This enabled to group the test compounds according to their individual steroid patterns. Additionally, gene expression analysis, cell-free activity assays and molecular docking calculations contributed to providing initial mechanistic information.

Besides direct effects on adrenal steroidogenesis, xenobiotic-induced alterations in circulating steroid hormone levels may arise due to altered feedback regulation or disturbed peripheral steroid metabolism. Thus, in a further part of this thesis drug-induced changes in steroid hormone levels were studied by measuring steroid profiles in human blood and urine samples.

In a clinical study, plasma levels of steroid hormones and adrenocorticotropic hormone (ACTH) were analyzed in healthy volunteers administered a single dose of slow-release lisdexamfetamine (100 mg) or immediate-release D-amphetamine (40.3 mg) at equimolar doses. Importantly, lisdexamfetamine and D-amphetamine similarly enhanced the levels of glucocorticoids, androgen precursors and ACTH, suggesting an acute stimulation of the hypothalamic-pituitary-adrenal (HPA) axis. Although lisdexamfetamine showed a delayed time of increase and peak levels of plasma D-amphetamine concentrations compared to the D-amphetamine treatment, drug exposure and drug effects seemed to be comparable between the two formulations.

In a clinical case study, a comprehensive analysis of blood and urinary steroid profiles was conducted in samples from two patients receiving posaconazole, an antifungal agent associated with hypertension and hypokalemia due to mineralocorticoid excess. Steroid analyses indicated inter-individual differences in the mechanism of mineralocorticoid-based hypertension with preferential CYP11B inhibition in one patient and predominant inhibition of 11β-HSD2 in the second patient. These results show that steroid profiling in plasma and urine samples can not only reveal disturbances of steroid homeostasis but also provide initial mechanistic information.

Together, these findings emphasize that molecular modeling combined with biological evaluation represents a valuable approach for the identification and characterization of chemicals potentially interfering with corticosteroid production and to provide initial mechanistic insights. However, *in vivo* investigations are unavoidable to study the impact of chemicals acting on the HPA axis.

Xenobiotics may not only affect steroid hormone production, feedback regulation or pre-receptor control of corticosteroid metabolism, but may also interfere directly with the receptor and steroid signal transduction. In order to understand potential disturbances of glucocorticoid action by xenobiotics, it is important to further clarify the signaling pathways involved in glucocorticoid receptor (GR) activation. Therefore, another part of this thesis focused on the impact of the serine/threonine-specific protein phosphatase PP1α on the activity of the GR. PP1α was found to increase GR activity, and preliminary mechanistic investigations showed that levels of phosphorylated GR-Ser211 were altered and glycogen synthase kinase 3 might be involved. Hence, PP1α appeared to modulate the cellular response to glucocorticoids, implying that impairment of its activity could lead to aberrant glucocorticoid hormone action.

In conclusion, these studies identified a novel GR regulating protein that enhances cortisol stimulation by controlling GR phosphorylation. A profound understanding of glucocorticoid signaling might provide the basis for developing cell models and conditions for the detection of chemicals disturbing glucocorticoid sensitivity and thereby contributing to diseases.

2. Introduction

Synthetic chemicals play a pivotal role in the industrialized world. A large number of chemicals used to increase agricultural yields, extend food shelf-life and as constituents of beauty and care products are produced each year. However, only a small portion of them underwent adequate toxicological evaluation, posing risks and hazards to humans, animals and the environment. The issue of exposure to potentially toxic chemicals received increasing public and political attention and their identification and characterization is of high priority for several regulatory authorities. The Registration, Evaluation, Authorization and Restriction of Chemicals (REACH) regulation of the European Union (EU), the U.S. Environmental Protection Agency's (EPA's) Endocrine Disruptor Screening Program (EDSP), Toxicology in the 21st Century (Tox21) interagency collaboration program and the Toxicity Forecaster (ToxCast) aim to better protect human health and the environment by assessing the potential toxicity of chemicals [1-5]. Recently, the EU Commission adopted a communication on endocrine disrupting chemicals (EDCs), addressing a new strategy for protecting the population and the environment from overall exposure to hazardous chemicals [6]. However, the published strategic approach failed to provide a concrete action plan, including specific measurements, targets to be tested, or a timeline and a budget for the next steps towards the identification of possible EDCs.

The EU defines an endocrine disruptor as an "exogenous substance or mixture that alters function(s) of the endocrine system and consequently causes adverse health effects in an intact organism, or its progeny, or (sub)populations" [7]. These EDCs have the ability to interfere with virtually every aspect of hormone action, as for instance with the biosynthesis and metabolism of steroidal hormones by modulating enzymes involved in steroidogenesis or hormonal signaling by affecting nuclear hormone receptors. Since EDCs can disturb different tissues and organs, they may increase the risk of developing numerous diseases, including infertility and development, obesity, diabetes, cardiovascular diseases, allergies, neurobehavioral disorders and cancer [8, 9]. Currently, the focus of investigations into EDCs lies on developmental and reproductive toxicity, and nuclear hormone receptors such as estrogen receptors (ER) and androgen receptors (AR) are among the most extensively studied targets due to disruption of sex hormone action. Interferences of xenobiotics with adrenocortical function and other receptors including the glucocorticoid receptor (GR) and the mineralocorticoid receptor (MR) are rather neglected [10, 11]. This is inconsistent with the important function of the adrenal gland in the endocrine system and the essential role of GR and MR in the regulation of important physiological processes. Disturbances of glucocorticoid action have been associated with pathophysiological consequences including metabolic and cardiovascular diseases, osteoporosis, asthma and chronic obstructive pulmonary disease (COPD), cataracts, immune diseases, mood and cognitive disorders and cancer, while impaired mineralocorticoid action has been related to hypertension and cardiovascular diseases [11, 12]. Thus, xenobiotics disrupting corticosteroid hormone action are likely to contribute

to the increasing incidence of allergic diseases, metabolic disturbances and cancer in the industrialized countries.

Glucocorticoids and mineralocorticoids are almost exclusively produced in the adrenal cortex [13] (see Fig. 1 for a general overview of steroid hormone synthesis), and corticosteroid homeostasis is mainly regulated by the hypothalamic-pituitary-adrenal (HPA) axis. Since the HPA axis plays a crucial role in stress responses, the adrenal gland is the most severely affected toxicological target in the endocrine system [14]. In toxicity studies, the administration of high doses of chemicals often leads to toxic insults, resulting in stress and HPA axis activation to enhance adrenocorticotropic hormone (ACTH) secretion [15]. Additional factors predisposing the adrenal cortex to toxicity include high vascularity ensuring exposures to toxicants, lipophilicity due to a large amount of steroids and unsaturated fatty acids in cell membranes, as well as the presence of cytochrome P450 (CYP) enzymes producing toxic metabolites and free radicals [15, 16].

An important enzyme involved in adrenal steroidogenesis is 11β-hydroxylase (CYP11B1), which is responsible for the conversion of 11-deoxycortisol to the potent glucocorticoid cortisol. Inhibition of CYP11B1 leads to reduced cortisol synthesis and an accumulation of the mineralocorticoids 11-deoxycortisol and 11-deoxycorticosterone (11-DOC) [17]. Reduced levels of cortisol in peripheral tissues stimulate adrenal steroidogenesis by an elevation of ACTH, leading to further production of 11-deoxycortisol and 11-DOC, thereby causing excessive MR activation, hypertension and hypokalemia along with low renin and aldosterone levels. In addition, a diminished CYP11B1 activity results in enhanced levels of adrenal androgens due to the ACTH-induced positive feedback, stimulating the adrenal gland and ultimately leading to hyperplasia [17, 18]. Another essential enzyme is aldosterone synthase (CYP11B2), which catalyzes the conversion of 11-DOC via corticosterone and 18-hydroxycorticosterone to the potent mineralocorticoid aldosterone [19]. Deficiency of CYP11B2 abolishes aldosterone production and leads to hypotension and hyperkalemia [20].

Etomidate, an anesthetic induction drug, is a classic example of drugs inducing fatal adrenocortical insufficiency. Due to potent CYP11B inhibition, etomidate markedly decreased cortisol and aldosterone levels, leading to Addisonian crisis, cardiovascular collapse and death [21-23]. Another fundamental example is torcetrapib, a promising drug candidate developed as lipid reducing agent to treat hypercholesterolemia [24]. Its development was terminated when phase III clinical trials showed increased morbidity and mortality in the treatment group. Torcetrapib induced the expression of CYP11B1 and CYP11B2, resulting in enhanced aldosterone plasma levels and blood pressure elevation, thus promoting cardiovascular events [25, 26]. In conclusion, this emphasizes the importance to identify chemicals that potentially interfere with adrenocortical function and disrupt glucocorticoid and mineralocorticoid action.

The present thesis aimed to apply molecular modeling including pharmacophore-based virtual screening and docking calculations in combination with biological assays for the identification and initial characterization of adrenocortical endocrine disruptors. Moreover, this thesis intended to further elucidate the post-translational modification of the GR and effects on signaling pathways in order to better understand the mechanisms of impaired glucocorticoid action. This might provide a possible basis for developing suitable cell-based models and optimizing existing readouts to screen for chemicals potentially interfering with glucocorticoid responses. It is important to gain insights into the effects of potential endocrine disruptors, which might not directly alter glucocorticoid production or bind to GR but act via pathways that affect the phosphorylation status of the GR and thereby its function. The evaluation of EDCs must go beyond the analysis of direct interaction of xenobiotics with a given receptor and also consider mechanisms contributing to receptor function such as post-translational modifications, transcriptional regulation, protein stability and protein-protein interactions.

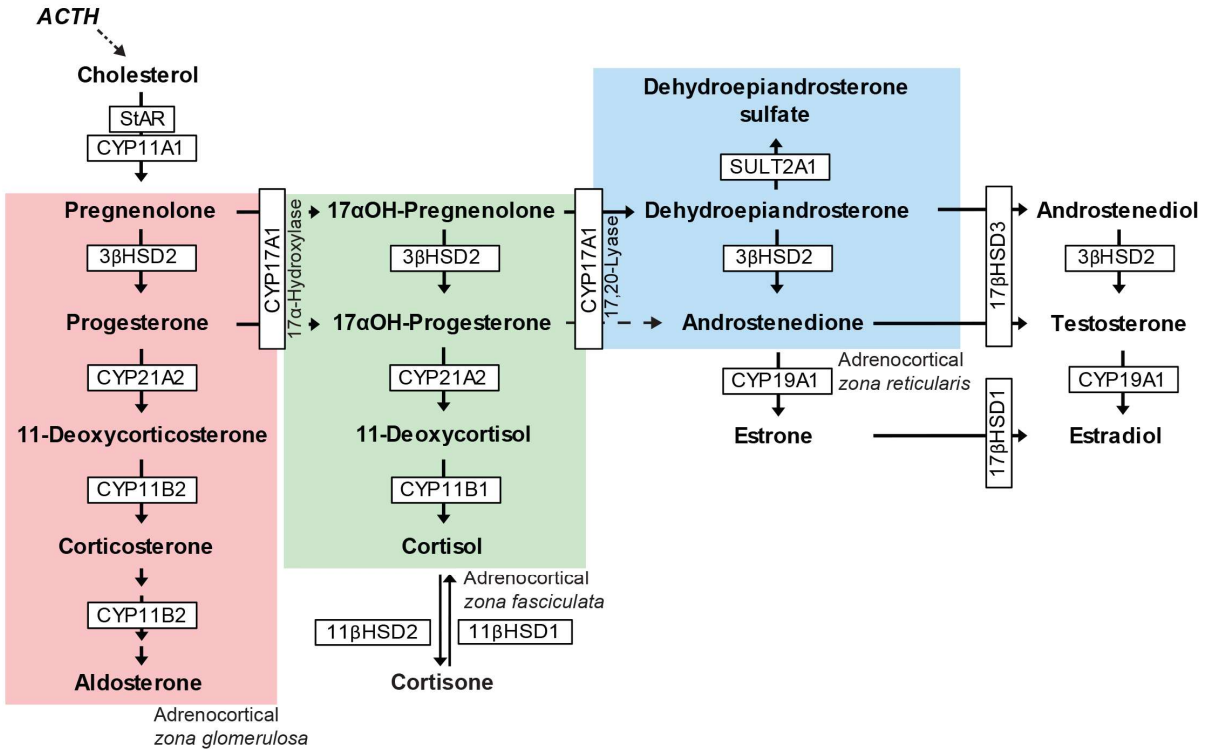

Figure 1. Schematic representation of major human adrenal and peripheral steroidogenesis.

(Figure adapted from Patt M et al., manuscript submitted, 2019). Enzymes and steroids involved in adrenocortical and peripheral steroidogenesis are presented. CYP = cytochrome P450; HSD = hydroxysteroid dehydrogenase; SULT = sulfotransferase; StAR = steroidogenic acute regulatory protein; ACTH = adrenocorticotropic hormone. The three small arrows below corticosterone indicate the conversion of corticosterone via 18-hydroxycorticosterone to the potent mineralocorticoid aldosterone. The dotted arrow represents low flux from 17α-hydroxyprogesterone to androstenedione, since CYP17A1 catalyzes this reaction with only about 2% of its activity to convert 17α-hydroxypregnenolone to dehydroepiandrosterone (DHEA) [27]. Thus, human androgen production proceeds mainly via DHEA but not via androstenedione. 3βHSD2 activity decreases in the *zona reticularis* during adrenarche, resulting in increased production of the adrenal androgen precursor DHEA, which is efficiently sulphated to dehydroepiandrosterone sulfate (DHEA-S), the most abundant steroid in the human circulation [28, 29].

3. Disruption of adrenocortical steroid synthesis and corticosteroid homeostasis by xenobiotics

3.1. *In silico* and *in vitro* approaches to identify endocrine disrupting chemicals interfering with adrenal steroidogenesis

Although it is well recognized that disturbances of adrenal steroidogenesis might lead to adrenocortical insufficiency and despite the evidence that steroidogenic enzymes can be affected by EDCs, only limited information is available regarding the identity of such EDCs and how they affect adrenal function. There is a need to develop novel strategies to identify EDCs interfering with adrenal steroidogenesis.

In drug discovery, computational methods are already well established and pharmacophore models are applied for filtering huge compound libraries in the search for novel drug candidates [30]. A pharmacophore represents a three-dimensional arrangement of the main chemical functionalities required for the interaction with a specific target molecule [31]. This pharmacophore-based virtual screening is a powerful *in silico* tool able to exclude compounds that do not have the desired properties, resulting in an enrichment of active compounds [32, 33]. Therefore, virtual screening has been proven to be a suitable technique to narrow down the list of potential candidates and to set priorities for *in vitro* studies, since biological testing is time- and cost-intensive.

Pharmacophore modeling and virtual screening have also been used successfully in toxicological investigations for example to support and facilitate the identification of chemicals acting on enzymes with essential functions in the endocrine system. Other *in silico* approaches such as molecular docking can be used to predict the interaction of xenobiotics with macromolecules mediating potentially hazardous effects [34-40].

Regarding the demand for extensive toxicological testing of chemicals that potentially act as EDCs, there is a great interest in establishing reliable *in silico* approaches with high predictability [37]. Nevertheless, successful application of *in silico* methods and subsequent validation of the hits requires appropriate bioassays. The regulatory need for *in vitro* assessment of the effects of EDCs on steroidogenesis pathways was addressed with the H295R steroidogenesis assay guideline developed by the Organisation for Economic Co-operation and Development (OECD) and the EPA [41, 42]. The H295R cell line is currently the most widely used *in vitro* cell-based model for the evaluation of biological pathways involved in adrenocortical function and mechanisms of toxicity [43, 44]. This cell line was derived from a human adrenocortical carcinoma and expresses genes encoding for all key steroidogenic enzymes (see Fig. 1 for an overview of steroid biosynthesis, chapter 2. Introduction). This is a unique characteristic, since the expression of the steroidogenic genes *in vivo* is dependent on the

adrenal zones (i.e. *glomerulosa*, *fasciculata* and *reticularis*) as well as the developmental stage [45, 46]. Thus, the H295R cell line can be applied to study steroidogenic pathways and provides a useful model to assess the effects of adrenocortical endocrine disruptors [47]. The OECD test guideline No. 456 based on H295R cells is validated to identify chemicals potentially interfering with the production of 17β-estradiol and testosterone [41, 42]. However, this test exhibits several limitations affecting the ability to confidently interpret the data obtained and leaving room for improvements. For example, estradiol and testosterone are two hormones typically not produced by the adrenal cortex, the method for quantification is not defined, and additional controls that would enhance the value of the data obtained are not included in this OECD test guideline No. 456.

This thesis aimed to establish a refined H295R steroidogenesis assay by extending the readout to mineralocorticoids, glucocorticoids and adrenal androgens, using a mass spectrometry-based method and including gene expression analyses for a more comprehensive understanding of steroid disturbances and to provide initial mechanistic information on the mode-of-action of potential EDCs. Furthermore, *in silico* methods, including pharmacophore-based virtual screening and molecular docking, combined with biological assessment were applied for the identification and characterization of potential EDCs.

In the published article, 'Steroid profiling in H295R cells to identify chemicals potentially disrupting the production of adrenal steroids' [48], described in detail in chapter 3.1.1, ultra-high performance liquid chromatography tandem mass spectrometry (UHPLC-MS/MS) was applied to selectively and simultaneously quantify a panel of steroid analytes. Additionally, reference compounds with known mechanisms and a medium control at the beginning of the experiment were included for an improved data interpretation. Gene expression analysis was performed to support the steroid profile changes induced by a chemical of interest.

The refined H295R steroidogenesis assay was then further developed to biologically evaluate three selected hits from an *in silico* screening of environmental chemical databases using ligand-based pharmacophore models of CYP11B1 and CYP11B2 [49]. In addition to using H295R cells in their basal state, cells activated by treatment with torcetrapib, a potent inducer of CYP11B1/2, were applied to more easily assess inhibitory effects of the tested compounds on cortisol and aldosterone production. This study is presented in more detail in the published article 'Identification of the fungicide epoxiconazole by virtual screening and biological assessment as inhibitor of human 11β-hydroxylase and aldosterone synthase' [49], in chapter 3.1.2.

In order to obtain a more general stimulation of adrenal steroidogenesis for studying the inhibitory capacity of test compounds, forskolin-activated H295R cells were employed in the most recent study 'Profiling of anabolic androgenic steroids and selective androgen receptor modulators for interference

with adrenal steroidogenesis' (see chapter 3.1.3). The improved protocol was used to examine the effects of 19 anabolic androgenic steroids (AAS) and 3 selective androgen receptor modulators (SARMs) on adrenal steroidogenesis, followed by gene expression analysis, cell-free activity assays and molecular docking calculations for selected compounds (see Appendix Fig. A1 and A2 for 2D-structures of AAS and SARMs, respectively).

3.1.1 Published article:

Steroid profiling in H295R cells to identify chemicals potentially disrupting the production of adrenal steroids

Petra Strajhar[a,c], David Tonoli[b,c], Fabienne Jeanneret[b,c], Raphaella M. Imhof[a], Vanessa Malagnino[a], Melanie Patt[a,c], Denise V. Kratschmar[a], Julien Boccard[b], Serge Rudaz[b,c], Alex Odermatt[a,c], Toxicology. 2017 Apr 15;381:51-63.

[a]Division of Molecular and Systems Toxicology, Department of Pharmaceutical Sciences, University of Basel, Klingelbergstrasse 50, 4056 Basel, Switzerland

[b]School of Pharmaceutical Sciences, University of Geneva and University of Lausanne, Pavillon des Isotopes 20, Boulevard d'Yvoy, 1211 Geneva, Switzerland

[c]Swiss Centre for Applied Human Toxicology (SCAHT), Universities of Basel and Geneva, Basel, Switzerland

Contribution:

Performed gene expression analysis and analyzed data.

Toxicology 381 (2017) 51–63

Contents lists available at ScienceDirect

Toxicology

journal homepage: www.elsevier.com/locate/toxicol

Steroid profiling in H295R cells to identify chemicals potentially disrupting the production of adrenal steroids

Petra Strajhar[a,c], David Tonoli[b,c], Fabienne Jeanneret[b,c], Raphaella M. Imhof[a], Vanessa Malagnino[a], Melanie Patt[a,c], Denise V. Kratschmar[a], Julien Boccard[b], Serge Rudaz[b,c], Alex Odermatt[a,c,*]

[a] Division of Molecular and Systems Toxicology, Department of Pharmaceutical Sciences, University of Basel, Klingelbergstrasse 50, 4056 Basel, Switzerland
[b] School of Pharmaceutical Sciences, University of Geneva and University of Lausanne, Pavillon des Isotopes 20, Boulevard d'Yvoy, 1211 Geneva, Switzerland
[c] Swiss Centre for Applied Human Toxicology (SCAHT), Universities of Basel and Geneva, Basel, Switzerland

ARTICLE INFO

Article history:
Received 13 October 2016
Received in revised form 9 February 2017
Accepted 16 February 2017
Available online 22 February 2017

Keywords:
Adrenal toxicity
Endocrine disrupting chemical
H295R
Steroid
Profiling

ABSTRACT

The validated OECD test guideline 456 based on human adrenal H295R cells promotes measurement of testosterone and estradiol production as read-out to identify potential endocrine disrupting chemicals. This study aimed to establish optimal conditions for using H295R cells to detect chemicals interfering with the production of key adrenal steroids. H295R cells' supernatants were characterized by liquid chromatography–mass spectrometry (LC–MS)-based steroid profiling, and the influence of experimental conditions including time and serum content was assessed. Steroid profiles were determined before and after incubation with reference compounds and chemicals to be tested for potential disruption of adrenal steroidogenesis. The H295R cells cultivated according to the OECD test guideline produced progestins, glucocorticoids, mineralocorticoids and adrenal androgens but only very low amounts of testosterone. However, testosterone contained in Nu-serum was metabolized during the 48 h incubation. Thus, inclusion of positive and negative controls and a steroid profile of the complete medium prior to the experiment ($t = 0$ h) was necessary to characterize H295R cells' steroid production and indicate alterations caused by exposure to chemicals. Among the tested chemicals, octyl methoxycinnamate and acetyl tributylcitrate resembled the corticosteroid induction pattern of the positive control torcetrapib. Gene expression analysis revealed that octyl methoxycinnamate and acetyl tributylcitrate enhanced CYP11B2 expression, although less pronounced than torcetrapib. Further experiments need to assess the toxicological relevance of octyl methoxycinnamate- and acetyl tributylcitrate-induced corticosteroid production. In conclusion, the extended profiling and appropriate controls allow detecting chemicals that act on steroidogenesis and provide initial mechanistic evidence for prioritizing chemicals for further investigations.

1. Introduction

The adrenals produce active glucocorticoids (*i.e.* cortisol, corticosterone) and mineralocorticoids (*i.e.* aldosterone, 11-deoxycorticosterone), which are essential for the regulation of electrolyte balance, blood pressure, immune system and energy homeostasis. They also produce progestins (*i.e.* progesterone, 17α-hydroxyprogesterone) and adrenal androgens (*i.e.* Δ4-androstene-3,17-dione(androstenedione), dehydroepiandrosterone) that serve as precursors for peripheral formation of active sex steroids. Impaired adrenal steroidogenesis has been associated with cardiometabolic, immune and psychiatric diseases (Gallo-Payet and Battista, 2014; Miller and Auchus, 2011). In Addison's disease, insufficient glucocorticoid synthesis leads to hypotension, fatigue, muscle weakness, weight loss and depression. In Cushing's disease, an over production of glucocorticoids results in visceral obesity, insulin resistance, skin and skeletal muscle atrophy and impaired wound healing. An over function of the adrenal cortex can also

Abbreviations: DMEM, Dulbecco's modified Eagle's medium; DMSO, dimethyl sulfoxide; EDCs, endocrine disrupting chemicals; LC–MS, liquid chromatography–mass spectrometry; LOD, limit of detection; LLOQ, lower limit of quantification; MTT, 3-(4,5-dimethylthiazol-2-yl)-2,5-diphenyl tetrazolium bromide; OECD, Organization for Economic Co-operation and Development; REACH, Registration, Evaluation, Authorization and Restriction of Chemicals.

* Corresponding author at: Division of Molecular and Systems Toxicology, Department of Pharmaceutical Sciences, University of Basel, Klingelbergstrasse 50, 4056 Basel, Switzerland.
E-mail address: alex.odermatt@unibas.ch (A. Odermatt).

http://dx.doi.org/10.1016/j.tox.2017.02.010
0300-483X/

cause hyperaldosteronism, associated with cardiovascular disease, and hyperandrogenism, associated with hirsutism. This emphasizes the importance to evaluate or test for adrenal toxicity chemicals that are contained in pharmaceuticals, food and consumer products or are released into the environment.

Drug-induced adrenal toxicity is a well-recognized clinical problem; however, in contrast to the investigations into endocrine disruption affecting sex steroid action, disruption of adrenal steroidogenesis has been neglected in the endocrine disrupting chemicals (EDCs) regulatory testing strategy despite compelling evidence for the existence of chemicals contained in consumer products and environmental pollutants that can cause adrenal toxicity (FDA, 2013; Harvey, 2016; Harvey and Everett, 2003; Harvey et al., 2007; Harvey and Sutcliffe, 2010; Hinson and Raven, 2006; Martinez-Arguelles and Papadopoulos, 2015). Also, the interference of industrial chemicals besides PCBs (Johansson et al., 1998, 2005), arsenic (Gosse et al., 2014; Kaltreider et al., 2001) and the organotin dibutyltin (Gumy et al., 2008) with glucocorticoid and mineralocorticoid hormone action requires further research (Macikova et al., 2014; Neel et al., 2013; Odermatt and Gumy, 2008; Stavreva et al., 2012).

The human adrenal cortical cell line H295R exhibits the main steroidogenic properties (Gazdar et al., 1990; Gracia et al., 2006) and has been validated to assess chemical effects on testosterone and estradiol production (Hecker et al., 2011; OECD, 2011). For the identification of EDCs, this protocol can be significantly extended by including progestins, adrenal androgens, glucocorticoids and mineralocorticoids (for a general overview of steroid synthesis see Fig. 1) (Odermatt et al., 2016). In fact, several studies addressed this issue and included several steroid metabolites in their analytical method (Feng et al., 2016; Karmaus et al., 2016; Mangelis et al., 2016; Nakano et al., 2016; Rijk et al., 2012; Saito et al., 2016; Tonoli et al., 2015; van den Dungen et al., 2015; Wang et al., 2015). Besides, the OECD testing guideline does not explicit the analytical method to be used as well as determined the read-out after a 48 h incubation period without inclusion of a control at the start of the experiment. Because improved testing protocols are especially important for situations where no clinical studies are performed, *e.g.* chemicals contained in cosmetics, UV-filters, food additives, drugs of abuse and designer steroids, the aim of the present study was to establish conditions for the LC–MS-based detection of changes of a series of progestins, adrenal androgens, glucocorticoids and mineralocorticoids upon exposure to reference chemicals and to chemicals that based on evidence from the literature might exert endocrine disrupting effects by disturbance of steroid hormone action.

2. Materials and methods

2.1. Chemicals and reagents

Test and reference compounds (angiotensin II (CAS Nr. 4474-91-3), forskolin (CAS Nr. 66575-29-9), prochloraz (CAS Nr. 67747-09-5), etomidate (CAS Nr. 33125-97-2), abiraterone acetate (CAS Nr. 154229-18-2), formestane (CAS Nr. 566-48-3), trilostan (CAS Nr. 13647-35-3), torcetrapib (CAS Nr. 262352-17-0), abietic acid (CAS Nr. 514-10-3), benzophenone-1 (CAS Nr. 131-56-6), chlorophene (CAS Nr. 120-32-1), enoxolone (CAS Nr. 471-53-4), escitalopram oxalate (CAS Nr. 219861-08-2), genistein (CAS Nr. 446-72-0), mitotane (CAS Nr. 53-19-0), rofecoxib (CAS Nr. 162011-90-7), sotalol (CAS Nr. 959-24-0), triclocarban (CAS Nr. 101-20-2), valproic acid sodium salt (CAS Nr. 1069-66-5), yohimbine hydrochloride (CAS Nr. 65-19-0), zidovudine (CAS Nr. 30516-87-1), octocrylene (CAS Nr. 6197-30-4), octyl methoxycinnamate (CAS Nr. 5466-77-3), acetyl tributylcitrate (CAS Nr. 77-90-7), linuron (CAS Nr. 330-55), digoxin (CAS Nr. 20830-75-5), digitoxin (CAS Nr. 71-63-6), amiodarone hydrochloride (CAS Nr. 19774-82-4), clofazimine (CAS Nr. 2030-63-9), sulforaphane (CAS Nr. 142825-10-3), and CDDO methyl ester (CAS Nr. 218600-53-4)) of the highest grade available were obtained from Sigma–Aldrich (Buchs, Switzerland). Stock solutions (10 mM) were prepared in dimethyl sulfoxide (DMSO). UHPLC-grade purity methanol, acetonitrile and formic acid were obtained from Biosolve (Dieuze, France). Aldosterone, 11-deoxycorticosterone, corticosterone, dehydroepiandrosterone-3-sulfate, androstenedione, testosterone, pregnenolone and [2,2,4,6,6,21,21-$^{2}H_{7}$]-aldosterone (98% isotopic purity) were purchased from Sigma-Aldrich. 11-Dehydrocorticosterone, dehydroepiandrosterone, progesterone, 17α-hydroxyprogesterone, 17α-hydroxypregnenolone, 11-deoxycortisol, cortisol and cortisone were purchased from Steraloids (Newport, RI). [1,2-$^{2}H_{2}$]-Testosterone (98% isotopic purity), [2,2,4,6,6,16,16-$^{2}H_{7}$]-4-androstene-3,17-dione (98% isotopic purity) and [2,2,4,6,6,17α,21,21-$^{2}H_{8}$]-corticosterone (98% isotopic purity) were purchased from C/D/N Isotopes Inc. (Pointe-Claire, Canada). Deuterated analogues [2,2,4,6,6,21,21,21-$^{2}H_{8}$]-17α-hydroxyprogesterone and [9,11,12,12-$^{2}H_{4}$]-cortisol were purchased from Toronto Research Chemicals (Toronto, ON, Canada). Stock solutions (10 mM and/or 1 mM) of above mentioned steroids were prepared in ethanol or methanol.

2.2. Cell culture and H295R steroidogenesis assay

The human adrenocortical carcinoma cell line H295R was obtained from American Type Culture Collection (ATCC, Manassas, USA) and grown in Dulbecco's modified Eagle's medium (DMEM)/Ham's nutrient mixture F-12 (1:1, v/v) (Life Technologies, Zug, Switzerland), supplemented with 1% (v/v) IST + Premix (BD Bioscience, Bedford, MA, USA), 2.5% (v/v) Nu-serum (Lot: 2342913, BD Bioscience, Bedford, MA, USA), 15 mM HEPES buffer and 1% (v/v) penicillin–streptomycin (Sigma–Aldrich) at 37 °C with a humidified 5% CO_2 atmosphere. The Nu-serum consists of 25% newborn calf serum and 75% of a proprietary formulation containing epidermal growth factor, endothelial cell growth supplement, insulin, transferrin, triiodothyronine, progesterone, estradiol, testosterone, cortisol, selenous acid, o-phosphorylethanolamine, glucose, amino acids, vitamins and other trace elements and nutrients in its Ham's F12 medium base. The concentrations of the supplements are not declared by the supplier.

The H295R steroidogenesis assay was performed according to the OECD test guideline (OECD, 2011). Briefly, cells at passages between 5 and 10 were seeded in 24-well plates at a density of 200,000 cells/ml in complete medium. The medium was replaced 24 h later with fresh medium containing test and reference compounds where indicated. DMSO (0.1% (v/v)) served as vehicle control. For studying time-dependent steroid production, cells were incubated for either 4, 8, 24 or 48 h in separate wells, and culture supernatants were collected and frozen at −20 °C until further analysis. For the other experiments, cells were incubated for

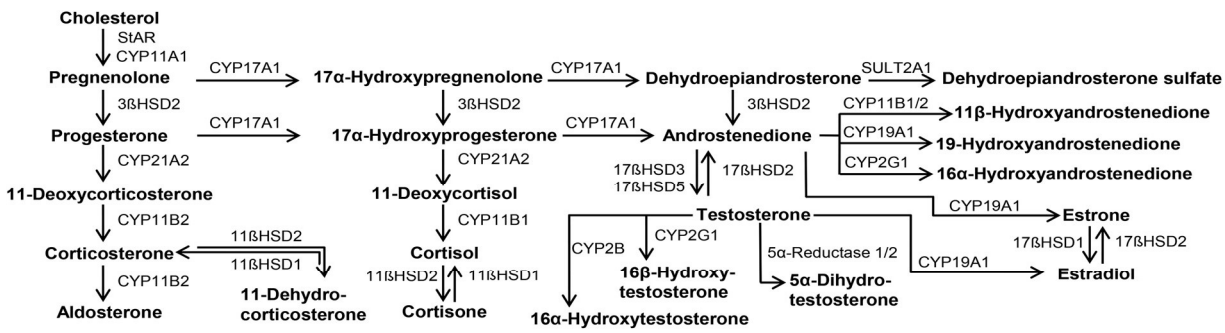

Fig. 1. Overview of steroidogenesis. Steroids are indicated in *bold*, the key enzymes in *regular* and the corresponding catalyzing reactions by *arrows*. CYP = cytochrome P450; HSD = hydroxysteroid dehydrogenase; SULT = sulfotransferase; StAR = steroidogenic acute regulatory protein.

48 h. Complete medium prior to adding to the cells ($t = 0$ h) served as control. To study the impact of serum, the complete medium was replaced 24 h after seeding by Nu-serum-free medium, followed by incubation for 48 h and collection of culture supernatants. All experiments were performed three times independently and in triplicates, with the exception of the untargeted analysis of steroid changes upon treatment with test and reference compounds; this experiment was performed two times independently, each in triplicates.

2.3. Assessment of cytotoxicity

The 3-(4,5-dimethylthiazol-2-yl)-2,5-diphenyl tetrazolium bromide (MTT) assay was used to evaluate possible effects of the test compounds on cellular metabolic activity. Briefly, H295R cells were seeded in 96-well plates (30,000 cells/100 μl complete medium). The medium was replaced after 24 h and cells were incubated with fresh medium containing the compounds of interest in a range of 0.04–50 μM, as indicated in the figures and tables. After 48 h, cells were inspected under the microscope. None of the treatments shown in this study, for both H295R cells kept in complete medium and cells kept in Nu serum-free medium, resulted in morphological changes. Then, 20 μl of MTT (5 mg/ml) was added to the medium, followed by incubation for another 3 h. For dissolving of the formed formazan crystals, the medium was aspirated and 100 μl of Sorenson's glycine buffer was added to each well. The plates were analyzed after 5 min at 565 and 650 nm (reference wavelength). The MTT assay was performed three times independently with technical triplicates. The conditions and concentrations used for the experiments presented in this study did not result in reduced cellular metabolic activity (values lower than 80% compared to vehicle control). Signs of cytotoxicity were observed, however, when incubating cells in the absence of Nu-serum with 10 μM forskolin. For this reason, the lower forskolin concentration of 5 μM was used for experiments with Nu-serum free medium.

2.4. Targeted steroid quantification

Targeted analysis of steroid hormone levels in H295R culture supernatants was performed as previously described with minor adaptations (Strajhar et al., 2016). Briefly, for solid-phase extraction, 1 ml of each H295R cell supernatant was mixed with 0.1 ml of protein precipitation solution (0.8 M zinc sulfate in water/methanol 50/50, v/v) that contained deuterium-labeled aldosterone, corticosterone, androstenedione and testosterone as internal standards. After incubating the samples in a shaker for 10 min at 4 °C with thorough shaking (1300 rotations/min), they were centrifuged for 10 min at 16,000 × g at 4 °C. The supernatants (950 μl) were transferred to Oasis HLB SPE cartridges, preconditioned with methanol and water. Steroids were eluted with 1 ml of methanol after washing once with 1 ml of water and twice with 1 ml of methanol/water (10/90, v/v). The samples were evaporated to dryness and then reconstituted in 25 μl of methanol. The separation and quantification of the steroids was performed by ultra-high pressure LC–MS/MS (UHPLC–MS/MS) using an Agilent 1290 UPLC coupled to an Agilent 6490 triple quadrupole mass spectrometer equipped with a jet-stream electrospray ionization interface. The steroids were separated using a reverse-phase column (Waters Acquity UPLC BEH C18, 1.7 μm, 2.1 mm × 150 mm) and a mobile phase A and B, consisting of water–acetonitrile–formic acid (95/5/0.1; v/v/v) and (5/95/0.1; v/v/v), respectively. For data acquisition and analysis, Mass Hunter software (Agilent Technologies) was used. Lower limits of quantification (LLOQ) are shown in Table 1. The steroid levels measured in all supernatants of incubated H295R cells were above the LLOQ. Recoveries for all steroids analyzed were between 80% and 120%.

2.5. Steroid quantification using an untargeted acquisition mode

Protein precipitation was performed adding 0.5 volume of protein precipitation solution in cell culture supernatant (1 ml). Precipitation solution was prepared adding 0.4 ml of 17α-hydroxyprogesterone-d8, cortisol-d4 at 1 μg/ml in methanol, and 0.2 ml of testosterone-d3 at 1 μg/ml in methanol (final concentrations in the cellular medium equal to 4, 4 and 2 ng/ml, respectively) into 49 ml of 6% perchloric acid solution in water. Samples were mixed for 10 min at 1400 rotations/min and 15 °C with a Thermomixer (Vaudaux-Eppendorf, Buchs, Switzerland). Samples underwent then centrifugation for 10 min at 4 °C and 12,000 × g. Supernatant was then loaded onto Oasis HLB cartridges (Waters, Milford, MA, USA) in 96-well plate format (30 mg, 30 μm particle size). Prior to supernatant deposition, cartridges were conditioned with 1 ml of methanol, dried for 10 min at 10 in Hg, and equilibrated with two times 1 ml of water. Cartridges were then washed three times successively with 1 ml of water/methanol (90:10, v/v) and dried for 1 min at 10 in Hg before elution with 1 ml of methanol. Fractions were then transferred into 1.5 ml polypropylene tubes and evaporated to dryness under vacuum with a centrifugal evaporator (RC1022, Jouan, Instrumenten Gesellschaft AG, Zürich, Switzerland). Samples were then reconstituted in 50 μl of water + 0.1% formic acid/acetonitrile + 0.1% formic acid (90:10, v/v) and homogenized in a Thermomixer for 10 min at 20 °C and 1400 rotations/min (Vaudaux-Eppendorf, Buchs, Switzerland) before 10 μl injection into the LC–MS system. Separation was performed with an UHPLC Acquity H-Class (Waters) including a quaternary solvent manager (QSM), a sample manager (SM-FTN) and a column manager (CM-A). The separation was performed on a Kinetex C18 column (2.1 mm × 150 mm, 1.7 μm) (Phenomenex, Torrance, CA) with a SecurityGuard ULTRA C18 (2.1 mm × 2 mm) (Phenomenex). Mobile phase A was water + 0.1% formic acid, and mobile phase B was acetonitrile + 0.1% formic acid. The flowrate was set at 300 μl/min. The composition in mobile phase B was increased linearly from 5% up to 80% in 14 min, then up to 90% in 0.5 min (hold for 1.5 min) and equilibrated back to original mobile phase conditions in 0.1 min for 6 min. Total analysis time was of 22.1 min per sample. Column was kept at 30 °C during the analysis while samples were kept at 8 °C in the autosampler. The automatic calibration procedure was performed as described by Tonoli et al. (2015). MaXis 3G QTOFMS (Bruker, Bremen, Germany) was equipped with an electrospray ionization source operated in positive mode. Source parameters were as follows: end plate offset was set at −500 V, nebulizer pressure at 1.8 bar, dry gas flowrate at 5.5 l/min, and temperature at 225 °C. Capillary voltage was set at −4.7 kV. Accumulation time was set at 1 s and mass range monitored was from *m/z* 50 to *m/z* 1000. Acquisition was performed in profile mode. Data were acquired using Compass v1.5 SR3 software suite from Bruker and HyStar v 3.2 SR2. UHPLC was controlled using plug-in for Waters Acquity UPLC v.1.5.

Table 1
Targeted quantification of steroids by LC–MS. Subset of 11 steroids used for quantification with their respective lower limits of quantification (LLOQ) values in nM.

Analyte	LLOQ (nM)
Progesterone	0.05
17α-Hydroxyprogesterone	0.78
11-Deoxycorticosterone	0.78
Aldosterone	0.20
Corticosterone	0.98
11-Deoxycortisol	0.78
Cortisol	1.95
Dehydroepiandrosterone	3.91
Dehydroepiandrosterone 3-sulfate	19.5
Androstenedione	0.78
Testosterone	0.39

2.6. Analysis of mRNA expression

Following a medium change and 48 h of incubation of H295R cells with the respective compounds, RNA was extracted using Tri-reagent (Sigma–Aldrich) and purified with the Direct-Zol RNA Mini Prep kit (Zymo research, Irvine, CA, USA) according to the manufacturer's instructions. RNA quality and yield was assessed using a Nano-Drop ND-1000 spectrophotometer (NanoDrop Technologies). Complementary DNA (cDNA) was synthesized from RNA using Superscript III reverse transcriptase (Invitrogen, Carlsbad, CA, USA) as previously described (Chantong et al., 2014). RT-qPCR was performed using KAPA SYBR FAST qPCR kit (Kapasystems, Boston, MA, USA) with the primers for the genes *CYP11B2*, *CYP17A1*, *CYP21A2*, *HSD3B2*, *CYP11A1*, *StAR*, and *CYP19A1* (Hilscherova et al., 2004), *CYP11B1* (Xu et al., 2006), *GAPDH* (Tanaka et al., 2008), and *HSD17B1*, *HSD17B2*, *HSD17B3*, *AKR1C3* (sequences of oligonucleotide primers are listed in Table S1 in the Supporting Information) and using the rotor-gene 6000 (Corbett Research, Sydney, Australia). Relative gene expression compared with the internal control GAPDH was determined using the 2-(ΔCt sample-ΔCt control) method. GAPDH was chosen as reference gene because its expression did not change between the various experimental conditions and time points applied in the present study. S18 RNA and PPIA were also analyzed but did not fulfill the quality criteria to be used as reference in these experiments (Taylor et al., 2010). Each sample was analyzed in triplicate.

2.7. Statistics

Computational analysis was performed in MATLAB® 8 environment (The MathWorks, Natick, USA). For analysis of data obtained from three independent steroid profiling experiments each performed in triplicate ($n = 9$), Shapiro–Wilk test was used to verify the normality of data. One-way analysis of variance (ANOVA) and Dunnett's multiple-comparison test were performed to evaluate differences between chemical treatments compared to the solvent control. Differences in gene expression were evaluated using a one-sample *t*-test of the fold changes after log2 transformation. Differences with $p < 0.05$ were considered to be significant. For analysis of data obtained from a representative experiment performed in triplicate ($n = 3$), Kruskal–Wallis test followed by Dunn's test was used.

3. Results

According to the OECD test guideline 456, H295R cells are incubated in medium containing 2.5% Nu-serum with the chemical of interest for 48 h, followed by determination of testosterone and estradiol as read-out and expression of the results as relative changes in hormone production compared with the solvent

controls (Hecker et al., 2011; OECD, 2011). In the present study, an untargeted LC–MS-based acquisition mode was chosen for the initial characterization of the H295R cell model and for a qualitative assessment of changes in the profile of 14 steroids upon exposure to various reference and test chemicals. In a second step, a targeted LC–MS-based method was used for quantification of steroid profiles upon exposure of cells to selected chemicals. This methods covered 11 adrenal steroids, including progestins, adrenal androgens, glucocorticoids and mineralocorticoids; however, not estrogens as they did not properly ionize under the conditions applied.

3.1. Time-dependent production of steroids in H295R cells

As a first analytical step, untargeted signal acquisition led to the detection of approximately 130 steroid-like metabolites annotated automatically based on exact mass. Starting from this panel of candidate compounds, 14 main steroids were unambiguously

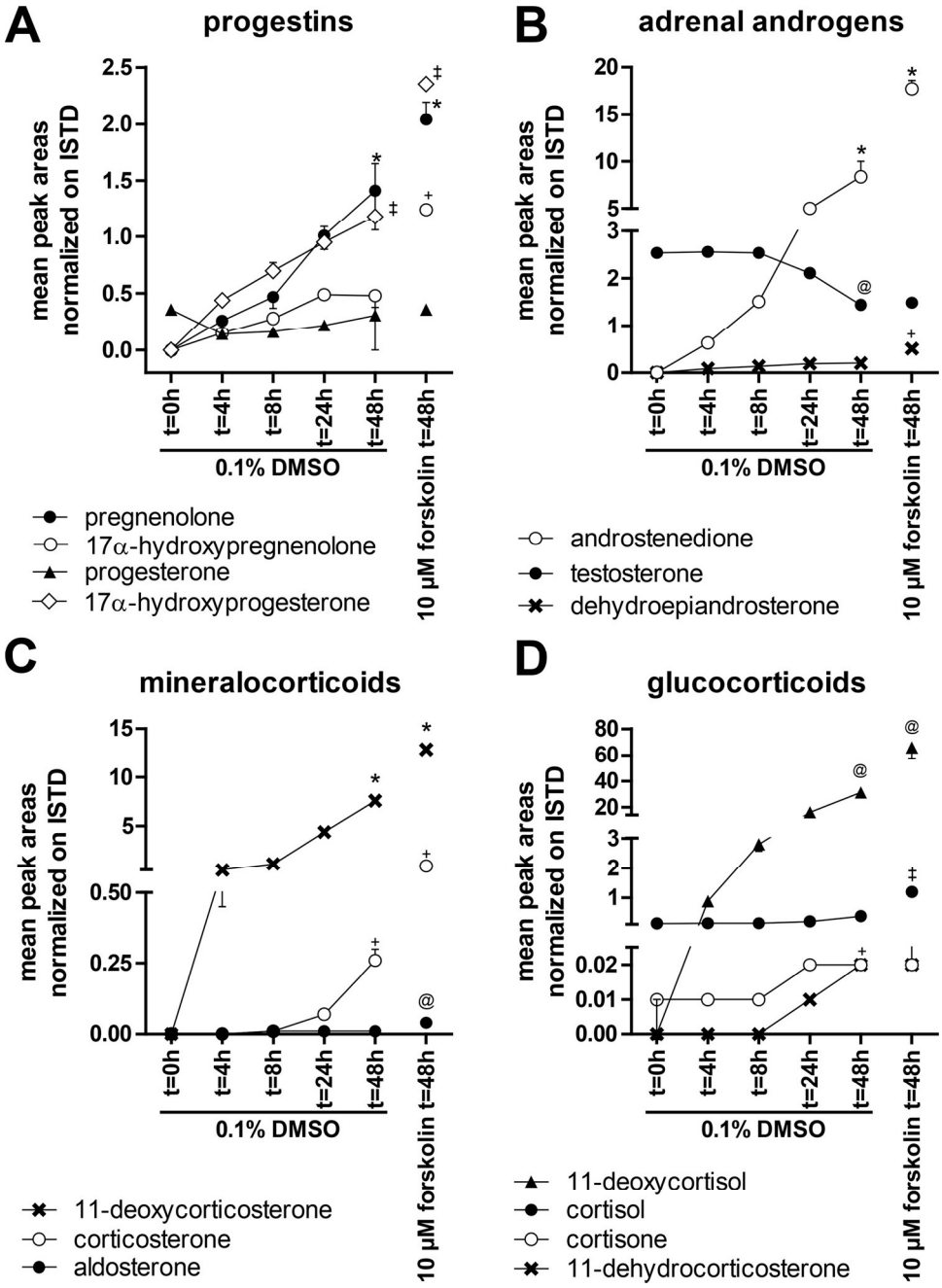

Fig. 2. Time-dependent steroid synthesis in H295R cells. H295R cells were cultivated following a medium change for 48 h in complete medium in the presence of vehicle (0.1% DMSO) or 10 μM forskolin as positive control to stimulate steroidogenesis. The secretion of (A) progestins, (B) adrenal androgens, (C) mineralocorticoids and (D) glucocorticoids into the medium was measured in culture supernatants by LC–MS. Kruskal–Wallis test followed by Dunn's test was used for statistical analysis. Data represent peak areas normalized to internal standard (ISTD), median with range, from one (out of three) representative experiment, performed in triplicate ($n = 3$). Significant differences ($p < 0.05$) for hormones (pregnenolone (*), 17α-hydroxypregnenolone (+), 17α-hydroxyprogesterone (‡), 11-deoxycorticosterone (*), corticosterone (+), aldosterone (@), 11-deoxycortisol (@), cortisol (‡), cortisone (+), androstenedione (*), testosterone (@), and dehydroepiandrosterone (+)) compared to vehicle (0.1% DMSO) at starting time point ($t = 0$ h) are indicated by the respective symbols.

identified by comparison with reference standards. Based on mean peak areas, a relative abundance comparison was conducted at 0, 4, 8, 24 and 48 h of incubation of the cells in complete medium containing 2.5% Nu-serum (Fig. 2). Additionally, steroidogenesis was stimulated in H295R cells by adding 10 μM forskolin and incubating the cells for 48 h.

Inclusion of steroid measurements of the complete medium prior to adding it to the cells at the start of the experiment ($t = 0$ h) revealed the presence of steroids that are added by the producer of Nu-serum (BD Bioscience), *i.e.* progesterone, testosterone and cortisol (estradiol is also added but was not measured by the method applied in this study) as well as cortisone in the complete medium (Fig. 2). While progesterone levels were not significantly altered upon incubation for up to 48 h, even in the presence of forskolin, the progestins pregnenolone, 17α-hydroxypregnenolone and 17α-hydroxyprogesterone showed time-dependent increases and were further enhanced upon treatment for 48 h with forskolin (Fig. 2A). A similar time-dependent increase was observed for the androgens androstenedione and, much less pronounced, for dehydroepiandrosterone (Fig. 2B), as well as for the corticosteroids 11-deoxycorticosterone, corticosterone, 11-deoxycortisol, and, less pronounced, for aldosterone, cortisone and cortisol (Fig. 2C and D). An exception was testosterone that was lower after 48 h of incubation (Fig. 2B). Also, the presence of forskolin did not stimulate the production of testosterone, and, although not reaching significance, a trend decrease was observed. These results show that H295R cells, in line with adrenal steroidogenesis, produce progestins, adrenal androgens, mineralocorticoids and glucocorticoids, reaching significant levels under the conditions applied after 48 h of incubation. In contrast, the testosterone contributed by addition of the Nu-serum seemed to be metabolized by the H295R cells.

3.2. De novo *synthesis of androstenedione but very low amounts of testosterone*

The production of androgens was further studied in H295R cells incubated for 48 h in the presence or absence of Nu-serum. This confirmed the presence of testosterone in the Nu-serum (compare DMSO control at $t = 0$ h in Fig. 3A and B) and that only very low amounts were produced *de novo* by the H295R cells (Fig. 3B). After 48 h of incubation in the absence of Nu-serum the amount of

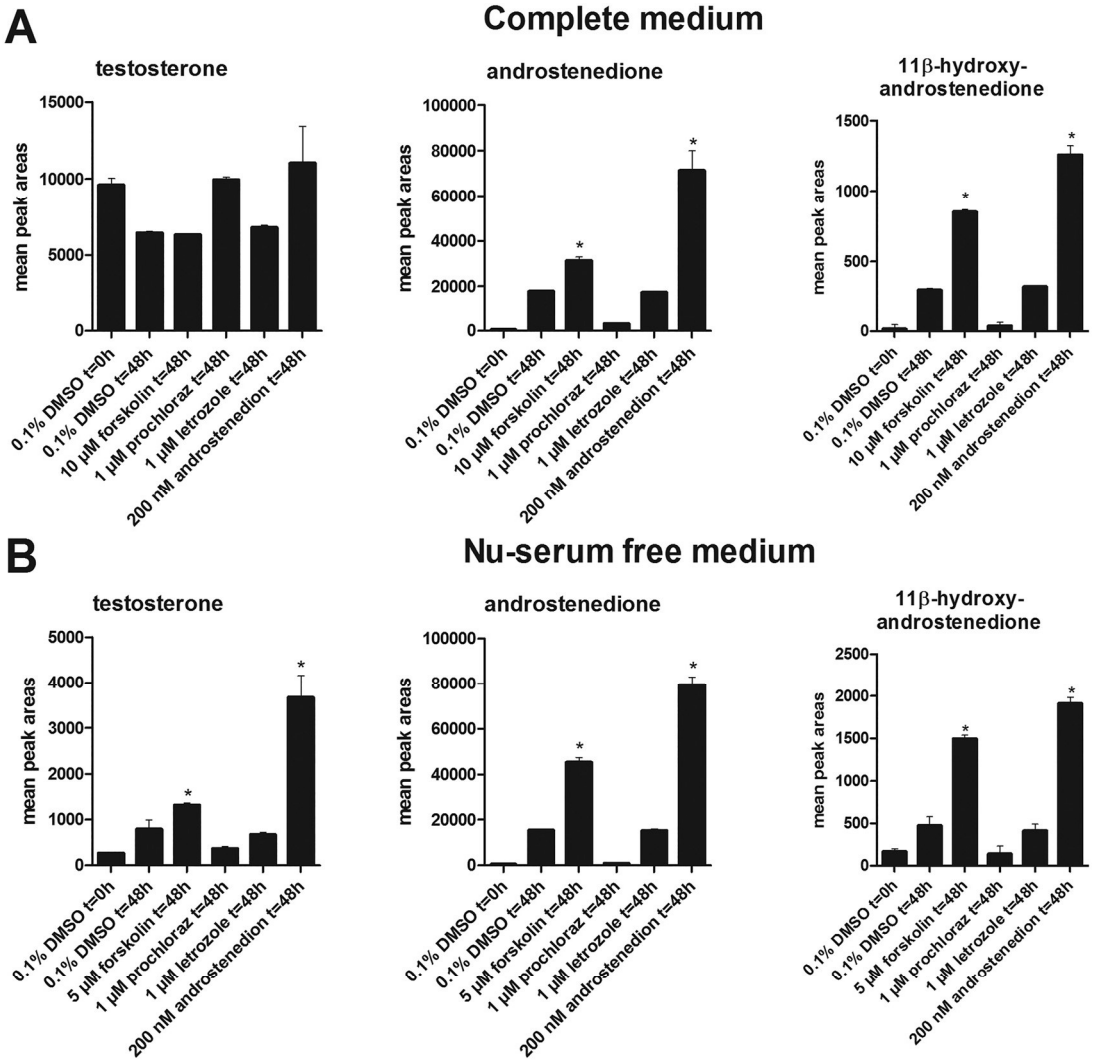

Fig. 3. *De novo* synthesis of testosterone, androstenedione and 11β-hydroxyandrostenedione by H295R cells. Steroids were quantitated in culture supernatants of H295R cells incubated either in complete medium (A) or in Nu-serum-free medium (B) for 48 h with vehicle (0.1% DMSO solvent control), 10 μM forskolin, 1 μM prochloraz, 1 μM letrozole or 200 nM androstenedione. Controls for complete medium and Nu-serum-free medium ($t = 0$ h) were included for comparison. Steroids (mean peak areas) were measured by LC–MS and represent median with range from one (out of three) representative experiment, performed in triplicate ($n = 3$). Kruskal–Wallis test followed by Dunn's test was used to analyze significant difference ($p < 0.05$) of solvent control at $t = 0$ to chemical treatment at $t = 48$ h (*).

testosterone produced was approximately 10-fold lower than the level present in the complete medium containing Nu-serum, thus masking *de novo* testosterone synthesis in cells kept in complete medium. Interestingly, forskolin did not affect the amount of testosterone in cells kept in the complete medium compared to vehicle control (Fig. 3A, DMSO control at $t = 48$ h), despite of an activation of testosterone formation observed in serum-free medium (Fig. 3B). The metabolism of testosterone from Nu-serum in cells kept in complete medium (Fig. 3A, also seen in Fig. 2B) could be prevented by the CYP17A1/CYP21A2 inhibitor prochloraz but not by the CYP19A1 inhibitor letrozole, suggesting that metabolism to estradiol had at best a minor contribution to the observed decrease of testosterone from the complete medium. However, formation of estrone and estradiol was not analyzed in this study because the LC–MS method applied was not designed to quantify these estrogens. Addition of androstenedione led to a trend increase (1.7-fold) in testosterone amounts in cells kept in complete medium, but a more pronounced increase (4.5-fold) that was further enhanced upon forskolin treatment (7.5-fold) in cells in the absence of serum, demonstrating the capability of H295R cells to produce testosterone (Fig. 3B). A comparison of H295R cells cultivated in complete medium with cells kept in Nu-serum-free medium revealed that androstenedione was synthesized *de novo* and that its production was further enhanced by forskolin (Fig. 3A and B). Also, 11β-hydroxyandrostenedione, a steroid produced by the human adrenals and found at higher concentration than androstenedione in adrenal vein sampling (Rege et al., 2013; Swart et al., 2013), was produced *de novo* by the H295R cells and was further enhanced upon forskolin treatment. While prochloraz abolished the formation of androstenedione and 11β-hydroxyandrostenedione, letrozole had no effect on the amounts of these steroids, suggesting that CYP19A1 plays a minor role under these conditions and that these androgens were not converted in substantial amounts to estrogens.

The adrenals can also form other hydroxylated metabolites of androstenedione and testosterone (Ford et al., 1975; Wang et al., 2010). For example, as shown in Fig. S1 (see Supplementary information), 16α- and 19α-hydroxyandrostenedione were found to be produced by the H295R cells and further increased by forskolin treatment, both in the presence and absence of Nu-serum. Also, 16α- and 16β-hydroxytestosterone were produced by the H295R cells and further enhanced by forskolin, and these metabolites were not present at substantial amounts in the complete medium. Thus, hydroxylation of testosterone by cytochrome P450 enzymes provides a possible explanation for the observed decrease of testosterone added by the complete medium upon incubation of H295R cells.

3.3. Impact of Nu-serum and forskolin on mRNA expression of steroidogenic genes

In order to assess the impact of Nu-serum removal on steroidogenic gene expression, H295R cells were subjected to a medium change and incubated in Nu-serum-free medium for 48 h in the presence of 0.1% DMSO. The comparison of mRNA expression levels with cells kept in complete medium revealed only minor differences in basal gene expression with CYP11B2 and StAR being expressed at about 2-fold lower levels (Table 2). Next, the stimulation of steroidogenesis by forskolin was analyzed. The most pronounced increase in mRNA expression was observed for 3β-HSD2 followed by CYP21A2, CYP11B2 and CYP19A1. All genes involved in steroidogenesis were induced at least 2-fold upon treatment with forskolin. Additionally, the expression of genes involved in the final steps of testosterone and estradiol synthesis were measured. 17β-HSD3 (converting androstenedione to testosterone), 17β-HSD1 (converting estrone to estradiol) and 17β-HSD2 (converting estradiol to estrone, testosterone to androstenedione) were not expressed at substantial levels. AKR1C3 mRNA was well expressed; thus, the enzyme responsible for the last step of *de novo* testosterone formation in H295R cells seems to be AKR1C3 and not 17β-HSD3, the key enzyme in Leydig cell testosterone formation (Miller and Auchus, 2011). AKR1C3 decreased 2-fold upon forskolin treatment in both cells kept in complete medium and in cells incubated in Nu-serum-free medium. Forskolin stimulation of steroidogenesis was in general more pronounced in Nu-serum-free medium, which may be explained by higher free concentrations of the compound in the absence of binding to serum proteins. At forskolin concentrations of 10 μM and higher, morphological changes indicating cytotoxicity were observed in cells incubated in Nu-serum-free medium (not shown); therefore a forskolin concentration of 5 μM, which did not lead to morphological changes, changes in the MTT assay, or changes in the expression levels of the GAPDH control, was chosen for these experiments.

3.4. Qualitative effects of reference and test compounds on the steroid profile in H295R cells

In the present study, H295R cells were incubated in medium containing 2.5% Nu-serum (complete medium) with the compounds of interest for 48 h, followed by collection of culture supernatants, according to the OECD test guideline. Relative amounts of the identified steroids, including the main adrenal steroids plus testosterone, were compared to those of cells incubated with vehicle (0.1% DMSO) (Fig. 4). The steroid profile of the complete medium at the start of the experiment ($t = 0$ h) was

Table 2
Impact of serum and forskolin on mRNA expression of steroidogenic genes. H295R cells were cultivated for 48 h in complete medium or in Nu-serum free medium in the presence or absence of 10 μM or 5 μM of forskolin, respectively, followed by quantification of mRNA expression by qPCR. Data represent mean ± SD from three independent experiments ($n = 9$), each performed in triplicates. GOIs = genes of interest; GAPDH = glycerinaldehyde-3-phosphatedehydrogenase; Ct = cycle threshold. Differences in gene expression were evaluated using a one-sample *t*-test of the fold changes after log2 transformation. Differences with $p < 0.05$ were considered to be significant.

	Complete medium		Nu-serum-free medium	
	Ct value DMSO 0.1%	Fold change GOI/GAPDH Forskolin 10 μM	Ct value DMSO 0.1%	Fold change GOI/GAPDH Forskolin 5 μM
GAPDH	13.7 ± 0.5	1.0 ± 0.4	13.6 ± 0.7	1.0 ± 0.1
StAR	15.9 ± 0.5	2.2 ± 0.4*	17.0 ± 0.4	5.6 ± 1.1*
CYP11A1	17.5 ± 0.5	2.4 ± 0.8*	17.9 ± 0.6	3.1 ± 0.3*
3β-HSD2	24.6 ± 0.6	27.9 ± 5.2*	25.0 ± 0.2	25.8 ± 10*
CYP17A1	19.5 ± 0.4	3.4 ± 0.6*	20.0 ± 0.5	7.3 ± 2.3*
CYP21A2	20.0 ± 0.7	8.0 ± 1.9*	20.8 ± 0.8	19 ± 5.9*
CYP11B1	29.1 ± 0.7	2.9 ± 1.0*	29.1 ± 0.9	5.3 ± 3.2*
CYP11B2	25.9 ± 0.6	9.1 ± 2.1*	26.9 ± 0.5	14.3 ± 5.7*
CYP19A1	23.4 ± 0.5	7.7 ± 1.6*	23.0 ± 0.3	10.5 ± 1.1*
AKR1C3	21.6 ± 0.6	0.5 ± 0.1*	22.0 ± 0.5	0.5 ± 0.0*

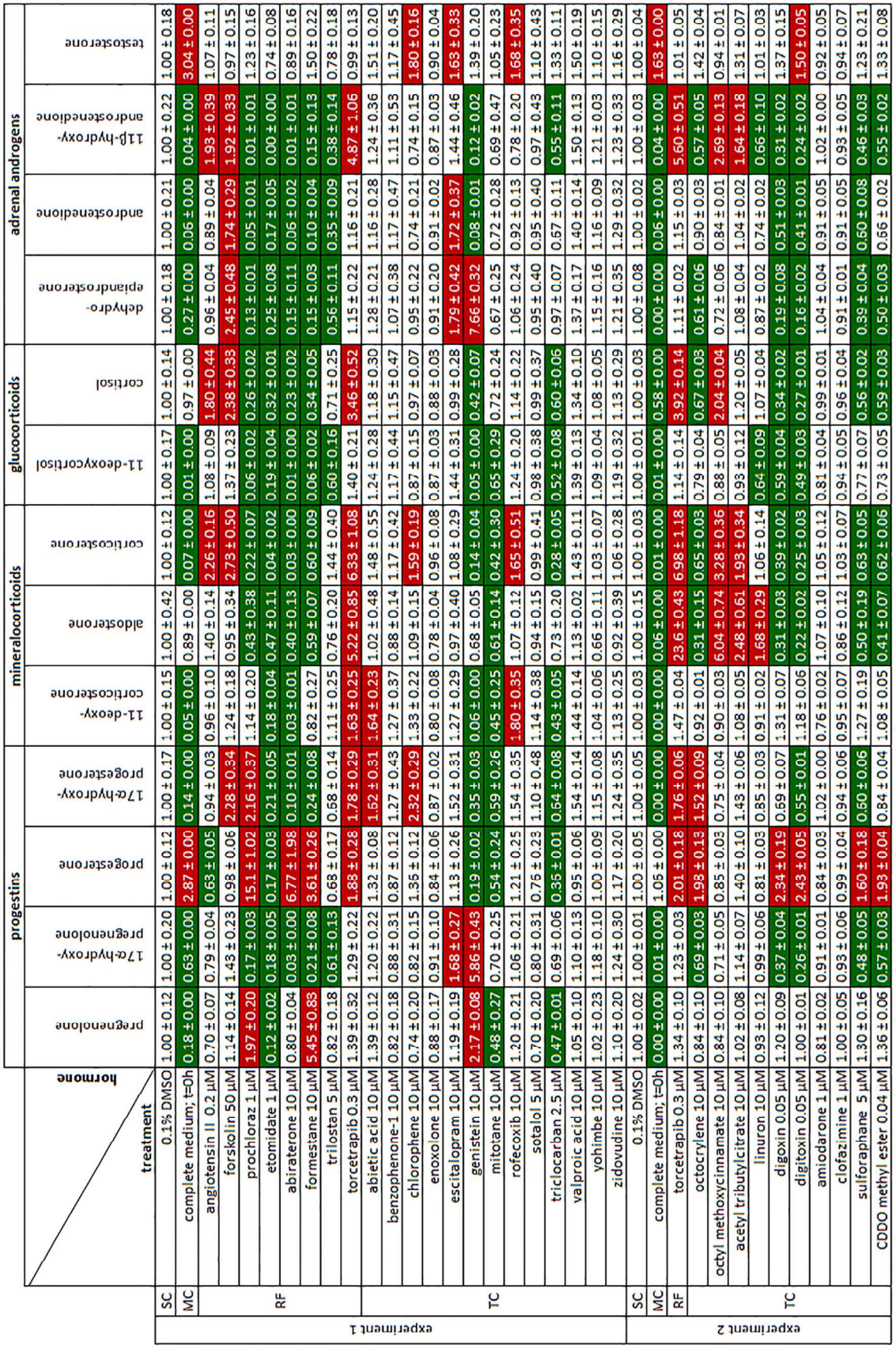

experiment		treatment \ hormone	pregnenolone	17α-hydroxy-pregnenolone	progesterone	17α-hydroxy-progesterone	11-deoxy-corticosterone	aldosterone	corticosterone	11-deoxycortisol	cortisol	dehydro-epiandrosterone	androstenedione	11β-hydroxy-androstenedione	testosterone
experiment 1	SC	0.1% DMSO	1.00 ± 0.12	1.00 ± 0.20	1.00 ± 0.12	1.00 ± 0.17	1.00 ± 0.15	1.00 ± 0.42	1.00 ± 0.12	1.00 ± 0.17	1.00 ± 0.14	1.00 ± 0.18	1.00 ± 0.21	1.00 ± 0.22	1.00 ± 0.18
	MC	complete medium; t=0h	0.18 ± 0.00	0.63 ± 0.00	2.87 ± 0.00	0.14 ± 0.00	0.05 ± 0.00	0.89 ± 0.00	0.07 ± 0.00	0.01 ± 0.00	0.97 ± 0.00	0.27 ± 0.00	0.06 ± 0.00	0.04 ± 0.00	3.04 ± 0.00
	RF	angiotensin II 0.2 μM	0.70 ± 0.07	0.79 ± 0.04	0.63 ± 0.05	0.94 ± 0.03	0.96 ± 0.10	1.40 ± 0.14	2.26 ± 0.16	1.08 ± 0.09	1.80 ± 0.44	0.96 ± 0.04	0.89 ± 0.04	1.93 ± 0.39	1.07 ± 0.11
		forskolin 50 μM	1.14 ± 0.14	1.43 ± 0.23	0.98 ± 0.06	2.28 ± 0.34	1.24 ± 0.18	0.95 ± 0.34	2.73 ± 0.50	1.37 ± 0.23	2.38 ± 0.33	2.45 ± 0.48	1.74 ± 0.29	1.92 ± 0.33	0.97 ± 0.15
		prochloraz 1 μM	1.97 ± 0.20	0.17 ± 0.03	15.1 ± 1.02	2.16 ± 0.37	1.14 ± 0.20	0.43 ± 0.38	0.22 ± 0.07	0.06 ± 0.02	0.26 ± 0.02	0.13 ± 0.01	0.05 ± 0.01	0.01 ± 0.01	1.23 ± 0.16
		etomidate 1 μM	0.12 ± 0.02	0.18 ± 0.05	0.17 ± 0.03	0.21 ± 0.05	0.18 ± 0.04	0.47 ± 0.11	0.04 ± 0.02	0.19 ± 0.04	0.32 ± 0.01	0.25 ± 0.08	0.17 ± 0.05	0.00 ± 0.00	0.74 ± 0.08
		abiraterone 10 μM	0.80 ± 0.04	0.03 ± 0.00	6.77 ± 1.98	0.10 ± 0.01	0.03 ± 0.01	0.40 ± 0.13	0.03 ± 0.00	0.01 ± 0.00	0.23 ± 0.02	0.15 ± 0.11	0.06 ± 0.02	0.01 ± 0.01	0.89 ± 0.16
		formestane 10 μM	5.45 ± 0.83	0.21 ± 0.08	3.61 ± 0.26	0.24 ± 0.08	0.82 ± 0.27	0.59 ± 0.07	0.60 ± 0.09	0.06 ± 0.02	0.34 ± 0.05	0.15 ± 0.03	0.10 ± 0.04	0.15 ± 0.13	1.50 ± 0.22
		trilostan 5 μM	0.82 ± 0.18	0.61 ± 0.13	0.68 ± 0.17	0.68 ± 0.14	1.11 ± 0.25	0.76 ± 0.20	1.44 ± 0.40	0.60 ± 0.16	0.71 ± 0.25	0.56 ± 0.11	0.35 ± 0.09	0.38 ± 0.14	0.78 ± 0.18
		torcetrapib 0.3 μM	1.39 ± 0.32	1.29 ± 0.22	1.88 ± 0.28	1.78 ± 0.29	1.63 ± 0.25	5.22 ± 0.85	6.33 ± 1.08	1.40 ± 0.21	3.46 ± 0.52	1.15 ± 0.22	1.16 ± 0.21	4.87 ± 1.06	0.99 ± 0.13
	TC	abietic acid 10 μM	1.39 ± 0.12	1.20 ± 0.22	1.32 ± 0.08	1.62 ± 0.31	1.64 ± 0.23	1.02 ± 0.48	1.48 ± 0.55	1.24 ± 0.28	1.18 ± 0.30	1.28 ± 0.21	1.16 ± 0.28	1.24 ± 0.36	1.51 ± 0.20
		benzophenone-1 10 μM	0.82 ± 0.18	0.88 ± 0.31	0.87 ± 0.12	1.27 ± 0.43	1.27 ± 0.37	0.88 ± 0.14	1.17 ± 0.42	1.17 ± 0.44	1.15 ± 0.47	1.07 ± 0.38	1.17 ± 0.47	1.11 ± 0.53	1.17 ± 0.45
		chlorophene 10 μM	0.74 ± 0.20	0.82 ± 0.15	1.35 ± 0.12	2.32 ± 0.29	1.33 ± 0.22	1.09 ± 0.15	1.59 ± 0.19	0.87 ± 0.15	0.97 ± 0.07	0.95 ± 0.22	0.74 ± 0.21	0.74 ± 0.15	1.80 ± 0.16
		enoxolone 10 μM	0.88 ± 0.17	0.91 ± 0.10	0.84 ± 0.06	0.87 ± 0.02	0.80 ± 0.08	0.78 ± 0.04	0.96 ± 0.08	0.87 ± 0.03	0.88 ± 0.03	0.91 ± 0.20	0.91 ± 0.02	0.87 ± 0.03	0.90 ± 0.04
		escitalopram 10 μM	1.19 ± 0.19	1.68 ± 0.27	1.13 ± 0.26	1.52 ± 0.31	1.27 ± 0.29	0.97 ± 0.40	1.08 ± 0.29	1.44 ± 0.31	0.99 ± 0.28	1.79 ± 0.42	1.72 ± 0.37	1.44 ± 0.46	1.63 ± 0.33
		genistein 10 μM	2.17 ± 0.08	5.86 ± 0.43	0.19 ± 0.02	0.35 ± 0.03	0.06 ± 0.00	0.68 ± 0.05	0.14 ± 0.04	0.05 ± 0.00	0.42 ± 0.07	7.66 ± 0.32	0.08 ± 0.01	0.12 ± 0.02	1.39 ± 0.20
		mitotane 10 μM	0.48 ± 0.27	0.70 ± 0.25	0.54 ± 0.24	0.59 ± 0.26	0.45 ± 0.25	0.61 ± 0.14	0.42 ± 0.30	0.65 ± 0.29	0.72 ± 0.24	0.67 ± 0.25	0.72 ± 0.28	0.69 ± 0.47	1.05 ± 0.23
		rofecoxib 10 μM	1.20 ± 0.21	1.06 ± 0.21	1.21 ± 0.25	1.54 ± 0.35	1.80 ± 0.35	1.07 ± 0.12	1.65 ± 0.51	1.24 ± 0.20	1.14 ± 0.22	1.06 ± 0.24	0.92 ± 0.13	0.78 ± 0.20	1.68 ± 0.35
		sotalol 5 μM	0.70 ± 0.20	0.80 ± 0.31	0.76 ± 0.23	1.10 ± 0.48	1.14 ± 0.38	0.94 ± 0.15	0.99 ± 0.41	0.98 ± 0.38	0.99 ± 0.37	0.95 ± 0.40	0.95 ± 0.40	0.97 ± 0.43	1.10 ± 0.43
		triclocarban 2.5 μM	0.47 ± 0.01	0.69 ± 0.06	0.35 ± 0.01	0.64 ± 0.08	0.43 ± 0.05	0.73 ± 0.20	0.28 ± 0.05	0.52 ± 0.08	0.60 ± 0.06	0.97 ± 0.07	0.67 ± 0.11	0.55 ± 0.11	1.33 ± 0.11
		valproic acid 10 μM	1.05 ± 0.10	1.10 ± 0.13	0.95 ± 0.06	1.54 ± 0.14	1.44 ± 0.14	1.13 ± 0.02	1.43 ± 0.11	1.39 ± 0.13	1.34 ± 0.10	1.37 ± 0.17	1.40 ± 0.14	1.50 ± 0.13	1.50 ± 0.19
		yohimbe 10 μM	1.02 ± 0.23	1.18 ± 0.10	1.00 ± 0.09	1.15 ± 0.08	1.04 ± 0.06	0.66 ± 0.11	1.03 ± 0.07	1.09 ± 0.04	1.08 ± 0.05	1.15 ± 0.16	1.16 ± 0.09	1.21 ± 0.03	1.10 ± 0.15
		zidovudine 10 μM	1.10 ± 0.20	1.24 ± 0.30	1.17 ± 0.20	1.24 ± 0.35	1.13 ± 0.25	0.92 ± 0.39	1.06 ± 0.28	1.19 ± 0.32	1.13 ± 0.29	1.21 ± 0.35	1.29 ± 0.32	1.23 ± 0.33	1.16 ± 0.29
experiment 2	SC	0.1% DMSO	1.00 ± 0.02	1.00 ± 0.01	1.03 ± 0.05	1.00 ± 0.05	1.00 ± 0.03	1.00 ± 0.15	1.00 ± 0.03	1.00 ± 0.01	1.00 ± 0.03	1.00 ± 0.08	1.00 ± 0.02	1.00 ± 0.03	1.00 ± 0.04
	MC	complete medium; t=0h	0.00 ± 0.00	0.01 ± 0.00	1.05 ± 0.00	0.00 ± 0.00	0.00 ± 0.00	0.06 ± 0.00	0.01 ± 0.00	0.01 ± 0.00	0.58 ± 0.00	0.00 ± 0.00	0.06 ± 0.00	0.04 ± 0.00	1.63 ± 0.00
	RF	torcetrapib 0.3 μM	1.34 ± 0.10	1.23 ± 0.03	2.01 ± 0.18	1.76 ± 0.06	1.47 ± 0.04	23.6 ± 0.43	6.98 ± 1.18	1.14 ± 0.14	3.92 ± 0.14	1.11 ± 0.02	1.15 ± 0.03	5.60 ± 0.51	1.01 ± 0.05
	TC	octocrylene 10 μM	0.84 ± 0.10	0.69 ± 0.03	1.98 ± 0.13	1.52 ± 0.09	0.92 ± 0.01	0.31 ± 0.15	0.65 ± 0.03	0.79 ± 0.04	0.67 ± 0.03	0.61 ± 0.06	0.90 ± 0.03	0.57 ± 0.05	1.42 ± 0.04
		octyl methoxycinnamate 10 μM	0.84 ± 0.10	0.71 ± 0.05	0.85 ± 0.03	0.75 ± 0.04	0.90 ± 0.03	6.04 ± 0.74	3.28 ± 0.36	0.88 ± 0.05	2.04 ± 0.04	0.72 ± 0.06	0.84 ± 0.01	2.69 ± 0.13	0.94 ± 0.01
		acetyl tributylcitrate 10 μM	1.02 ± 0.08	1.14 ± 0.07	1.40 ± 0.10	1.43 ± 0.06	1.08 ± 0.05	2.48 ± 0.61	1.93 ± 0.34	0.93 ± 0.12	1.20 ± 0.05	1.08 ± 0.04	1.04 ± 0.02	1.64 ± 0.18	1.31 ± 0.07
		linuron 10 μM	0.93 ± 0.12	0.99 ± 0.06	0.81 ± 0.03	0.85 ± 0.03	0.91 ± 0.02	1.68 ± 0.29	1.06 ± 0.14	0.64 ± 0.09	1.07 ± 0.04	0.87 ± 0.02	0.74 ± 0.02	0.66 ± 0.10	1.01 ± 0.03
		digoxin 0.05 μM	1.20 ± 0.09	0.37 ± 0.04	2.34 ± 0.19	0.69 ± 0.07	1.31 ± 0.07	0.31 ± 0.03	0.39 ± 0.02	0.59 ± 0.04	0.34 ± 0.02	0.19 ± 0.08	0.51 ± 0.03	0.31 ± 0.02	1.37 ± 0.15
		digitoxin 0.05 μM	1.00 ± 0.01	0.26 ± 0.01	2.43 ± 0.05	0.55 ± 0.01	1.18 ± 0.06	0.22 ± 0.02	0.25 ± 0.03	0.49 ± 0.03	0.27 ± 0.01	0.16 ± 0.02	0.41 ± 0.01	0.24 ± 0.02	1.50 ± 0.05
		amiodarone 1 μM	0.81 ± 0.02	0.91 ± 0.01	0.84 ± 0.03	1.02 ± 0.00	0.76 ± 0.02	1.07 ± 0.10	1.05 ± 0.12	0.81 ± 0.04	0.99 ± 0.01	1.04 ± 0.04	0.91 ± 0.05	1.02 ± 0.00	0.92 ± 0.05
		clofazimine 1 μM	1.00 ± 0.05	0.93 ± 0.06	0.99 ± 0.04	0.94 ± 0.06	0.95 ± 0.07	0.86 ± 0.12	1.03 ± 0.07	0.94 ± 0.05	0.96 ± 0.04	0.91 ± 0.01	0.91 ± 0.05	0.93 ± 0.05	0.94 ± 0.07
		sulforaphane 5 μM	1.30 ± 0.16	0.48 ± 0.05	1.60 ± 0.18	0.60 ± 0.06	1.27 ± 0.19	0.50 ± 0.19	0.63 ± 0.05	0.77 ± 0.07	0.56 ± 0.02	0.39 ± 0.04	0.60 ± 0.08	0.46 ± 0.03	1.23 ± 0.21
		CDDO methyl ester 0.04 μM	1.36 ± 0.06	0.57 ± 0.03	1.93 ± 0.04	0.84 ± 0.04	1.08 ± 0.05	0.41 ± 0.07	0.62 ± 0.06	0.73 ± 0.05	0.59 ± 0.03	0.50 ± 0.03	0.66 ± 0.02	0.55 ± 0.02	1.33 ± 0.08

SC: solvent control; MC: medium control; RF: reference compound; TC: test compound

Fig. 4. Qualitative analysis of effects of reference and test chemicals on the H295R steroid profile. H295R cells were incubated following a medium change in complete medium for 48 h with vehicle (0.1% DMSO) or the respective reference or test compound at the indicated concentration. Changes in steroid levels were measured by LC–MS. Data are expressed as a fold change relative to the solvent control and represent mean ± SD from one (out of two) representative experiment, performed in triplicate ($n = 3$). Steroid metabolites down regulated by 1.5-fold or more are indicated in green and steroids up regulated 1.5-fold or higher are depicted in red in order to indicate trend changes. The complete medium control was taken at the start of the experiment ($t = 0$ h). RF: reference compound; TC: test compound; SC: solvent control; MC: medium control.

included to distinguish steroids produced by the cells from steroids contributed by the Nu-serum. Progesterone, testosterone and cortisol were mainly contributed by the Nu-serum. Aldosterone was present at very low levels in unstimulated cells and varied in the medium control of the two experiments, thereby affecting the fold increase upon stimulation.

Next, in a qualitative experiment, the effects of various reference compounds were analyzed. As expected, angiotensin II and forskolin both enhanced the production of corticosterone, cortisol as well as the CYP11B product 11β-hydroxyandrostenedione (Fig. 4). Forskolin additionally enhanced the levels of 17α-hydroxyprogesterone, dehydroepiandrosterone and androstenedione, in line with an overall stimulation of the steroidogenesis. Prochloraz, which besides CYP17A1 also inhibits CYP21A2 (Ohlsson et al., 2009), prevented the further metabolism of progesterone, resulting in its accumulation, and led to reduced levels of corticosteroids and adrenal androgens. As mentioned above, the metabolism of testosterone from the Nu-serum was not affected by prochloraz treatment. Etomidate, at the concentration used in the present study, was found to inhibit CYP11B1, CYP11B2 and CYP11A1 (Hahner et al., 2010), explaining the almost complete block of steroidogenesis observed. Abiraterone, a known inhibitor of CYP17A1 and 3β-HSD2 (Jarman et al., 1998; Li et al., 2012), resulted in the simultaneous increase in progesterone and decrease in adrenal androgens and corticosteroids. Formestane at 10 μM exhibited a similar inhibition pattern with the exception of enhanced pregnenolone levels. The 3β-HSD inhibitor trilostane (Cooke, 1996) led to reduced adrenal androgen production. Since one of the aims of the present study was to establish conditions to identify chemicals disrupting corticosteroid synthesis, torcetrapib was used as a positive control. Torcetrapib was initially developed as a lipid lowering drug for treatment of cardiovascular disease but failed in phase III clinical trials due to excessive production of corticosteroids (Clerc et al., 2010; Hu et al., 2009). As expected, incubation of H295R cells with torcetrapib enhanced the CYP11B1/CYP11B2 products aldosterone, corticosterone, cortisol and 11β-hydroxyandrostenedione. The steroid profiles obtained for these reference compounds should facilitate classifying effects of test chemicals that yield a similar pattern, providing initial mechanistic insight and helping to prioritize further investigations.

Numerous test compounds were then analyzed for potential disruption of adrenal steroidogenesis. Several of them did not affect the steroid profile and/or presented very moderate effects. A general reduction of steroid production was observed for triclocarban, as reported earlier (Tonoli et al., 2015), and for mitotane, although the effects were moderate. Genistein led to enhanced pregnenolone, 17α-hydroxypregnenolone and dehydroepiandrosterone, but reduced progesterone, 17α-hydroxyprogesterone, corticosteroids and 3β-HSD-dependent androgens, in line with earlier findings of an inhibition of 3β-HSD activity (Sirianni et al., 2001). Five compounds, the UV-filter octocrylene, the cardiac glycosides digoxin and digitoxin, and the Nrf2 activators sulforaphane and CDDO methyl ester, resembled the steroid profile of abiraterone, suggesting inhibition and/or down regulation of CYP17A1 as an underlying mechanism. Two compounds, the UV-filter oxtyl methoxycinnamate and the phthalate replacement compound acetyl tributylcitrate, resembled the steroid profile of torcetrapib, suggesting an induction of CYP11B1 and CYP11B2 expression and activity.

3.5. Concentration-response study of selected chemicals on steroid production and impact on gene expression

To confirm the impact on the steroidogenesis of various concentrations of three important compounds, namely octocrylene, acetyl tributylcitrate and octyl methoxycinnamate, a supplementary set of experiments was conducted. For this purpose, targeted analyses on a QqQ system were then carried out to complement the first screening and determination of the extended steroid profiles with quantitative data. The use of targeted MS analysis of 11 reference steroid compounds allowed to unambiguously identify the concentration-dependent effects of the selected compounds on the alteration of steroid production. Incubation of H295R cells in complete medium containing 10 μM of octocrylene confirmed the increased progesterone and 17α-hydroxyprogesterone levels but suggested only a weak trend decrease for the corticosteroids 11-deoxycortisol, cortisol and corticosterone (Fig. 5). Exposure of H295R cells to acetyl tributylcitrate tended to increase the synthesis of the corticosteroids corticosterone and aldosterone and increased 11-deoxycorticosterone production. As seen with torcetrapib, acetyl tributylcitrate enhanced progesterone and 17α-hydroxyprogesterone levels. Octyl methoxycinnamate enhanced corticosterone and aldosterone and tended to increase cortisol levels. Hence, these results suggest that acetyl tributylcitrate and octyl methoxycinnamate increase mineralocorticoid production at concentrations of 10 μM, while none of these steroid metabolites were altered at lower concentrations.

As the initial goal of this study was to search for chemicals enhancing corticosteroid production and thereby contributing to hyperaldosteronism and hypercortisolism, the effect of acetyl tributylcitrate and octyl methoxycinnamate on the expression of key steroidogenic genes was determined (Fig. 6). As positive control, torcetrapib led to a profound up regulation of the expression of CYP11B2 and 3β-HSD2 and a more moderate induction of CYP11B1, CYP21A2, StAR, CYP11A1 and CYP17A1. The elevated expression of 3β-HSD2 explains the increased production of progesterone and 17α-hydroxyprogesterone, whereas the enhanced CYP11B1, CYP11B2 and CYP21A2 are responsible for the observed increase in aldosterone, cortisol, corticosterone and 11β-hydroxyandrostenedione. At concentrations of 10 μM, octyl methoxycinnamate and acetyl tributylcitrate both increased CYP11B2, 3β-HSD2 and CYP21A2 expression. They also increased or tended to increase CYP11B1 expression, thus explaining the torcetrapib-like effects previously observed in the qualitative assessment on the extended steroid profile.

4. Discussion

The OECD test guideline 456 describes a steroidogenesis assay validated for using the H295R cell line in its basal state to detect chemicals affecting the levels of testosterone and estradiol as endpoints (Hecker et al., 2006; OECD, 2011). According to the test guideline, the cells are incubated with the chemicals for 48 h. Testosterone and estradiol levels are being compared between cells exposed to vehicle and cells exposed to the test chemical (relative concentration determination). The steroidogenesis inhibitor prochloraz (1 μM) and the inducer forskolin (10 μM) are suggested as relevant controls. The present study proposes several suggestions for improvement of using H295R cells to detect chemicals interfering with adrenal steroid production. Using MS-based methods an extended panel of adrenal steroids can be quantified in culture supernatants of H295R cells at the start of the experiment ($t = 0$ h) and upon incubation ($t = 48$ h), allowing distinguishing between steroids produced by the cells and steroids contributed by the serum. Additionally, comparison of the observed changes caused by a given test chemical in the steroid profile with that of reference compounds acting on specific steroidogenic enzymes can provide initial mechanistic information.

First, because H295R cells and the complete medium with 2.5% Nu-serum represent a complex biological matrix already

treatment \ hormone	progestins		mineralocorticoids			glucocorticoids		adrenal androgens			
	progesterone	17α-hydroxyprogesterone	11-deoxycorticosterone	aldosterone	corticosterone	11-deoxycortisol	cortisol	dehydroepiandrosterone	dehydroepiandrosterone sulfate	androstenedione	testosterone
0.1% DMSO	1.41 ± 0.75	7.93 ± 0.51	14.8 ± 5.97	0.29 ± 0.14	3.61 ± 1.47	226.6 ± 71.5	22.8 ± 1.40	5.57 ± 0.78	53.2 ± 13.3	43.4 ± 7.59	3.77 ± 0.55
complete medium; t=0	1.39 ± 0.75	1.37 ± 0.85*	1.10 ± 0.72*	0.25 ± 0.17	<LLOQ	<LLOQ	14.3 ± 6.12	<LLOQ	<LLOQ	<LLOQ	6.44 ± 2.24*
torcetrapib 0.3 µM	4.00 ± 0.76*	14.4 ± 3.70*	33.4 ± 7.12*	2.45 ± 0.92*	37.0 ± 9.24*	376.2 ± 87.2*	64.0 ± 23.04*	7.17 ± 3.13	48.6 ± 26.6	54.5 ± 9.84*	4.12 ± 0.86
octocrylene 10 µM	3.20 ± 0.82*	12.2 ± 2.92*	18.0 ± 3.79	0.25 ± 0.18	2.70 ± 0.64	201.0 ± 25.5	17.5 ± 4.83	6.21 ± 3.10	50.0 ± 36.1	38.5 ± 3.54	7.01 ± 1.11*
octocrylene 5 µM	2.70 ± 0.46*	9.90 ± 0.81	19.5 ± 3.26	0.26 ± 0.22	5.12 ± 2.56	234.9 ± 22.1	20.4 ± 2.47	5.91 ± 0.46	37.4 ± 16.1	42.6 ± 4.87	5.16 ± 0.54*
octocrylene 1 µM	1.86 ± 0.51	9.77 ± 0.82	19.9 ± 2.32	0.27 ± 0.21	4.53 ± 0.17	267.8 ± 10.4	20.6 ± 4.5	6.04 ± 0.69	41.5 ± 16.8	43.6 ± 4.80	4.46 ± 0.32
octocrylene 0.5 µM	2.01 ± 0.62	10.4 ± 2.04	18.4 ± 1.76	0.27 ± 0.17	3.73 ± 0.99	277.9 ± 43.2	19.4 ± 4.3	5.86 ± 0.38	41.9 ± 16.0	47.2 ± 11.4	4.35 ± 0.30
octocrylene 0.1 µM	2.18 ± 0.77	9.90 ± 0.80	19.2 ± 3.57	0.25 ± 0.19	3.25 ± 0.76	263.7 ± 31.9	19.7 ± 3.36	5.64 ± 1.20	39.7 ± 14.4	42.4 ± 5.17	4.62 ± 0.59
octyl methoxycinnamate 10 µM	1.37 ± 0.43	7.32 ± 2.85	17.5 ± 3.98	0.87 ± 0.27*	13.5 ± 2.96*	242.6 ± 62.6	34.2 ± 5.72	6.81 ± 4.06	34.1 ± 25.6	37.4 ± 8.53	4.04 ± 0.78
octyl methoxycinnamate 5 µM	1.65 ± 0.75	8.37 ± 1.14	16.0 ± 4.41	0.30 ± 0.17	3.48 ± 0.59	249.5 ± 24.0	19.8 ± 5.48	5.63 ± 0.45	41.3 ± 18.6	40.9 ± 5.51	4.10 ± 0.81
octyl methoxycinnamate 1 µM	1.97 ± 0.75	9.27 ± 1.13	18.1 ± 4.35	0.31 ± 0.16	3.43 ± 1.14	254.3 ± 18.1	19.6 ± 3.9	5.58 ± 0.57	40.5 ± 17.4	42.1 ± 5.70	4.34 ± 0.46
octyl methoxycinnamate 0.5 µM	2.07 ± 0.74	9.88 ± 0.81	19.1 ± 4.09	0.30 ± 0.16	3.32 ± 1.04	261.2 ± 7.38	19.4 ± 4.03	5.79 ± 0.91	41.3 ± 20.1	42.6 ± 4.78	4.41 ± 0.48
octyl methoxycinnamate 0.1 µM	1.71 ± 0.46	10.0 ± 0.48	19.6 ± 4.80	0.29 ± 0.16	3.12 ± 0.80	263.2 ± 4.36	18.3 ± 6.36	5.80 ± 1.26	42.1 ± 20.6	42.1 ± 2.95	4.58 ± 0.78
acetyl tributylcitrate 10 µM	2.34 ± 1.12*	12.1 ± 3.17*	20.6 ± 4.67*	0.56 ± 0.46	6.93 ± 2.96	273.2 ± 89.3	21.8 ± 5.83	6.66 ± 0.51	37.4 ± 26.3	49.9 ± 11.8	5.82 ± 0.75*
acetyl tributylcitrate 5 µM	1.98 ± 0.89	10.9 ± 2.23*	17.9 ± 3.81	0.36 ± 0.25	3.91 ± 1.36	272.9 ± 36.4	21.9 ± 2.45	6.66 ± 0.67	42.8 ± 18.4	45.0 ± 4.46	4.47 ± 0.49
acetyl tributylcitrate 1 µM	2.03 ± 0.81	10.1 ± 0.92	18.9 ± 4.14	0.31 ± 0.17	3.63 ± 0.71	268.7 ± 26.4	19.9 ± 3.85	5.93 ± 0.82	39.7 ± 16.7	44.2 ± 3.39	4.40 ± 0.43
acetyl tributylcitrate 0.5 µM	2.08 ± 0.83	10.3 ± 0.98	19.2 ± 4.32	0.30 ± 0.16	3.60 ± 0.95	273.6 ± 32.0	19.7 ± 3.76	5.86 ± 0.73	40.7 ± 15.3	43.7 ± 3.89	4.23 ± 0.59
acetyl tributylcitrate 0.1 µM	2.25 ± 0.75	10.3 ± 0.38	19.7 ± 3.44	0.30 ± 0.16	3.45 ± 0.75	276.3 ± 18.2	20.3 ± 4.15	5.71 ± 0.83	42.9 ± 18.6	43.4 ± 6.34	4.43 ± 0.76

SC: solvent control; MC: medium control; RF: reference compound; TC: test compound

Fig. 5. Concentration-dependent effects of octocrylene, octyl methoxycinnamate and acetyl tributylcitrate on the H295R steroid profile. H295R cells were incubated following a medium change for 48 h with 0.1% DMSO (solvent control), 0.3 µM torcetrapib (reference compound) or the test compounds at the concentrations indicated. A complete medium control ($t = 0$ h) was included for comparison. Targeted quantification of steroids was performed by LC–MS. Data depicted in nM (mean ± SD; $n = 9$) were obtained from three independent experiments, each performed in triplicates. Steroid levels are shown as absolute values in nM. Values are depicted in a color code; where down regulation (>1.5-fold) is indicated in green and up regulation (>1.5-fold) in red compared to vehicle control. Shapiro–Wilk test was used to verify the normality of data. One-way analysis of variance (ANOVA) and Dunnett's multiple-comparison test were performed to evaluate differences between chemical treatments compared to the solvent control. Differences with $p < 0.05$ were considered to be significant. $^{*}p < 0.05$.

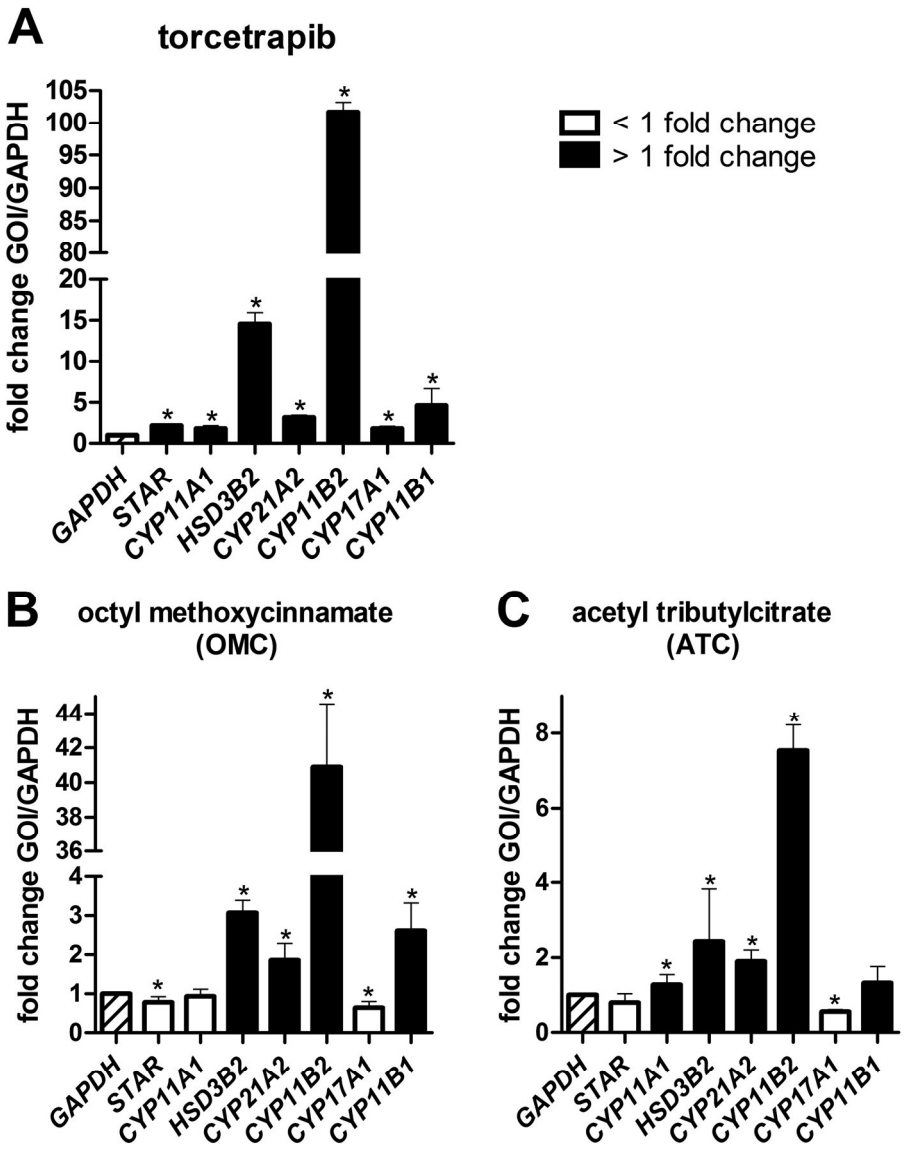

Fig. 6. Impact of torcetrapib, octyl methoxycinnamate and acetyl tributyl citrate on steroidogenic gene expression. H295R cells were incubated for 48 h with 0.3 μM torcetrapib, 10 μM octyl methoxycinnamate (OMC) or 10 μM acetyl tributyl citrate (ATC), followed by determination of the mRNA expression of steroidogenic genes of interest (GOIs). Values were normalized to glycerinaldehyde-3-phosphatedehydrogenase (GAPDH) and represent fold change over DMSO control (solid bars: up regulation; open bars: down regulation). Data, obtained from three independent experiments each performed in triplicates, are expressed as mean ± SD; $n = 9$. Differences in gene expression were evaluated using a one-sample t-test of the fold changes after log2 transformation. Differences with $p < 0.05$ were considered to be significant. $^{*}p < 0.05$ compared to control.

containing about 30 different steroids (Gazdar et al., 1990; Rainey et al., 1993, 1994), appropriate analytical methods, *i.e.* LC–MS and GC–MS, should be applied to obtained a sufficient analytical selectivity and the specific quantification of individual steroids. Antibody-based methods often fail to discriminate between similar steroid metabolites, resulting in an over estimation of the concentration of an individual steroid metabolite. For example, antibodies recognizing testosterone might also bind 6-, 11-, 16- and 19-hydroxylated or 5α-reduced metabolites, thus explaining the higher values obtained compared to MS-based quantification methods (Handelsman et al., 2015). The specificity analysis of commercially available antibody-based steroid quantification kits usually includes only a few steroid metabolites, thus the application of such kits should be restricted to well-defined samples. Also, a comparison of antibody-based kits revealed heterogeneity regarding recovery and linearity of steroid quantification (Buttler et al., 2013; Haisenleder et al., 2011; Handelsman and Wartofsky, 2013; Rosner et al., 2007). These issues emphasize the use of hyphenated approaches such as LC–MS and GC–MS methods for quantification of steroids, already considered as routine use determination in other important scientific fields such as doping analysis (Badoud et al., 2011). Moreover, untargeted LC–MS acquisition allows the retrospective analysis of the data without the need to reprocess the samples (Boccard et al., 2011). Such an approach constitutes therefore an appealing alternative for future developments of an extended profiling of the molecular actors involved in steroidogenesis, to complement the OECD reference guideline.

Second, to distinguish between changes in levels of steroids produced by the H295R cells from changes of steroids contributed by the Nu-serum, a control sample of the complete medium at the start of the experiment ($t = 0$ h) should be included. The composition of Nu-serum shows batch-dependent variations that are not defined by the vendor; besides varying concentrations of

testosterone and other steroids (own observations), other components such as growth factors may show Nu-serum batch-dependent differences, which may explain some of the inter-laboratory differences of steroid values and responses reported for this cell line (LeBaron et al., 2014). The Nu-serum used in the present study contained a relatively high concentration of testosterone (6.4 nM in complete medium containing 2.5% Nu-serum), and upon incubation with the cells part of this exogenously added testosterone was metabolized by enzyme(s) that could be inhibited by prochloraz (Fig. 3A and Fig. S1), likely involving CYP enzymes. In an earlier report, Zhang et al. reported the presence of testosterone in the culture medium (1260 pg/ml, corresponding to 4.4 nM) (Zhang et al., 2011); however, in their study they observed testosterone formation in complete medium (470 pg/ml, 1.6 nM) and forskolin led to a 2.9-fold increase in testosterone production. In the present study, the H295R cells in the absence of Nu-serum produced 0.55 nM testosterone, which was increased to 0.87 nM (158%) upon forskolin treatment, in line with the OECD guideline standard for induction/inhibition of testosterone synthesis (OECD, 2011). However, the H295R cells used in this study seemed to be less responsive to forskolin and they seemed to have a higher capacity to metabolize testosterone than the cells used by Zhang et al. (2011).

A limitation of the present study includes that estrone and estradiol, generated from androstenedione and testosterone by CYP19A1, were not quantified. Nevertheless, an induction of CYP19A1 by forskolin was observed, as reported in other studies focusing on CYP19A1 expression and activity (Caron-Beaudoin et al., 2016; Sanderson et al., 2000, 2002; Zhang et al., 2011). Compared with androstenedione synthesis, the capacity of H295R cells to produce estrogens seems to be rather low. For example Zhang et al. found approximately 50% lower amounts of estradiol produced compared to testosterone (Zhang et al., 2011). The present study showed that androstenedione was synthesized by the H295R cells, reaching an estimated concentration of 39 nM after incubation for 48 h in Nu-serum free medium (Fig. 3B). This compares with the much lower levels of testosterone generated under Nu-serum free conditions (0.55 nM), indicating inefficient 17-oxoreduction, and, as indicated by the study of Zhang et al. (2011) of estradiol, thus providing an explanation why incubation with the potent CYP19A1 inhibitors letrozole and formestane did not result in an accumulation of androstenedione and testosterone upon blocking the conversion to the corresponding estrogens.

Whilst comparison of treatment with vehicle *versus* chemical allows detecting compounds that cause changes in steroid levels, the inclusion of a complete medium control ($t = 0$ h) within any experimental design is mandatory to distinguish between steroids produced by the cells and steroids from the Nu-serum that then might be metabolized by the cells, thereby providing mechanistic information. For example, in the present study in the presence of Nu-serum, treatment of cells with prochloraz resulted in higher testosterone levels (Fig. 3A), which could be misinterpreted as a testosterone inducing chemical effect if no $t = 0$ h control were included and if no comparison with cells incubated in Nu-serum-free medium would have been analyzed. Thus, the use of H295R cells in the absence of serum represents a useful alternative for testing of chemicals interfering with steroidogenesis. Nevertheless, due to the higher unbound fraction of chemicals in the absence of serum, cytotoxicity of test compounds might be higher and should be excluded under these conditions.

Third, the simultaneous quantification of a panel of progestins, adrenal androgens, glucocorticoids and mineralocorticoids can provide initial mechanistic insight into the effects of a new test chemical. Measuring a group of important steroids provides more reliable information than determination of a single steroid. For example, ratios between selected compounds could be used to improve analytical reproducibility. Upon stimulation of CYP11B1 expression, the corticosteroids corticosterone, cortisol and 11β-hydroxyandrostenedione are expected to increase, whereas the progestins progesterone, 17α-hydroxyprogesterone, pregnenolone and 17α-hydroxypregnenolone remain unchanged or tend to decrease. A modulation of adrenal androgens is indicated if dehydroepiandrosterone, its sulfated form, androstenedione and its 11β-hydroxylated form are altered. Testosterone appears not to be a reliable marker, since it is present at a substantial level in Nu-serum (Zhang et al., 2011) and can be metabolized, thereby masking the production by the H295R cells. Furthermore, inhibition of the initial steps of steroidogenesis, *i.e.* StAR or CYP11A1, is indicated by a pattern resembling that of the complete medium at the start of the experiment, thus further emphasizing the inclusion of this important control.

Fourth, the use of several reference compounds with known mechanisms allows classifying effects of new test chemicals. As shown in this study, for the UV-filter chemical octocrylene a steroid profile similar to that of abiraterone (Mangelis et al., 2016; Rijk et al., 2012), with enhanced progesterone but slightly decreased corticosteroids and adrenal androgens was observed (Fig. 4), suggesting further mechanistic studies on whether octocrylene might inhibit and/or down regulate the expression of CYP17A1 and 3β-HSD2. The toxicological relevance of the observed effects of octocrylene needs to be investigated in a follow-on study. The observed inhibitory concentration was high and reliable concentrations in exposed individuals need to be established; however, mixtures of UV-filter chemicals need also to be considered in such follow-on studies. Similarly, future experiments should investigate whether the cardiac glycosides digoxin and digitoxin and the Nrf2 activators sulforaphane and CDDO methyl ester indeed act on CYP17A1. For this purpose, the use of forskolin stimulated cells should be considered because H295R cells produce rather moderate levels of adrenal androgens and corticosteroids in their basal state. The use of stimulated cells will facilitate the identification of chemicals inhibiting different steps of steroidogenesis. Also, the use of reference inhibitor compounds such as etomidate (Hahner et al., 2010; Rijk et al., 2012; Ulleras et al., 2008) and abiraterone (Mangelis et al., 2016; Rijk et al., 2012) can be optimized to use concentrations where a more selective inhibition of CYP11B1/CYP11B2 and CYP17A1, respectively, is achieved.

Using a corticosteroid inducer such as torcetrapib as a reference compound (Clerc et al., 2010; Hu et al., 2009), the two chemicals octyl methoxycinnamate and acetyl tributylcitrate were found to have a similar pattern. A supplementary concentration-dependence experiment revealed that only the highest concentration of 10 μM showed corticosteroid inducing effects (Fig. 5). Although it seems unlikely that such high concentrations are reached *in vivo* in the adrenals, a significant contribution of this compound when present in mixtures cannot be excluded and further studies should address this important issue of potential synergistic effect between EDCs. Furthermore, torcetrapib may serve as a useful reference compound to induce corticosteroid production and search for chemicals that are associated with hypocortisolism and hypoaldosteronism by inhibiting corticosteroid production. Determination of incubation time and type of inducer is important for such studies. In a recent study, Karmaus et al. used H295R cells that were stimulated for 48 h with forskolin prior to incubation with the test chemicals for profiling a large number of chemical effects on steroidogenesis, aiming at the categorization of action (Karmaus et al., 2016).

Finally, as shown in the present study, the steroid profile changes induced by a given chemical should ideally be confirmed or at least combined with gene expression analysis. As demonstrated for octyl methoxycinnamate and acetyl tributylcitrate, the

torcetrapib-like steroid pattern with increased corticosteroids could be explained by elevated expression of CYP11B2 and 3β-HSD2 mRNA levels (Fig. 6). Thus, these compounds do not directly modulate the activity of these enzymes but rather alter their expression levels. Follow-on investigations need to show whether L-type calcium channels might be involved in the mode of action and whether the increased CYP11B2 expression is a result of enhanced activation of the nuclear receptor NR4A2 as reported for torcetrapib expressed H295R cells (Clerc et al., 2010). Often, mRNA expression does not translate into protein expression; thus, determination of protein expression and/or enzyme activity measurements can complement mRNA expression analysis.

5. Conclusion

H295R cells represent an invaluable tool for the detection of hazardous chemicals interfering with steroidogenesis. The simultaneous measurements of a panel of progestins, adrenal androgens, glucocorticoids and mineralocorticoids by separation techniques hyphenated to MS such as LC–MS or GC–MS, as well as inclusion of a complete medium control at the start of the experiment allow identifying chemicals altering adrenal steroid production and provide initial mechanistic insight into the effects of such chemicals. Comparison with the steroid profiles of suitable reference compounds further allows classifying new test chemicals, thereby facilitating the prioritization of follow-on *in vitro* and *in vivo* experiments.

The results of the test chemicals suggest that the UV-filter octocrylene, the cardiac glycosides digoxin and digitoxin and the Nrf2 activators sulforaphane and CDDO methyl ester affect steroidogenesis by inhibiting or down regulating CYP17A1. Further, octyl methoxycinnamate and acetyl tributylcitrate increase corticosteroid production *via* induction of CYP11B2 and 3β-HSD2 expression. Further studies need to address the toxicological relevance of these observations. Finally, additional investigations of the untargeted steroid profiles will be carried out to extend the number of potential biomarkers and offer a more complete picture of the biochemical events resulting from H295R exposure to possible EDCs.

Conflict of interest

The authors declare no conflict of interest.

Transparency document

The http://dx.doi.org/10.1016/j.tox.2017.02.010 associated with this article can be found in the online version.

Acknowledgements

This study was supported by the Swiss Center for Applied Human Toxicology (SCAHT). A.O. was supported as Chair for Molecular and Systems Toxicology by the Novartis Research Foundation.

Appendix A. Supplementary data

Supplementary data associated with this article can be found, in the online version, at http://dx.doi.org/10.1016/j.tox.2017.02.010.

References

Badoud, F., Grata, E., Boccard, J., Guillarme, D., Veuthey, J.L., Rudaz, S., Saugy, M., 2011. Quantification of glucuronidated and sulfated steroids in human urine by ultra-high pressure liquid chromatography quadrupole time-of-flight mass spectrometry. Anal. Bioanal. Chem. 400, 503–516.

Boccard, J., Badoud, F., Grata, E., Ouertani, S., Hanafi, M., Mazerolles, G., Lanteri, P., Veuthey, J.L., Saugy, M., Rudaz, S., 2011. A steroidomic approach for biomarkers discovery in doping control. Forensic Sci. Int. 213, 85–94.

Buttler, R.M., Kruit, A., Blankenstein, M.A., Heijboer, A.C., 2013. Measurement of dehydroepiandrosterone sulphate (DHEAS): a comparison of isotope-dilution liquid chromatography tandem mass spectrometry (ID-LC–MS/MS) and seven currently available immunoassays. Clin. Chim. Acta 424, 22–26.

Caron-Beaudoin, E., Denison, M.S., Sanderson, J.T., 2016. Effects of neonicotinoids on promoter-specific expression and activity of aromatase (CYP19) in human adrenocortical carcinoma (H295R) and primary umbilical vein endothelial (HUVEC) cells. Toxicol. Sci. 149, 134–144.

Chantong, B., Kratschmar, D.V., Lister, A., Odermatt, A., 2014. Inhibition of metabotropic glutamate receptor 5 induces cellular stress through pertussis toxin-sensitive Gi-proteins in murine BV-2 microglia cells. J. Neuroinflamm. 11, 190.

Clerc, R.G., Stauffer, A., Weibel, F., Hainaut, E., Perez, A., Hoflack, J.C., Benardeau, A., Pflieger, P., Garriz, J.M., Funder, J.W., Capponi, A.M., Niesor, E.J., 2010. Mechanisms underlying off-target effects of the cholesteryl ester transfer protein inhibitor torcetrapib involve L-type calcium channels. J. Hypertens. 28, 1676–1686.

Cooke, G.M., 1996. Differential effects of trilostane and cyanoketone on the 3 beta-hydroxysteroid dehydrogenase-isomerase reactions in androgen and 16-androstene biosynthetic pathways in the pig testis. J. Steroid Biochem. Mol. Biol. 58, 95–101.

FDA, 2013. Endocrine Disruption Potential of Drugs: Nonclinical Evaluation. Draft Guidance. Federal Register 78 183, 57859. .

Feng, Y., Jiao, Z., Shi, J., Li, M., Guo, Q., Shao, B., 2016. Effects of bisphenol analogues on steroidogenic gene expression and hormone synthesis in H295R cells. Chemosphere 147, 9–19.

Ford, H.C., Wheeler, R., Engel, L.L., 1975. Hydroxylation of testosterone at carbons 1, 2, 6, 7, 15 and 16 by the hepatic microsomal fraction from adult female C57BL/6J mice. Eur. J. Biochem. 57, 9–14.

Gallo-Payet, N., Battista, M.C., 2014. Steroidogenesis-adrenal cell signal transduction. Compr. Physiol. 4, 889–964.

Gazdar, A.F., Oie, H.K., Shackleton, C.H., Chen, T.R., Triche, T.J., Myers, C.E., Chrousos, G.P., Brennan, M.F., Stein, C.A., La Rocca, R.V., 1990. Establishment and characterization of a human adrenocortical carcinoma cell line that expresses multiple pathways of steroid biosynthesis. Cancer Res. 50, 5488–5496.

Gosse, J.A., Taylor, V.F., Jackson, B.P., Hamilton, J.W., Bodwell, J.E., 2014. Monomethylated trivalent arsenic species disrupt steroid receptor interactions with their DNA response elements at non-cytotoxic cellular concentrations. J. Appl. Toxicol. 34, 498–505.

Gracia, T., Hilscherova, K., Jones, P.D., Newsted, J.L., Zhang, X., Hecker, M., Higley, E.B., Sanderson, J.T., Yu, R.M., Wu, R.S., Giesy, J.P., 2006. The H295R system for evaluation of endocrine-disrupting effects. Ecotoxicol. Environ. Saf. 65, 293–305.

Gumy, C., Chandsawangbhuwana, C., Dzyakanchuk, A.A., Kratschmar, D.V., Baker, M. E., Odermatt, A., 2008. Dibutyltin disrupts glucocorticoid receptor function and impairs glucocorticoid-induced suppression of cytokine production. PLoS ONE 3, e3545.

Hahner, S., Sturmer, A., Fassnacht, M., Hartmann, R.W., Schewe, K., Cochran, S., Zink, M., Schirbel, A., Allolio, B., 2010. Etomidate unmasks intraadrenal regulation of steroidogenesis and proliferation in adrenal cortical cell lines. Horm. Metab. Res. 42, 528–534.

Haisenleder, D.J., Schoenfelder, A.H., Marcinko, E.S., Geddis, L.M., Marshall, J.C., 2011. Estimation of estradiol in mouse serum samples: evaluation of commercial estradiol immunoassays. Endocrinology 152, 4443–4447.

Handelsman, D.J., Jimenez, M., Singh, G.K., Spaliviero, J., Desai, R., Walters, K.A., 2015. Measurement of testosterone by immunoassays and mass spectrometry in mouse serum, testicular, and ovarian extracts. Endocrinology 156, 400–405.

Handelsman, D.J., Wartofsky, L., 2013. Requirement for mass spectrometry sex steroid assays. J. Clin. Endocrinol. Metab. 98, 3971–3973.

Harvey, P.W., 2016. Adrenocortical endocrine disruption. J. Steroid Biochem. Mol. Biol. 155, 199–206.

Harvey, P.W., Everett, D.J., 2003. The adrenal cortex and steroidogenesis as cellular and molecular targets for toxicity: critical omissions from regulatory endocrine disrupter screening strategies for human health? J. Appl. Toxicol. 23, 81–87.

Harvey, P.W., Everett, D.J., Springall, C.J., 2007. Adrenal toxicology: a strategy for assessment of functional toxicity to the adrenal cortex and steroidogenesis. J. Appl. Toxicol. 27, 103–115.

Harvey, P.W., Sutcliffe, C., 2010. Adrenocortical hypertrophy: establishing cause and toxicological significance. J. Appl. Toxicol. 30, 617–626.

Hecker, M., Hollert, H., Cooper, R., Vinggaard, A.M., Akahori, Y., Murphy, M., Nellemann, C., Higley, E., Newsted, J., Laskey, J., Buckalew, A., Grund, S., Maletz, S., Giesy, J., Timm, G., 2011. The OECD validation program of the H295R steroidogenesis assay: Phase 3. Final inter-laboratory validation study. Environ. Sci. Pollut. Res. Int. 18, 503–515.

Hecker, M., Newsted, J.L., Murphy, M.B., Higley, E.B., Jones, P.D., Wu, R., Giesy, J.P., 2006. Human adrenocarcinoma (H295R) cells for rapid in vitro determination of effects on steroidogenesis: hormone production. Toxicol. Appl. Pharmacol. 217, 114–124.

Hilscherova, K., Jones, P.D., Gracia, T., Newsted, J.L., Zhang, X., Sanderson, J.T., Yu, R. M., Wu, R.S., Giesy, J.P., 2004. Assessment of the effects of chemicals on the

expression of ten steroidogenic genes in the H295R cell line using real-time PCR. Toxicol. Sci. 81, 78–89.
Hinson, J.P., Raven, P.W., 2006. Effects of endocrine-disrupting chemicals on adrenal function. Best Pract. Res. Clin. Endocrinol. Metab. 20, 111–120.
Hu, X., Dietz, J.D., Xia, C., Knight, D.R., Loging, W.T., Smith, A.H., Yuan, H., Perry, D.A., Keiser, J., 2009. Torcetrapib induces aldosterone and cortisol production by an intracellular calcium-mediated mechanism independently of cholesteryl ester transfer protein inhibition. Endocrinology 150, 2211–2219.
Jarman, M., Barrie, S.E., Llera, J.M., 1998. The 16,17-double bond is needed for irreversible inhibition of human cytochrome p45017alpha by abiraterone (17-(3-pyridyl)androsta-5, 16-dien-3beta-ol) and related steroidal inhibitors. J. Med. Chem. 41, 5375–5381.
Johansson, M., Johansson, N., Lund, B.O., 2005. Xenobiotics and the glucocorticoid receptor: additive antagonistic effects on tyrosine aminotransferase activity in rat hepatoma cells. Basic Clin. Pharmacol. Toxicol. 96, 309–315.
Johansson, M., Nilsson, S., Lund, B.O., 1998. Interactions between methylsulfonyl PCBs and the glucocorticoid receptor. Environ. Health Perspect. 106, 769–772.
Kaltreider, R.C., Davis, A.M., Lariviere, J.P., Hamilton, J.W., 2001. Arsenic alters the function of the glucocorticoid receptor as a transcription factor. Environ. Health Perspect. 109, 245–251.
Karmaus, A.L., Toole, C.M., Filer, D.L., Lewis, K.C., Martin, M.T., 2016. High-throughput screening of chemical effects on steroidogenesis using H295R human adrenocortical carcinoma cells. Toxicol. Sci. 150, 323–332.
LeBaron, M.J., Coady, K.K., O'Connor, J.C., Nabb, D.L., Markell, L.K., Snajdr, S., Sue Marty, M., 2014. Key learnings from performance of the U.S. EPA Endocrine Disruptor Screening Program (EDSP) Tier 1 in vitro assays. Birth Defect. Res. B Dev. Reprod. Toxicol. 101, 23–42.
Li, R., Evaul, K., Sharma, K.K., Chang, K.H., Yoshimoto, J., Liu, J., Auchus, R.J., Sharifi, N., 2012. Abiraterone inhibits 3beta-hydroxysteroid dehydrogenase: a rationale for increasing drug exposure in castration-resistant prostate cancer. Clin. Cancer Res. 18, 3571–3579.
Macikova, P., Groh, K.J., Ammann, A.A., Schirmer, K., Suter, M.J., 2014. Endocrine disrupting compounds affecting corticosteroid signaling pathways in Czech and Swiss waters: potential impact on fish. Environ. Sci. Technol. 48, 12902–12911.
Mangelis, A., Dieterich, P., Peitzsch, M., Richter, S., Juhlen, R., Hubner, A., Willenberg, H.S., Deussen, A., Lenders, J.W., Eisenhofer, G., 2016. Computational analysis of liquid chromatography-tandem mass spectrometric steroid profiling in NCI H295R cells following angiotensin II, forskolin and abiraterone treatment. J. Steroid Biochem. Mol. Biol. 155, 67–75.
Martinez-Arguelles, D.B., Papadopoulos, V., 2015. Mechanisms mediating environmental chemical-induced endocrine disruption in the adrenal gland. Front. Endocrinol. 6, 29.
Miller, W.L., Auchus, R.J., 2011. The molecular biology, biochemistry, and physiology of human steroidogenesis and its disorders. Endocr. Rev. 32, 81–151.
Nakano, Y., Yamashita, T., Okuno, M., Fukusaki, E., Bamba, T., 2016. In vitro steroid profiling system for the evaluation of endocrine disruptors. J. Biosci. Bioeng. 122, 370–377.
Neel, B.A., Brady, M.J., Sargis, R.M., 2013. The endocrine disrupting chemical tolylfluanid alters adipocyte metabolism via glucocorticoid receptor activation. Mol. Endocrinol. 27, 394–406.
Odermatt, A., Gumy, C., 2008. Glucocorticoid and mineralocorticoid action: why should we consider influences by environmental chemicals? Biochem. Pharmacol. 76, 1184–1193.
Odermatt, A., Strajhar, P., Engeli, R.T., 2016. Disruption of steroidogenesis: cell models for mechanistic investigations and as screening tools. J. Steroid Biochem. Mol. Biol. 158, 9–21.
OECD, 2011. OECD Guideline for the Testing of Chemicals. Test No. 456: H295R Steroidogenesis Assay. OECD Guidelines for the Testing of Chemicals, Section 4: Health Effects. .
Ohlsson, A., Ulleras, E., Oskarsson, A., 2009. A biphasic effect of the fungicide prochloraz on aldosterone, but not cortisol, secretion in human adrenal H295R cells – underlying mechanisms. Toxicol. Lett. 191, 174–180.
Rainey, W.E., Bird, I.M., Mason, J.I., 1994. The NCI-H295 cell line: a pluripotent model for human adrenocortical studies. Mol. Cell. Endocrinol. 100, 45–50.
Rainey, W.E., Bird, I.M., Sawetawan, C., Hanley, N.A., McCarthy, J.L., McGee, E.A., Wester, R., Mason, J.I., 1993. Regulation of human adrenal carcinoma cell (NCI-H295) production of C19 steroids. J. Clin. Endocrinol. Metab. 77, 731–737.
Rege, J., Nakamura, Y., Satoh, F., Morimoto, R., Kennedy, M.R., Layman, L.C., Honma, S., Sasano, H., Rainey, W.E., 2013. Liquid chromatography–tandem mass spectrometry analysis of human adrenal vein 19-carbon steroids before and after ACTH stimulation. J. Clin. Endocrinol. Metab. 98, 1182–1188.
Rijk, J.C., Peijnenburg, A.A., Blokland, M.H., Lommen, A., Hoogenboom, R.L., Bovee, T. F., 2012. Screening for modulatory effects on steroidogenesis using the human H295R adrenocortical cell line: a metabolomics approach. Chem. Res. Toxicol. 25, 1720–1731.
Rosner, W., Auchus, R.J., Azziz, R., Sluss, P.M., Raff, H., 2007. Position statement: utility, limitations, and pitfalls in measuring testosterone: an Endocrine Society position statement. J. Clin. Endocrinol. Metab. 92, 405–413.
Saito, R., Terasaki, N., Yamazaki, M., Masutomi, N., Tsutsui, N., Okamoto, M., 2016. Estimation of the mechanism of adrenal action of endocrine-disrupting compounds using a computational model of adrenal steroidogenesis in NCI-H295R cells. J. Toxicol. 2016, 4041827.
Sanderson, J.T., Boerma, J., Lansbergen, G.W., van den Berg, M., 2002. Induction and inhibition of aromatase (CYP19) activity by various classes of pesticides in H295R human adrenocortical carcinoma cells. Toxicol. Appl. Pharmacol. 182, 44–54.
Sanderson, J.T., Seinen, W., Giesy, J.P., van den Berg, M., 2000. 2-Chloro-s-triazine herbicides induce aromatase (CYP19) activity in H295R human adrenocortical carcinoma cells: a novel mechanism for estrogenicity? Toxicol. Sci. 54, 121–127.
Sirianni, R., Sirianni, R., Carr, B.R., Pezzi, V., Rainey, W.E., 2001. A role for src tyrosine kinase in regulating adrenal aldosterone production. J. Mol. Endocrinol. 26, 207–215.
Stavreva, D.A., George, A.A., Klausmeyer, P., Varticovski, L., Sack, D., Voss, T.C., Schiltz, R.L., Blazer, V.S., Iwanowicz, L.R., Hager, G.L., 2012. Prevalent glucocorticoid and androgen activity in US water sources. Sci. Rep. 2, 937.
Strajhar, P., Schmid, Y., Liakoni, E., Dolder, P.C., Rentsch, K.M., Kratschmar, D.V., Odermatt, A., Liechti, M.E., 2016. Acute effects of lysergic acid diethylamide on circulating steroid levels in healthy subjects. J. Neuroendocrinol. 28, 12374.
Swart, A.C., Schloms, L., Storbeck, K.H., Bloem, L.M., Toit, T., Quanson, J.L., Rainey, W. E., Swart, P., 2013. 11beta-hydroxyandrostenedione, the product of androstenedione metabolism in the adrenal, is metabolized in LNCaP cells by 5alpha-reductase yielding 11beta-hydroxy-5alpha-androstanedione. J. Steroid Biochem. Mol. Biol. 138, 132–142.
Tanaka, H., Kamita, S.G., Wolf, N.M., Harris, T.R., Wu, Z., Morisseau, C., Hammock, B. D., 2008. Transcriptional regulation of the human soluble epoxide hydrolase gene EPHX2. Biochim. Biophys. Acta 1779, 17–27.
Taylor, S., Wakem, M., Dijkman, G., Alsarraj, M., Nguyen, M., 2010. A practical approach to RT-qPCR-Publishing data that conform to the MIQE guidelines. Methods 50, S1–S5.
Tonoli, D., Furstenberger, C., Boccard, J., Hochstrasser, D., Jeanneret, F., Odermatt, A., Rudaz, S., 2015. Steroidomic footprinting based on ultra-high performance liquid chromatography coupled with qualitative and quantitative high-resolution mass spectrometry for the evaluation of endocrine disrupting chemicals in H295R cells. Chem. Res. Toxicol. 28, 955–966.
Ulleras, E., Ohlsson, A., Oskarsson, A., 2008. Secretion of cortisol and aldosterone as a vulnerable target for adrenal endocrine disruption – screening of 30 selected chemicals in the human H295R cell model. J. Appl. Toxicol. 28, 1045–1053.
van den Dungen, M.W., Rijk, J.C., Kampman, E., Steegenga, W.T., Murk, A.J., 2015. Steroid hormone related effects of marine persistent organic pollutants in human H295R adrenocortical carcinoma cells. Toxicol. In Vitro 29, 769–778.
Wang, C., Ruan, T., Liu, J., He, B., Zhou, Q., Jiang, G., 2015. Perfluorooctyl iodide stimulates steroidogenesis in H295R cells via a cyclic adenosine monophosphate signaling pathway. Chem. Res. Toxicol. 28, 848–854.
Wang, H., Xu, D., Peng, R.X., Yue, J., 2010. Testosterone-metabolizing capacity and characteristics of adrenal microsomes in human fetus in vitro. J. Pediatr. Endocrinol. Metabol. 23, 143–152.
Xu, Y., Yu, R.M., Zhang, X., Murphy, M.B., Giesy, J.P., Lam, M.H., Lam, P.K., Wu, R.S., Yu, H., 2006. Effects of PCBs and MeSO2-PCBs on adrenocortical steroidogenesis in H295R human adrenocortical carcinoma cells. Chemosphere 63, 772–784.
Zhang, F., Rick, D.L., Kan, L.H., Perala, A.W., Geter, D.R., LeBaron, M.J., Bartels, M.J., 2011. Simultaneous quantitation of testosterone and estradiol in human cell line (H295R) by liquid chromatography/positive atmospheric pressure photoionization tandem mass spectrometry. Rapid Commun. Mass. Spectrosc. 25, 3123–3130.

Supplementary information

Steroid profiling in H295R cells to identify chemicals potentially disrupting the production of corticosteroids and adrenal androgens

Petra Strajhar,[a,c] David Tonoli,[b,c] Fabienne Jeanneret,[b,c] Raphaella M. Imhof,[a] Vanessa Malagnino,[a] Melanie Patt,[a] Denise V. Kratschmar,[a] Julien Boccard,[b] Serge Rudaz,[b,c] Alex Odermatt[a,c,*]

Table S1: Sequences of oligonucleotide primers used for qPCR

Gene	Sense primer (sequence 5'-3')	Antisense primer (sequence 5'-3')
GAPDH	CAGCCTCAAGATCATCAGCA	TTCTAGACGGCAGGTCAGGT
STAR	GTCCCACCCTGCCTCTGAAG	CATACTCTAAACACGAACCCCACC
CYP11A1	GAGATGGCACGCAACCTGAAG	CTTAGTGTCTCCTTGATGCTGGC
HSD3B2	TGCCAGTCTTCATCTACACCAG	TTCCAGAGGCTCTTCTTCGTG
CYP17A1	AGCCGCACACCAACTATCAG	TCACCGATGCTGGAGTCAAC
CYP21A2	CGTGGTGCTGACCCGACTG	GGCTGCATCTTGAGGATGACAC
CYP11B1	GGTTTGCCAGGCTAAGC	CAAACTGCCCAGAGGACAG
CYP11B2	TCCAGGTGTGTTCAGTAGTTCC	GAAGCCATCTCTGAGGTCTGTG
CYP19A1	AGGTGCTATTGGTCATCTGCTC	TGGTGGAATCGGGTCTTTATGG
AKR1C3	GGATTTGGCACCTATGCACCTC	CTATATGGCGGAACCCAGCTTCTA
HSD17B1	GAAGGCTTATGCGAGAGT	GAAGGTGTGGATGTCCGT
HSD17B2	AAAGGGAGGCTGGTGAAT	GCAACTTTAATTCCCCAC
HSD17B3	TGCTTCCAAACCTTCTCCC	AGACCTTTCTGCCTTGATTCC

Fig. S1. *De novo* synthesis of 16α-hydroxyandrostenedione, 19-hydroxyandrostenedione, 16α-hydroxytestosterone and 16β-hydroxytestosterone by H295R cells. Steroids were quantified in culture supernatants of H295R cells incubated either in complete medium (A) or in Nu-serum-free medium (B) for 48 h with vehicle (0.1% DMSO solvent control), 10 µM (in A) or 5 µM (in B) forskolin, 1 µM prochloraz, 1 µM letrozole or 200 nM androstenedione. Controls for complete medium and Nu-serum-free medium (t=0 h) were included for comparison. Steroids (mean peak areas) were measured by LC-MS and represent median with range from one (out of three) representative experiment, performed in triplicate (n=3). Kruskal-Wallis test followed by Dunn's test was used to analyze significant difference ($p < 0.05$) of solvent control at t=0 to chemical treatment at t=48 h (*).

3.1.2 Published article:

Identification of the fungicide epoxiconazole by virtual screening and biological assessment as inhibitor of human 11β-hydroxylase and aldosterone synthase

Muhammad Akram[a,b,1], Melanie Patt[c,1], Teresa Kaserer[a], Veronika Temml[a], Watcharee Waratchareeyakul[d], Denise V. Kratschmar[c], Joerg Haupenthal[e], Rolf W. Hartmann[e,f], Alex Odermatt[c], Daniela Schuster[a,b], J Steroid Biochem Mol Biol. 2019 Sep;192:105358.

[1]These authors contributed equally to the present study.

[a]Institute of Pharmacy / Pharmaceutical Chemistry and Center for Molecular Biosciences Innsbruck, University of Innsbruck, Innrain 80-82, 6020, Innsbruck, Austria

[b]Department of Medicinal and Pharmaceutical Chemistry, Institute of Pharmacy, Paracelsus Medical University, Strubergasse 22, 5020, Salzburg, Austria

[c]Swiss Centre for Applied Human Toxicology and Division of Molecular and Systems Toxicology, Department of Pharmaceutical Sciences, University of Basel, Klingelbergstrasse 50, 4056, Basel, Switzerland

[d]Department of Chemistry, Faculty of Science and Technology, Rambhai Barni Rajabhat University, 22000, Chanthaburi, Thailand

[e]Department of Drug Design and Optimization, Helmholtz Institute for Pharmaceutical Research Saarland (HIPS), Universitätscampus E8 1, 66123, Saarbrücken, Germany

[f]Department of Pharmaceutical and Medicinal Chemistry, Saarland University, Campus C2.3, 66123, Saarbrücken, Germany

Contribution:

Performed all experiments in H295R cells, analyzed data, wrote and revised the manuscript.

Journal of Steroid Biochemistry and Molecular Biology 192 (2019) 105358

Contents lists available at ScienceDirect

Journal of Steroid Biochemistry and Molecular Biology

journal homepage: www.elsevier.com/locate/jsbmb

Identification of the fungicide epoxiconazole by virtual screening and biological assessment as inhibitor of human 11β-hydroxylase and aldosterone synthase

Muhammad Akram[a,b,1], Melanie Patt[c,1], Teresa Kaserer[a], Veronika Temml[a], Watcharee Waratchareeyakul[d], Denise V. Kratschmar[c], Joerg Haupenthal[e], Rolf W. Hartmann[e,f], Alex Odermatt[c,**], Daniela Schuster[a,b,*]

[a] Institute of Pharmacy / Pharmaceutical Chemistry and Center for Molecular Biosciences Innsbruck, University of Innsbruck, Innrain 80-82, 6020, Innsbruck, Austria
[b] Department of Medicinal and Pharmaceutical Chemistry, Institute of Pharmacy, Paracelsus Medical University, Strubergasse 22, 5020, Salzburg, Austria
[c] Swiss Centre for Applied Human Toxicology and Division of Molecular and Systems Toxicology, Department of Pharmaceutical Sciences, University of Basel, Klingelbergstrasse 50, 4056, Basel, Switzerland
[d] Department of Chemistry, Faculty of Science and Technology, Rambhai Barni Rajabhat University, 22000, Chanthaburi, Thailand
[e] Department of Drug Design and Optimization, Helmholtz Institute for Pharmaceutical Research Saarland (HIPS), Universitätscampus E8 1, 66123, Saarbrücken, Germany
[f] Department of Pharmaceutical and Medicinal Chemistry, Saarland University, Campus C2.3, 66123, Saarbrücken, Germany

ARTICLE INFO

Keywords:
Steroidogenesis
Pharmacophore modeling
Virtual screening
Endocrine disruption
Fungicide
Environmental chemical
Cortisol synthase
Aldosterone synthase

ABSTRACT

Humans are constantly exposed to a multitude of environmental chemicals that may disturb endocrine functions. It is crucial to identify such chemicals and uncover their mode-of-action to avoid adverse health effects. 11β-hydroxylase (CYP11B1) and aldosterone synthase (CYP11B2) catalyze the formation of cortisol and aldosterone, respectively, in the adrenal cortex. Disruption of their synthesis by exogenous chemicals can contribute to cardio-metabolic diseases, chronic kidney disease, osteoporosis, and immune-related disorders. This study applied *in silico* screening and *in vitro* evaluation for the discovery of xenobiotics inhibiting CYP11B1 and CYP11B2. Several databases comprising environmentally relevant pollutants, chemicals in body care products, food additives and drugs were virtually screened using CYP11B1 and CYP11B2 pharmacophore models. A first round of biological testing used hamster cells overexpressing human CYP11B1 or CYP11B2 to analyze 25 selected virtual hits. Three compounds inhibited CYP11B1 and CYP11B2 with IC_{50} values below 3 μM. The most potent inhibitor was epoxiconazole (IC_{50} value of 623 nM for CYP11B1 and 113 nM for CYP11B2, respectively); flurprimidol and ancymidol were moderate inhibitors. In a second round, these three compounds were tested in human adrenal H295R cells endogenously expressing CYP11B1 and CYP11B2, confirming the potent inhibition by epoxiconazole and the more moderate effects by flurprimidol and ancymidol. Thus, the *in silico* screening, prioritization of chemicals for initial biological tests and use of H295R cells to provide initial mechanistic information

Abbreviations: EDCs, endocrine disrupting chemicals; ACTH, adrenocorticotrophic hormone; CYP11B1, 11β-hydroxylase; DOC, 11-deoxycorticosterone; CAH, congenital adrenal hyperplasia; Na^+, sodium; K^+, potassium; CYP450, cytochrome P450; CYP11B2, aldosterone synthase; ID_{50}, infectious dose; 3β-HSD, 3β-hydroxysteroid dehydrogenase; PCBs, polychlorinated biphenyls; VS, virtual screening; 3D, three dimensional; HBD, hydrogen bond donors; HBA, hydrogen bond acceptors; AR, aromatic ring interactions; XVOLs, exclusion volumes; HTS, high throughput screening; APs, alanwood pesticides, EUC, EU-cosmetics; INCI, international nomenclature of cosmetics ingredients; EUFFA, EU food flavoring agents; EUFCM, EU food contact materials; ICs, industrial chemicals; SA, Sigma-Aldrich; DB, drug bank; CAS, chemical abstracts service; MOE, molecular operating environment; DMSO, dimethyl sulfoxide; DMEM, Dulbecco's Modified Eagle's Medium; FBS, fetal bovine serum; HPLC, high performance liquid chromatography; IC_{50}, half maximal inhibitory concentration; G6P, glucose-6-phosphate; 2D, two dimensional; sd, structure data; RMSD, root mean square deviation; PDB, protein data bank; VS, virtual screening; EtOH, ethyl alcohol

* Corresponding author at: Institute of Pharmacy / Pharmaceutical Chemistry and Center for Molecular Biosciences Innsbruck, University of Innsbruck, Innrain 80-82, 6020, Innsbruck, Austria.
** Corresponding author.
E-mail addresses: Muhammad.Akram@pmu.ac.at (M. Akram), Melanie.Patt@unibas.ch (M. Patt), Teresa.Kaserer@uibk.ac.at (T. Kaserer), Veronika.Temml@uibk.ac.at (V. Temml), Watcharee.W@rbru.ac.th (W. Waratchareeyakul), Denise.Kratschmar@unibas.ch (D.V. Kratschmar), Joerg.Haupenthal@helmholtz-hips.de (J. Haupenthal), Rolf.Hartmann@helmholtz-hzi.de (R.W. Hartmann), Alex.Odermatt@unibas.ch (A. Odermatt), Daniela.Schuster@uibk.ac.at (D. Schuster).
[1] These authors contributed equally to the present study.

https://doi.org/10.1016/j.jsbmb.2019.04.007
Received 23 December 2018; Received in revised form 5 April 2019; Accepted 6 April 2019
Available online 06 April 2019
0960-0760/

is a promising strategy to identify potential endocrine disruptors inhibiting corticosteroid synthesis. A critical assessment of human exposure levels and *in vivo* evaluation of potential corticosteroid disrupting effects by epoxiconazole is required.

1. Introduction

Humans are exposed to a large number of xenobiotics from various sources during their entire life. Exposure to such chemicals can cause adverse health effects and contribute to diseases. Chemicals causing acute toxic effects and genotoxic chemicals are usually identified during their production and/or introduction to industrial processes. In contrast, the identification of xenobiotics causing more subtle disturbances such as impairment of endocrine functions is more challenging. Therefore, there is a great interest to develop new strategies to identify chemicals interfering with endocrine functions. Several large projects currently aim to identify potential endocrine disrupting chemicals (EDCs), such as the European Registration, Evaluation, Authorization and Restriction of Chemicals (REACH; http://ec.europa.eu/growth/sectors/chemicals/reach/index_en.htm), the EPA's EDSP (Environmental Protection Agency's Endocrine Disruptor Screening Program, http://www.epa.gov/endo/) and the FDA's (U.S. Food and Drug Administration) drug development guidelines (http://www.fda.gov/Drugs/GuidanceComplianceRegulatoryInformation/Guidances/); thus a huge number of chemicals needs to be tested. Considerable efforts focused on the search for potential EDCs acting through estrogen and androgen receptors, and other nuclear hormone receptors by using both wet lab and *in silico* methods [1–3]. Nevertheless, steroidogenic enzymes such as cortisol synthase (11β-hydroxylase, CYP11B1) and aldosterone synthase (CYP11B2) play essential roles in steroid hormone homeostasis and should be included in the assessment of potential EDCs.

CYP11B1 is a mitochondrial enzyme belonging to the cytochrome P450 (CYP) family and uses NADPH as co-factor to catalyze the last and rate-limiting step in the synthesis of cortisol by 11β-oxidation of 11-deoxycortisol in the *zona fasciculata* of the adrenal cortex (Fig. 1) [4]. The synthesis of cortisol underlies feedback regulation *via* adrenocorticotrophic hormone (ACTH), which is secreted by the anterior pituitary gland [5]. Cortisol is produced when circulating glucose levels drop and under situations of stress. Furthermore, cortisol acts as an intrinsic immune-modulatory agent with an essential role in inflammation. It also regulates developmental and metabolic processes in the body. Therefore, maintenance of an un-interrupted synthesis of cortisol is crucial.

A deficiency in CYP11B1 results in a decrease of glucocorticoids, which ultimately leads to the development of an Addisonian crisis, cardiovascular collapse, and death [6]. Under normal circumstances, CYP11B1 produces also low amounts of corticosterone from its precursor 11-deoxycorticosterone (DOC) [7]. CYP11B1 deficiency leads to elevated levels of ACTH, DOC, 11-deoxycortisol, and a shift towards androgen production. Upon inhibition of CYP11B1, the increase in the mineralocorticoid DOC results in an extracellular fluid volume expansion, essential hypertension, and hypokalemia, with a concomitant suppression of the renin-angiotensin-aldosterone system [8,9]. The most pronounced form of CYP11B1 deficiency is seen in patients with genetic defects suffering from congenital adrenal hyperplasia (CAH) [10–12].

Aldosterone synthase (CYP11B2) is mainly located in mitochondria in the *zona glomerulosa* of the adrenal cortex, requires NADPH as a cofactor, and catalyzes three steps in the synthesis of aldosterone. First, it hydroxylates DOC at the 11β-position to corticosterone; second, it hydroxylates corticosterone at position 18 to form 18-hydroxycorticosterone; and third, it oxidizes this metabolite at position 18 to generate aldosterone (Fig. 1) [13]. Aldosterone is the major mineralocorticoid controlling the reabsorption of Na^+ and the excretion of K^+ by activating mineralocorticoid receptors (MR) in the distal convoluted tubules and the cortical collecting ducts of the nephron. It maintains plasma volume and regulates atrial blood pressure. Inhibition of CYP11B2 in normal individuals can result in life-threatening hyponatremia, hyperkalemia, and postural hypotension [14]. The most severe form is observed in patients with genetic defects [15–17].

CYP11B1 and CYP11B2 share 93% amino acid sequence identity [18], suggesting that xenobiotics rather unselectively inhibit CYP11B enzymes. Ayub et al. determined the IC_{50} values of several azole-based antifungals towards rat CYP enzymes and reported inhibitory potency for CYP11B1 of ketoconazole > bifonazole > clotrimazole > miconazole > econazole > isoconazole > tioconazole [19]. Furthermore, the anti-tumor drug mitotane and an analog of mitotane named 3-methylsulfonyl-DDE (3-$MeSO_2$-DDE), as well as some methylsulfonyl polychlorinated biphenyls ($MeSO_2$-PCBs), were found to inhibit CYP11B1 in a mouse adrenal cell line [20]. In a follow-up study, the inhibition of steroidogenesis by 3-$MeSO_2$-DDE was confirmed using the H295R cell model [21]. Xu et al. also used H295R cells and reported inhibition of steroidogenesis by polychlorinated biphenyls (PCBs) and $MeSO_2$-PCBs [22]. However, none of these earlier studies analyzed

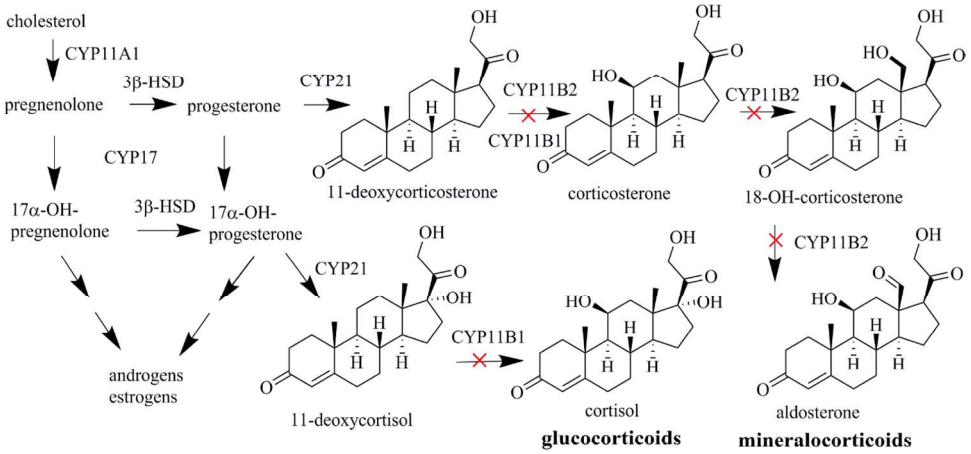

Fig. 1. The biosynthesis pathways of cortisol and aldosterone. The crucial role of CYP11B1 and CYP11B2 for the synthesis of glucocorticoids and mineralocorticoids, respectively, is shown.

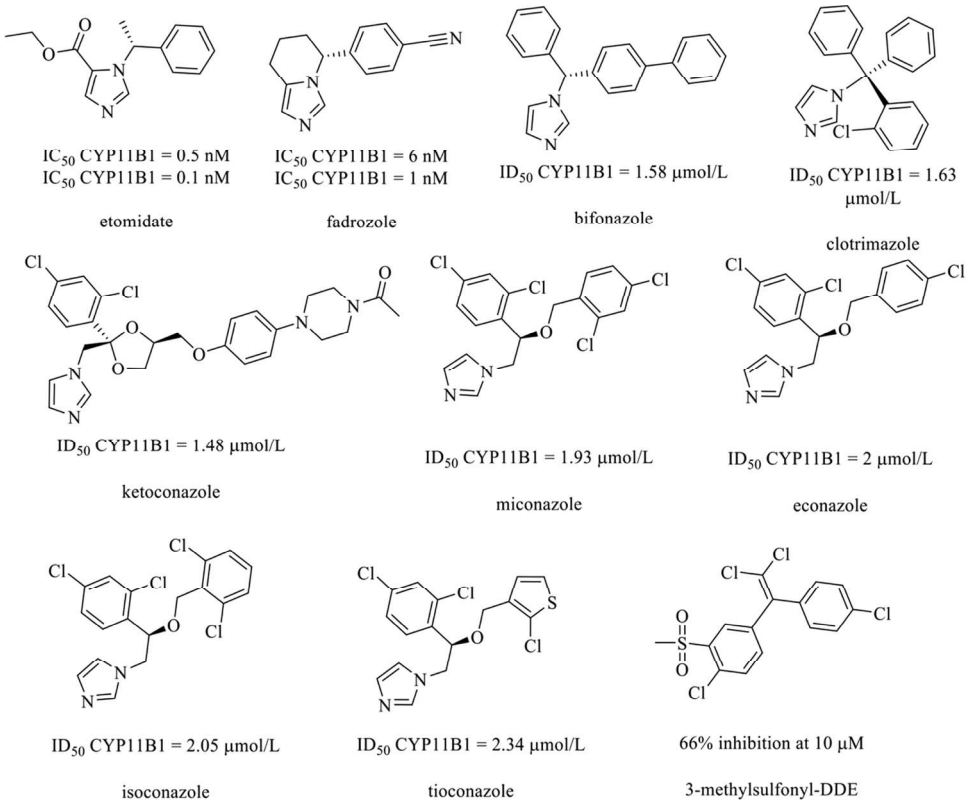

Fig. 2. Drugs, antifungals, and environmental pollutants that were found to interfere with steroidogenesis by inhibiting CYP11B1 or CYP11B2 [19,21,76–78].

CYP11B2. Inhibition of CYP11B1 and CYP11B2 by the already marketed drugs aminoglutethimide and etomidate (Fig. 2) raised concerns of fatal adrenal insufficiency in patients [23], and drug-induced adrenal toxicity has been recognized by the regulators [24]. Despite this, interference with the production of the two essential hormones cortisol and aldosterone has been neglected in the assessment of potential EDCs [25].

Due to their important physiological roles, CYP11B1 and CYP11B2 can be considered as anti-targets in drug development and they should be considered in the evaluation of potential EDCs. In order to screen large numbers of chemicals and for prioritization of biological assessment, *in silico* methods have been applied to discover potential lead compounds for drug development and to identify potential EDCs (reviewed in [26–31]. While previous *in silico* studies of CYP11B1 and CYP11B2 focused on the optimized ligand design and the synthesis of potential therapeutic inhibitors [32–36], the present study was designed to find potential EDCs inhibiting CYP11B1 and CYP11B2 by *in silico* screening and *in vitro* evaluation of selected virtual hits. To the best of our knowledge, this study is the first to focus on the identification of potential EDCs acting through CYP11B1 and CYP11B2 using pharmacophore-based virtual screening (VS) combined with *in vitro* approaches.

2. Materials and methods

2.1. Pharmacophore model optimization

In order to identify xenobiotics inhibiting CYP11B1 and/or CYP11B2, a pharmacophore-based screening strategy to enrich active molecules in a virtual hit list was applied. Two previously reported pharmacophore models [36] were optimized according to their experimental validation data. In brief, four structurally diverse, mostly subnanomolar active CYP11B1 and CYP11B2 inhibitors were used to develop two common features ligand-based pharmacophore models. Both models consisted of aromatic ring and hydrophobic features as well as hydrogen bond acceptors (Supporting information Figure S1 and S2). The model was validated by testing 24 predicted active compounds. These results were then used for model refinement.

The following parameters were used to assess the improved model quality:

$$Sensitivity = \frac{true\ positive}{true\ positive\ in\ the\ database} \quad (1)$$

$$Specificity = \frac{true\ negative}{true\ negative\ in\ the\ database} \quad (2)$$

$$Yield\ of\ active = \frac{true\ positive + false\ positive}{total\ number\ of\ hits} \quad (3)$$

$$accuracy = \frac{true\ positive + true\ negative}{true\ positive + false\ positive + true\ negative + false\ negative} \quad (4)$$

The performance of the models was analyzed before and after the refinement using sensitivity, specificity, yield of active, and accuracy (Eqs 1–4). Sensitivity of the given model is defined as the ratio between true positive compounds found by the model to the total number of true positives present in the dataset (Eq. 1). Specificity refers to the ratio of true negatives (discarded inactives) to the true negative dataset. Yield of active is the total number of compounds (true positive and false positive) found by the model to the total number of compounds in the dataset. Accuracy is the ratio of found active and discarded inactive to the total number of active and inactive dataset [37,38].

2.2. Pharmacophore-based anti-target screening

The improved models were used to screen the Alanwood pesticides (APs), EU cosmetics (EUC), International nomenclature of cosmetic ingredients (INCI), EU food flavoring agents (EUFFA), EU food contact

Table 1
Origin of chemical databases used in virtual screening.

Database	Description	No. of entries	Source	Access date/version
Pesticides				
APs	Collection of pesticide common names	7,221	http://www.alanwood.net/pesticides/index.html	07-05-2014
Cosmetics				
EUC	List of cosmetics ingredients provided by the EU	16,948	http://ec.europa.eu/growth/tools-databases/cosing/	28-05-2014
INCI	Manually compiled list of cosmetics ingredients	5,622	inhouse	
Food				
EUFFA	List of food flavorings provided by the EU	3,733	http://ec.europa.eu/dgs/health_food-safety/information_systems/index_en.htm	14-05-2014
EUFCM	List of food contact materials provided by the EU	2,105	http://ec.europa.eu/dgs/health_consumer/information_systems/index_en.htm	26-05-2014
Drugs				
DB	Drugs that are approved by the FDA	1,526	https://www.drugbank.ca/releases/latest#structures	08-09-2014
Chemicals produced by the industry				
ICs	List of chemicals from ECHA used in European industries	2,556	https://echa.europa.eu/	08-04-2016
SA	Full catalogue of chemicals of Sigma-Aldrich	73,003	https://www.sigmaaldrich.com/chemistry/chemistry-services/selected-structure.html	28-04-2014
Potential endocrine disrupting chemicals				
EDCs	This database was constructed from publicly available version 2 of the endocrine disruptors priority setting database of the U.S. Environmental Protection Agency.	76,677	[75]	17-05-2009

materials (EUFCM), industrial chemicals (ICs), Sigma-Aldrich (SA), DrugBank (DB), and endocrine disrupting chemicals (EDCs) databases (Table 1). OMEGA-FAST settings were used to generate the 500 conformers for every single entry of all environmental chemical databases. VS was performed within LigandScout 3.12 using default settings (*zero omitted pharmacophore features*, *pharmacophore-fit* as a scoring function, and in presence of exclusion volumes (XVOLs)). Test compounds were selected from the virtual hit lists by pharmacophore-fit scores, consensus hits, and compounds with high consumer exposure.

2.3. Description of chemical databases for virtual screening

Lists of relevant environmental chemicals were mainly collected from regulatory sources (Table 1). First, the chemical abstracts service (CAS) numbers of the xenobiotic chemicals shown in Table 1 were collected. The structures of the compounds were retrieved as sd files from PubChem using a Pipeline Pilot [39] script (version 9.1). In case multiple structures were obtained for a given CAS number, only the entry with the highest number of defined stereo-centers was kept. Salts and counter-ions were removed using the 'wash molecules' protocol in Molecular Operating Environment (MOE) version 2011.10 [40]. Discovery Studio version 4.0 [41] was employed to generate tautomers and stereoisomers (in case of undefined stereo-centers) using the default settings. OpenEye's OMEGA [42,43], implemented in LigandScout, was used for conformer generation in FAST mode, allowing for a maximum of 500 conformers for every single entry of all databases.

2.4. Biological evaluation

2.4.1. Chemicals and reagents

Torcetrapib (CAS Nr. 262352-17-0), etomidate (CAS Nr. 33125-97-2), epoxiconazole (CAS Nr. 133855-98-8), flurprimidol (CAS Nr. 56425-91-3) and ancymidol (CAS Nr. 12771-68-5) of the highest grade available were purchased from Sigma-Aldrich (Buchs, Switzerland). Compounds were dissolved in dimethyl sulfoxide (DMSO; Sigma-Aldrich) to stock solutions of 10 mM. To maintain stability, multiple aliquots were made, frozen at −20 °C, and each stock solution was tested once only. For the testing in hamster cells, the inhibitors were diluted with 99.9% ethanol to the desired concentrations. Aldosterone, deoxycorticosterone (DOC), corticosterone and androstenedione were purchased from Sigma-Aldrich. Progesterone, 17α-hydroxyprogesterone, 11-deoxycortisol, and cortisol were obtained from Steraloids (Newport, RI). Deuterated analogues [2,2,4,6,6,16,16-$^{2}H_{7}$]-4-androstene-3,17-dione (98% isotopic purity), [2,2,4,6,6,17α,21,21-$^{2}H_{8}$]-corticosterone (98% isotopic purity) were purchased from C/D/N Isotopes Inc. (Pointe-Claire, Canada) and [2,2,4,6,6,21,21-$^{2}H_{7}$]-aldosterone (98% isotopic purity) from Sigma-Aldrich. Steroid stock solutions (10 mM and/or 1 mM) were prepared in ethanol or methanol. UHPLC-grade purity methanol, acetonitrile, and formic acid were purchased from Biosolve (Dieuze, France). Milli-Q water was obtained using a Milli-Q water purification system (Millipore, USA).

2.4.2. Cell culture

Hamster V79MZh cells expressing recombinant human CYP11B1 and CYP11B2 were grown in Dulbecco's modified Eagle medium high glucose (DMEM), supplemented with 5% fetal bovine serum (FBS), 100 U/mL penicillin/streptomycin, 4 mM glutamine and 1 mM sodium pyruvate. The H295R human adrenocortical carcinoma cell line was obtained from the American Type Culture Collection (ATCC, Manassas, USA) and cultured in DMEM/Ham's nutrient mixture F-12 (1:1, v/v) (Life Technologies, Zug, Switzerland), supplemented with 1% (v/v) ITS + Premix (BD Bioscience, Bedford, MA, USA), 2.5% (v/v) Nu-Serum (Lot: 2342913, BD Bioscience), 15 mM HEPES buffer and 1% (v/v) penicillin-streptomycin (Sigma-Aldrich).

2.4.3. CYP11B1 and CYP11B2 activity assays in hamster V79MZh cells

The virtual hits were examined for their inhibition of recombinant human CYP11B1 and CYP11B2 expressed in hamster V79MZh cells [44,45]. Approximately 8 million cells/well in 1 ml DMEM were grown in a 24-well plate for 24 h, followed by adding fresh medium (450 µl) containing ketoconazole at a concentration of 50 nM, test compound, or 100% ethanol. The non-selective CYP11B1 and CYP11B2 inhibitor ketoconazole was used as positive control [46]. The assay was started by adding 50 µl of the DOC mixture (78 µl of [^{3}H]-DOC (60 Ci/mmol), 124 µl of 0.2 mM DOC in 100% ethanol, 1098 µl of 100% ethanol) into each well. CYP11B1 cells were incubated for 15–60 min and CYP11B2 cells for 50–120 min. The incubation time depended on the conversion of DOC to corticosterone in negative control samples to reach a conversion of 15–30%. The assay was stopped by transferring the reaction mixture into a plastic tube containing ethyl acetate (500 µl) at 4 °C. Samples were mixed (10 min) and centrifuged (12,500 rpm, 5 min, 4 °C). The upper organic layer (450 µl) was separated into a fresh tube and dried using a speedVac vacuum centrifuge. The dried steroids were re-dissolved in methanol/water (65/35, v/v) solution (40 µl) and analyzed by reverse phase radio-HPLC using the Nucleodur C18ec column [44,45] and an Agilent 1200 HLPC system. Steroids were eluted under isocratic conditions using 0.1% trifluoroacetic acid (TFA), methanol (65%)/water at a flow rate of 0.6 ml/min and a pressure of about 25 MPa. For each analysis 10 µl were injected by an Agilent 1100 autosampler cooled to 4 °C. The product [^{3}H]-corticosterone and the substrate [^{3}H]-DOC were eluted at 3.4 and 5.0 min, respectively. The HPLC chromatogram was integrated by using the ChemStation software (Agilent). The conversion of DOC to corticosterone was determined by peak areas of the chromatogram. The inhibition was calculated by using the reduced substrate conversion caused by the inhibitor.

2.4.4. CYP17A1 activity assay

Recombinant human CYP17A1 was expressed in *E.coli* and the prepared bacterial membrane pellet was re-suspended in phosphate buffer (50 mM, pH 7.4, 1 mM $MgCl_2$, 0.1 mM EDTA, and 0.1 mM dithiothreitol) with 20% glycerol as described [47,48]. The enzyme activity was measured as follows: A solution containing phosphate buffer (140 µl), NADPH regeneration system (50 µl) (12.5 µl of 10 mM $NADP^+$, 25 µl of 100 mM glucose-6-phosphate, and 12.5 µl of 2.5 U glucose-6-phosphate dehydrogenase, all prepared in phosphate buffer), inhibitor solution (5 µl in DMSO), and radiolabeled progesterone (5 µl) (63.3 µl of [^{3}H]-progesterone (99.1 Ci/mmol), 125 µl of 10 mM progesterone in methanol, 811.7 µl of methanol) was pre-incubated (37 °C, 5 min). The reaction was started by adding CYP17A1 (1:4 dilution in phosphate buffer, 50 µl, approx. 1 mg) and the mixture was incubated (37 °C, 30 min) in a water bath. The reaction was stopped by adding HCl (50 µl, 1 N). Ethyl acetate (1 ml) was added to extract the steroids and the mixture was vortexed (10 min) and centrifuged (12,500 rpm, 5 min, 4 °C). The steroid layer (900 µl) was washed with phosphate buffer (500 µl, as above and 50 µl of 1 N HCl), shook (10 min), and centrifuged (12,500 rpm, 5 min, 4 °C). The washed steroid layer (800 µl) was collected in fresh plastic tubes and dried using a SpeedVac vacuum centrifuge. The dried steroids were dissolved in methanol (40 µl) and analyzed by radio-HPLC [44,45]. Negative control wells were supplemented with DMSO (5 µl) and positive control wells with abiraterone (5 µl, 100 nM in DMSO) and ketoconazole (5 µl, 4 µM in DMSO) [47]. Steroids were separated by HPLC and eluted under isocratic conditions by using 0.1% TFA, methanol (72%)/water at a flow rate of 0.6 ml/min and a pressure of 23 MPa. The substrate [^{3}H]-progesterone was eluted at 4.4 min. The hydroxylation by CYP17A1 produced 17α-hydroxyprogesterone and 16α-hydroxyprogesterone (byproduct), which were eluted at 3.0 min and 2.2 min, respectively. The HPLC peaks were integrated by using Agilent ChemStation software and the inhibition was calculated.

2.4.5. Steroidogenesis assay in H295R cells

The H295R steroidogenesis assay was conducted according to the OECD Test No. 456 guidelines (OECD, 2011), with some modifications [49]. Briefly, cells at passages between 5 and 10 were seeded in 24-well plates at a density of 200,000 cells/ml of complete medium. Following a 24 h acclimation period, the medium was replaced with fresh medium containing 0.3 µM torcetrapib and either test or reference compound. Each plate contained medium controls and DMSO (0.1% v/v) vehicle control. Torcetrapib (0.3 µM) was used as a control to stimulate and etomidate (1 µM) to inhibit corticosteroid production. Cells were incubated for 48 h, followed by a collection of culture supernatants and freezing at −20 °C until further analysis by ultra-high performance liquid chromatography-tandem mass spectrometry (UHPLC-MS/MS). Steroid profiles were only assessed from treatments showing no cytotoxic effects.

2.4.6. Cell viability assay in H295R cells

Cytotoxic effects of compounds were evaluated by the CellTiter-Glo® Luminescent Cell Viability Assay (Promega, Madison, WI, USA). Briefly, H295R cells were seeded in 96-well plates (30,000 cells/100 µl complete medium). The medium was replaced 24 h later by fresh medium containing 0.3 µM torcetrapib and the compound of interest at a concentration between 3.3 and 10 µM with the exception of etomidate, where 1 µM was the highest concentration tested. After 48 h of exposure, cells were examined under the microscope to check for morphological changes, followed by a 30 min equilibration period at room temperature. CellTiter-Glo® Reagent (100 µl) was added and cells lyzed for 2 min with shaking. The plates were incubated at room temperature for another 10 min to stabilize the luminescent signal, which was recorded at 470 nm using a SpectraMax L microplate reader (Molecular Devices, Sunnyvale, CA, USA). Control wells containing complete medium served as a value for background luminescence. The cell viability test was performed two times independently with technical triplicates.

2.4.7. Targeted steroid quantification and data analysis

Eight major adrenal steroids, *i.e.* androstenedione, progesterone, 17α-hydroxyprogesterone, DOC, corticosterone, aldosterone, 11-deoxycortisol, and cortisol were simultaneously analyzed in supernatants from treated H295R cells using UHPLC-MS/MS as described earlier, with minor modifications [50]. Briefly, 100 µl of protein precipitation solution (0.8 M zinc sulfate in water/methanol 50/50, v/v) supplemented with deuterium-labeled aldosterone, corticosterone and androstenedione as internal standards were added to 1 ml cell supernatant. Samples were incubated for 10 min at 4 °C in a thermoshaker, centrifuged for 10 min at 16,000 × g at 4 °C, and supernatants (950 µl) were transferred to Oasis HLB 1 cc solid-phase extraction (SPE) cartridges (30 mg, 30 µm particle size, Waters, Massachusetts, USA), preconditioned with 1 ml methanol and 1 ml Milli-Q water. The columns were washed twice with 1 ml of water and once with 1 ml of methanol/water (10/90, v/v). Steroids were eluted by methanol (two times with 0.5 ml), followed by evaporation of solvent at 35 °C using a Genevac EZ-2 plus evaporator (Genevac, Suffolk, UK) and reconstitution in 25 µl of methanol. Steroids were separated and quantified by UHPLC-MS/MS on an Agilent 1290 UHPLC connected to an Agilent 6490 triple quadrupole mass spectrometer equipped with a jet-stream electrospray ionization source. A reverse-phase column (Waters Acquity UPLC BEH C18, 1.7 µm, 2.1 × 150 mm) and a mobile phase A and B, consisting of water-acetonitrile-formic acid (95/5/0.1; v/v/v) and (5/95/0.1; v/v/v), respectively, were used for steroid separation. Data were acquired and analyzed using Mass Hunter software version B.09.00 (Agilent Technologies). Steroid concentrations were calculated in proportion to the mean steroid levels of the torcetrapib control to obtain the normalized data. Further computational analysis was performed in GraphPad Prism version 5.04. To visualize the changes in steroid profiles, the relative steroid concentrations were plotted as mean ± SD.

Four parameters log-logistic curves were fitted (data not shown) and IC_{50} values were calculated using a non-linear regression analysis.

2.5. Molecular docking

Molecular docking has been successfully used to predict binding modes of active fungicides after predictive pharmacophore-based virtual screening [51]. Molecular docking was performed after the biological testing to estimate the potential binding pose of biologically active hits. The crystal structure of human CYP11B2 in complex with fadrozole (Protein Data Bank entry 4FDH) was used for this purpose [52] because of its good resolution (2.71 Å) and because an azole-based inhibitor was co-crystallized. Also our active hits contained a terminal nitrogen-containig aromatic ring as well as they were similar in size compared to fadrozole. Therefore, we expected the binding site to have a conformation suitable to bind this kind of molecules.

The docking calculations were performed using GOLD software version 5.2 (Cambridge Crystallographic Data Centre, Cambridge, UK) [53,54]. The binding pocket was defined as a sphere with a 6 Å radius around the co-crystallized ligand. In order to obtain the optimum docking orientations, the default docking template for CYP450 *Goldscore-P450* was used. Goldscore was applied as a scoring function to predict the binding position of the docked ligands by considering H-bonding energy, Van der Waals energy, metal interaction and ligand torsion strain [55]. Interactions between the ligands and the CYP11B2 binding pocket found by the docking calculations were evaluated using LigandScout 3.12 (inte:ligand GmbH, Vienna, Austria) [56]. In order to investigate whether the original binding orientation of the co-crystallized ligand could be restored, fadrozole was deleted from the binding site and re-docked. The applied docking settings could be validated with a RMSD value of 0.111 Å.

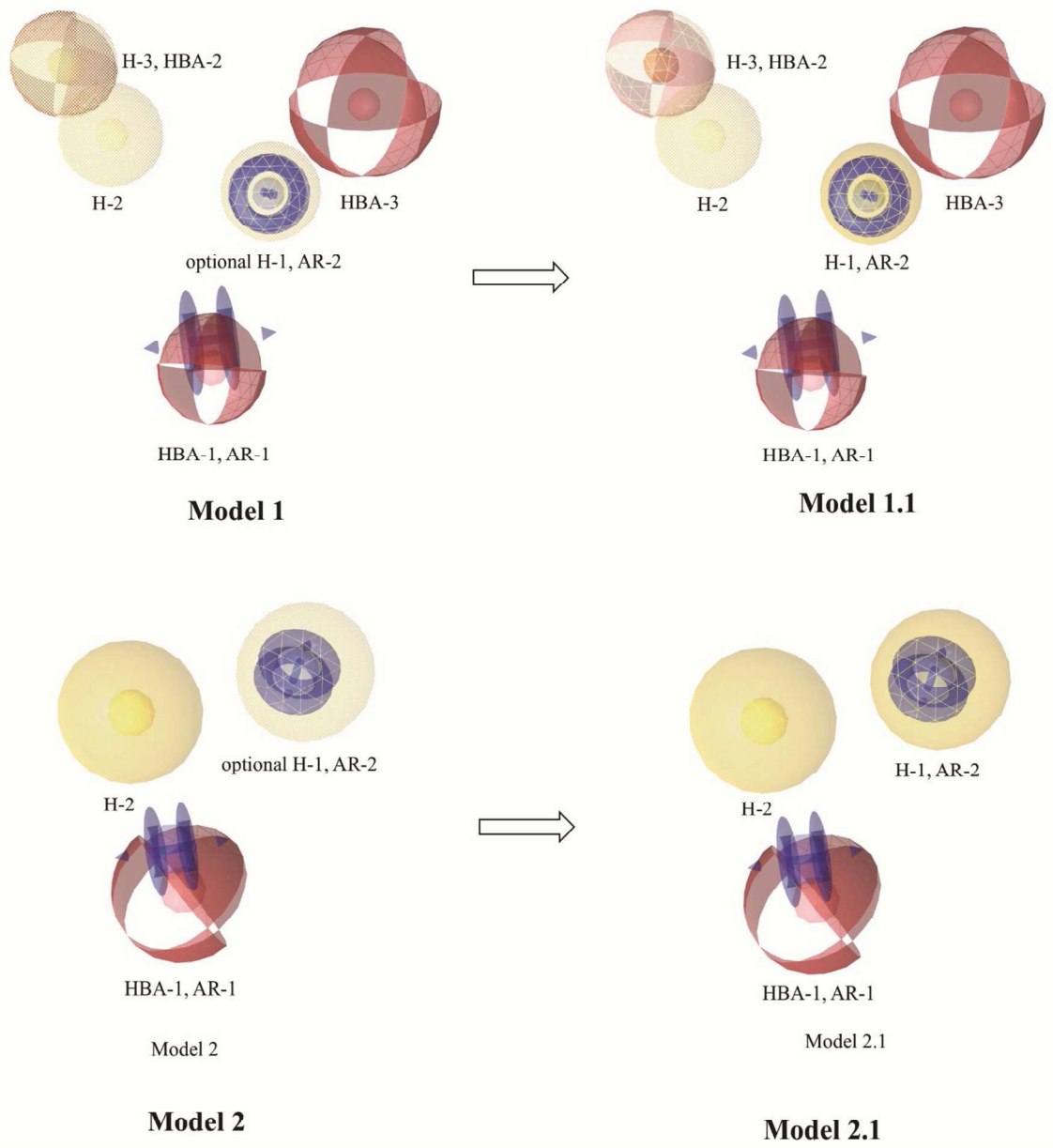

Fig. 3. Modification of previously published models 1 and 2. The H-1 feature of both model 1 and 2 was made obligatory. The pharmacophore features are color-coded. Yellow spheres represent hydrophobic interactions, blue rings signify AR features, HBA features are shown as red spheres. Dotted spheres represent the optional features. The modified model 1.1 had a total of 8 features and 47 XVOLs (not shown). Model 2.1 had 5 features and 33 XVOLs (not shown).

3. Results

3.1. Modification of pharmacophore models and virtual screening

The previously validated pharmacophore models (Fig. 3) trained with CYP11B1 and CYP11B2 inhibitors [36] were modified based on the biological test results of their evaluation. In this former study, we found 5 active compounds out of 24 tested virtual hits. Model 1 found 2 active substances and model 2 found 4, among them one consensus hit. The refinement aimed at finding more actives and fewer inactive compounds, respectively. All biologically active hits among the tested hits from previous study were fitted and overlaid into the models. We then visually analyzed, which features were mapped by all active compounds and which weren't. Based on this, the feature modification was done. The previously optional hydrophobic feature H-1 was defined from optional to mandatory, because all active compounds mapped on it. The HBA-2 and H-3 features of model 1.1 were marked as disabled because some active compounds failed to map these features accordingly. This change resulted in a higher hit rate (model 1.1) and higher model restrictivity (model 2.1, Table 2): The modification of model 1 improved sensitivity and yield of actives from 0.40 to 0.75 and 0.036 to 0.068, respectively, by modified model 1.1. The modification of model 2 increased the specificity and accuracy from 0.53 to 0.95 and 0.66 to 0.85, respectively, by modified model 2.1 (Table 2).

The modified pharmacophore models (Fig. 3) were then used to search for novel xenobiotics inhibiting CYP11B1 and CYP11B2. Both models were employed for the VS of APs, EUC, EDCs, EUFCM, EUFFA, INCI, ICs, SA, and DB databases, respectively (Table 3). The VS was performed in LigandScout 3.12 [56]. In total, the VS resulted in 213 unique hits, including 198 hits found by the more sensitive model 1.1 and 18 hits found by the more restrictive model 2.1, respectively (Table 3). Finally, 25 virtual hits were selected for biological testing based on one of three criteria: High pharmacophore fit value, commonly used compounds, and consensus hits of both models.

3.2. Inhibition of recombinant CYP11B1 and CYP11B2 expressed in hamster V79MHz cells

The selected 25 virtual hits were analyzed in an *in vitro* overexpression cell system [44,45] for their potential to inhibit CYP11B1 and CYP11B2. Initially, all of the selected virtual hits from both modified pharmacophore models 1.1 and 2.1 were tested against both CYP11B1 and CYP11B2 enzymes at a concentration of 10 µM. In this screening run, epoxiconazole, flurprimidol, ancymidol, and 1,1-thiocarbonyldiimidazole (Fig. 4) displayed an inhibitory activity on CYP11B1 and CYP11B2 of more than 50% (Table 4). Epoxiconazole was found to be a potent inhibitor of both CYP11B1 and CYP11B2 with IC_{50} values of 623 and 113 nM, respectively. The IC_{50} values for CYP11B1 inhibition of flurprimidol, ancymidol, and 1,1-thiocarbonyldiimidazole were 796 nM, 1.30 µM, and 8.2 µM, respectively; and for CYP11B2 939 nM, 2.40 µM, and 14 µM, respectively (Table 4). Ozagrel HCl was a very weak inhibitor of CYP11B1 and CYP11B2 and therefore its IC_{50} value was not determined. Epoxiconazole, ancymidol, flurprimidol, and ozagrel HCl were found by model 1.1, 1,1-thiocarbonyldiimidazole was predicted by model 2.1, and ancymidol and flurprimidol were consensus hits found by both models.

Table 2
Qualitative analysis of performance of modified pharmacophore models based on biological testing.

Quality metrices	Previously validated models [36]		Modified models	
	Model 1	Model 2	Model 1.1	Model 2.1
True positive	2/5	4/5	3/4	3/4
False positive	9/19	9/19	20/21	1/21
True negative	10/19	10/19	1/21	20/21
False negative	3/5	1/5	1/4	1/4
Sensitivity	0.4	0.8	0.75	0.75
Specificity	0.53	0.53	0.05	0.95
Yield of active	0.036	0.053	0.068	0.032
Accuracy	0.46	0.66	0.40	0.85
Individual success rate	18.18 %	30.77 %	14.29 %	75 %
Overall success rate	21 %		16 %	

Table 3
VS details of xenobiotic chemicals databases.

Database name	Entries	Calculated entries	Hits found by model 1	Hits found by model 1.1	Hits found by model 2	Hits found by model 2.1
APs	7,221	7,206	18	29	5	5
EUC	16,948	16,265	6	12	0	0
EDCs	76,677	76,150	92	146	10	10
EUFCM	2,105	1,980	0	6	0	0
EUFFA	3,733	3,717	0	0	0	0
INCI	5,622	5,298	1	6	0	0
ICs	2,556	2,531	2	9	0	0
SA	73,003	41,041	31	76	7	7
DB	1,526	1,526	5	7	2	2
Total	189,391	155,714	155	291	24	24
Unique hits			133	198	18	18

3.3. Inhibition of recombinant CYP17A1 in a cell-free assay

CYP17A1 hydroxylase activity was measured using progesterone as a substrate. Epoxiconazole and ancymidol were very weak inhibitors of CYP17A1, while flurprimidol, 1,1-thiocarbonyldiimidazole, and ozagrel HCl were almost inactive and showed only very weak activity if any.

3.4. Inhibition of corticosteroid synthesis by the selected hits in H295R cells

In order to characterize the potential of the three selected hits epoxiconazole, flurprimidol and ancymidol to interfere with adrenal steroidogenesis, a modified version of the OECD test 456 using the human adrenal adenocarcinoma cell line H295R was employed [49,57]. For facilitated detection of xenobiotics inhibiting corticosteroid production, cells were stimulated with torcetrapib and treated with the compounds for 48 h. Torcetrapib is a potent inducer of CYP11B1 and CYP11B2 and stimulated the production of the CYP11B1/CYP11B2 products aldosterone, corticosterone, and cortisol, which was most prominent for aldosterone with an approximately 14-fold increase (Supplementary Fig. S4) [58]. The reference compound etomidate blocked steroidogenesis almost completely as expected [49,58]. The effects of epoxiconazole, flurprimidol and ancymidol were normalized to the steroid levels of torcetrapib treated cells. Whereas flurprimidol showed weak inhibition of CYP11B1 and CYP11B2 with effects at 10 µM on aldosterone, corticosterone and cortisol (Supplementary Fig. S5), ancymidol was a very weak inhibitor with only aldosterone being more than 1.5-fold decreased at 10 µM (Supplementary Fig. S6). In contrast, epoxiconazole was found to be a potent steroidogenesis inhibitor with evidence for most pronounced inhibition of CYP11B2 (seen at the lowest concentration), inhibition of CYP11B2 and CYP11B1 at a medium concentration, and inhibition of CYP11B2, CYP11B1 and CYP17A1 at a high concentration (Fig. 5). CYP21A2, CYP11A1 and 3β-HSD2 seemed not to be inhibited at any concentration tested based on the steroid profile observed at the highest epoxiconazole concentration. Considering cortisol and aldosterone production as markers for CYP11B1 and CYP11B2, estimated IC_{50} values of 610 ± 139 and 320 ± 54 nM, respectively, were obtained (Fig. 6).

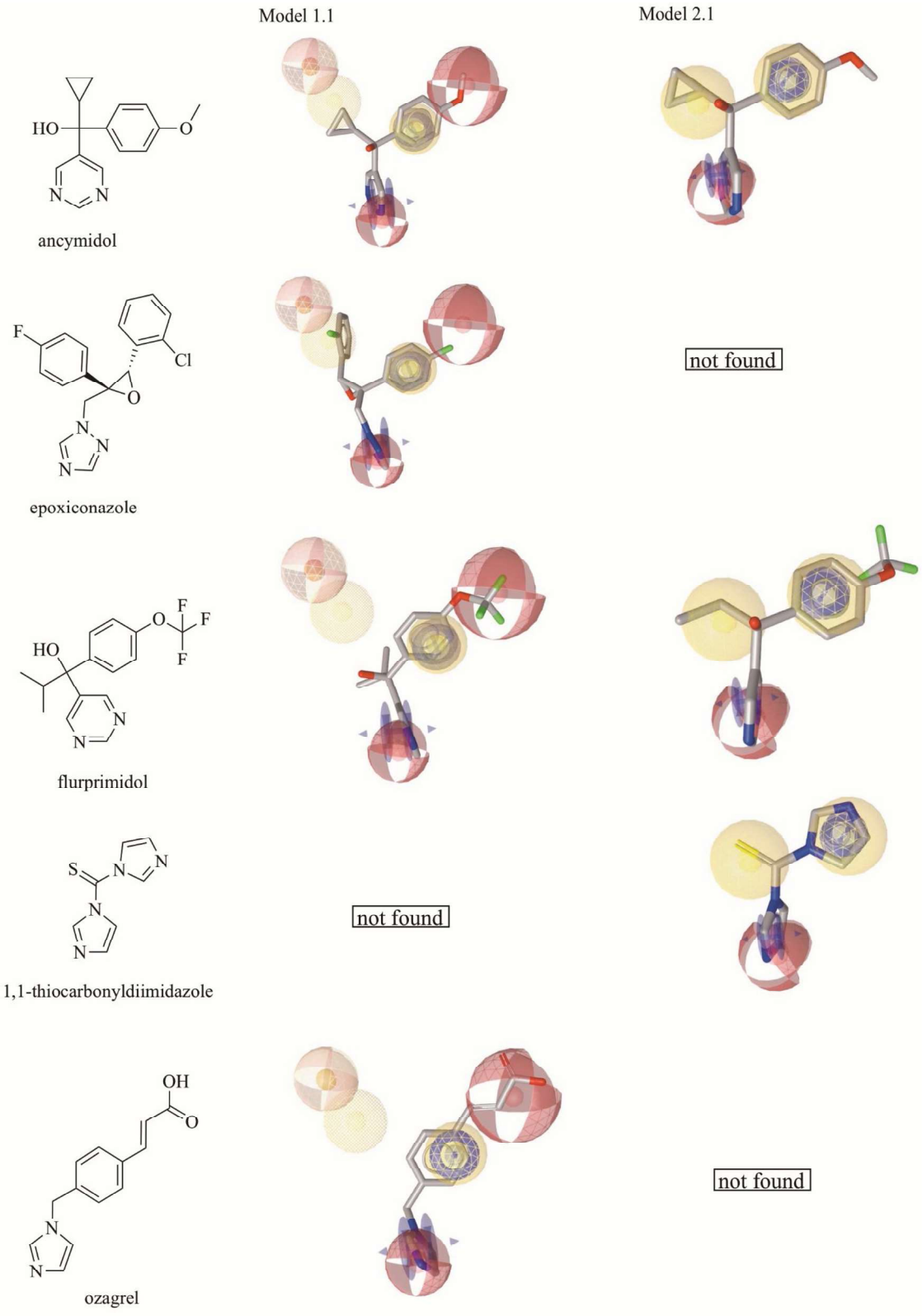

Fig. 4. Newly identified xenobiotics inhibiting CYP11B1 and CYP11B2 along with their fittings in the modified pharmacophore models.

3.5. *Possible binding pose predictions*

The proposed binding poses of the novel inhibitors were calculated using GOLD 5.2 [53,54]. In 2014, Yin et al. proposed that the binding affinity of CYP11B2 is highly dependent on the coordination geometry between the iron of the heme and the nitrogen of the aromatic ring of the inhibitor [59]. In addition to this interaction, the strength of inhibition of CYP enzymes varies with the hydrogen bond and hydrophobic interactions [60,61]. In the present study, ancymidol was found as a moderate novel inhibitor of CYP11B1 and CYP11B2. The docked

Table 4
Inhibition of CYP11B1, CYP11B2, CYP17A1, and CYP19A1 by newly identified xenobiotics.

Target enzyme		Ancymidol	Epoxiconazole	Flurprimidol	1,1-thiocarbonyl-diimidazole	Ozagrel HCl
CYP11B1[a,i]	IC_{50} (nM)[b]	1298	623	796	8208	32%[h]
	SD[c] (nM)	167	93	327	2047	
	CI LL[d] (nM)	884	392	−17	3124	
	CI UL[e] (nM)	1712	853	1608	13293	
CYP11B2[a,i]	IC_{50} (nM)[b]	2404	113	939	14021	11%[h]
	SD[c] (nM)	673	21	153	3192	
	CI LL[d] (nM)	733	61	558	6092	
	CI UL[e] (nM)	4075	116	1320	21950	
hCYP17 inhibition at 10 µM[f]		18%	13%	7%	4%	6%
Found by model		both	1.1	both	2.1	1.1
Database name		Aps	Aps	SA, Aps, EDCs	SA, EDCs	EDCs

nd = not determined.
[a] recombinant CYP11B1 and CYP11B2 enzymes expressed in hamster fibroblast cells.
[b] mean value of at least three experiments, substrate 0.10 µM 11-deoxycorticosterone.
[c] standard deviation.
[d] 95% confidence interval lower limit.
[e] 95% confidence interval upper limit.
[f] recombinant CYP17A1 enzyme expressed in Escherichia coli, substrate 25 µM progesterone, percentage inhibition.
[h] inhibition was measured at 10 µM concentration.
[i] ketoconazole at 50 nM was used as positive control, mean inhibition of CYP11B1 and CYP11B2 was 39% and 58%, respectively. An inhibition review by positive control is given in Table S2.

		progestins		mineralocorticoids			glucocorticoids		adrenal androgens
	treatment \ homone	progesterone	17α-hydroxy-progesterone	11-deoxy-corticosterone	corticosterone	aldosterone	11-deoxycortisol	cortisol	androstenedione
RC	torcetrapib 0.3 µM	1.00 ± 0.10	1.00 ± 0.06	1.00 ± 0.08	1.00 ± 0.05	1.00 ± 0.10	1.00 ± 0.05	1.00 ± 0.12	1.00 ± 0.07
	etomidate 1 µM + 0.3 µM tor	0.07 ± 0.04	0.07 ± 0.04	0.08 ± 0.02	0.00 ± 0.00	n.d.	0.09 ± 0.01	0.04 ± 0.03	0.08 ± 0.02
TC	epoxiconazole 3.33 µM + 0.3 µM tor	0.67 ± 0.18	0.51 ± 0.07	0.93 ± 0.14	0.19 ± 0.03	0.09 ± 0.02	0.58 ± 0.05	0.11 ± 0.03	0.61 ± 0.11
	epoxiconazole 1.11 µM + 0.3 µM tor	0.67 ± 0.15	0.70 ± 0.06	0.95 ± 0.09	0.43 ± 0.06	0.21 ± 0.03	0.91 ± 0.08	0.28 ± 0.06	0.95 ± 0.09
	epoxiconazole 0.37 µM + 0.3 µM tor	0.76 ± 0.14	0.86 ± 0.08	0.98 ± 0.10	0.74 ± 0.06	0.47 ± 0.04	1.10 ± 0.05	0.74 ± 0.07	1.10 ± 0.10

< 1.5 fold change/tor

Fig. 5. Effect of epoxiconazole on the torcetrapib-stimulated H295R steroid profile. H295R cells were treated for 48 h with 0.3 µM torcetrapib (reference stimulating compound) and either 0.1% DMSO (solvent control) or the inhibitors at the concentrations indicated. Steroids were quantified by UHPLC-MS/MS. Data were obtained from four independent experiments, each performed in duplicates, and normalized to the respective steroid concentration in torcetrapib treated cells. Fold change expressed as mean ± SD is depicted. Values are shown in a color code: green represents > 1.5-fold down regulation compared with torcetrapib control. RC: reference compound; TC: test compound.

orientation of ancymidol showed the presence of metal binding interaction of the sp^2-hybridized pyrimidine-nitrogen with the iron of the heme. The angle of this interaction was 106.8°. The amino acid side chains that were involved in the hydrophobic interactions included Phe130, The318, Val378, Phe487, and Ile488 (Fig. 7). The docked pose of the most potent hit, the fungicide epoxiconazole, showed an iron-binding interaction of the sp^2-hybridized triazole nitrogen with the iron of the heme at the binding site at an angle of 98.26° (Fig. 7). This interaction is probably crucial for the inhibition of the catalytic process of the target enzyme. It also showed multiple hydrophobic interactions with Phe130, Leu227, Met230, Phe231, Ala313, Val316, Thr318, Val378, Phe487, and Ile488, providing an explanation for the potent inhibition. The docked pose of flurprimidol showed the crucial iron binding interaction of the sp^2-hybridized pyrimidine-nitrogen with the iron of the heme at the binding site (Fig. 7). The interaction angle was 95.17°. It also showed several hydrophobic contacts with Phe130, Thr318, Phe381, Val378, Phe487, and Ile488.

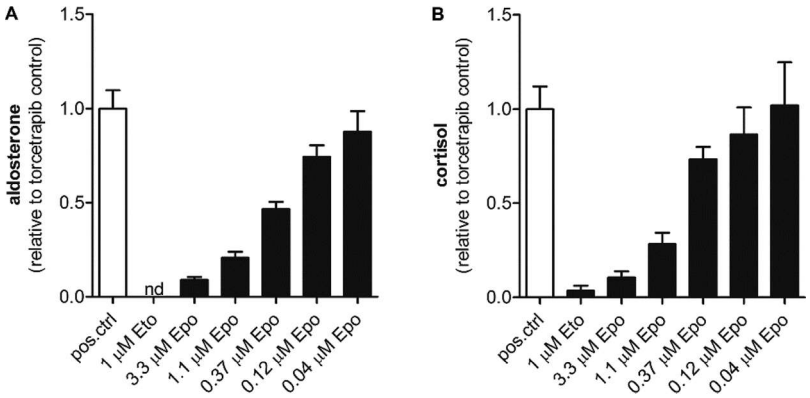

Fig. 6. Concentration-dependence of epoxiconazole-dependent inhibition of aldosterone and cortisol production in H295R cells. H295R cells were stimulated with torcetrapib and treated with epoxiconazole at different concentrations for 48 h, followed by quantification of steroids in the cell culture supernatants. Data obtained from four independent experiments, each performed in duplicates are expressed as fold change relative to the torcetrapib control and represent mean ± SD. A, aldosterone production; B, cortisol production. Etomidate served as a reference inhibitor. Eto, etomidate; Epo, epoxiconazole; pos. crtl, positive control torcetrapib only.

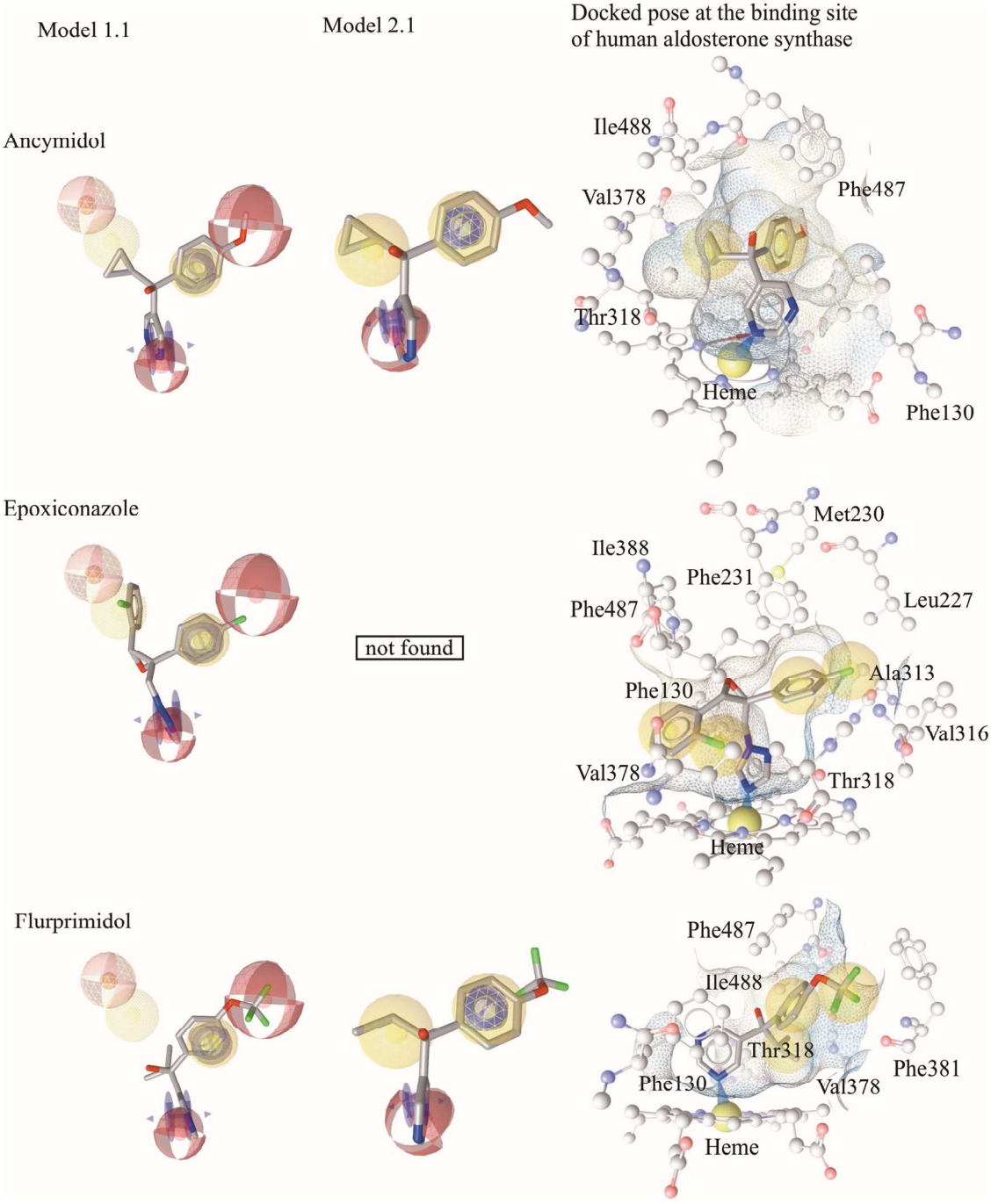

Fig. 7. Predicted binding modes of the three selected hits and their fittings in the modified pharmacophore models. Ancymidol, epoxiconazole, and flurprimidol in the binding site of human CYP11B2 (PDB code = 4FDH). The hydrophobic contacts and metal binding interactions of ancymidol corresponded to its fitting in both of the modified pharmacophore models. Epoxiconzole mapped the aromatic ring interaction, HBA, and two hydrophobic contact points in the modified model 1.1. It showed two additional hydrophobic interactions at the binding site in the proposed docked pose. Flurprimidol mapped both modified pharmacophore models. Its proposed binding pose showed the similar pharmacophore points and an additional hydrophobic point at the trifluormethoxy substituent. Yellow spheres denote the hydrophobic interactions, red spheres show the HBA feature, blue rings represent the aromatic ring interaction, and blue wedge show metal binding interaction. The wireframe network represents the surface of the binding pocket and is color-coded, aggregated lipophilicity is shown in grey/ hydrophilicity in blue.

4. Discussion

In order to maintain high pharmacophore quality, a regular analysis of performance of models is very important. In this study, a model refinement was performed using new biological data generated in the course of the validation of the models [37]. Not only had the quality metrics of the models improved in this process, but also this refinement enabled the identification of epoxiconazole as potential endocrine disruptor, because our initial models would have not reported it as a virtual hit. However, structural bias in the hit lists was identified due to the lack of structurally diverse data for the inhibition of human CYP11B1 and CYP11B2. Most of the known CYP11B1 and CYP11B2 inhibitors have an aromatic nitrogen. So if a model finds this scaffold, it usually recognizes all of the known imidazole/pyrimidine-based CYP11B1 and CYP11B2 inhibitors. Epoxiconazole structurally belongs to the highly similar class of triazoles. In order to identify chemically

novel hits, a less restrictive model with a probably higher false positive hit rate would have to be applied. Individually, model 1 was less sensitive in our previous study and we tried to improve the sensitivity to find more active hits. Although the overall accuracy deteriorated that way, we wanted to have this kind of general model for this type of study, which is anti-target screening. The discovery of the most potent hit epoxiconazole by model 1.1 proved us right in this respect (Table 2).

In summary, the *in silico* approach applied turned out to be useful for the identification of novel inhibitors. However, it needs to be noticed that the false negative rate of the ligand-based pharmacophore models used is 25%, meaning that in our validation database 25% of active compounds were mistaken for inactive compounds by the models. Thus, a limitation of this strategy is that it cannot be applied to exclude CYP11B inhibitory effects of chemicals in a virtual screening. Nevertheless, the models are very useful to identify novel inhibitors for prioritization of test compounds from environmental chemical databases. Based on these results, further investigations on the newly identified compounds and of structurally related compounds can be planned.

In a virtual screening - apart from the missing of some active compounds - there is the issue of incorrectly classifying inactive compounds as such. However, there are several reasons for the inactivity of compounds selected in the initial CYP11B1 and CYP11B2 activity assay, using intact hamster V79MHz cells (Fig. S3). Assays using intact cells have the limitation that a given compound does not have direct access to the target of interest due to inappropriate uptake or efflux by transport proteins [62]. The development of cell-free assays would greatly enhance the analysis of the performance of the *in silico* methods. However, cell-based assays have other advantages, for example, chemicals acting at allosteric sites or altering posttranslational modifications or gene expression can potentially be detected in intact cell assays.

The further biological evaluation of the three most potent hits epoxiconazole, flurprimidol and ancymidol using torcetrapib-stimulated H295R cells supported the observations from the initial screening. Furthermore, the simultaneous quantification of major adrenal steroids proved useful in case of epoxiconazole to demonstrate that additional CYP enzymes were inhibited at increasing concentrations in the order CYP11B2 > CYP11B1 > CYP17A1, without evidence for interference with other key steroidogenic enzymes such as CYP11A1, CYP21A2 and 3β-HSD2. The fact that epoxiconazole had almost no activity in the cell-free assay (13% inhibition at 10 µM), but showed inhibition of adrenal androgen production in the H295R assay at a concentration of 3.3 µM, indicates inhibition of CYP17A1 17,20-lyase activity rather than 17α-hydroxylase activity. Thus, the results obtained in torcetrapib-stimulated H295R cells provided preliminary mechanistic information on the concentration-dependent mode-of-action of epoxiconazole-mediated disruption of steroidogenesis. The modified version of the OECD test 456 constitutes a suitable *in vitro* model for studying the effects of CYP11B1 and CYP11B2 inhibitors.

Ancymidol and flurprimidol are used as plant growth inhibitors in greenhouse crops. Animal experimentation showed reproductive, developmental and acute toxicity of the two compounds [63,64], but there are currently no studies on potential toxicity in human. Based on the observed IC_{50} values of about 1 µM of flurprimidol and ancymidol for CYP11B1 and CYP11B2, it is unlikely that such concentrations can be reached in the general population upon exposure to contaminated products and that inhibition of CYP11B enzymes would contribute to their toxicity.

Epoxiconazole is widely used as an antifungal agent in agriculture and is currently listed in the approved EU pesticides (Reg. (EU) No. 1107/2009) database [65]. It was developed to interfere with the fungal plasma membrane synthesis by inhibiting the ergosterol producing 14α-demethylase (CYP51) [66]. Besides inhibiting CYP51, azole fungicides are known to affect many other CYPs, including those involved in steroidogenesis [67–69]. For these reasons, the agricultural application of epoxiconazole as well as the consumption of epoxiconazole-contaminated food raises the potential of endocrine disruption [70].

Studies in rats provided evidence for potential endocrine disrupting effects of epoxiconazole; however, the animals were treated with relatively high doses [66,71]. Treatment of rats for four weeks with 3000 ppm epoxiconazole led to decreased estradiol as well as decreased corticosterone and increased ACTH levels, in line with an inhibition of CYP19 and CYP11B1 [70]. Increased adrenal weight in the treated animals provided further evidence for an inhibition of adrenal steroidogenesis. Additionally, in females reduced aldosterone levels were reported, in line with an inhibition of CYP11B2. To further address possible interference with estrogen production, several cell-based studies focused on the evaluation of epoxiconazole-mediated effects on CYP19A1 (aromatase) [67,72,73], with a reported IC_{50} of 1.44 µM [74]. To our knowledge, the present study is the first to address an effect of epoxiconazole on CYP11B enzymes (with an IC_{50} for CYP11B2 being an order of magnitude lower than that for CYP19A1). Thus, future studies on potential corticosteroid-mediated effects upon epoxiconazole exposure should be performed.

There is currently no literature available describing the adverse effects associated with epoxiconazole exposure in humans. However, Chambers et al. estimated the human risk of epoxiconazole and concluded that based on the available knowledge (rodent and cell-based studies, anti-estrogenic effects) and anticipated human exposure the safety margin for reproductive effects would be about three orders of magnitude [70]. Therefore, even when considering an approximately 10-fold higher potency of epoxiconazole to inhibit CYP11B2 compared with CYP19A1, the safety margin for adverse cardiovascular and metabolic effects caused by inhibition of the CYP11B enzymes would still be estimated to be one or two orders of magnitude. Thus, for the general population, exposure to epoxiconazole by consumption of treated products seems to be of little toxicological concern; however, it could contribute to effects in mixtures and in situations of occupational exposure where higher levels can be reached.

5. Conclusion

This study demonstrated that *in silico/in vitro* activity profiling is a useful approach for predicting novel inhibitors. Epoxiconazole was identified as a potent CYP11B1 and CYP11B2 inhibitor; flurprimidol, ancymidol, and 1,1-thiocarbonyldiimidazole were less potent. Epoxiconazole contains a triazole ring, ancymidol, and flurprimidol a pyrimidine ring, and 1,1-thiocarbonyldiimidazole two imidazole rings. This study reinforces the importance of aromatic nitrogen for the inhibition of CYP11B1 and CYP11B2. The use of torcetrapib-stimulated H295R cells and the simultaneous quantification by mass spectrometry-based methods of several steroids not only allowed detecting disturbances of steroidogenesis but also provided additional insight into the mode of interference by epoxiconazole. Further research needs to address human exposure: epoxiconazole concentrations to inhibit CYP11B1 and CYP11B2 are unlikely reached through environmental exposure in the general population; however, a contribution to effects of mixtures and of occupational exposure needs to be investigated.

Author contributions

Each author contributed to this project. DS planned the study and supervised the molecular modeling. MA, TK, VT, and WW were responsible for the computational part. VT did modification of pharmacophore models and helped in the VS and selection of hits. MA performed VS and selection of hits for biological testing under the supervision of DS. MA did *in vitro* analysis in cooperation with JH and RH. AO and MP planned the biological analyses using H295R cells and analysed and interpreted the data. MP performed biological testing. All authors analysed the data, were involved in the preparation of the manuscript and approved the final version.

Conflict of interest

The authors declare that the research was conducted in the absence of any commercial or financial relationships that could be construed as a potential conflict of interest.

Acknowledgement

This study was funded by the Austrian Science Fund (FWF), project "safety of environmental chemicals" (P26782) and a Young Talents Grants from the University of Innsbruck. M.A. is grateful to the Standortagentur Tirol for providing financial support *via* the ERASMUS$^+$ program for doing *in vitro* assays at the Helmholtz Institute for Pharmaceutical Research in Saarland, Germany. D.S. is an Ingeborg Hochmair Professor at the University of Innsbruck. A.O. thanks the Swiss Centre for Applied Human Toxicology (SCAHT). We are thankful to InteLigand and OpenEye Inc. for providing academic software licenses for LigandScout and OMEGA, respectively. Many thanks to Bojan Lazic and Julia Kirchmair for generating the ICs and cosmetic ingredients database, respectively.

Appendix A. Supplementary data

Supplementary material related to this article can be found, in the online version, at doi:https://doi.org/10.1016/j.jsbmb.2019.04.007.

References

[1] L.J. Guillette Jr., Endocrine disrupting contaminants–beyond the dogma, Environ. Health Perspect. 114 (Suppl 1) (2006) 9–12.
[2] D.W. Singleton, S.A. Khan, Xenoestrogen exposure and mechanisms of endocrine disruption, Front. Biosci. 8 (2003) s110–118.
[3] S. De Coster, N. van Larebeke, Endocrine-disrupting chemicals: associated disorders and mechanisms of action, J. Environ. Public Health 2012 (2012) 52.
[4] F.P. Guengerich, Mechanisms of cytochrome P450 substrate oxidation: MiniReview, J. Biochem. Mol. Toxicol. 21 (2007) 163–168.
[5] C. Tsigos, G.P. Chrousos, Hypothalamic–pituitary–adrenal axis, neuroendocrine factors and stress, J. Psychosom. Res. 53 (2002) 865–871.
[6] P.W. Harvey, Adrenocortical endocrine disruption, J. Steroid Biochem. Mol. Biol. 155 (Part B) (2016) 199–206.
[7] K. Yanagibashi, C.H. Shackleton, P.F. Hall, Conversion of 11-deoxycorticosterone and corticosterone to aldosterone by cytochrome P-450 11 beta-/18-hydroxylase from porcine adrenal, J. Steroid Biochem. 29 (1988) 665–675.
[8] P.C. White, K.M. Curnow, L. Pascoe, Disorders of steroid 11β-Hydroxylase isozymes*, Endocr. Rev. 15 (1994) 421–438.
[9] G. de Simone, A.P. Tommaselli, R. Rossi, R. Valentino, R. Lauria, F. Scopacasa, G. Lombardi, Partial deficiency of adrenal 11-hydroxylase. A possible cause of primary hypertension, Hypertension (Dallas, Tex.: 1979) 7 (1985) 204–210.
[10] D. El-Maouche, W. Arlt, D.P. Merke, Congenital adrenal hyperplasia, Lancet 390 (2017) 2194–2210.
[11] A. Khattab, S. Haider, A. Kumar, S. Dhawan, D. Alam, R. Romero, J. Burns, D. Li, J. Estatico, S. Rahi, S. Fatima, A. Alzahrani, M. Hafez, N. Musa, M. Razzghy Azar, N. Khaloul, M. Gribaa, A. Saad, I.B. Charfeddine, B. Bilharinho de Mendonça, A. Belgorosky, K. Dumic, M. Dumic, J. Aisenberg, N. Kandemir, A. Alikasifoglu, A. Ozon, N. Gonc, T. Cheng, U. Kuhnle-Krahl, M. Cappa, P.-M. Holterhus, M.A. Nour, D. Pacaud, A. Holtzman, S. Li, M. Zaidi, T. Yuen, M.I. New, Clinical, genetic, and structural basis of congenital adrenal hyperplasia due to 11β-hydroxylase deficiency, Proc. Natl. Acad. Sci. U. S. A. 114 (2017) E1933–E1940.
[12] P.C. White, M.I. New, Molecular genetics of congenital adrenal hyperplasia, Baillieres Clin. Endocrinol. Metab. 2 (1988) 941–965.
[13] M. Lisurek, R. Bernhardt, Modulation of aldosterone and cortisol synthesis on the molecular level, Mol. Cell. Endocrinol. 215 (2004) 149–159.
[14] R.A. DeFronzo, Hyperkalemia and hyporeninemic hypoaldosteronism, Kidney Int. 17 (1980) 118–134.
[15] M. Peter, L. Fawaz, S.L. Drop, H.K. Visser, W.G. Sippell, Hereditary defect in biosynthesis of aldosterone: aldosterone synthase deficiency 1964-1997, J. Clin. Endocrinol. Metab. 82 (1997) 3525–3528.
[16] L. Pascoe, K.M. Curnow, L. Slutsker, A. Rosler, P.C. White, Mutations in the human CYP11B2 (aldosterone synthase) gene causing corticosterone methyloxidase II deficiency, Proc. Natl. Acad. Sci. U. S. A. 89 (1992) 4996–5000.
[17] Y. Mitsuuchi, T. Kawamoto, Y. Naiki, K. Miyahara, K. Toda, I. Kuribayashi, T. Orii, K. Yasuda, K. Miura, K. Nakao, et al., Congenitally defective aldosterone biosynthesis in humans: the involvement of point mutations of the P-450C18 gene (CYP11B2) in CMO II deficient patients, Biochem. Biophys. Res. Commun. 182 (1992) 974–979.
[18] N.V. Belkina, M. Lisurek, A.S. Ivanov, R. Bernhardt, Modelling of three-dimensional structures of cytochromes P450 11B1 and 11B2, J. Inorg. Biochem. 87 (2001) 197–207.
[19] M. Ayub, M.J. Levell, Inhibition of human adrenal steroidogenic enzymes in vitro by imidazole drugs including ketoconazole, J. Steroid Biochem. 32 (1989) 515–524.
[20] M. Johansson, C. Larsson, A. Bergman, B.O. Lund, Structure-activity relationship for inhibition of CYP11B1-dependent glucocorticoid synthesis in Y1 cells by aryl methyl sulfones, Pharmacol. Toxicol. 83 (1998) 225–230.
[21] M.K. Johansson, J.T. Sanderson, B.O. Lund, Effects of 3-MeSO2-DDE and some CYP inhibitors on glucocorticoid steroidogenesis in the H295R human adrenocortical carcinoma cell line, Toxicol. In Vitro 16 (2002) 113–121.
[22] Y. Xu, R.M.K. Yu, X. Zhang, M.B. Murphy, J.P. Giesy, M.H.W. Lam, P.K.S. Lam, R.S.S. Wu, H. Yu, Effects of PCBs and MeSO2–PCBs on adrenocortical steroidogenesis in H295R human adrenocortical carcinoma cells, Chemosphere 63 (2006) 772–784.
[23] J.P. Hinson, P.W. Raven, Effects of endocrine-disrupting chemicals on adrenal function, Best Pract. Res. Clin. Endocrinol. Metab. 20 (2006) 111–120.
[24] FDA, Endocrine disruption potential of drugs: nonclinical evaluation, Draft Guidance, Fed. Regist. 78 (183) (2013) 57859.
[25] P.W. Harvey, Adrenocortical endocrine disruption, J. Steroid Biochem. Mol. Biol. 155 (2016) 199–206.
[26] A. Vuorinen, A. Odermatt, D. Schuster, In silico methods in the discovery of endocrine disrupting chemicals, J. Steroid Biochem. Mol. Biol. 137 (2013) 18–26.
[27] T.M. Steindl, D. Schuster, G. Wolber, C. Laggner, T. Langer, High-throughput structure-based pharmacophore modelling as a basis for successful parallel virtual screening, J. Comput. Aided Mol. Des. 20 (2006) 703–715.
[28] K.R. Beck, T. Kaserer, D. Schuster, A. Odermatt, Virtual screening applications in short-chain dehydrogenase/reductase research, J. Steroid Biochem. Mol. Biol. 171 (2017) 157–177.
[29] T. Kaserer, K.R. Beck, M. Akram, A. Odermatt, D. Schuster, Pharmacophore models and pharmacophore-based virtual screening: concepts and applications exemplified on hydroxysteroid dehydrogenases, Molecules 20 (2015) 22799–22832.
[30] J. Kirchmair, S. Distinto, D. Schuster, G. Spitzer, T. Langer, G. Wolber, Enhancing drug discovery through in silico screening: strategies to increase true positives retrieval rates, Curr. Med. Chem. 15 (2008) 2040–2053.
[31] J. Bajorath, Integration of virtual and high-throughput screening, Nat. Rev. Drug Discov. 1 (2002) 882–894.
[32] S. Gobbi, Q. Hu, M. Negri, C. Zimmer, F. Belluti, A. Rampa, R.W. Hartmann, A. Bisi, Modulation of cytochromes P450 with xanthone-based molecules: from aromatase to aldosterone synthase and steroid 11β-Hydroxylase inhibition, J. Med. Chem. 56 (2013) 1723–1729.
[33] S. Lucas, R. Heim, M. Negri, I. Antes, C. Ries, K.E. Schewe, A. Bisi, S. Gobbi, R.W. Hartmann, Novel aldosterone synthase inhibitors with extended carbocyclic skeleton by a combined ligand-based and structure-based drug design approach, J. Med. Chem. 51 (2008) 6138–6149.
[34] S. Lucas, M. Negri, R. Heim, C. Zimmer, R.W. Hartmann, Fine-tuning the selectivity of aldosterone synthase inhibitors: structure−activity and structure−selectivity insights from studies of heteroaryl substituted 1,2,5,6-Tetrahydropyrrolo[3,2,1-ij]quinolin-4-one derivatives, J. Med. Chem. 54 (2011) 2307–2319.
[35] S. Ulmschneider, M. Negri, M. Voets, R.W. Hartmann, Development and evaluation of a pharmacophore model for inhibitors of aldosterone synthase (CYP11B2), Bioorg. Med. Chem. Lett. 16 (2006) 25–30.
[36] M. Akram, W. Waratchareeyakul, J. Haupenthal, R.W. Hartmann, D. Schuster, Pharmacophore modeling and in Silico/in vitro screening for human cytochrome P450 11B1 and cytochrome P450 11B2 inhibitors, Front. Chem. 5 (2017).
[37] A. Vuorinen, L.G. Nashev, A. Odermatt, J.M. Rollinger, D. Schuster, Pharmacophore model refinement for 11β-Hydroxysteroid dehydrogenase inhibitors: search for modulators of intracellular glucocorticoid concentrations, Mol. Inform. 33 (2014) 15–25.
[38] M. Jacobsson, P. Lidén, E. Stjernschantz, H. Boström, U. Norinder, Improving structure-based virtual screening by multivariate analysis of scoring data, J. Med. Chem. 46 (2003) 5781–5789.
[39] I. Accelrys, Pipeline Pilot, San Diego (2011).
[40] C.C.G. Inc, Molecular Operating Environment (MOE), Chemical Computing Group Inc 1010 Sherbooke St. West, Suite# 910, Montreal, 2011.
[41] Accelrys, Discovery Studio, Biovia, 5005 Wateridge Vista Drive, San Diego, CA 92121 USA, 2015.
[42] P.C.D. Hawkins, A. Nicholls, Conformer generation with OMEGA: learning from the data set and the analysis of failures, J. Chem. Inf. Model. 52 (2012) 2919–2936.
[43] P.C.D. Hawkins, A.G. Skillman, G.L. Warren, B.A. Ellingson, M.T. Stahl, Conformer generation with OMEGA: algorithm and validation using high quality structures from the protein databank and Cambridge structural database, J. Chem. Inf. Model. 50 (2010) 572–584.
[44] K. Denner, J. Doehmer, R. Bernhardt, Cloning of CYP11B1 and CYP11B2 from normal human adrenal and their functional expression in COS-7 and V79 Chinese hamster cells, Endocr. Res. 21 (1995) 443–448.
[45] P.B. Ehmer, M. Bureik, R. Bernhardt, U. Müller, R.W. Hartmann, Development of a test system for inhibitors of human aldosterone synthase (CYP11B2): screening in fission yeast and evaluation of selectivity in V79 cells, J. Steroid Biochem. Mol. Biol. 81 (2002) 173–179.
[46] U.E. Hille, C. Zimmer, C.A. Vock, R.W. Hartmann, First selective CYP11B1 inhibitors for the treatment of cortisol-dependent diseases, ACS Med. Chem. Lett. 2 (2011) 2–6.
[47] P.B. Ehmer, J. Jose, R.W. Hartmann, Development of a simple and rapid assay for the evaluation of inhibitors of human 17alpha-hydroxylase-C(17,20)-lyase (P450cl7) by coexpression of P450cl7 with NADPH-cytochrome-P450-reductase in Escherichia coli, J. Steroid Biochem. Mol. Biol. 75 (2000) 57–63.
[48] T.U. Hutschenreuter, P.B. Ehmer, R.W. Hartmann, Synthesis of hydroxy derivatives

of highly potent non-steroidal CYP 17 inhibitors as potential metabolites and evaluation of their activity by a non cellular assay using recombinant human enzyme, J. Enzyme Inhib. Med. Chem. 19 (2004) 17–32.
[49] P. Strajhar, D. Tonoli, F. Jeanneret, R.M. Imhof, V. Malagnino, M. Patt, D.V. Kratschmar, J. Boccard, S. Rudaz, A. Odermatt, Steroid profiling in H295R cells to identify chemicals potentially disrupting the production of adrenal steroids, Toxicology 381 (2017) 51–63.
[50] P. Strajhar, Y. Schmid, E. Liakoni, P.C. Dolder, K.M. Rentsch, D.V. Kratschmar, A. Odermatt, M.E. Liechti, Acute effects of lysergic acid diethylamide on circulating steroid levels in healthy subjects, J. Neuroendocrinol. 28 (2016) 12374.
[51] L. Xiong, X.-L. Zhu, H.-W. Gao, Y. Fu, S.-Q. Hu, L.-N. Jiang, W.-C. Yang, G.-F. Yang, Discovery of potent succinate-ubiquinone oxidoreductase inhibitors via pharmacophore-linked fragment virtual screening approach, J. Agric. Food Chem. 64 (2016) 4830–4837.
[52] N. Strushkevich, A.A. Gilep, L. Shen, C.H. Arrowsmith, A.M. Edwards, S.A. Usanov, H.-W. Park, Structural insights into aldosterone synthase substrate specificity and targeted inhibition, Mol. Endocrinol. 27 (2013) 315–324.
[53] G. Jones, P. Willett, R.C. Glen, Molecular recognition of receptor sites using a genetic algorithm with a description of desolvation, J. Mol. Biol. 245 (1995) 43–53.
[54] G. Jones, P. Willett, R.C. Glen, A.R. Leach, R. Taylor, Development and validation of a genetic algorithm for flexible docking1, J. Mol. Biol. 267 (1997) 727–748.
[55] M.L. Verdonk, J.C. Cole, M.J. Hartshorn, C.W. Murray, R.D. Taylor, Improved protein-ligand docking using GOLD, Proteins 52 (2003) 609–623.
[56] G. Wolber, T. Langer, LigandScout: 3-D pharmacophores derived from protein-bound ligands and their use as virtual screening filters, J. Chem. Inf. Model. 45 (2005) 160–169.
[57] OECD, OECD Guideline for the Testing of Chemicals. Test No. 456: H295R Steroidogenesis Assay, OECD Guidelines for the Testing of Chemicals, Section 4: Health Effects, 2011.
[58] R.G. Clerc, A. Stauffer, F. Weibel, E. Hainaut, A. Perez, J.C. Hoflack, A. Benardeau, P. Pflieger, J.M. Garriz, J.W. Funder, A.M. Capponi, E.J. Niesor, Mechanisms underlying off-target effects of the cholesteryl ester transfer protein inhibitor torcetrapib involve L-type calcium channels, J. Hypertens. 28 (2010) 1676–1686.
[59] L. Yin, Q. Hu, J. Emmerich, M.M.-C. Lo, E. Metzger, A. Ali, R.W. Hartmann, Novel pyridyl- or isoquinolinyl-substituted indolines and indoles as potent and selective aldosterone synthase inhibitors, J. Med. Chem. 57 (2014) 5179–5189.
[60] Z. Guan, X. Chai, S. Yu, H. Hu, Y. Jiang, Q. Meng, Q. Wu, Synthesis, molecular docking, and biological evaluation of novel triazole derivatives as antifungal agents, Chem. Biol. Drug Des. 76 (2010) 496–504.
[61] X. Chai, J. Zhang, H. Hu, S. Yu, Q. Sun, Z. Dan, Y. Jiang, Q. Wu, Design, synthesis, and biological evaluation of novel triazole derivatives as inhibitors of cytochrome P450 14α-demethylase, Eur. J. Med. Chem. 44 (2009) 1913–1920.
[62] R.W. Johnstone, A.A. Ruefli, M.J. Smyth, Multiple physiological functions for multidrug transporter P-glycoprotein? Trends Biochem. Sci. 25 (2000) 1–6.
[63] EFSA, E.F.S. Authority (Ed.), Draft Assessment Report (DAR) Conclusion on the Peer Review of the Pesticide Risk Assessment of the Active Substance Flurprimidol, 2011, p. 1962 Parma, Italy.
[64] U.S.E.P.A.A.D. Ancymidol, R.E.D FACTS Ancymidol, to Pesticide Docket, Public Response and Program Resources Branch, Field Operations Division (7506C), Office of Pesticide Programs (OPP), US EPA, Washington, DC 20460, US Environmental Protection Agency, Science Advisory Board, 1995.
[65] E. Commission, Endocrine Disruptors: Study on Gathering Information on 435 Substances with Insufficient Data, RPS BKH Consultants B.V. Electronikaweg 2, 2628 XG Delft, Netherlands, 2002.
[66] EPA, EPA Pesticides Fact Sheet, United States Environmental Protection Agency Office of Prevention, Pesticides and Toxic Substances (7505P), 2006.
[67] J.A. Zarn, B.J. Bruschweiler, J.R. Schlatter, Azole fungicides affect mammalian steroidogenesis by inhibiting sterol 14 alpha-demethylase and aromatase, Environ. Health Perspect. 111 (2003) 255–261.
[68] J.T. Sanderson, J. Boerma, G.W.A. Lansbergen, M. van den Berg, Induction and inhibition of aromatase (CYP19) activity by various classes of pesticides in H295R human adrenocortical carcinoma cells, Toxicol. Appl. Pharmacol. 182 (2002) 44–54.
[69] M.J.E. Roelofs, A.H. Piersma, M. van den Berg, M.B.M. van Duursen, The relevance of chemical interactions with CYP17 enzyme activity: assessment using a novel in vitro assay, Toxicol. Appl. Pharmacol. 268 (2013) 309–317.
[70] J.E. Chambers, H. Greim, R.J. Kendall, H. Segner, R.M. Sharpe, G. Van Der Kraak, Human and ecological risk assessment of a crop protection chemical: a case study with the azole fungicide epoxiconazole, Crit. Rev. Toxicol. 44 (2014) 176–210.
[71] C. Taxvig, U. Hass, M. Axelstad, M. Dalgaard, J. Boberg, H.R. Andeasen, A.M. Vinggaard, Endocrine-disrupting activities in vivo of the fungicides tebuconazole and epoxiconazole, Toxicol. Sci. 100 (2007) 464–473.
[72] M.B. Kjærstad, C. Taxvig, C. Nellemann, A.M. Vinggaard, H.R. Andersen, Endocrine disrupting effects in vitro of conazole antifungals used as pesticides and pharmaceuticals, Reprod. Toxicol. 30 (2010) 573–582.
[73] A. Vinggaard, C. Hnida, V. Breinholt, J.C. Larsen, Screening of selected pesticides for inhibition of CYP19 aromatase activity in vitro, Toxicol. In Vitro 14 (2000) 227–234.
[74] E.R. Trösken, K. Scholz, R.W. Lutz, W. Völkel, J.A. Zarn, W.K. Lutz, Comparative assessment of the inhibition of recombinant human CYP19 (Aromatase) by azoles used in agriculture and as drugs for humans, Endocr. Res. 30 (2004) 387–394.
[75] L.G. Nashev, D. Schuster, C. Laggner, S. Sodha, T. Langer, G. Wolber, A. Odermatt, The UV-filter benzophenone-1 inhibits 17β-hydroxysteroid dehydrogenase type 3: Virtual screening as a strategy to identify potential endocrine disrupting chemicals, Biochem. Pharmacol. 79 (2010) 1189–1199.
[76] U.E. Hille, C. Zimmer, J. Haupenthal, R.W. Hartmann, Optimization of the first selective Steroid-11β-hydroxylase (CYP11B1) inhibitors for the treatment of cortisol dependent diseases, ACS Med. Chem. Lett. 2 (2011) 559–564.
[77] M.A.E. Pinto-Bazurco Mendieta, Q. Hu, M. Engel, R.W. Hartmann, Highly potent and selective nonsteroidal dual inhibitors of CYP17/CYP11B2 for the treatment of prostate Cancer To reduce risks of cardiovascular diseases, J. Med. Chem. 56 (2013) 6101–6107.
[78] S. Lucas, M. Negri, R. Heim, C. Zimmer, R.W. Hartmann, Fine-tuning the selectivity of aldosterone synthase inhibitors: structure—Activity and structure—Selectivity insights from studies of heteroaryl substituted 1,2,5,6-Tetrahydropyrrolo[3,2,1-ij] quinolin-4-one derivatives, J. Med. Chem. 54 (2011) 2307–2319.

Supplementary Material

Identification of the fungicide epoxiconazole by virtual screening and biological assessment as inhibitor of human 11β-hydroxylase and aldosterone synthase

Muhammad Akram[a,b,#], Melanie Patt[c,#], Teresa Kaserer[a], Veronika Temml[a], Watcharee Waratchareeyakul[d], Denise V. Kratschmar[c], Joerg Haupenthal[e], Rolf W. Hartmann[e,f], Alex Odermatt[c,*], Daniela Schuster[a,b*]

[a]*Institute of Pharmacy / Pharmaceutical Chemistry and Center for Molecular Biosciences Innsbruck, University of Innsbruck, Innrain 80-82, 6020 Innsbruck Austria*

[b]*Department of Medicinal and Pharmaceutical Chemistry, Institute of Pharmacy, Paracelsus Medical University, Strubergasse 21, 5020 Salzburg Austria*

[c]*Swiss Centre of Applied Human Toxicology and Division of Molecular and Systems Toxicology, Department of Pharmaceutical Sciences, University of Basel, Klingelbergstrasse 50, 4056 Basel, Switzerland*

[d]*Department of Chemistry, Faculty of Science and Technology, Rambhai Barni Rajabhat University, Chanthaburi, Thailand*

[e]*Department of Drug Design and Optimization, Helmholtz Institute for Pharmaceutical Research Saarland (HIPS), Universitätscampus E8 1 66123 Saarbrücken Germany*

[f]*Department of Pharmaceutical and Medicinal Chemistry, Saarland University, Campus C2.3, 66123 Saarbrücken, Germany*

[#] These authors contributed equally to the present study.
* Correspondence to D.S. for molecular modeling and to A.O. for biology.

Generation of ligand-based pharmacophore models

Ligand-based pharmacophore models were created using the espresso function of LigandScout 3.12 [1]. This workflow first assigns pharmacophore features to all of the conformations of the training compounds. Then, the features of the two most rigid training compounds are aligned to create intermediate common feature pharmacophore models. These intermediate models are ranked according to a selected scoring function.

The ligand-based, common feature pharmacophore model 1 was generated from two training compounds (Figure S1-A) [2]. *Pharmacophore-fit and atom overlap* was used as scoring function. Among the 10 reported pharmacophore queries, the model with the highest score (0.9084) and highest pharmacophore-fit score of training compounds was selected for further refinement. This

pharmacophore model was composed of two aromatic ring features (AR-1 and AR-2), three hydrophobic contacts (H-1, H-2, and H-3), three hydrogen bond acceptors (HBA-1, HBA-2, and HBA-3), and 47 XVOLs (Figures S1-B,C). HBA-1 represents the heterocyclic nitrogen of the training compounds, which is hypothesized to form a complex with the heme of the CYP enzymes. The remaining pharmacophore features represent various common features of the training compounds. Model 1 was optimized by; (1) increasing the feature tolerance of AR-1, AR-2, and HBA-3 from default 1 to 1.6, 1.3, and 1.75 Å, respectively, (2) and marking the H-1, H-2, H-3, and HBA-2 features as optional [3].

Ligand-based pharmacophore model 2 was generated from two training compounds [4, 5] (Figure S2-A) using the same settings as for model 1. The model which achieved the highest score (0.9174) and highest pharmacophore-fit score for the training compounds was selected for further optimization. It consisted of two AR features (AR-1, AR-2), two hydrophobic (H-1 and H-2) contacts, one HBA (HBA-1), and 33 XVOLs (Figures S2-B,C). The shared HBA feature of both of the training compounds was derived from the nitrogen of pyrimidine and imidazole rings. This model was optimized by marking the hydrophobic feature H-1 as optional [3].

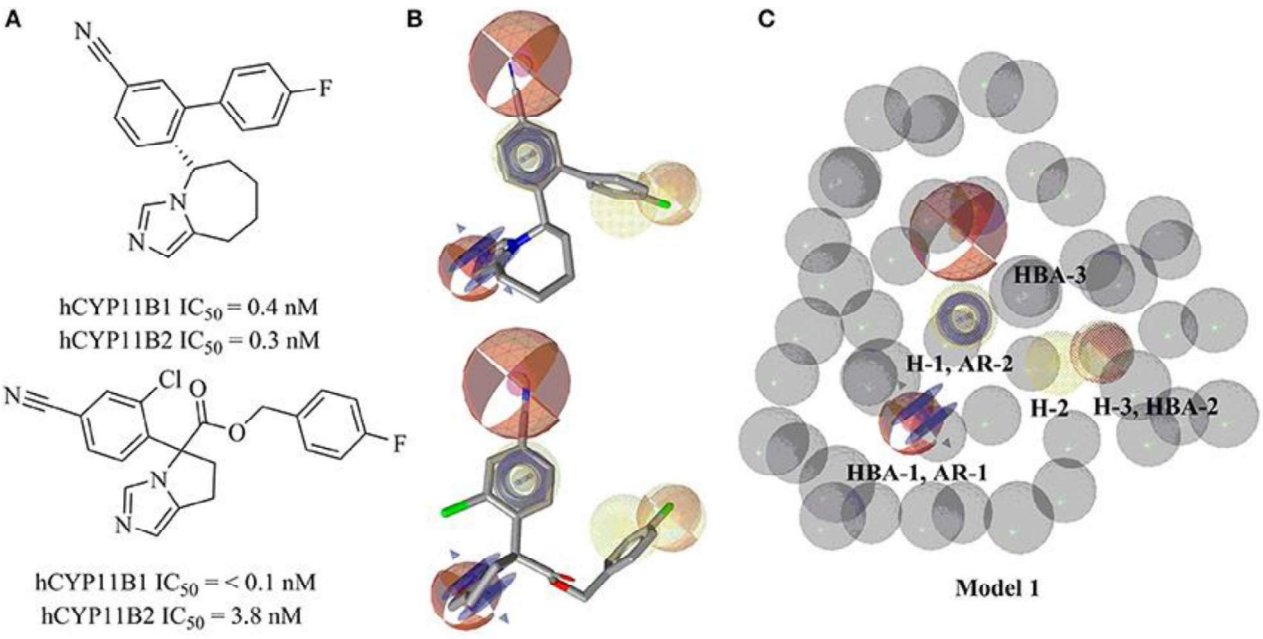

Figure S1. Ligand-based pharmacphore model 1. (A) 2D training compounds with their IC_{50} values are drawn. (B) Training compounds mapped into the model. (C) Final pharmacophore model 1 with color-coded features (yellow—hydrophobic contacts, blue rings—AR, red—HBA, dotted

style—optional features). The model consisted of 3 hydrophobic contacts, 3 HBAs, 2 AR features, and 47 XVOLs. This figure is taken from [3].

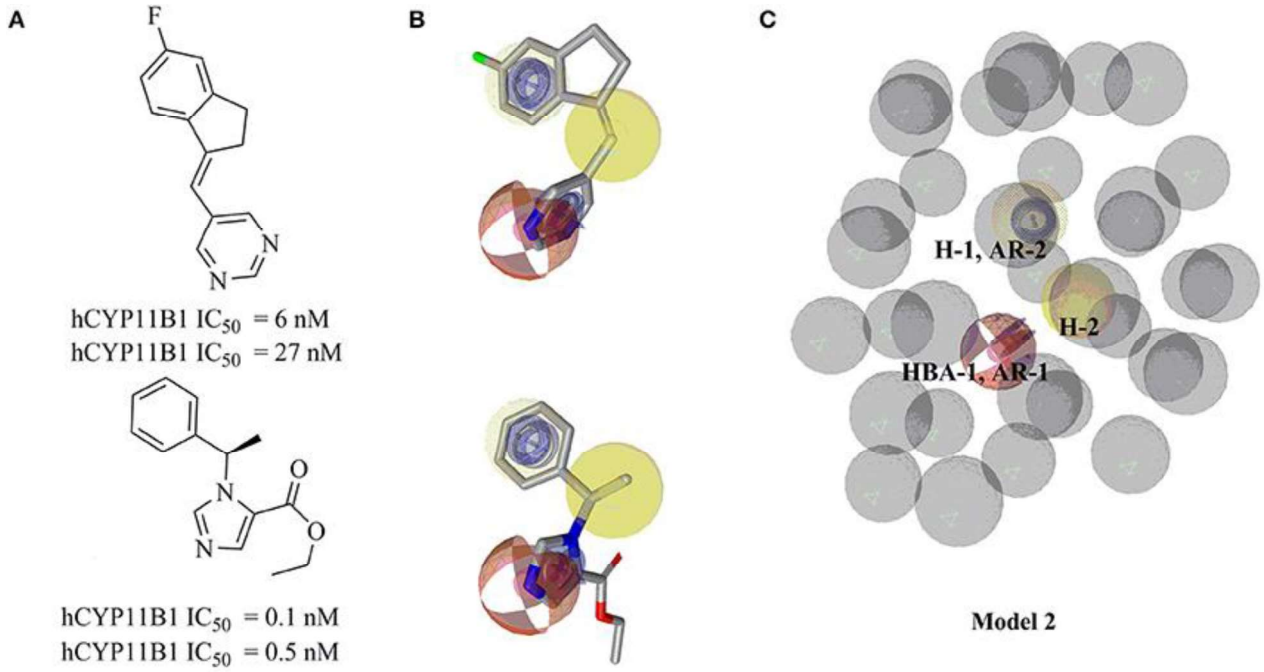

Figure S2. Ligand-based pharmacophore model 2. (A) Two training compounds with their IC_{50} values are drawn. (B) Mapping of training compounds with the model are shown. (C) The pharmacophore model is shown. Pharmacophore features are marked by colors. Model 2 comprised of 2 hydrophobic features, 2 AR features, 1 HBA feature, and 33 XVOLs. This figure is taken from [3].

Modification of previously used pharmacophore models

Two previously reported pharmacophore models [3] served as a basis. These models consisted of three-dimensional features defining interaction types such as HBD/HBA, H, AR, and XVOLs. A qualitative refinement of pharmacophore models was performed based on their specificity and/or sensitivity. In general, specificity was slightly improved by adding the spatial restrictions in the form of XVOLs or shapes. The sensitivity was partly increased by making the models less restrictive, deleting or adjusting the size of features, making some features optional, and/or removing the spatial restrictions.

The modified pharmacophore model 1.1 had three H (H-1, H-2, and H-3), two AR interactions (AR-1 and AR-2), three HBA features (HBA-1, HBA-2, and HBA-3), and 47 XVOLs (Fig. 3A). The

modified model 1.1 had H-2 as an optional feature. The modified model 2.1 had two H (H-1 and H-2), two AR interactions (AR-1 and AR-2), one HBA-1 feature, and 33 XVOLs (Fig. 3B).

The theoretical dataset used for the training of the models 1 and 2 in our previous study was used as reference dataset to compare the performance of validated (model 1 and 2) and modified models (model 1.1 and 2.1). The modified models 1.1 and 2.1 were employed for the virtual screening of reference dataset of active 442 compounds. The modified models 1.1 and 2.1 found 91 and 37 active hits, respectively. Hence, the sensitivity for model 1.1 and 2.1 was 0.21 and 0.08, respectively (Table S1). Our previously published models 1 and 2 found 92 and 40 active hits, respectively (Table S1). Hence the sensitivity value for models 1 and 2 was 0.21 and 0.1, respectively [3]. The yield of active of models 1, 1.1, 2, and 2.1 was 0.01031, 0.00872, 0.00305, and 0.00280, respectively (Table S1). The accuracy of models 1, 1.1, 2, and 2.1 was 0.97394, 0.97540, 0.97485, and 0.97473, respectively (Table S1).

Table S1. Quality analysis of both previously published [3] and modified models.

Matrices for quality evaluation	Previously published models [3]		Modified models	
	Model 1	Model 2	Model 1.1	Model 2.1
True positive [6]	92/442	40/442	91/442	37/442
True negative [6]	15869/15946	15936/15946	15894/15946	15937/15946
False negative [6]	350/442	402/442	351/442	405/442
False positive [6]	77/15946	10/15946	52/15946	9/15946
Yield of actives [6]	0.01031	0.00305	0.00872	0.00280
Sensitivity [6]	0.20814	0.09049	0.20588	0.08371
Specificity [6]	0.99517	0.99937	0.99673	0.99943
Accuracy [6]	0.97394	0.97485	0.97540	0.97473

True positive = found active, true negative = discarded inactive, false positive = found inactive, false negative = discarded active

Table S2. A review of percentage inhibition of human CYP11B1 and CYP11B2 by novel environmental compound in relation to the positive control

	CYP11B1				CYP11B2			
Ancymidol								
Concentration (μM)	0.05*	4	2	1	0.05*	4	2	1
Inhibition (%)	37	83	61	39	50	70	50	29
Flurprimidol								
Concentration (μM)	0.05*	2.5	1.25	0.625	0.05*	2.5	1.25	0.625
Inhibition (%)	36	86	71	49	54	82	59	42
Epoxiconazole								
Concentration (μM)	0.05*	1.5	0.75	0.375	0.05*	0.2	0.1	0.05
Inhibition (%)	36	68	51	34	54	61	42	26
1,1-thiocarbonyldiimidazole								
Concentration (μM)	0.05*	10	7	3.5	0.05*	20	15	10
Inhibition (%)	24	63	51	34	48	58	49	33
Ozagrel								
Concentration (μM)	0.05*	10	10	-	0.05*	10	10	-

Inhibition (%)	29	32	32	-	56	10	13	-

*** Ketoconazole (50 nM) was used as a positive control.**

Figure S3. The tested hits, which were inactive against CYP11B1, CYP11B2, CYP17, and CYP19 enzymes.

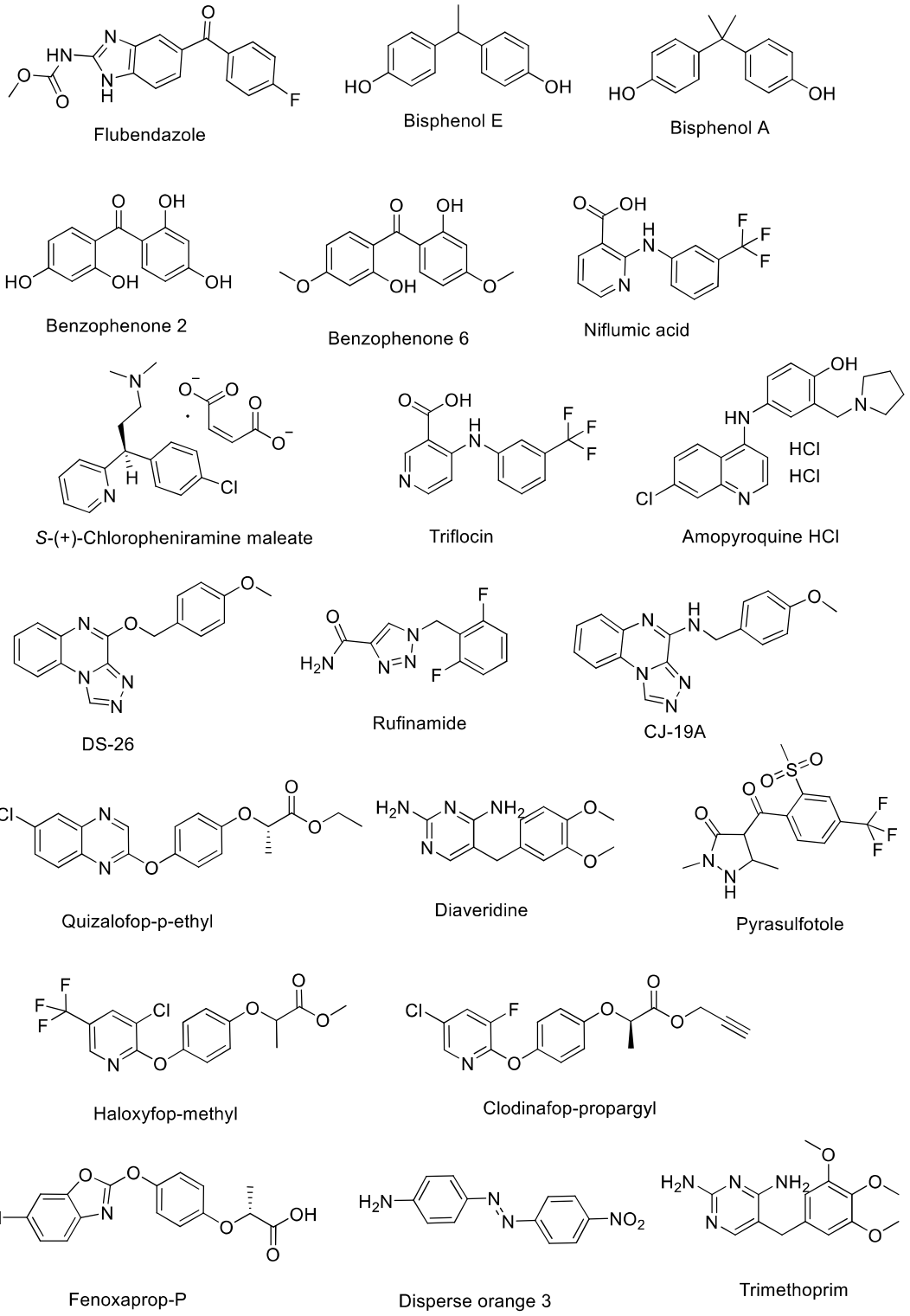

Figure S4. Effect of torcetrapib and etomidate on the H295R steroid profile. H295R cells were treated for 48 h with 0.3 µM torcetrapib (reference inducer) or 1 µM etomidate (reference inhibitor) or 0.1% DMSO (solvent control). Steroids were quantified by UHPLC-MS/MS. Data were obtained from four independent experiments, each performed in duplicates, and normalized to the respective steroid concentration in DMSO treated control cells. Fold change expressed as mean ± SD is depicted. Values are shown in a color code: green represents >1.5-fold down regulation and red >1.5-fold up regulation compared with DMSO control. RC: reference compound; SC: solvent control.

		progestins		mineralocorticoids			glucocorticoids		adrenal androgens
	treatment \ hormone	progesterone	17α-hydroxy-progesterone	11-deoxy-corticosterone	corticosterone	aldosterone	11-deoxycortisol	cortisol	androstenedione
SC	DMSO 0.1%	1.00 ± 0.03	1.00 ± 0.07	1.00 ± 0.06	1.00 ± 0.07	1.00 ± 0.10	1.00 ± 0.04	1.00 ± 0.05	1.00 ± 0.04
RC	torcetrapib 0.3 µM	2.14 ± 0.21	2.25 ± 0.20	1.61 ± 0.19	4.83 ± 1.72	13.7 ± 3.09	1.30 ± 0.10	4.24 ± 1.38	1.20 ± 0.09
	etomidate 1 µM + 0.3 µM tor	0.19 ± 0.02	0.16 ± 0.09	0.12 ± 0.02	0.02 ± 0.02	n.d.	0.12 ± 0.01	0.13 ± 0.09	0.09 ± 0.02

< 1.5 fold change/tor
> 1.5 fold change/tor

Figure S5. Effect of flurprimidol on the torcetrapib-stimulated H295R steroid profile. H295R cells were treated for 48 h with 0.3 μM torcetrapib (reference stimulating compound) and either 0.1% DMSO (solvent control) or flurprimidol at the concentrations indicated. Steroids were quantified by UHPLC-MS/MS. Data were obtained from two independent experiments, each performed in duplicates, and normalized to the respective steroid concentration in torcetrapib treated cells. Fold change expressed as mean ± SD is depicted. Values are shown in a color code: green represents >1.5-fold down regulation compared with torcetrapib control. RC: reference compound; TC: test compound.

		progestins		mineralocorticoids			glucocorticoids		adrenal androgens
	hormone / treatment	progesterone	17α-hydroxy-progesterone	11-deoxy-corticosterone	corticosterone	aldosterone	11-deoxycortisol	cortisol	androstenedione
RC	torcetrapib 0.3 μM	1.00 ± 0.10	1.00 ± 0.06	1.00 ± 0.08	1.00 ± 0.05	1.00 ± 0.10	1.00 ± 0.05	1.00 ± 0.12	1.00 ± 0.07
	etomidate 1 μM + 0.3 μM tor	0.07 ± 0.04	0.07 ± 0.04	0.08 ± 0.02	0.00 ± 0.00	n.d.	0.09 ± 0.01	0.04 ± 0.03	0.08 ± 0.02
TC	flurprimidol 10 μM + 0.3 μM tor	0.72 ± 0.07	0.62 ± 0.05	0.70 ± 0.04	0.45 ± 0.11	0.33 ± 0.09	0.79 ± 0.09	0.54 ± 0.16	0.69 ± 0.09
	flurprimidol 3.33 μM + 0.3 μM tor	0.72 ± 0.08	0.66 ± 0.06	0.76 ± 0.09	0.74 ± 0.08	0.71 ± 0.09	0.86 ± 0.05	0.94 ± 0.24	0.83 ± 0.10
	flurprimidol 1.11 μM + 0.3 μM tor	0.67 ± 0.06	0.73 ± 0.06	0.79 ± 0.10	0.90 ± 0.18	0.88 ± 0.20	0.98 ± 0.04	1.00 ± 0.21	0.81 ± 0.05

< 1.5 fold change/tor

Figure S6. Effect of ancymidol on the torcetrapib-stimulated H295R steroid profile. H295R cells were treated for 48 h with 0.3 µM torcetrapib (reference stimulating compound) and either 0.1% DMSO (solvent control) or ancymidol at the concentrations indicated. Steroids were quantified by UHPLC-MS/MS. Data were obtained from an experiments performed in duplicate, and normalized to the respective steroid concentration in torcetrapib treated cells. Fold change expressed as mean ± SD is depicted. Values are shown in a color code: green represents >1.5-fold down regulation compared with torcetrapib control. RC: reference compound; TC: test compound.

		progestins		mineralocorticoids			glucocorticoids		adrenal androgens
	treatment \ hormone	progesterone	17α-hydroxy-progesterone	11-deoxy-corticosterone	corticosterone	aldosterone	11-deoxycortisol	cortisol	androstenedione
RC	torcetrapib 0.3 µM	1.00 ± 0.10	1.00 ± 0.06	1.00 ± 0.08	1.00 ± 0.05	1.00 ± 0.10	1.00 ± 0.05	1.00 ± 0.12	1.00 ± 0.07
RC	etomidate 1 µM + 0.3 µM tor	0.07 ± 0.04	0.07 ± 0.04	0.08 ± 0.02	0.00 ± 0.00	n.d.	0.09 ± 0.01	0.04 ± 0.03	0.08 ± 0.02
TC	ancymidol 10 µM + 0.3 µM tor	0.78 ± 0.01	0.75 ± 0.00	0.91 ± 0.01	0.74 ± 0.02	0.51 ± 0.03	1.00 ± 0.04	1.30 ± 0.08	0.95 ± 0.05
TC	ancymidol 3.33 µM + 0.3 µM tor	0.68 ± 0.02	0.71 ± 0.03	0.73 ± 0.02	0.83 ± 0.01	0.72 ± 0.06	0.95 ± 0.05	1.40 ± 0.38	0.86 ± 0.07
TC	ancymidol 1.11 µM + 0.3 µM tor	0.75 ± 0.01	0.88 ± 0.01	0.76 ± 0.01	1.10 ± 0.08	0.85 ± 0.07	1.10 ± 0.04	1.60 ± 0.32	0.97 ± 0.02

< 1.5 fold change/tor

References

[1] Y. Krautscheid, C.J.Å. Senning, S.B. Sartori, N. Singewald, D. Schuster, H. Stuppner, Pharmacophore Modeling, Virtual Screening, and in Vitro Testing Reveal Haloperidol, Eprazinone, and Fenbutrazate as Neurokinin Receptors Ligands, Journal of Chemical Information and Modeling, 54 (2014) 1747-1757.

[2] E.L. Meredith, G. Ksander, L.G. Monovich, J.P.N. Papillon, Q. Liu, K. Miranda, P. Morris, C. Rao, R. Burgis, M. Capparelli, Q.-Y. Hu, A. Singh, D.F. Rigel, A.Y. Jeng, M. Beil, F. Fu, C.-W. Hu, D. LaSala, Discovery and in Vivo Evaluation of Potent Dual CYP11B2 (Aldosterone Synthase) and CYP11B1 Inhibitors, ACS Med. Chem. Lett., 4 (2013) 1203-1207.

[3] M. Akram, W. Waratchareeyakul, J. Haupenthal, R.W. Hartmann, D. Schuster, Pharmacophore Modeling and in Silico/in Vitro Screening for Human Cytochrome P450 11B1 and Cytochrome P450 11B2 Inhibitors, Frontiers in Chemistry, 5 (2017).

[4] U.E. Hille, C. Zimmer, C.A. Vock, R.W. Hartmann, First Selective CYP11B1 Inhibitors for the Treatment of Cortisol-Dependent Diseases, ACS Med. Chem. Lett., 2 (2011) 2-6.

[5] S. Ulmschneider, U. Müller-Vieira, C.D. Klein, I. Antes, T. Lengauer, R.W. Hartmann, Synthesis and Evaluation of (Pyridylmethylene)tetrahydronaphthalenes/-indanes and Structurally Modified Derivatives: Potent and Selective Inhibitors of Aldosterone Synthase, J. Med. Chem., 48 (2005) 1563-1575.

[6] M. Jacobsson, P. Lidén, E. Stjernschantz, H. Boström, U. Norinder, Improving Structure-Based Virtual Screening by Multivariate Analysis of Scoring Data, Journal of Medicinal Chemistry, 46 (2003) 5781-5789.

3.1.3 Submitted manuscript:

Profiling of anabolic androgenic steroids and selective androgen receptor modulators for interference with adrenal steroidogenesis

Melanie Patt[1,2], Katharina R. Beck[1,2], Tobias Di Marco[2], Marie-Christin Jäger[1,2], Victor González-Ruiz[1,3], Julien Boccard[1,3], Serge Rudaz[1,3], Rolf W. Hartmann[4,5], Mohamed Salah[5], Chris J. van Koppen[5], Matthias Grill[6], Alex Odermatt[1,2], manuscript submitted to Biochem Pharmacol. 2019 Oct.

[1]Swiss Centre for Applied Human Toxicology (SCAHT), University of Basel, Basel, Switzerland

[2]Division of Molecular and Systems Toxicology, Department of Pharmaceutical Sciences, University of Basel, Klingelbergstrasse 50, 4056 Basel, Switzerland

[3]Institute of Pharmaceutical Sciences of Western Switzerland, University of Geneva, Geneva 4, Switzerland

[4]Department Drug Design and Optimization (DDOP), Helmholtz Institute for Pharmaceutical Research Saarland (HIPS), Universitätscampus E8 1, 66123 Saarbrücken, Germany

[5]Department of Pharmaceutical and Medicinal Chemistry, Universitätscampus C2.3, 66123 Saarbrücken, Germany

[6]Lipomed AG, Fabrikmattenweg 4, 4144 Arlesheim, Switzerland

Contribution:

Performed experiments with H295R cells, analyzed data, wrote the manuscript.

Profiling of anabolic androgenic steroids and selective androgen receptor modulators for interference with adrenal steroidogenesis

Melanie Patt[1,2], Katharina R. Beck[1,2&], Tobias Di Marco[2], Marie-Christin Jäger[1,2], Victor González-Ruiz[1,3], Julien Boccard[1,3], Serge Rudaz[1,3], Rolf W. Hartmann[4,5], Mohamed Salah[5], Chris J. van Koppen[5], Matthias Grill[6], Alex Odermatt[1,2*]

[1]Swiss Centre for Applied Human Toxicology (SCAHT), University of Basel, Basel, Switzerland.

[2]Division of Molecular and Systems Toxicology, Department of Pharmaceutical Sciences, University of Basel, Klingelbergstrasse 50, 4056 Basel, Switzerland. MP: melanie.patt@unibas.ch; KRB: katharina.beck@unibas.ch; TD: tobias.dimarco@outlook.com; MCJ: m.jaeger@unibas.ch; AO: alex.odermatt@unibas.ch.

[3]Institute of Pharmaceutical Sciences of Western Switzerland, University of Geneva, Geneva 4, Switzerland. VG: Victor.Gonzalez@unige.ch; JB: Julien.Boccard@unige.ch. SR: Serge.Rudaz@unige.ch.

[4]Department Drug Design and Optimization (DDOP), Helmholtz Institute for Pharmaceutical Research Saarland (HIPS), Universitätscampus E8 1, 66123 Saarbrücken, Germany. RWH: rolf.hartmann@helmholtz-hzi.de.

[5]Department of Pharmaceutical and Medicinal Chemistry, Universitätscampus C2.3, 66123 Saarbrücken, Germany. MS: mohamed.rezk87@hotmail.com; CVK: vankoppen@elexopharm.de.

[6]Lipomed AG, Fabrikmattenweg 4, 4144 Arlesheim, Switzerland. MG: grill78@web.de.

[&]Current address: Labormedizinisches Zentrum Dr. Risch, Lagerstrasse 30, 9470 Buchs, Switzerland.

*Address of correspondence: Dr. Alex Odermatt, Swiss Centre for Applied Human Toxicology and Division of Molecular and Systems Toxicology, Department of Pharmaceutical Sciences, University of Basel, Klingelbergstrasse 50, 4056 Basel, Switzerland.
Alex.Odermatt@unibas.ch; Phone: + 41 61 207 1530.

Abstract

Anabolic-androgenic steroids (AAS) are testosterone derivatives developed for steroid-replacement and treatment of debilitating conditions. They are widely used by athletes in elite sports and bodybuilding due to their muscle building and performance enhancing properties. Excessive AAS use is associated with cardiovascular diseases, mood changes and endocrine and metabolic disorders; however, the underlying mechanisms remain incompletely understood. Selective androgen receptor modulators (SARMs) aim to reduce adverse androgenic AAS effects, while maximizing anabolic effects. This study assessed potential steroidogenesis disturbances of 19 AAS and 3 SARMs in human adrenocortical carcinoma H295R cells, comparing basal and forskolin-activated states by using mass spectrometry-based quantification of nine major adrenal steroids. Mesterolone, mestanolone and methenolone increased mineralocorticoid but decreased adrenal androgen production, indicating CYP17A1 dysfunction. Cell-free activity assays failed to detect direct CYP17A1 inhibition, supported by molecular modeling, and CYP17A1 mRNA expression was unaffected, suggesting indirect inhibition involving post-translational modification and/or impaired protein stability. Clostebol and oxymetholone decreased corticosteroid but increased dehydroepiandrosterone synthesis in H295R cells, indicating CYP21A2 inhibition, supported by molecular modeling. None of the SARMs tested interfered with steroidogenesis. The chosen approach allowed to group AAS according to their steroidogenesis-interfering effects and provided initial mechanistic information. Mesterolone, mestanolone and methenolone potentially promote hypertension and cardiovascular diseases via excessive mineralocorticoid synthesis. Clostebol and oxymetholone might cause metabolic disturbances by suppressing corticosteroid production and result in adrenal hyperplasia due to negative feedback induction of ACTH. The non-steroidal SARMs exhibit an improved safety profile and represent a preferred therapeutic option.

Keywords

Adrenal gland; steroid synthesis; hypertension; cardiovascular disease; H295R; adverse effect; hormone

1. Introduction

Anabolic androgenic steroids (AAS) are synthetic derivatives of the male sex hormone testosterone developed to increase bioavailability and reduce adverse androgenic properties, while maximizing anabolic effects. Traditional indications for the use of AAS have been advanced breast cancer, osteoporosis and anemia associated with leukemia and kidney failure. Nowadays, AAS are clinically used in hormone replacement therapies, including hypogonadism and aging, and to treat muscle wasting due to cancer, AIDS, severe burns, chronic renal failure and pulmonary diseases [1-7]. Therapeutic doses of synthetic testosterone aim to raise serum testosterone concentrations to the mid-normal range between 350 ng/dL (14 nmol/L) and 600 ng/dL (25 nmol/L) [8, 9], and treatment with testosterone analogues should achieve equivalent activity corresponding to this range. Although improvements in the chemical scaffold of testosterone were made, a clear dissociation of anabolic from androgenic effects in the respective testosterone analogues has not yet been achieved [10]. The undesirable androgenic properties of AAS including acne, hirsutism and alopecia are responsible for their limited clinical use [8, 9].

The beneficial effects of AAS on muscle mass and bone mineral density have led to the development of tissue-selective alternatives with reduced adverse effects. Selective androgen receptor modulators (SARMs) are supposed to act as full agonists in anabolic tissues such as muscle and bone with ideally no or minimal activation of the androgen receptor (AR) in prostate, heart or liver [11, 12]. Most SARMs are non-steroidal compounds, expected to exhibit fewer interactions with steroid metabolizing enzymes and possessing a better side effect profile. Currently, SARMs are studied in phase I and II clinical trials to assess their efficacy in treatment

of cachexia, benign prostatic hyperplasia, prostate cancer, breast cancer and stress urinary incontinence in postmenopausal women [13].

Besides therapeutic applications, AAS are used as anabolic agents to enhance muscle mass and burn fat by athletes to enhance performance and by the general population to improve body shape. AAS are the most frequently detected doping agents with about 44% of adverse analytical findings in WADA-accredited laboratories in 2017 [14]. Due to frequent doping tests, AAS misuse cannot be considered a serious health risk among elite athletes; however, it has become a public health concern [15]. The majority of AAS users are individuals striving for a muscular body shape without competitive athletic ambitions. According to the latest 'Monitoring the Future' statistics (2017), an annual survey on drug abuse in adolescents across the United States funded by the National Institute on Drug Abuse, the lifetime prevalence of AAS use is 1.4% for young adults (ages 19-28) [16]. Nevertheless, these data do not accurately reflect the population encountering serious adverse effects, since most of those arise during long-term AAS use. Prolonged AAS use can be assumed to be more prevalent in fitness and strength training environments. Higher estimates of AAS misuse have been documented among gym-goers, bodybuilders and security personnel compared to the general population [15, 17, 18]. Whereas the medical use of AAS aims to achieve a physiologic replacement level on a continuous basis, recreational users usually take supraphysiologic doses of AAS, reaching 10 to 100 times the physiological level. Furthermore, AAS are often applied in a sophisticated multidrug regimen involving varying doses, time courses and simultaneously using oral and intramuscular preparations [19-22]. High-dose AAS use is associated with a wide range of adverse health effects including liver toxicity, kidney diseases, psychological disorders, endocrine disturbances and dermatologic effects [23-25]. Additionally, AAS affect the cardiovascular system. Several studies described cardiovascular consequences occurring after abusive AAS use including hypertension, myocardial hypertrophy, cardiomyopathy, myocardial infarction and sudden cardiac death [26, 27].

Mechanisms involving steroidogenesis have been suggested to contribute to the hypertensive effects of AAS. In bovine adrenal cells, testosterone hemisuccinate stimulated the membrane binding of angiotensin as well as aldosterone synthesis [28]. Another mechanism leading to hypertension includes the elevation of the mineralocorticoid 11-deoxycorticosterone (DOC), which may be caused by a testosterone-dependent decrease in cytochrome P450 11B1 (CYP11B1, 11β-hydroxylase) mRNA levels [29, 30]. In addition, inhibition of cytochrome P450 17A1 (CYP17A1, 17α-hydroxylase-17, 20-lyase) is accompanied with mineralocorticoid excess, since the lack of CYP17A1 activity forces steroid substrates to pass through the biosynthetic pathway of aldosterone via corticosterone and DOC [31-33]. The feedback regulation via adrenocorticotropic hormone (ACTH) upon inhibition of cortisol synthesis further stimulates adrenal steroidogenesis, thereby enhancing mineralocorticoid production. A well-known example of the consequences of drug-induced CYP17A1 inhibition is the anti-prostate cancer drug abiraterone, a synthetic androgen derivative (3β-acetoxy-17-(3-pyridyl)androsta-5,16-diene). Patients are usually co-treated with glucocorticoids to prevent feedback stimulation and avoid mineralocorticoid excess, and/or mineralocorticoid receptor (MR) antagonists [34]. The mineralocorticoids regulate sodium reabsorption and potassium excretion by acting through MR. An excess of mineralocorticoids is characterized by hypokalemia, hypernatremia, fluid retention, edema, and hypertension. Although the adverse cardiovascular effects of AAS misuse are well recognized, the underlying molecular mechanisms are still not fully understood.

The current study examined the effects of 19 AAS and 3 SARMs on adrenal steroidogenesis, aiming to identify compounds that increase the production of mineralocorticoids and potentially contribute to the development of hypertension and cardiovascular diseases [35]. The use of a modified protocol of the OECD test guideline 456, based on human H295R adrenocortical carcinoma cells, and subsequent quantification of all major adrenal steroids ([36], see Fig. 1 for an overview of steroid biosynthesis), provided initial insight into the mechanism of interference

by different AAS. Finally, this study allowed a comparison of the potential steroidogenesis-disrupting effects of AAS and SARMs as a first insight of chemical grouping in the context of system toxicology.

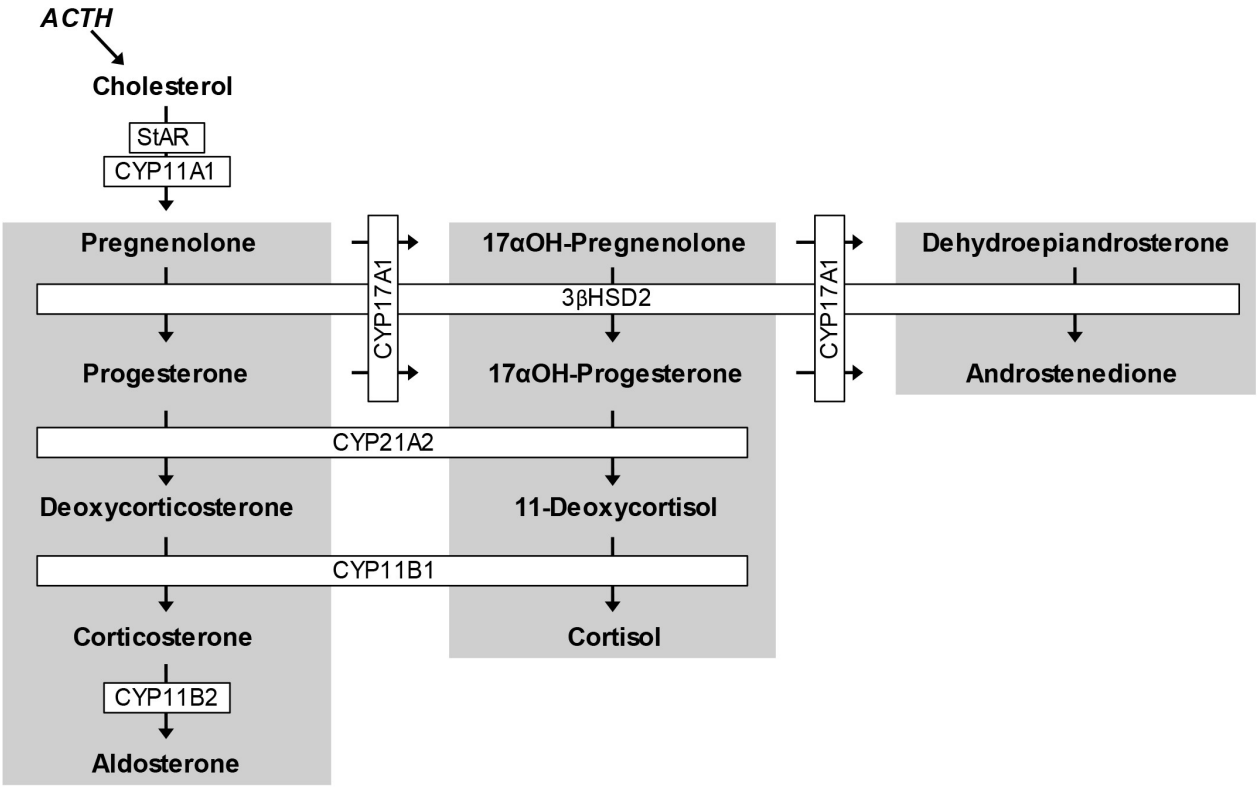

Fig. 1. Schematic representation of adrenal steroidogenesis. Major enzymes and steroids involved in mineralo- and glucocorticoid as well as adrenal androgen biosynthesis are shown.

2. Materials and methods

2.1. Chemicals and reagents

Danazol (CAS 17230-88-5), fluoxymesterone (CAS 76-43-7), mestanolone (CAS 521-11-9), methandienone (CAS 72-63-9), nandrolone (CAS 434-22-0), oxandrolone (CAS 53-39-4), oxymesterone (CAS 145-12-0), oxymetholone (CAS 434-07-1), stanozolol (CAS 10418-03-8), trenbolone (CAS 10161-33-8), and ostarin (CAS 841205-47-8) were obtained from Lipomed (Arlesheim, Switzerland) at the highest purity available. Boldenone (CAS 846-48-0), clostebol (CAS 1093-58-9), drostanolone (CAS 58-19-5), methasterone (CAS 3381-88-2), LDG-2226 (CAS 328947-93-9), LDG-4033 (CAS 1165910-22-4), and oxystanolone (2-hydroxymethylene-androstan-17β-ol-3-one or 4,5α-dihydro-2-(hydroxymethylene)testosterone) were synthesized as described elsewhere (Methods-X, submitted). Mesterolone (CAS 1424-00-6) and turinabol (clostebol acetate, CAS 855-19-6) were kindly provided by Dr. Daniela Schuster (Paracelsus Medical University, Salzburg, Austria). Methenolone (CAS 153-00-4) and norbolethone (CAS 1235-15-0) were purchased from Cerilliant Corporation (Round Rock, TX, USA), and the reference compounds forskolin (CAS 66575-29-9) and prochloraz (CAS 67747-09-5) from Sigma Aldrich (Buchs, Switzerland) at the highest purity available. Stock solutions (10 mM or 5 mM) were prepared in dimethyl sulfoxide (DMSO, AppliChem, Darmstadt, Germany). UPLC-grade purity methanol, acetonitrile and formic acid were purchased from Biosolve (Dieuze, France). Aldosterone, corticosterone, 11-deoxycorticosterone, androstenedione, testosterone and [2,2,4,6,6,21,21-$^{2}H_{7}$]-aldosterone (98% isotopic purity) were obtained from Sigma-Aldrich. 11-Dehydrocorticosterone, dehydroepiandrosterone, progesterone, 17α-hydroxyprogesterone, 11-deoxycortisol, cortisol and cortisone were purchased from Steraloids (Newport, RI, USA). [1,2-$^{2}H_{2}$]-Testosterone (98% isotopic purity), [2,2,4,6,6,16,16-$^{2}H_{7}$]-Δ4-androstene-3,17-dione (98% isotopic purity) and [2,2,4,6,6,17α,21,21-$^{2}H_{8}$]-corticosterone (98% isotopic purity) were

purchased from C/D/N Isotopes Inc. (Pointe-Claire, Canada). Stock solutions (10 mM and/or 1 mg/mL) of above-mentioned steroids were prepared in methanol.

2.2. Cell culture and H295R steroidogenesis assay

H295R human adrenocortical carcinoma cells were obtained from the American Type Culture Collection (ATCC, Manassas, VA, USA) and cultured in Dulbecco's modified Eagle's medium (DMEM)/Ham's nutrient mixture F-12 (1:1, v/v) (Life Technologies, Zug, Switzerland), supplemented with 1% (v/v) ITS + Premix (BD Bioscience, Bedford, MA, USA), 2.5% (v/v) Nu-Serum (Lot: 2342913, BD Bioscience, Bedford, MA, USA), 15 mM HEPES buffer, pH 7.4, and 1% (v/v) penicillin-streptomycin (Sigma-Aldrich). The H295R steroidogenesis assay was performed following the OECD Test 456 guidelines [37], with some modifications [38]. Briefly, cells (at passages 5-10) were seeded in 24-well plates at a density of 200,000 cells/mL. The medium was changed after 24 h to fresh medium containing reference or test compound (1 μM). DMSO (0.01% (v/v)) was used as vehicle control, forskolin (10 μM) as positive control to stimulate and prochloraz (1 μM) as negative control to inhibit adrenal steroidogenesis, respectively. In addition to using cells in their basal state, cells were activated by exposure to 10 μM forskolin in combination with the test compound (1 μM). Forskolin (10 μM) served as a vehicle control for stimulated steroidogenesis. Supplemented medium prior to adding the cells served as control at time zero. After 48 h of exposure, cell supernatants were collected and stored at -20 °C until steroid hormone analysis was performed. Experiments were carried out three times independently, each in duplicates.

2.3. Cell viability assay

Possible effects of tested compounds on cell viability were evaluated using 2,3-bis(2-methoxy-4-nitro-5-sulfophenyl)-2H-tetrazolium-5-carboxanilide (XTT) and phenazine methosulfate (PMS) as an electron-coupling reagent. Briefly, H295R cells were seeded in 96-well plates at a density of 30,000 cells/100 µL complete medium. After 24 h, the medium was replaced by fresh phenol red-free medium containing test compound at a concentration of 0.1 µM, 1 µM or 10 µM with or without 10 µM forskolin. Digitoxin (10 µM) was used as a cytotoxicity control. After 48 h of incubation, cells were subjected to microscopic inspection for morphological changes, and 25 µL of XTT/PMS solution (1 mg/mL and 7.5 µg/mL) was added to each well, followed by incubation for another 2 h. Absorbance was then recorded at 450 and 650 nm (reference wavelength). Control wells containing phenol red-free medium were used as a value for background absorbance. Experiments were performed three times independently with technical triplicates.

2.4. Targeted steroid quantification

The concentrations of nine steroid hormones in H295R culture supernatants were quantified using ultra-high performance liquid chromatography tandem mass spectrometry (UHPLC-MS/MS) as described previously with minor adaptations [36, 38]. Briefly, 1 mL of cell supernatant was spiked with deuterium-labeled aldosterone, corticosterone and androstenedione as internal standards. The samples were then extracted using Oasis HLB 1 cc SPE cartridges (30 mg, 30 µm particle size, Waters, Massachusetts, USA), preconditioned with 1 mL ethyl acetate and 1 mL Milli-Q water. After washing the columns three times with water and a mixture of methanol/water (10/90, v/v), steroids were eluted twice with 0.5 mL of ethyl acetate. The eluates were evaporated to dryness, and reconstituted with 50 µL of methanol. Steroids were separated on a reverse-phase column (Waters Acquity UPLC BEH C18, 1.7 µm, 2.1 mm × 150 mm) using an Agilent 1290 UHPLC system. Mobile phases A and B consisted

of water-acetonitrile-formic acid (95/5/0.1; v/v/v) and (5/95/0.1; v/v/v), respectively. Detection was performed using an Agilent 6490 triple quadrupole mass spectrometer equipped with a jet-stream electrospray ionization source. Mass Hunter software version B.07.01 (Agilent Technologies) was used to analyze the acquired data.

2.5. Gene expression analysis

Following the indicated treatment, RNA was isolated using the RNeasy Mini Kit (QIAGEN, Hilden, Germany) on a QIAcube extraction robot (QIAGEN, Hilden, Germany) according to the manufacturer. Complementary DNA (cDNA) was synthesized and quantitative polymerase chain reaction (qPCR) was performed as described previously [36].

2.6. Determination of CYP17A 17α-hydroxylase activity in cell lysates

Lysates of recombinant *E. coli* pJL17/OR co-expressing human CYP17A1 and rat NADPH-P450-reductase were prepared as described earlier [39, 40]. The 17α-hydroxylase activity of CYP17A1 was determined by measuring the conversion of progesterone to 17α-hydroxyprogesterone and the byproduct 16α-hydroxyprogesterone by UV spectroscopy. Test substance or vehicle control (DMSO at a final concentration of 2%) were included in the incubation medium at the concentrations indicated.

2.7. Molecular modeling

Based on the crystal structures of human CYP17A1 co-crystallized with abiraterone (PDB code 3RUK [41]) and human CYP21A2 in complex with 17α-hydroxyprogesterone (PDB code 5VBU [42]), docking calculations were performed using GOLD 5.2 (The Cambridge Crystallographic Data Centre, Cambridge, UK, [43]). In a first step, the co-crystallized ligands of each crystal structure were deleted and re-docked into the corresponding enzyme's substrate binding pocket in order to determine whether the original binding orientation could be restored

and thus the adapted docking settings could be validated. The root mean square deviation (RMSD) values obtained were 0.522 for CYP17A1 and 0.384 for CYP21A2 using the following settings: the ligand binding pockets were defined as spheres with a 10 Å radius around the coordinates X = 28.53, Y = -8.76, Z = 36.51 for CYP17A1 and X = -35.87, Y = -2.26, Z = 28.00 for CYP21A2. ChemPLP was used as scoring function for all docking calculations. The binding poses predicted by GOLD were then further analyzed using LigandScout 4.1 (Inte:Ligand GmbH, Vienna, Austria) [44].

2.8. Statistics

Statistical evaluation was performed in GraphPad Prism version 7.04. Shapiro-Wilk normality test was performed to verify the normality of data (N = k × n) obtained from three independent steroid profiling experiments (k = 3) each performed in duplicate (n = 2). One-way analysis of variance (ANOVA) and Dunnett's multiple-comparison test were used to compare chemical treatments to the solvent control, followed by a Bonferroni correction to adjust the false discovery rate. Differences were considered significant at a p-value <0.05.

3. Results

3.1. *Effects of AAS and SARMs on cell viability*

Cell viability was assessed after 48 h of incubation with the respective compound using cells in the basal state and upon forskolin stimulation by visual inspection under a microscope and by performing an XTT assay. No alteration of the normal morphology nor any signs of cytotoxicity were observed at the tested concentrations up to 10 μM (data not shown).

3.2. *Effects of AAS and SARMs on steroid profiles in H295R cells in the basal and stimulated state*

H295R cells were incubated with the respective compound in the basal state, allowing easy detection of compounds inducing the production of steroids, and upon forskolin stimulation of steroidogenesis, to facilitate identification of inhibitory effects. The amounts of nine adrenal steroids were quantified by UHPLC-MS/MS to investigate effects of the compounds in cells at the basal state (treated with vehicle: 0.01% DMSO, Table 1) and in stimulated cells (treated with 10 μM forskolin, Table 2). Since the Nu-serum already contained a significant amount of progesterone and cortisol, steroid measurements of the complete medium at the beginning of the experiment (t = 0 h) were assessed in order to distinguish between steroids produced by the cells and those contributed by the Nu-serum [36]. Following the OECD test guideline 456, forskolin (10 μM) and prochloraz (1 μM) were included in non-stimulated cells as reference compounds to verify responsiveness. As expected, forskolin, a known inducer of adenylyl cyclase that increases cAMP levels [45], significantly increased the production of the progestin 17α-hydroxyprogesterone, the mineralocorticoids 11-deoxycorticosterone, corticosterone and aldosterone as well as the glucocorticoids 11-deoxycortisol and cortisol and the adrenal androgens dehydroepiandrosterone and androstenedione, in accordance with an overall stimulation of adrenal steroidogenesis.

		progestins		mineralocorticoids			glucocorticoids		adrenal androgens	
	treatment \ steroid	progesterone	17α-hydroxy-progesterone	11-deoxy-corticosterone	corticosterone	aldosterone	11-deoxycortisol	cortisol	dehydro-epiandrosterone	androstenedione
SC	0.01% DMSO	1.00 ± 0.02	1.00 ± 0.04	1.00 ± 0.03	1.00 ± 0.05	1.00 ± 0.06	1.00 ± 0.04	1.00 ± 0.06	1.00 ± 0.04	1.00 ± 0.05
MC	complete medium; t=0	1.00 ± 0.13	n.d.	0.01 ± 0.00	n.d.	n.d.	0.02 ± 0.01	0.30 ± 0.13	n.d.	0.03 ± 0.00
RC	forskolin 10 µM	1.20 ± 0.20	3.90 ± 0.32	1.30 ± 0.20	4.50 ± 0.33	2.50 ± 0.28	2.60 ± 0.36	5.30 ± 1.50	3.90 ± 0.96	4.00 ± 0.33
	prochloraz 1 µM	16.0 ± 1.80	1.70 ± 0.23	1.70 ± 0.24	0.35 ± 0.06	0.35 ± 0.06	0.09 ± 0.01	0.32 ± 0.16	n.d.	0.08 ± 0.01
AAS	clostebol	0.87 ± 0.05	1.40 ± 0.09	0.67 ± 0.06	n.d.	0.24 ± 0.10	0.94 ± 0.07	0.48 ± 0.13	1.90 ± 0.23	1.40 ± 0.07
	turinabol	0.62 ± 0.06	1.30 ± 0.11	0.47 ± 0.07	n.d.	0.22 ± 0.13	0.75 ± 0.04	0.35 ± 0.11	2.80 ± 0.45	0.92 ± 0.06
	oxymetholone	0.73 ± 0.12	1.10 ± 0.08	0.57 ± 0.11	0.43 ± 0.06	0.46 ± 0.11	0.81 ± 0.11	0.92 ± 0.22	2.10 ± 0.54	0.95 ± 0.05
	mesterolone	2.30 ± 0.08	0.57 ± 0.03	2.30 ± 0.04	2.50 ± 0.17	2.70 ± 0.32	0.42 ± 0.04	0.70 ± 0.29	n.d.	0.30 ± 0.02
	mestanolone	2.00 ± 0.09	0.77 ± 0.06	1.90 ± 0.11	1.90 ± 0.33	1.70 ± 0.19	0.65 ± 0.05	0.81 ± 0.13	n.d.	0.50 ± 0.03
	methenolone	1.30 ± 0.17	0.98 ± 0.06	1.40 ± 0.16	1.80 ± 0.18	1.80 ± 0.21	0.84 ± 0.06	0.95 ± 0.29	n.d.	0.74 ± 0.06
	stanozolol	3.60 ± 0.35	2.80 ± 0.44	1.40 ± 0.10	1.60 ± 0.10	1.80 ± 0.41	0.62 ± 0.06	0.86 ± 0.18	0.65 ± 0.39	0.48 ± 0.03
	drostanolone	2.20 ± 0.22	1.40 ± 0.16	1.70 ± 0.16	1.60 ± 0.21	1.90 ± 0.31	0.85 ± 0.10	1.10 ± 0.27	0.82 ± 0.48	0.92 ± 0.10
	danazol	0.68 ± 0.06	0.41 ± 0.04	0.90 ± 0.03	0.89 ± 0.12	0.87 ± 0.16	0.30 ± 0.03	0.54 ± 0.14	0.57 ± 0.18	0.20 ± 0.03
	methandienone	1.80 ± 0.35	1.80 ± 0.31	1.20 ± 0.13	0.61 ± 0.08	0.83 ± 0.11	0.96 ± 0.10	0.78 ± 0.21	0.79 ± 0.34	1.20 ± 0.10
	boldenone	3.10 ± 0.30	2.80 ± 0.28	1.50 ± 0.09	0.95 ± 0.09	1.00 ± 0.15	1.00 ± 0.08	0.58 ± 0.12	0.78 ± 0.12	1.10 ± 0.05
	methasterone	1.20 ± 0.06	1.10 ± 0.09	1.30 ± 0.06	1.00 ± 0.10	0.99 ± 0.17	0.91 ± 0.05	0.88 ± 0.19	0.93 ± 0.15	0.85 ± 0.05
	oxystanolone	1.30 ± 0.04	1.00 ± 0.07	1.30 ± 0.05	1.20 ± 0.10	1.10 ± 0.13	0.91 ± 0.05	0.82 ± 0.17	0.82 ± 0.23	0.83 ± 0.05
	fluoxymesterone	1.00 ± 0.03	0.98 ± 0.04	0.98 ± 0.03	0.69 ± 0.15	1.20 ± 0.11	1.00 ± 0.13	1.20 ± 0.20	0.91 ± 0.12	0.95 ± 0.05
	nandrolone	1.20 ± 0.08	1.30 ± 0.07	1.20 ± 0.06	0.89 ± 0.07	0.75 ± 0.13	1.00 ± 0.08	0.88 ± 0.17	0.85 ± 0.22	1.20 ± 0.05
	norbolethone	1.00 ± 0.10	1.10 ± 0.11	1.00 ± 0.10	1.10 ± 0.08	1.20 ± 0.17	1.00 ± 0.09	1.20 ± 0.09	1.00 ± 0.11	1.00 ± 0.07
	oxandrolone	0.94 ± 0.03	1.10 ± 0.02	0.85 ± 0.05	0.75 ± 0.10	0.70 ± 0.15	0.98 ± 0.08	1.10 ± 0.20	1.40 ± 0.08	1.20 ± 0.03
	oxymesterone	1.10 ± 0.11	1.10 ± 0.07	0.97 ± 0.05	0.75 ± 0.07	0.77 ± 0.14	0.98 ± 0.14	1.00 ± 0.25	1.00 ± 0.17	1.00 ± 0.07
	trenbolone	1.00 ± 0.08	1.20 ± 0.09	0.97 ± 0.04	0.86 ± 0.05	0.76 ± 0.14	1.00 ± 0.09	1.10 ± 0.25	1.20 ± 0.28	1.20 ± 0.06
SARMs	LGD-2226	1.10 ± 0.03	0.96 ± 0.05	1.00 ± 0.03	1.20 ± 0.06	1.30 ± 0.19	0.89 ± 0.05	1.00 ± 0.20	0.84 ± 0.11	0.94 ± 0.03
	LGD-4033	0.98 ± 0.08	1.00 ± 0.14	0.96 ± 0.08	1.20 ± 0.07	1.40 ± 0.19	0.97 ± 0.07	1.20 ± 0.18	0.98 ± 0.15	1.00 ± 0.14
	ostarin	0.90 ± 0.06	0.94 ± 0.07	0.95 ± 0.06	1.10 ± 0.07	1.30 ± 0.18	0.93 ± 0.09	1.10 ± 0.19	0.86 ± 0.31	0.97 ± 0.08

Table 1. Effects of AAS and SARMs on steroid profile in H295R cells in the basal state. H295R cells were incubated for 48 h with vehicle (solvent control (SC); 0.01% DMSO) or the respective anabolic androgenic steroid (AAS) or selective androgen modulator (SARM) at a final concentration of 1 µM. Forskolin (10 µM) and prochloraz (1 µM) served as reference compound (RC). A complete medium control (MC; t = 0 h) taken at the start of the experiment was included for comparison. Steroid hormone levels were quantified by UHPLC-MS/MS. Data are expressed as fold changes relative to SC and are depicted as mean ± SD from three independent experiments, each performed in duplicate. Steroids significantly downregulated compared to SC are represented in green and those significantly upregulated in red. Differences with $p < 0.05$ were considered significant.

		progestins		mineralocorticoids			glucocorticoids		adrenal androgens	
	steroid / treatment	progesterone	17α-hydroxy-progesterone	11-deoxy-corticosterone	corticosterone	aldosterone	11-deoxycortisol	cortisol	dehydro-epiandrosterone	androstenedione
FC	forskolin 10 µM	1.00 ± 0.03	1.00 ± 0.03	1.00 ± 0.03	1.00 ± 0.05	1.00 ± 0.06	1.00 ± 0.05	1.00 ± 0.11	1.00 ± 0.05	1.00 ± 0.02
MC	complete medium; t=0	0.84 ± 0.07	n.d.	0.01 ± 0.00	n.d.	n.d.	0.01 ± 0.01	0.07 ± 0.04	n.d.	0.01 ± 0.00
AAS	clostebol	0.74 ± 0.06	1.10 ± 0.04	0.60 ± 0.07	0.28 ± 0.03	0.21 ± 0.03	0.98 ± 0.12	0.58 ± 0.21	2.60 ± 0.26	1.10 ± 0.10
AAS	turinabol	0.59 ± 0.09	0.96 ± 0.06	0.43 ± 0.10	0.19 ± 0.03	0.19 ± 0.04	0.72 ± 0.12	0.38 ± 0.12	3.10 ± 0.22	0.73 ± 0.12
AAS	oxymetholone	0.70 ± 0.08	0.90 ± 0.03	0.52 ± 0.12	0.50 ± 0.08	0.54 ± 0.06	0.89 ± 0.05	1.00 ± 0.36	2.60 ± 0.74	0.81 ± 0.07
AAS	mesterolone	2.10 ± 0.22	0.83 ± 0.09	2.20 ± 0.25	1.80 ± 0.19	2.10 ± 0.36	0.74 ± 0.02	0.73 ± 0.03	0.55 ± 0.11	0.52 ± 0.06
AAS	mestanolone	1.70 ± 0.22	1.00 ± 0.08	1.70 ± 0.19	1.40 ± 0.09	1.40 ± 0.13	0.90 ± 0.05	0.73 ± 0.16	0.86 ± 0.13	0.68 ± 0.08
AAS	methenolone	1.20 ± 0.12	0.97 ± 0.09	1.40 ± 0.24	1.40 ± 0.24	1.60 ± 0.14	0.95 ± 0.17	0.94 ± 0.04	0.85 ± 0.12	0.74 ± 0.10
AAS	stanozolol	3.30 ± 0.31	3.00 ± 0.29	1.40 ± 0.12	1.30 ± 0.12	1.40 ± 0.15	0.99 ± 0.04	1.00 ± 0.39	1.00 ± 0.12	0.61 ± 0.06
AAS	drostanolone	1.40 ± 0.14	1.10 ± 0.07	1.30 ± 0.13	1.20 ± 0.12	1.60 ± 0.13	1.10 ± 0.07	1.10 ± 0.46	0.94 ± 0.08	0.90 ± 0.09
AAS	danazol	1.30 ± 0.13	0.60 ± 0.03	1.40 ± 0.21	0.90 ± 0.09	1.10 ± 0.13	0.45 ± 0.06	0.31 ± 0.08	0.66 ± 0.07	0.20 ± 0.02
AAS	methandienone	1.20 ± 0.15	1.30 ± 0.11	1.00 ± 0.12	0.68 ± 0.06	0.68 ± 0.09	1.10 ± 0.08	0.69 ± 0.11	1.30 ± 0.18	1.10 ± 0.10
AAS	boldenone	1.60 ± 0.14	1.60 ± 0.07	1.30 ± 0.12	1.00 ± 0.07	0.92 ± 0.03	1.10 ± 0.10	0.84 ± 0.31	0.81 ± 0.12	0.97 ± 0.07
AAS	methasterone	1.00 ± 0.03	0.93 ± 0.07	1.20 ± 0.06	0.93 ± 0.10	1.20 ± 0.13	1.20 ± 0.10	0.84 ± 0.22	0.96 ± 0.12	0.86 ± 0.11
AAS	oxystanolone	1.10 ± 0.04	0.98 ± 0.09	1.10 ± 0.04	1.20 ± 0.15	1.20 ± 0.20	1.10 ± 0.08	1.10 ± 0.44	1.00 ± 0.25	0.92 ± 0.15
AAS	fluoxymesterone	0.98 ± 0.10	1.00 ± 0.07	1.00 ± 0.06	0.59 ± 0.08	1.10 ± 0.10	1.00 ± 0.11	0.94 ± 0.15	1.00 ± 0.17	1.10 ± 0.14
AAS	nandrolone	1.10 ± 0.12	1.10 ± 0.12	1.10 ± 0.13	1.10 ± 0.07	0.71 ± 0.08	1.10 ± 0.14	1.10 ± 0.29	1.10 ± 0.21	1.10 ± 0.12
AAS	norbolethone	0.92 ± 0.09	0.99 ± 0.08	0.98 ± 0.09	1.10 ± 0.04	1.10 ± 0.22	1.10 ± 0.17	0.96 ± 0.23	1.00 ± 0.16	1.00 ± 0.11
AAS	oxandrolone	0.89 ± 0.03	0.96 ± 0.08	0.79 ± 0.04	0.84 ± 0.10	0.86 ± 0.10	1.00 ± 0.05	1.10 ± 0.33	1.40 ± 0.35	0.99 ± 0.11
AAS	oxymesterone	0.92 ± 0.05	1.00 ± 0.07	0.91 ± 0.08	0.86 ± 0.04	0.86 ± 0.07	1.00 ± 0.09	0.96 ± 0.16	1.10 ± 0.10	1.00 ± 0.12
AAS	trenbolone	0.89 ± 0.10	1.10 ± 0.07	0.82 ± 0.08	0.95 ± 0.10	0.70 ± 0.11	1.10 ± 0.07	1.00 ± 0.33	1.40 ± 0.30	0.98 ± 0.10
SARMs	LGD-2226	1.00 ± 0.05	1.00 ± 0.07	1.00 ± 0.06	1.10 ± 0.13	1.30 ± 0.05	1.00 ± 0.10	1.00 ± 0.16	1.00 ± 0.15	0.96 ± 0.05
SARMs	LGD-4033	0.84 ± 0.08	0.94 ± 0.07	0.89 ± 0.05	0.97 ± 0.05	1.10 ± 0.10	0.91 ± 0.04	1.00 ± 0.14	1.10 ± 0.12	1.10 ± 0.13
SARMs	ostarin	0.91 ± 0.03	0.98 ± 0.05	0.97 ± 0.06	0.97 ± 0.10	1.10 ± 0.12	0.92 ± 0.07	0.97 ± 0.19	1.00 ± 0.13	1.10 ± 0.11

Table 2. Effects of AAS and SARMs on steroid profiles in forskolin-stimulated H295R cells.

H295R cells were incubated for 48 h with 10 µM forskolin (reference stimulating control, FC) and the corresponding anabolic androgenic steroid (AAS) or selective androgen receptor modulator (SARM) at a concentration of 1 µM. A complete medium control (MC; t = 0 h) was taken at the start of the experiment. Quantitative analysis of steroid levels was performed by UHPLC-MS/MS. Data obtained from three independent experiments, each performed in duplicate, were normalized to the respective steroid concentration in forskolin treated cells. Fold changes are shown as means ± SD and depicted in a color code: green represents significant downregulation and red significant upregulation compared to FC. Differences with $p < 0.05$ were considered significant.

Prochloraz, known to inhibit CYP17A1 and CYP21A2 [46], led to a pronounced accumulation of the adrenal precursor steroid progesterone and a more moderate increase in the intermediates 17α-hydroxyprogesterone and 11-deoxycorticosterone, whilst the levels of the adrenal androgens and mineralo- and glucocorticoids were significantly decreased.

Next, the effects of various AAS and SARMs were analyzed for their potential to interfere with adrenal steroidogenesis. The three AAS mesterolone, mestanolone and methenolone significantly enhanced the levels of mineralocorticoids but decreased adrenal androgens (Table 1 and 2). The steroid patterns obtained in unstimulated and forskolin-activated cells exhibited an important overlap. Furthermore, the patterns resembled the steroid profile observed for abiraterone [47], indicating decreased CYP17A1 activity as an underlying mechanism. Whereas treatment with mesterolone led to high levels of progesterone and decreased 17α-hydroxyprogesterone and 11-deoxycortisol, suggesting potent inhibition of CYP17A1 activity, mestanolone resulted in high progesterone levels but had slightly weaker effects on the production of 17α-hydroxyprogesterone and 11-deoxycortisol. Methenolone exhibited the weakest CYP17A1 inhibition with only a trend to increase progesterone production and no change in 17α-hydroxyprogesterone. The effect of mesterolone, mestanolone and methenolone on 17α-hydroxylase enzymatic activity was estimated as the ratio of the product 17α-hydroxyprogesterone and the substrate progesterone. Similarly, CYP17A1 17/20-lyase activity and total activity were assessed as the ratio of androstenedione/17α-hydroxyprogesterone and androstenedione/progesterone, respectively (Fig. 2). Total CYP17A1 activity was decreased by a compound-dependent manner, with mesterolone showing the most potent inhibition and methenolone the weakest. Interestingly, these three AAS lowered 17α-hydroxylase activity more efficiently than 17/20-lyase activity.

A significantly increased synthesis of mineralocorticoids was similarly observed with stanozolol and drostanolone both in unstimulated and stimulated cells (Table 1 and 2). In addition, both AAS significantly enhanced the production of progestins. However, whereas

stanozolol significantly decreased the levels of androstenedione, drostanolone did not affect adrenal androgen synthesis. Stanozolol and drostanolone could be distinguished by the ratios of 17α-hydroxyprogesterone to progesterone reflecting CYP17A1 17α-hydroxylase activity, and androstenedione to 17α-hydroxyprogesterone denoting 17/20-lyase activity. The data suggest that stanozolol lowers CYP17A1 activity mainly through inhibition of 17/20-lyase activity, whereas drostanolone equally affected 17/20-lyase and 17α-hydroxylase activities (Fig. 2).

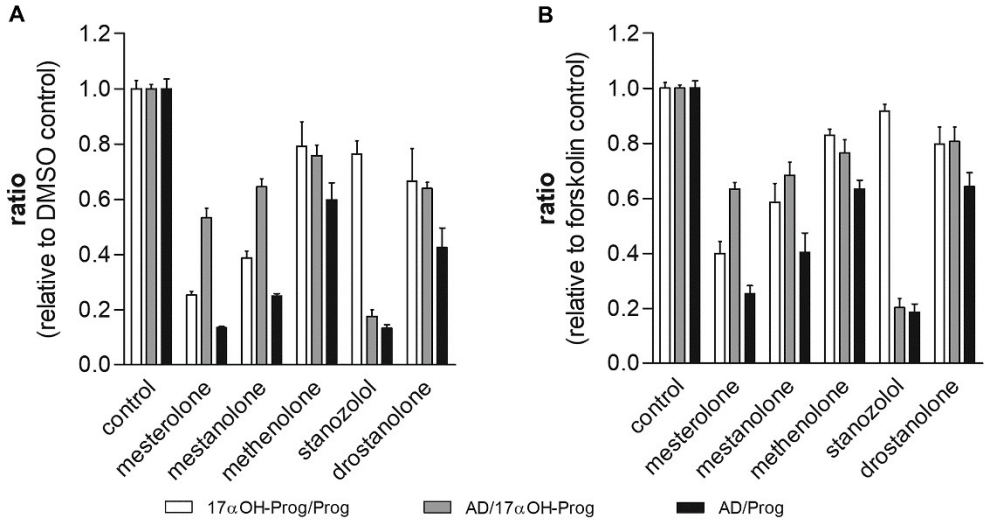

Fig. 2. Inhibition of apparent CYP17A1 enzyme activity by selected AAS. H295R cells in the basal (A) and forskolin-stimulated state (B) were incubated for 48 h with the indicated AAS at a concentration of 1 μM. Steroid metabolites were quantified using UHPLC-MS/MS and apparent CYP17A1 activities estimated from product to substrate ratios of secreted metabolites: 17α-hydroxyprogesterone/progesterone (17αOH-Prog/Prog, white bars) reflecting 17α-hydroxylase activity; androstenedione/17α-hydroxyprogesterone (AD/17αOH-Prog, grey bars) denoting CYP17,20-lyase activity; androstenedione/progesterone (AD/Prog, black bars) reporting total CYP17A1 activity.

A different steroid profile was observed upon treatment with clostebol, turinabol (clostebol acetate) and oxymetholone (Table 1 and 2). In cells in the basal state, these AAS led to significantly reduced levels of mineralocorticoids, enhanced dehydroepiandrosterone and a trend increase in 17α-hydroxyprogesterone. The observed steroid profiles resembled those obtained from cells in the forskolin-stimulated state, suggesting inhibition of CYP21A2 activity as mode-of-action. Since cortisol levels decreased or tended to decrease, an inhibition of CYP11B1/2 activity cannot be fully excluded.

All other AAS tested exerted very moderate effects (danazol, methandienone, boldenone, methasterone, oxystanolone and fluoxymesterone) or did not affect the steroid profiles (nandrolone, norbolethone, oxandrolone, oxymesterone and trenbolone) in unstimulated and stimulated cells. In particular, none of the tested SARMs (LGD-2226, LGD-4033 and ostarin) showed any effect on adrenal steroidogenesis.

3.3. *Evaluation of the effects of selected AAS on the mRNA expression of steroidogenic enzymes*

To test whether altered expression of steroidogenic enzymes contributed to the observed effects on the steroid profiles by the identified AAS (mesterolone, mestanolone, methenolone, clostebol, oxymetholone, stanozolol, and drostanolone), H295R cells were incubated with these AAS for 48 h and mRNA levels of *3β-HSD2*, *CYP17A1*, *CYP21A2*, *CYP11B1* and *CYP11B2* were determined by qPCR. At concentrations of 1 µM, none of the selected AAS affected the mRNA expression levels of the five key steroidogenic genes as compared to the DMSO vehicle control (data not shown).

3.4. *Effects of selected AAS on CYP17A1 17α-hydroxylase activity*

Next, the impact of mesterolone, mestanolone, methenolone, stanozolol and drostanolone on the conversion of progesterone to 17α-hydroxyprogesterone and the byproduct 16α-hydroxyprogesterone were tested in a cell-free CYP17A1 activity assay. Abiraterone served as a reference compound exhibiting an IC_{50} value of 15.6 nM. At a high concentration of 5 µM, the selected AAS showed very weak (mesterolone: less than 20% inhibition) or no inhibition (mestanolone, methenolone, stanozolol and drostanolone) of CYP17A1 17α-hydroxylase activity (data not shown).

3.5. *Predicted binding of the selected AAS to CYP17A1 and CYP21A2*

The potent irreversible inhibition of CYP17A1 by abiraterone is characterized by two key interactions: first, the heme iron forming a covalent coordinating bond with the nitrogen in the heterocycle of abiraterone, and second, the hydrogen bond between the C3-hydroxyl of abiraterone and the side chain of Asn^{202} in helix F, at a distance of 2.6 Å [41, 48] (Fig. 3). Additionally, hydrophobic interactions of the heterocycle ring and the two methyl groups with hydrophobic side chains of several residues on CYP17A1 contribute to the stabilization of abiraterone binding (Fig. 3C). The docking calculations predicted a similar binding mode for mesterolone and mestanolone but with an inverted orientation of the steroid backbone compared to abiraterone where the C3-carbonyl forms an interaction with the heme iron (Fig. 3A, B, D, E). Additionally, some stabilizing hydrophobic interactions by the methyl groups could be identified; however, the key stabilizing hydrogen bond interaction with Asn^{202} is absent and no hydrogen bonds of the C17-hydroxyl with CYP17A1 residues at a distance closer than 5 Å could be found. Methenolone showed even weaker effects on CYP17A1 activity in the H295R assay and docking calculations also did not reveal any stabilizing interactions with Asn^{202} (data not shown).

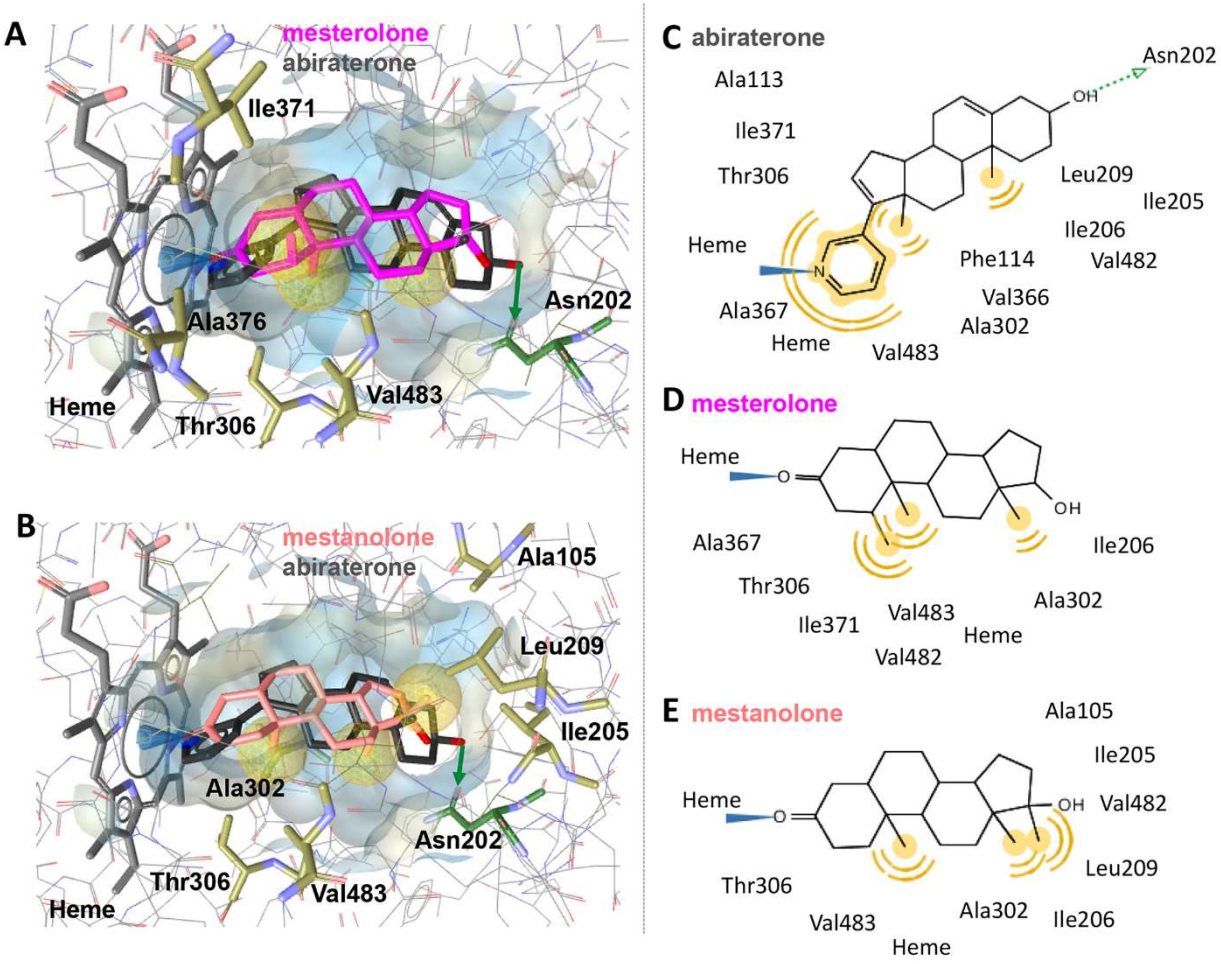

Fig. 3. Docking of mesterolone, mestanolone and abiraterone into the binding site of CYP17A1. The automatically generated pharmacophore maps the structural details of the compound for binding (yellow spheres: hydrophobic interactions; blue cone: iron binding location; green arrow: hydrogen bond donor). Binding mode of docked mesterolone (A) and mestanolone (B) together with co-crystallized abiraterone in CYP17A1. (A) and (B) show the iron binding interaction and hydrophobic features of the two AAS (not shown for abiraterone). The hydrogen bond of abiraterone with Asn^{202} is indicated, while the two AAS do not form a similar hydrogen bond. Two-dimensional representation of the binding interactions of abiraterone (C), mesterolone (D) and mestanolone (E).

17α-hydroxyprogesterone binding to CYP21A2 is characterized by a hydrogen bond (2.5 Å) of the C3-carbonyl on the A-ring with the guanidinium group on the Arg^{234} side chain (Fig. 4). The A-ring of 17α-hydroxyprogesterone is anchored by helix G such that the C21-methyl group faces the heme iron [49], facilitating C21-hydroxylation. Clostebol and oxymetholone, in all predictions, showed a 180° flipped orientation compared to 17α-hydroxyprogesterone with the A-ring facing the heme. Clostebol and oxymetholone showed an interaction with the heme iron. Furthermore, both steroids, like 17α-hydroxyprogesterone, are stabilized by the formation of a hydrogen bond with Arg^{234} (distance to Arg^{234} for clostebol of 2.93 Å and for oxymetholone of 3.14 Å). Moreover, all three steroids formed similar hydrophobic stabilizing interactions.

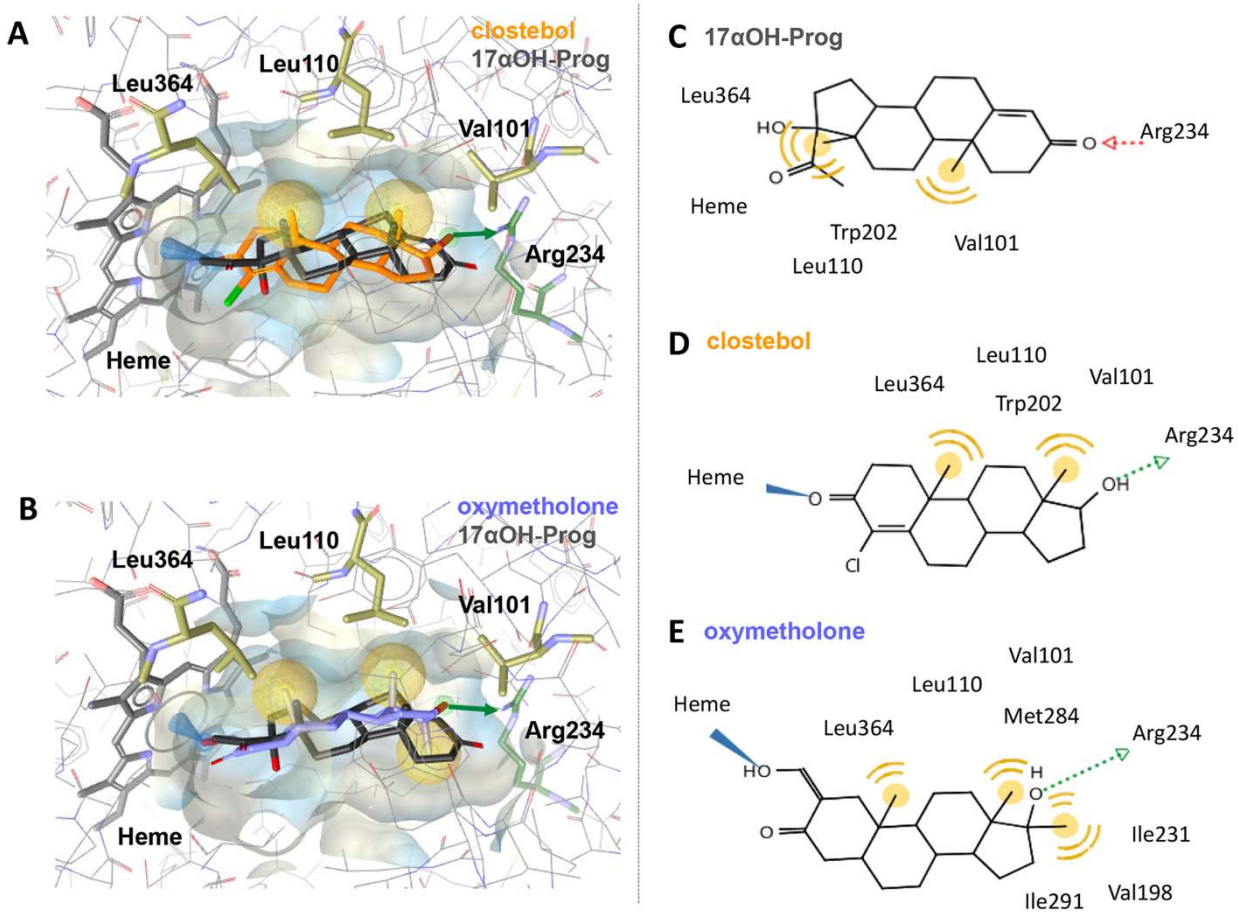

Fig. 4. Predicted binding of clostebol, oxymetholone and 17α-hydroxyprogesterone in CYP21A2.

The pharmacophore maps the structural details of the compound for binding (yellow spheres: hydrophobic interactions; blue cone: iron binding interaction; green arrow: hydrogen bond donor; red arrow: hydrogen bond acceptor). Binding mode of docked clostebol (A) and oxymetholone (B) together with co-crystallized 17α-hydroxyprogesterone (17αOH-Prog) in CYP21A2. (A) and (B) show the iron binding interaction, hydrophobic features and hydrogen bond of the two AAS (not shown for 17αOH-Prog). Two-dimensional representation of the binding interactions of 17αOH-Prog (C), clostebol (D) and oxymetholone (E).

4. Discussion

Evaluation of adverse cardiovascular effects associated with AAS use has mainly focused on heart structure and function by performing echocardiographic examinations. Increases in blood pressure are generally assumed to be due to enhanced cardiac output, arterial stiffness and peripheral arterial resistance [50, 51]. Another mechanism by which AAS might contribute to the development of hypertension and cardiovascular diseases includes the interference with adrenal steroidogenesis [35], leading to enhanced mineralocorticoid synthesis. An excess of mineralocorticoids is associated with an exaggerated activation of MR, which in turn contribute to increased blood pressure and cardiovascular diseases [52, 53].

The androgen derivative abiraterone is a drug well known to interfere with steroidogenesis, causing mineralocorticoid excess and resulting in hypertension and hypokalemia [33, 54]. Abiraterone is a drug designed to treat prostate cancer by suppressing testosterone synthesis through inhibition of CYP17A1, thereby blocking gonadal and adrenal androgen production. As a side effect of CYP17A1 inhibition, cortisol production is decreased. This results in an excessive activation of the hypothalamic-pituitary-adrenal (HPA) axis and elevated ACTH release in an attempt to correct for the lack of cortisol along with an excessive production of the mineralocorticoid aldosterone. To avoid the mineralocorticoid excess-related side effects of abiraterone, patients are co-administered prednisone to prevent the excessive HPA axis activation and ACTH release [55]. While patients receiving AAS in a therapeutic situation can be monitored for symptoms of mineralocorticoid excess (pseudo-hyperaldosteronism, hypertension, hypokalemia), this is not the case for recreational users. Their uncontrolled use of supraphysiologic AAS doses exposes them to serious health risks.

Despite the well-described adverse health events of AAS, very few of them have been assessed for their impact on adrenal steroidogenesis and the mechanisms of action of such compounds is poorly investigated. To our knowledge, this study is the first to compare numerous well-

known and widely used AAS as well as three non-steroidal SARMs with respect to their potential to interfere with adrenal steroid synthesis.

This analysis revealed three AAS (mesterolone, mestanolone and methenolone) exhibiting effects on the steroid profile of H295R cells in the basal state and upon forskolin-stimulation that resemble those of abiraterone [47], namely increased mineralocorticoids and decreased androgens. The similar bioactivity of these three AAS may be explained by their related chemical structures. They share C3-carbonyl and C17-hydroxyl groups. Mestanolone differs from mesterolone only by the lack or presence of a methyl group in C5 and C17, respectively. Moreover, methenolone has a double bond between C1 and C2 that is absent in mesterolone. The observed steroid profiles indicated decreased CYP17A1 enzyme activity (Table 1 and 2), mainly affecting 17α-hydroxylase activity, in the order mesterolone > mestanolone > methenolone (Fig. 2).

The mechanism by which these three AAS decrease CYP17A1 activity is distinct from that of abiraterone. Whereas abiraterone was found to irreversibly inhibit CYP17A1 activity by direct interaction with the substrate binding pocket due to its 16,17-double bond [56], mesterolone, mestanolone and methenolone lacking this important structural feature were unable to inhibit CYP17A1 17α-hydroxylase activity in a cell-free enzyme assay (not shown). Molecular docking indicated the lack of a stabilizing hydrogen bond between the C17-hydroxyl of mesterolone and mestanolone with residues on CYP17A1 such as Asn^{202} that forms a key interaction with the C3-hydroxyl of abiraterone (Fig. 3). Thus, the predicted lack of important stabilizing interactions is in line with the results of the activity assay that do not support a direct inhibition of CYP17A1 by these AAS. Moreover, gene expression analysis did not reveal an effect of mesterolone, mestanolone and methenolone on CYP17A1 mRNA levels, implying post-translational effects. Thus, further research should focus on post-translational modifications such as phosphorylation and glycosylation and on protein stability that have been found earlier to be involved in the regulation of CYP17A1 activity [57-61].

Increased mineralocorticoid but decreased androstenedione production was also observed for stanozolol (Table 1 and 2), with a strongly decreased androstenedione/17α-hydroxyprogesterone ratio, indicating inhibition of CYP17/20-lyase activity (Fig. 2). Stanozolol did not inhibit CYP17A1 17α-hydroxylase activity in the cell-free assay; however, since the 17/20-lyase reaction needs the allosteric action of cytochrome b5 to promote the interaction of CYP17A1 with P450 oxidoreductase (POR) [62, 63], our cell-free CYP17A1 activity assay did not consider 17/20-lyase activity. Drostanolone, which enhanced mineralocorticoid synthesis but showed little effect on androgen production, modestly decreased CYP17A1 activity in the cell-free assay. Both stanozolol and drostanolone did not alter the expression of steroidogenic genes. Thus, an enhanced mineralocorticoid production due to increased CYP11B2 gene expression, such as observed in an earlier study for the UV-filter octylmethoxycinnamate [36], seems unlikely. A limitation of the gene expression analysis includes the late time point, after 48 h of treatment, and it cannot be excluded that mRNA levels were altered at an earlier time point and returned to normal after 48 h. Further research is needed to uncover the mechanism of enhanced aldosterone production by stanozolol and drostanolone. The results of the current study show a direct effect of particular AAS on adrenal steroidogenesis to enhance aldosterone production. Aldosterone acts through mineralocorticoid receptors and regulates salt and water homeostasis and redox processes [64]. The uncontrolled and prolonged use of such AAS may cause excessive aldosterone secretion, increasing blood volume and blood pressure, decreasing potassium levels and promoting oxidative stress, thereby contributing to the development of cardiovascular diseases.

A different steroid pattern was observed for clostebol, turinabol and oxymetholone (Table 1 and 2). Considering that turinabol (clostebol acetate) is the non-active esterified pro-drug of clostebol and that such esters are rapidly hydrolyzed to the free active form, explains the almost identical steroid profiles obtained for these two compounds. Suppressed corticosteroid production along with increased dehydroepiandrosterone levels indicate inhibition of

CYP21A2 activity. Since there is no cell-free CYP21A2 activity assay available, molecular docking calculations were performed. Strong stabilizing interactions were found for clostebol and oxymetholone, supporting direct CYP21A2 inhibition (Fig. 4). Future work needs to establish a cell-free CYP21A2 activity assay and address the issue of direct or indirect inhibition.

In vivo, an inhibition of adrenal corticosteroid synthesis, as suggested for clostebol, turinabol and oxymetholone, is expected to result in negative feedback-mediated HPA axis activation, ultimately leading to adrenal hyperplasia. Consequently, the increased levels of steroid precursors may be mainly converted to androgens, as it is the case in patients with 21-hydroxylase deficiency suffering from congenital adrenal hyperplasia (CAH). A deficiency of gluco- and mineralocorticoids causes severe metabolic disturbances, ultimately leading to life-threatening adrenal crisis [65].

Not all of the tested AAS affected the adrenal steroid profile. While some of them exhibited only minor effects, one third showed no significant changes on steroid levels. Since AAS have been designed to act through the AR and only differ in their relative binding affinity, the observed effects on the adrenal steroid pattern are most likely AR-independent. In line with this, none of the SARMs tested interfered with adrenal steroidogenesis. Whereas the steroidal scaffold of the AAS bears a higher risk for interference with other steroid hormone receptors and steroid metabolizing enzymes, including steroidogenic CYPs, the non-steroidal SARMs possess an improved risk profile and should be preferably considered in clinical applications.

The (adverse) effects of AAS depend on the concentrations reached *in vivo* at the site of a given enzyme or receptor. To our knowledge, there are no data available on intra-adrenal concentrations of AAS and exposure has to be estimated from plasma levels. For example, plasma levels of testosterone undecanoate, the active ingredient of Andriol® Testocaps®, reach about 10 to 35 nmol/L (300-1000 ng/dL) and are considered to be within accepted therapeutic range [66, 67]. Bearing in mind that supraphysiologic AAS doses in non-therapeutic uses can

reach up to 100 times physiologic levels, the concentration of the AAS used in the present study may be achieved in AAS abusers. Although quantitative *in vitro* to *in vivo* extrapolation of concentration-effect correlations can be problematic, the concentrations used herein, causing significant effects on adrenal steroidogenesis, might be relevant in situations of AAS misuse. An obvious limitation of the current study is the lack of negative feedback regulation by the HPA axis in the adrenal cell model applied. Another limitation, regarding the analysis of the underlying mechanisms, includes that only one time point (48 h) was considered, and follow-on work will need to address earlier time points; nevertheless, initial mechanistic information could be gathered.

In conclusion, the use of H295R cells in their basal and forskolin-stimulated state together with the simultaneous quantification of the most important adrenal steroids by UHPLC-MS/MS allowed the detection of compound-specific interferences with adrenal steroidogenesis and provided preliminary information on the mode-of-action. The comparison of a series of AAS and SARMs in the same study allowed grouping compounds causing similar effects and potentially sharing the same mechanism. Mesterolone, mestanolone and methenolone were found to enhance mineralocorticoid and reduce adrenal androgen production by decreasing CYP17A1 activity, whereas clostebol, turinabol and oxymetholone lowered corticosteroid and enhanced dehydroepiandrosterone synthesis, likely via inhibition of CYP21A2. The non-steroidal SARMs displayed a more favorable safety profile than most of the AAS and they should be considered as preferred treatment option for various muscle wasting conditions.

Conflicts of Interest

Chris J. van Koppen was an employee of elexopharm, Germany, and Matthias Grill of Lipomed AG, Switzerland. The other authors declare no conflict of interest.

Acknowledgements

This work was supported by the Swiss Centre for Applied Human Toxicology (SCAHT). We thank Dr. Denise V. Kratschmar for advice in LC-MS analytics. We are grateful to Prof. Thierry Langer, University of Vienna, and Inte:Ligand GmbH, for providing the LigandScout software.

References

[1] S. Basaria, J.T. Wahlstrom, A.S. Dobs, Anabolic-Androgenic Steroid Therapy in the Treatment of Chronic Diseases, The Journal of Clinical Endocrinology & Metabolism 86(11) (2001) 5108-5117.

[2] U.R. Hengge, M. Baumann, R. Maleba, N.H. Brockmeyer, M. Goos, Oxymetholone promotes weight gain in patients with advanced human immunodeficiency virus (HIV-1) infection, The British journal of nutrition 75(1) (1996) 129-38.

[3] S. Bhasin, T.W. Storer, M. Javanbakht, N. Berman, K.E. Yarasheski, J. Phillips, M. Dike, I. Sinha-Hikim, R. Shen, R.D. Hays, G. Beall, Testosterone replacement and resistance exercise in HIV-infected men with weight loss and low testosterone levels, Jama 283(6) (2000) 763-70.

[4] J. Gold, M.J. Batterham, H. Rekers, M.K. Harms, T.B. Geurts, P.M. Helmyr, J. Silva de Mendonca, L.H. Falleiros Carvalho, G. Panos, A. Pinchera, F. Aiuti, C. Lee, A. Horban, J. Gatell, P. Phanuphak, W. Prasithsirikul, B. Gazzard, M. Bloch, S.A. Danner, Effects of nandrolone decanoate compared with placebo or testosterone on HIV-associated wasting, HIV medicine 7(3) (2006) 146-55.

[5] S. Bhasin, O.M. Calof, T.W. Storer, M.L. Lee, N.A. Mazer, R. Jasuja, V.M. Montori, W. Gao, J.T. Dalton, Drug insight: Testosterone and selective androgen receptor modulators as anabolic therapies for chronic illness and aging, Nature clinical practice. Endocrinology & metabolism 2(3) (2006) 146-59.

[6] I.M. Ferreira, I.T. Verreschi, L.E. Nery, R.S. Goldstein, N. Zamel, D. Brooks, J.R. Jardim, The influence of 6 months of oral anabolic steroids on body mass and respiratory muscles in undernourished COPD patients, Chest 114(1) (1998) 19-28.

[7] R.H. Demling, The role of anabolic hormones for wound healing in catabolic states, Journal of burns and wounds 4 (2005) e2.
[8] S. Bhasin, J.P. Brito, G.R. Cunningham, F.J. Hayes, H.N. Hodis, A.M. Matsumoto, P.J. Snyder, R.S. Swerdloff, F.C. Wu, M.A. Yialamas, Testosterone Therapy in Men With Hypogonadism: An Endocrine Society Clinical Practice Guideline, The Journal of clinical endocrinology and metabolism 103(5) (2018) 1715-1744.
[9] G. Hackett, M. Kirby, D. Edwards, T.H. Jones, K. Wylie, N. Ossei-Gerning, J. David, A. Muneer, British Society for Sexual Medicine Guidelines on Adult Testosterone Deficiency, With Statements for UK Practice, The journal of sexual medicine 14(12) (2017) 1504-1523.
[10] G.O. Potts, A. Arnold, A.L. Beyler, Dissociation of the Androgenic and Other Hormonal Activities from the Protein Anabolic Effects of Steroids, in: C.D. Kochakian (Ed.), Anabolic-Androgenic Steroids, Springer Berlin Heidelberg, Berlin, Heidelberg, 1976, pp. 361-406.
[11] W. Gao, P.J. Reiser, C.C. Coss, M.A. Phelps, J.D. Kearbey, D.D. Miller, J.T. Dalton, Selective Androgen Receptor Modulator Treatment Improves Muscle Strength and Body Composition and Prevents Bone Loss in Orchidectomized Rats, Endocrinology 146(11) (2005) 4887-4897.
[12] C.L. Smith, B.W. O'Malley, Coregulator Function: A Key to Understanding Tissue Specificity of Selective Receptor Modulators, Endocrine reviews 25(1) (2004) 45-71.
[13] NIH, U.S., National, Library, of, Medicine, Clinical Trials, [Online] https://www.clinicaltrials.gov [Accessed: September, 2019].
[14] World, Anti-Doping, Agency, Adverse analytical findings reported by accredited laboratories, [Online]http://www.wada-ama.org/sites/default/files/resources/files/2017_anti-doping_testing_figures_en_0.pdf (2017) [Accessed: November, 2018].
[15] G. Kanayama, H.G. Pope, History and epidemiology of anabolic androgens in athletes and non-athletes, Molecular and Cellular Endocrinology 464 (2018) 4-13.
[16] J.E. Schulenberg, L.D. Johnston, P.M. O'Malley, J.G. Bachman, R.A. Miech, M.E. Patrick, Monitoring the Future - National Survey Results on Drug Use: College Students and Adults Ages 19-55, [Online] http://monitoringthefuture.org//pubs/monographs/mtf-vol2_2017.pdf (2017) [Accessed: November, 2018].
[17] A. Donati, World traffic in doping substances, [Online] https://www.wada-ama.org/sites/default/files/resources/files/WADA_Donati_Report_On_Trafficking_2007.pdf (2007) [Accessed: November, 2018].
[18] H. Leifman, C. Rehnman, E. Sjöblom, S. Holgersson, Anabolic androgenic steroids--use and correlates among gym users--an assessment study using questionnaires and observations at

gyms in the Stockholm region, International journal of environmental research and public health 8(7) (2011) 2656-2674.
[19] M.R. Graham, B. Davies, F.M. Grace, A. Kicman, J.S.J.S.M. Baker, Anabolic Steroid Use, 38(6) (2008) 505-525.
[20] J.D. Wilson, Androgen abuse by athletes, Endocrine reviews 9(2) (1988) 181-99.
[21] A.J. Trenton, G.W.J.C.D. Currier, Behavioural Manifestations of Anabolic Steroid Use, 19(7) (2005) 571-595.
[22] D.R. Mottram, A.J. George, Anabolic steroids, Bailliere's best practice & research. Clinical endocrinology & metabolism 14(1) (2000) 55-69.
[23] H.G. Pope, Jr., R.I. Wood, A. Rogol, F. Nyberg, L. Bowers, S. Bhasin, Adverse health consequences of performance-enhancing drugs: an Endocrine Society scientific statement, Endocrine reviews 35(3) (2014) 341-75.
[24] C. Maravelias, A. Dona, M. Stefanidou, C. Spiliopoulou, Adverse effects of anabolic steroids in athletes: A constant threat, Toxicology letters 158(3) (2005) 167-175.
[25] A. Buttner, D. Thieme, Side effects of anabolic androgenic steroids: pathological findings and structure-activity relationships, Handb Exp Pharmacol (195) (2010) 459-84.
[26] P. Vanberg, D. Atar, Androgenic anabolic steroid abuse and the cardiovascular system, Handb Exp Pharmacol (195) (2010) 411-57.
[27] M.L. Sullivan, C.M. Martinez, P. Gennis, E.J. Gallagher, The cardiac toxicity of anabolic steroids, Progress in cardiovascular diseases 41(1) (1998) 1-15.
[28] J.E. Carroll, T.L. Goodfriend, Androgen modulation of adrenal angiotensin receptors, Science 224(4652) (1984) 1009-11.
[29] A.C. Brownie, S. Gallant, P.A. Nickerson, L.M. Joseph, The Occurrence of 11-Deoxycorticosterone (DOC)-Induced Hypertension in the Long-Evans Rat, Endocrine Research Communications 5(1) (1978) 71-80.
[30] S. Gallant, J. Alfano, M. Charpin, A.C. Brownie, The inhibition of rat adrenal cytochrome P-45011 beta gene expression by androgens, Endocr Res 18(2) (1992) 145-61.
[31] E.G. Biglieri, M.A. Herron, N. Brust, 17-hydroxylation deficiency in man, The Journal of Clinical Investigation 45(12) (1966) 1946-1954.
[32] O. Goldsmith, D.H. Solomon, R. Horton, Hypogonadism and Mineralocorticoid Excess, New England Journal of Medicine 277(13) (1967) 673-677.
[33] G. Attard, A.H. Reid, T.A. Yap, F. Raynaud, M. Dowsett, S. Settatree, M. Barrett, C. Parker, V. Martins, E. Folkerd, J. Clark, C.S. Cooper, S.B. Kaye, D. Dearnaley, G. Lee, J.S. de Bono, Phase I clinical trial of a selective inhibitor of CYP17, abiraterone acetate, confirms that

castration-resistant prostate cancer commonly remains hormone driven, Journal of clinical oncology : official journal of the American Society of Clinical Oncology 26(28) (2008) 4563-71.
[34] A. Pia, F. Vignani, G. Attard, M. Tucci, P. Bironzo, G. Scagliotti, W. Arlt, M. Terzolo, A. Berruti, Strategies for managing ACTH dependent mineralocorticoid excess induced by abiraterone, Cancer Treat Rev 39(8) (2013) 966-73.
[35] K.R. Beck, G.R. Thompson, 3rd, A. Odermatt, Drug-induced endocrine blood pressure elevation, Pharmacol Res (2019) 104311.
[36] P. Strajhar, D. Tonoli, F. Jeanneret, R.M. Imhof, V. Malagnino, M. Patt, D.V. Kratschmar, J. Boccard, S. Rudaz, A. Odermatt, Steroid profiling in H295R cells to identify chemicals potentially disrupting the production of adrenal steroids, Toxicology 381 (2017) 51-63.
[37] OECD, OECD guideline for the testing of chemicals. Test No. 456: H295R Steroidogenesis Assay, OECD Guidelines for the Testing of Chemicals, Section 4: Health Effects (2011).
[38] M. Akram, M. Patt, T. Kaserer, V. Temml, W. Waratchareeyakul, D.V. Kratschmar, J. Haupenthal, R.W. Hartmann, A. Odermatt, D. Schuster, Identification of the fungicide epoxiconazole by virtual screening and biological assessment as inhibitor of human 11beta-hydroxylase and aldosterone synthase, The Journal of steroid biochemistry and molecular biology (2019).
[39] P.B. Ehmer, J. Jose, R.W. Hartmann, Development of a simple and rapid assay for the evaluation of inhibitors of human 17alpha-hydroxylase-C(17,20)-lyase (P450cl7) by coexpression of P450cl7 with NADPH-cytochrome-P450-reductase in Escherichia coli, The Journal of steroid biochemistry and molecular biology 75(1) (2000) 57-63.
[40] T.U. Hutschenreuter, P.B. Ehmer, R.W. Hartmann, Synthesis of hydroxy derivatives of highly potent non-steroidal CYP 17 inhibitors as potential metabolites and evaluation of their activity by a non cellular assay using recombinant human enzyme, J Enzyme Inhib Med Chem 19(1) (2004) 17-32.
[41] N.M. DeVore, E.E. Scott, Structures of cytochrome P450 17A1 with prostate cancer drugs abiraterone and TOK-001, Nature 482(7383) (2012) 116-9.
[42] C. Wang, P.S. Pallan, W. Zhang, L. Lei, F.K. Yoshimoto, M.R. Waterman, M. Egli, F.P. Guengerich, Functional analysis of human cytochrome P450 21A2 variants involved in congenital adrenal hyperplasia, The Journal of biological chemistry 292(26) (2017) 10767-10778.

[43] G. Jones, P. Willett, R.C. Glen, A.R. Leach, R. Taylor, Development and validation of a genetic algorithm for flexible docking, Journal of molecular biology 267(3) (1997) 727-48.
[44] G. Wolber, T. Langer, LigandScout: 3-D pharmacophores derived from protein-bound ligands and their use as virtual screening filters, Journal of chemical information and modeling 45(1) (2005) 160-9.
[45] C. Pinto, D. Papa, M. Hubner, T.C. Mou, G.H. Lushington, R. Seifert, Activation and inhibition of adenylyl cyclase isoforms by forskolin analogs, J Pharmacol Exp Ther 325(1) (2008) 27-36.
[46] A. Ohlsson, E. Ulleras, A. Oskarsson, A biphasic effect of the fungicide prochloraz on aldosterone, but not cortisol, secretion in human adrenal H295R cells--underlying mechanisms, Toxicology letters 191(2-3) (2009) 174-80.
[47] A. Mangelis, P. Dieterich, M. Peitzsch, S. Richter, R. Juhlen, A. Hubner, H.S. Willenberg, A. Deussen, J.W. Lenders, G. Eisenhofer, Computational analysis of liquid chromatography-tandem mass spectrometric steroid profiling in NCI H295R cells following angiotensin II, forskolin and abiraterone treatment, The Journal of steroid biochemistry and molecular biology 155(Pt A) (2016) 67-75.
[48] R. Yadav, E.M. Petrunak, D.F. Estrada, E.E. Scott, Structural insights into the function of steroidogenic cytochrome P450 17A1, Mol Cell Endocrinol 441 (2017) 68-75.
[49] B. Zhao, L. Lei, N. Kagawa, M. Sundaramoorthy, S. Banerjee, L.D. Nagy, F.P. Guengerich, M.R. Waterman, Three-dimensional structure of steroid 21-hydroxylase (cytochrome P450 21A2) with two substrates reveals locations of disease-associated variants, The Journal of biological chemistry 287(13) (2012) 10613-22.
[50] M.E. Safar, J.P. Lehner, M.I. Vincent, M.T. Plainfosse, A.C. Simon, Echocardiographic dimensions in borderline and sustained hypertension, The American journal of cardiology 44(5) (1979) 930-5.
[51] A. Beutel, C.T. Bergamaschi, R.R. Campos, Effects of chronic anabolic steroid treatment on tonic and reflex cardiovascular control in male rats, The Journal of steroid biochemistry and molecular biology 93(1) (2005) 43-8.
[52] G. Lastra, S. Dhuper, M.S. Johnson, J.R. Sowers, Salt, aldosterone, and insulin resistance: impact on the cardiovascular system, Nature reviews. Cardiology 7(10) (2010) 577-84.
[53] M. Briet, E.L. Schiffrin, Aldosterone: effects on the kidney and cardiovascular system, Nature reviews. Nephrology 6(5) (2010) 261-73.
[54] J.S. de Bono, C.J. Logothetis, A. Molina, K. Fizazi, S. North, L. Chu, K.N. Chi, R.J. Jones, O.B. Goodman, Jr., F. Saad, J.N. Staffurth, P. Mainwaring, S. Harland, T.W. Flaig, T.E. Hutson,

T. Cheng, H. Patterson, J.D. Hainsworth, C.J. Ryan, C.N. Sternberg, S.L. Ellard, A. Flechon, M. Saleh, M. Scholz, E. Efstathiou, A. Zivi, D. Bianchini, Y. Loriot, N. Chieffo, T. Kheoh, C.M. Haqq, H.I. Scher, Abiraterone and increased survival in metastatic prostate cancer, The New England journal of medicine 364(21) (2011) 1995-2005.

[55] K. Fizazi, N. Tran, L. Fein, N. Matsubara, A. Rodriguez-Antolin, B.Y. Alekseev, M. Ozguroglu, D. Ye, S. Feyerabend, A. Protheroe, P. De Porre, T. Kheoh, Y.C. Park, M.B. Todd, K.N. Chi, Abiraterone plus Prednisone in Metastatic, Castration-Sensitive Prostate Cancer, The New England journal of medicine 377(4) (2017) 352-360.

[56] M. Jarman, S.E. Barrie, J.M. Llera, The 16,17-double bond is needed for irreversible inhibition of human cytochrome p45017alpha by abiraterone (17-(3-pyridyl)androsta-5, 16-dien-3beta-ol) and related steroidal inhibitors, Journal of medicinal chemistry 41(27) (1998) 5375-81.

[57] J.B. Lohr, W.N. Kuhn-Velten, Protein phosphorylation changes ligand-binding efficiency of cytochrome P450c17 (CYP17) and accelerates its proteolytic degradation: putative relevance for hormonal regulation of CYP17 activity, Biochemical and biophysical research communications 231(2) (1997) 403-8.

[58] A.V. Pandey, S.H. Mellon, W.L. Miller, Protein phosphatase 2A and phosphoprotein SET regulate androgen production by P450c17, The Journal of biological chemistry 278(5) (2003) 2837-44.

[59] M.K. Tee, W.L. Miller, Phosphorylation of human cytochrome P450c17 by p38alpha selectively increases 17,20 lyase activity and androgen biosynthesis, The Journal of biological chemistry 288(33) (2013) 23903-13.

[60] L.H. Zhang, H. Rodriguez, S. Ohno, W.L. Miller, Serine phosphorylation of human P450c17 increases 17,20-lyase activity: implications for adrenarche and the polycystic ovary syndrome, Proceedings of the National Academy of Sciences of the United States of America 92(23) (1995) 10619-23.

[61] S. Nakajin, P.F. Hall, Microsomal cytochrome P-450 from neonatal pig testis. Purification and properties of A C21 steroid side-chain cleavage system (17 alpha-hydroxylase-C17,20 lyase), The Journal of biological chemistry 256(8) (1981) 3871-6.

[62] M. Onoda, P.F. Hall, Cytochrome b5 stimulates purified testicular microsomal cytochrome P-450 (C21 side-chain cleavage), Biochemical and biophysical research communications 108(2) (1982) 454-460.

[63] A.V. Pandey, W.L. Miller, Regulation of 17,20 lyase activity by cytochrome b5 and by serine phosphorylation of P450c17, The Journal of biological chemistry 280(14) (2005) 13265-71.
[64] A. Odermatt, A.G. Atanasov, Mineralocorticoid receptors: emerging complexity and functional diversity, Steroids 74(2) (2009) 163-71.
[65] P.W. Speiser, R. Azziz, L.S. Baskin, L. Ghizzoni, T.W. Hensle, D.P. Merke, H.F.L. Meyer-Bahlburg, W.L. Miller, V.M. Montori, S.E. Oberfield, M. Ritzen, P.C. White, Congenital Adrenal Hyperplasia Due to Steroid 21-Hydroxylase Deficiency: An Endocrine Society Clinical Practice Guideline, The Journal of Clinical Endocrinology & Metabolism 95(9) (2010) 4133-4160.
[66] Merck, Canada, Inc., Andriol - Product Monograph, [Online] https://www.merck.ca/static/pdf/ANDRIOL-PM_E.pdf (2017) [Accessed: September, 2019].
[67] A.Y. Yin, M. Htun, R.S. Swerdloff, M. Diaz-Arjonilla, R.E. Dudley, S. Faulkner, R. Bross, A. Leung, S. Baravarian, L. Hull, J.A. Longstreth, S. Kulback, G. Flippo, C. Wang, Reexamination of pharmacokinetics of oral testosterone undecanoate in hypogonadal men with a new self-emulsifying formulation, Journal of andrology 33(2) (2012) 190-201.

Supplementary Information

Anabolic androgenic steroids (AAS) are frequently used either clinically, by athletes, or for body shaping due to their muscle building and performance enhancing properties. AAS misuse is associated with cardiovascular diseases, mood changes and endocrine issues. Despite the recognition of the severe adverse effects of AAS misuse, the underlying molecular mechanisms are insufficiently understood. Selective androgen receptor modulators (SARMs) are supposed to diminish the adverse androgenic AAS effects while maximizing anabolic effects. In order to obtain androgen receptor modulating compounds of high purity for mechanistic in vitro investigations, this study summarizes protocols of optimized chemical synthesis for five AAS and two SARMs.
The procedures described exhibit the following advantages:
1. straightforward, easily reproducible synthesis method
2. high purity achieved
3. low cost chemical synthesis

SPECIFICATIONS TABLE

Subject Area	Chemistry
More specific subject area	*Medicinal chemistry*
Method name	*Protective group synthesis of anabolic androgenic steroids and selective androgen receptor modulators*
Name and reference of original method	*[1] H.J. Ringold, E. Batres, O. Halpern, E. Necoechea, Steroids. CV.1 2-Methyl and 2-Hydroxymethylene-androstane Derivatives, Journal of the American Chemical Society 81(2) (1959) 427-432.* *[2] R.O. Clinton, R.L. Clarke, F.W. Stonner, A.J. Manson, K.F. Jennings, D.K. Phillips, Steroidal Heterocycles. VI.1 Formylation of A/B-cis 3-Ketosteroids.2 Preparation of 5β-Steroidal[3,2-c]pyrazoles, The Journal of Organic Chemistry 27(8) (1962) 2800-2807.* *[3] M. Miyashita, A. Yoshikoshi, P.A. Grieco, Pyridinium p-toluenesulfonate. A mild and efficient catalyst for the tetrahydropyranylation of alcohols, The Journal of Organic Chemistry 42(23) (1977) 3772-3774.* *[4] H.J. Ringold, E. Batres, O. Mancera, G. Rosenkranz, Steroids. LXXXII.1 Synthesis of 4-Halo Hormone Analogs, The Journal of Organic Chemistry 21(12) (1956) 1432-1435.* *[5] K. Chen, C. Liu, L. Deng, G. Xu, A practical Delta 1-dehydrogenation of Delta 4-3-keto-steroids with DDQ in the presence of TBDMSCl at room temperature, Steroids 75(7) (2010) 513-6.* *[6] A. van Oeveren, M. Motamedi, N.S. Mani, K.B. Marschke, F.J. Lopez, W.T. Schrader, A. Negro-Vilar, L. Zhi, Discovery of 6-N,N-bis(2,2,2-trifluoroethyl)amino- 4-trifluoromethylquinolin-2(1H)-one as a novel selective androgen receptor modulator, Journal of medicinal chemistry 49(21) (2006) 6143-6.* *[7] M. Marull, O. Lefebvre, M. Schlosser, An Improved Access to 4-Trifluoromethyl-2(1H)-quinolinones: The "Watering Protocol", 2004(1) (2004) 54-63.* *[8] L. Zhi, SELECTIVE ANDROGEN RECEPTOR MODULATORS (SARMS) AND USES THEREOF, PCT International Application, WO/2009/082437 (2009).*
Resource availability	*NMR: Bruker 300 Ultrashield; HPLC: ThermoFisher Ultimate 3000; MS: ThermoFisher ISQ EM Single Quadrupole; TLC: Macherey-Nagel Alugram Xtra SIL G* *Reagents: TCI Chemicals Europe, Sigma-Aldrich Chemie GmbH Switzerland*

***Method details**

Synthesis of drostanolone:

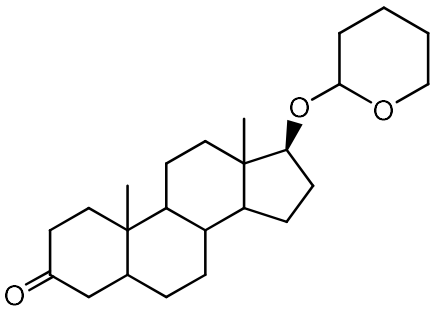

STEP I: Androstan-17β-((tetrahydro-2H-pyran-2-yl)oxy)-3-one (1)

Facilitating higher yields, the application of the tetrahydropyranyl-(THP)-group in order to protect the 17β-alcohol as a THP-ether was established:

3.53 g Dihydropyran was added dropwise to a solution of 10.2 g dihydrotestosterone in 200 ml dichloromethane under argon at room temperature, followed by the addition of a solution of 0.100 g pyridinium tosylate in 13 ml dichloromethane.

After 20 h stirring at room temperature, TLC showed 80% conversion. An additional amount of 0.420 g dihydropyran and 0.010 g pyridinium tosylate were added to the solution and stirring continued for another 24 h. After this period, a total conversion of approx. 90% could be monitored by TLC.

The reaction mixture was diluted with 200 ml dichloromethane and then washed with water and saturated sodium chloride solution. The combined organic extracts were dried over $MgSO_4$ and evaporated to yield 16.50 g of colorless foam.

The crude product was chromatographed on silica gel by using hexane-ethyl acetate (1:1) as an eluent. The isolated product was obtained as a colorless solid (13.10 g; **~ 99%**).

MS (ESI^+):
m/z = 374.89 (calculated MW: 374.56 g/mol)

R_f: 0.7 hexane/ethyl acetate 1:1 visualized by Seebach derivatization reagent

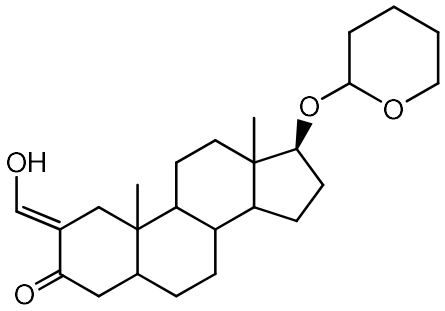

STEP II: 2-Hydroxymethylene-androstan-17β-((tetrahydro-2H-pyran-2-yl)oxy)-3-one (2)

13.00 g Intermediate (1) was completely dissolved in 200 ml dry tetrahydrofuran. 1.09 g Sodium hydride was added in small portions before the reaction mixture was flushed with argon and stirred at room temperature for 1 h. After this period, the dropwise addition of 7.77 g pure ethyl formate through the septum was administered. The reaction mixture was stirred over night at ambient temperature [1, 2].

On the next day, the reaction mixture has become a cloudy-orange suspension, which was evaporated to dryness. The remaining yellow solid was colloidally dissolved in water. By the addition of 1 M HCl, the pH-value (beginning 9-10) could be changed to pH 4 and orange suspension becomes a milky white, before some white solids start to precipitate. 14.80 g could be obtained as an amber solid. The crude product was still wet. This material was purified by column chromatography on silica gel by using hexane-ethyl acetate (8:2) as an eluent. 12.0 g light beige solid could be obtained as a purified product (**85%**).

MS (ESI^+):
m/z = 402.94 (calculated MW: 402.57 g/mol)

R_f: 0.6 hexane/ethyl acetate 7:3 UV active (254 nm) and visualized by Seebach derivatization reagent

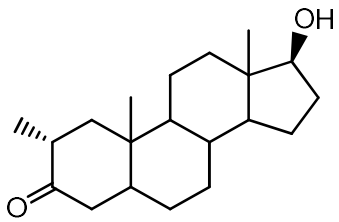

STEP III: 2α-Methyl-androstan-17β-ol-3-one (3)

In this “one-pot-reaction”-step the conversion to the 1α-methyl-group is performed simultaneously with the cleavage of the protective group at the 17β-alcohol:

10.60 g Hydroxymethylene-precusor **2** was nearly dissolved in 800 ml ethanol at 55°C. This solution was hydrogenated in a pressure vessel (Parr reactor) with 6.00 g palladium on charcoal (5%) at 4 bar and room temperature for 24 h. The mixture was filtered twice through paper and the corresponding ethanolic solution was evaporated, to yield 9.50 g colorless oil, still contains traces of charcoal and ethanol. The crude product was purified by column chromatography on silica gel by using hexane-ethyl acetate (8:2) as an eluent, to afford 5.45 g purified material as a colorless solid (**69%**) [1, 2].

MS (ESI^+):
m/z = 304.96 (calculated MW: 304.47 g/mol)

R_f: 0.35 hexane/ethyl acetate 7:3, visualized by Seebach derivatization reagent

^1H NMR(300 MHz, DMSO-d_6) : δ 4.42 (d, 1 H, OH), 3.42 (m, 1H, H_{CHOH}), 3.32 (s, 1H, CH), 2.37 (t, 1 H, CH), 1.99 (dd, 1 H,), 1.84 (dd, 1H), 1.78 – 1.84 (m, 1H), 1.72 (m, 1H), 1.61 (m, 1H), 1.22-1.58 (m, 8H), 1.08 – 1.22 (m, 1H), 1.03 (s, 3H, CH_3), 0.76-1.01 (m + d, 7H, 2α-CH_3 +X), 0.65 – 0.72 (m, 1H), 0.64 (s, 3H, CH_3).

Preparation of methasterone:

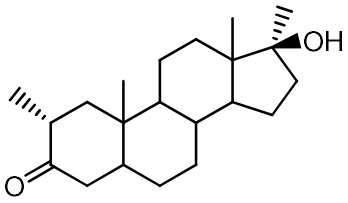

2α-17α-Dimethyl-androstan-17β-ol-3-one (4)

2.05 g Oxymetholone was dissolved in 160 ml ethanol at room temperature. This solution was hydrogenated in a pressure vessel (Parr reactor) with 2.50 g palladium on charcoal (5%) at 3 bar and room temperature for 36 h. The reaction seemed to be completed, since there is no starting material remaining. The formation of two major byproducts can be observed via TLC (Seebach-staining). The mixture was filtered through a short pad of silica and the corresponding ethanolic solution was evaporated to yield 1.90 g of a colorless solid [1, 2]. The crude product was purified by column chromatography on silica gel by using hexane-ethyl acetate (1:1), to afford 1.35 g of **4** as a colorless solid (**68%**).

MS (ESI^+):
m/z = 319.17 (calculated MW: 318.49 g/mol)

R_f: 0.80 hexane/ethyl acetate 1:1 visualized by Seebach derivatization reagent

^1H NMR(300 MHz, $CDCl_3$-d_3) : δ 2.49 (sept, 1 H, CH), 2.34 (t, 1H, CH), 2.13 – 2.05 (m, 2H, CH_2), 1.87 – 1.25 (m, 12 H), 1.23 (s, 3 H, CH_3), 1.22 – 1.12 (m, 2H), 1.10 (s, 3 H, CH_3), 1.02 (d, 3 H, CH_3), 1.00 – 0.91 (m, 1 H), 0.89 (s, 3 H, CH_3), 0.88 – 0.80 (m, 1H), 0.71 (td, 1H, CH).

Preparation of 4,5α-dihydro-2-(hydroxymethylene)testosterone (oxystanolone):

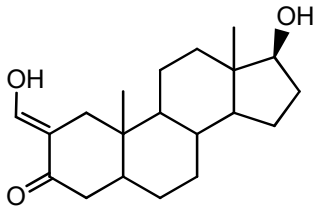

2-Hydroxymethylene-androstan-17β-ol-3-one (5)

To a solution of 0.95 g intermediate (2) in 55 ml of the solvent mixture tetrahydrofuran/methanol/water 7:2:1 pyridinium tosylate (1.15 g dissolved in 20 ml tetrahydrofuran/methanol/water 7:2:1) was added at room temperature. Subsequently, this was followed by 8 h stirring at 50°C. Monitoring via TLC still shows remaining starting material [3].

After evaporation of all solvents, the crude product was chromatographed on silica gel by using hexane-ethyl acetate (8:2). 0.385 g of **5** was obtained as a colorless solid (**52%**).

MS (ESI^+):
m/z = 318.95 (calculated MW: 318.45 g/mol)

R_f: 0.35 hexane/ethyl acetate 7:3 UV active (254 nm) and visualized by Seebach derivatization reagent

Preparation of clostebol:

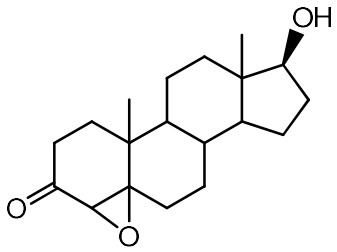

STEP I: 4,5-Epoxy-androstan-17β-ol-3-one (6)

10.0 g Testosterone was dissolved in 200 ml methanol and cooled to 0°C on ice. After cooling down, a chilled sodium hydroxide solution (1.40 g in 20 ml) was added dropwise, followed by the addition of 8 ml cold 30% hydrogen peroxide solution. The reaction was then stirred for 12 h at 0°C.

The reaction solution was then diluted with 500 ml water, before the resulting suspension was extracted several times with 200 ml dichloromethane. The combined organic phases were dried over Magnesium sulfate and all solvents were removed under vacuum [4]. This resulted in 8.50 g of **6** as a colorless foam (**85%**).

For further conversion to Clostebol (7), this intermediate was taken without any additional purification.

R_f: 0.45 hexane/ethyl acetate 1:1 visualized by Seebach derivatization reagent

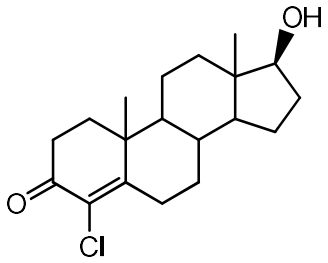

STEP II: 4-Chloro-androst-4-en-17β-ol-3-one (7)

8.50 g epoxide (6) was dissolved in 150 ml Acetone and treated with 14 ml of 25% hydrochloric acid. An immediate color shift of the reaction mixture from light yellow to deep blue can be observed. After stirring for 30 h at room temperature, a complete conversion of the epoxide (6) can be monitored by TLC. The reaction mixture was diluted with 400 ml water, leading to the formation of a blue-black solid precipitating from the solution.
After evaporation of acetone the remaining aqueous solution was extracted several times with 200 ml dichloromethane. The combined organic extracts were washed with saturated sodium bicarbonate solution and sodium chloride solution before drying over magnesium sulfate.

The crude product was chromatographed on silica gel by using hexane-ethyl acetat (1:1) and followed by a recrystallization from acetone [4]. The isolated product **7** was obtained as yellowish crystals (4.50 g; **51%**).

MS (ESI^+):
m/z = 322.83 + 324.80(^{37}Cl) (calculated MW: 322.87 g/mol)

R_f: 0.45 hexane/ethyl acetate 4:6 UV active (254) and visualized by Seebach derivatization reagent

^1H NMR(300 MHz, DMSO-d_6) : δ 4.48 (d, 1 H, OH), 3.44 (m, 1H, H_{CHOH}), 3.05 (m, 1H, 2-CH_2), 2.63 (m, 1H, 2-CH_2), 2.42 (m, 1H), 2.27 (m, 1H), 1.98 (m, 1H), 1.48 – 1.90 (m, 7H), 1.30 – 1.41 (m, 2H), 1.25 (m, 1H), 1.21 (s, 3H, CH_3), 0.84 – 1.03 (m, 4H), 0.69 (s, 3H, CH_3).

Preparation of boldenone:

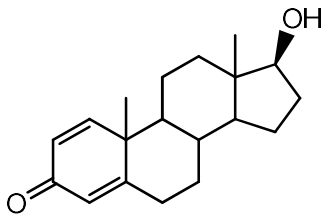

1,4-Androstdien-17β-ol-3-one (8)

29.0 g Testosterone was dissolved in 220 ml dioxan/THF 8:2 and cooled to 0°C on ice. After cooling down a solution of tert-butyldimethylsilyl chloride (46.0 g in 100 ml dioxan/THF 8:2) was added dropwise and stirred for 90 min at 0°C. Then a suspension of 32.0 g of DDQ in 200 ml dioxan/THF 8:2 was added in 4 equal portions over a period of 4 h. The reaction mixture was stirred for additional 12 h within coming from 0°C to room temperature.

The resulting suspension was then filtered over Celite and rinsed with 300 ml THF. The filtrate was evaporated and brown oil was obtained. The oil was diluted in 1500 ml DCM and washed with 500 ml of 5% aqueous sodium hydroxide. The yellow organic phase was washed with 400 ml water and 400 ml saturated sodium chloride solution, before drying over magnesium sulfate.

After evaporation, the crude product was chromatographed on silica gel by using hexane-ethyl acetate (3:7), followed by a recrystallization in ethyl acetate [5]. 16.50 g of **8** was obtained as an amber solid (**58%**).

MS (ESI^+):
m/z = 287.20 (calculated MW: 286.41 g/mol)

R_f: 0.30 hexane/ethyl acetate 3:7 UV active (254 nm) and visualized by Seebach derivatization reagent

^1H NMR(300 MHz, $CDCl_3$) : δ 7.05 (d, 1 H, H_{olefin}), 6.23 (d, 1 H, H_{olefin}), 6.07 (s, 1 H, H_{olefin}), 3.64 (t, 1H, H_{CHOH}), 2.42 – 2.51 (m, 1H), 2.32 – 2.39 (m, 1H), 2.02 – 2.12 (m, 1H), 1.91-1.99 (m, 1H), 1.84 – 1.90 (m, 1H), 1.56 – 1.80 (m, 4H), 1.41 – 1.51 (m, 2H), 1.28 – 1.39 (m, 1H), 1.24 (s, 3H, CH_3), 0.91 – 1.14 (m, 4H), 0.82 (s, 3H, CH_3).

Preparation of LGD-2226:

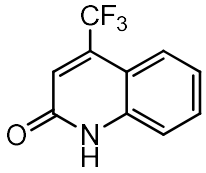

STEP I: 4-Trifluoromethylquinolin-2(1H)-one (9)

In a 1 L round flask fitted with a reflux condenser a mixture of 25.60 g aniline, 50.0 g ethyl-4,4,4-trifluoroacetoacetate 300 ml toluene was heated to reflux in an oil bath at 130 °C. After 20 min 3 ml water was added and the mixture was heated at reflux for another 24 h. the reaction mixture was cooled to room temperature and concentrated under reduced pressure. A round flask with 200 mL H_2SO_4 was heated to 80°C and the crude oil from the step before was added in portions to the H_2SO_4 keeping the internal temperature below 90°C, total addition time was approximately 40 min. After addition was complete, the mixture was stirred at 80°C for 1 h, cooled and poured onto 400 g crushed ice. The resulting solids were filtered, washed with water, and dried under vacuum at 40°C to give 33.0 g (**50%**) product (9) as a colorless solid [6, 7].

MS (ESI^+):
m/z = 214.13 (calculated MW: 213.16 g/mol)

R_f: 0.10 hexane/ethyl acetate 7:3 UV active (254 nm)

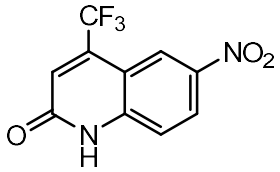

STEP II: 6-Nitro-4-trifluoromethylquinolin-2(1H)-one (10)

A milky suspension of 33.0 g in 200 mL H_2SO_4 was cooled in an ice-salt bath to -5°C. 14.3 g 70% HNO_3 was added dropwise, keeping the internal temperature below 7°C. After addition was complete, the mixture was stirred at 0-10°C for 1 h and then after removal of the ice bath the temperature raised to room temperature within the next hours. The yellow solution was then poured onto 600 g crushed ice and kept standing/stirring for the next 12 h. The resulting two phases were separated and the organic phase equals a yellow slurry, which was filtered by suction. The resulting solid was washed with water and dried under vacuum. After crystallization of 20 g crude product in 1 L ethanol a nearly colorless solid (10) (**43%**) was obtained [6, 7].

MS (ESI^-):
m/z = 257.08 + 514.96 (2*M) (calculated MW: 258.15 g/mol)

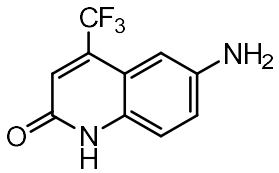

STEP III: 6-Amino-4-trifluoromethylquinolin-2(1H)-one (11)

A suspension of the 17.0 g Nitro-compound (10) in 400 ml ethanol in a 1 L round flask was flushed with argon and 2.0 g 5% Pd/C was added. The mixture was stirred under a hydrogen atmosphere for 2 days. Then filtered through silica and washed with 1500 mL ethanol. The filtrate was evaporated under vacuum to yield 14.0 g of a bright yellow solid 11 (**92%**).

Since the resulting solid has been monitored by TLC to exhibit high purity, the product was used without further purification for the next step.

MS (ESI^+):
m/z = 229.11 (calculated MW: 228.17 g/mol)

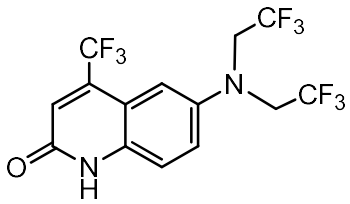

STEP IV: 6-N,N-Bis(2,2,2-trifluoroethyl)amino -4-trifluoromethylquinolin-2(1H)-one (12)

A 2 L round flask, under argon, was charged with a solution of the 14.00 g amine 11 in 350 ml trifluoroacetic acid. 5.80 g $NaBH_4$ was added within 1 h. The mixture was stirred at room temperature for 16 h. After that 4.50 g $NaBH_4$ was added and then heated to 70°C for 5 h. The heating bath was removed and it was stirred at room temperature over 2 d. In several portions water was carefully added. In total 1500 ml water was slowly added. The yellow-greenish precipitate was filtered and rinsed with water.

After drying, the crude product was purified by column chromatography on silica gel by using hexane-ethyl acetate (1:4), followed by a recrystallization in chloroform [6]. 18.1 g of **12** was obtained as a bright yellow solid (**76%**).

MS (ESI^+):
m/z = 392.86 (calculated MW: 392.22 g/mol)

R_f: 0.35 hexane/ethyl acetate 1:4 UV active (254 nm)

^1H NMR(300 MHz, DMSO-d_6) : δ 12.2 (bs, 1 H, NH), 7.57 (dd, 1H, H_{arom}), 7.39 (d, 1H, H_{arom}), 7.16 (s, 1 H, H_{arom}), 6.97 (s, 1 H, H_{olefin}), 4.39 (q, 4H, CH_2).

Preparation of LGD-4033:

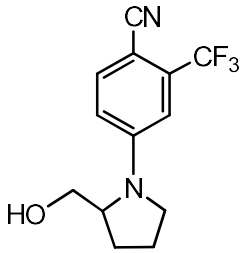

STEP I: 4-(2-(hydroxymethyl)-pyrrolidin-1-yl)-2-(trifluoromethyl)benzonitril (13)

10.0 g 4-Fluoro-2-(trifluoromethyl)benzonitril was dissolved in 200 ml tetrahydrofuran and 9.0 ml Hünig base was added dropwise. While stirring at room temperature, 5.0 g D-prolinol diluted in 100 ml tetrahydrofuran was added over a period of 15 min. The reaction mixture was stirred for 2 d at room temperature.

After evaporation, the crude product appears as a yellow oil, which was chromatographed on silica gel by using hexane-ethyl acetate (1:1) as a eluent to yield 11.40 g of **13** as a light yellow oil (**88%**) [8].

MS (ESI^+):
m/z = 270.89 (calculated MW: 270.25 g/mol)

R_f: 0.30 hexane/ethyl acetate 1:1 UV active (254 nm)

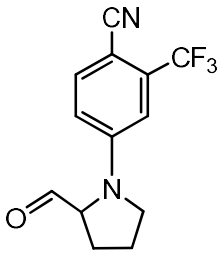

STEP II: 4-(2-(formylpyrrolidin-1-yl)-2-(trifluoromethyl)benzonitril (14)

6.99 g Oxalylchloride was diluted in 100 ml dichloromethane and cooled down to -78°C by dry ice/acetone bath. 9.83 g dimethylsulfoxide diluted in 50 ml dichloromethane was added via syringe over a period of 30 min. After stirring 20 min at -78°C, 11.4 g intermediate-alcohol 13 diluted in 60 ml dichloromethane is added dropwise over a period of 45 min. After stirring 45 min at -78°C, the addition of 29 ml triethylamine starts, following by 30 min stirring at -78°C.

Then the ice bath was removed and the reaction mixture was stirred 12 h at room temperature. The resulting yellow-milky suspension was stirred with 200 ml saturated sodium chloride solution. After the separation of the organic phase, the aqueous phase was extracted two times with 100 ml dichloromethane. The combined organic phases were dried over magnesium sulfate and evaporated. The resulting yellow

solid was purified by column chromatography on silica gel by using hexane-ethyl acetate (1:1) as a eluent [8]. 11.20 g of **14** was obtained as a yellow solid (**99%**).

MS (ESI^+):
m/z = 269.08 (calculated MW: 268.23 g/mol)

R_f: 0.40 hexane/ethyl acetate 1:1 UV active (254 nm)

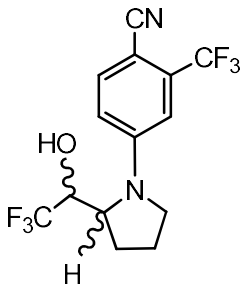

STEP III: 4-(2-(1-Hydroxyl-2,2,2-trifluoroethyl)pyrrolidin-1-yl)-2-(trifluoromethyl)benzonitril (15)

11.20 g Aldehyde 14 was dissolved in 300 ml dry tetrahydrofuran and 8.36 g CsF was added directly as a solid to the reaction mixture. It was cooled via ice bath to 0°C and stirred for 15 min. Then 25.00 g trimethyl(trifluoromethyl)silane was added via syringe over a period of 40 min. The reaction is stirred for 15 h coming from 0°C to room temperature over this time interval. The reaction solution shifts color from nearly colorless to dark brown.

For stopping the reaction, it was diluted with 100 ml saturated ammonium chloride solution and then evaporated. The resulting emulsion was extracted several times with ethyl acetate and the combined phases dried over magnesium sulfate. After evaporation of all volatiles, the intermediate silyl-ether can be obtained as red-brown oil.

This intermediate was converted to the final product **15** without any further purification.

The intermediate was diluted with 400 ml tetrahydrofuran and cooled to 0°C. A cooled potassium hydroxide solution (4.76 g in 400 ml water) was mixed with the diluted oil and stirred at 0°C for 2h. After quenching with 300 ml water, the organic solvent was removed via evaporation from the mixture. The remaining brown oil was extracted with dichloromethane and dried over magnesium sulfate, to yield a reddish-brown oil.

This crude product was chromatographed on silica gel by using hexane-ethyl acetat (8:2) as an eluent. During purification, different fractions with several product isomers can be collected [8].

The isolated products were obtained as 8.50 g yellowish oils (**61%**).

MS (ESI^+):
m/z = 338.97 (calculated MW: 338.25 g/mol)

R_f: 0.65 + 0.50 (isomers) hexane/ethyl acetate 1:1 UV active (254 nm + 366 nm)

^1H NMR(300 MHz, DMSO-d_6): δ 7.85 (d, 1H, H_{arom}), 6.94 (d, 1H, H_{arom}), 6.87 (dd, 1 H, H_{arom}), 6.53 (bd, 1 H, OH), 4.28 (m, 1H), 4.20 (m, 1H), 3.55 (m, 1H), 2.14 – 2.25 (m, 2H), 1.89 – 2.02 (m,2H).

Declaration of interests:

The authors declare the following financial interests/personal relationships which may be considered as potential competing interests:

Matthias Grill was an employee of Lipomed AG

***References:**

[1] H.J. Ringold, E. Batres, O. Halpern, E. Necoechea, Steroids. CV.1 2-Methyl and 2-Hydroxymethylene-androstane Derivatives, Journal of the American Chemical Society 81(2) (1959) 427-432.
[2] R.O. Clinton, R.L. Clarke, F.W. Stonner, A.J. Manson, K.F. Jennings, D.K. Phillips, Steroidal Heterocycles. VI.1 Formylation of A/B-cis 3-Ketosteroids.2 Preparation of 5β-Steroidal[3,2-c]pyrazoles, The Journal of Organic Chemistry 27(8) (1962) 2800-2807.
[3] M. Miyashita, A. Yoshikoshi, P.A. Grieco, Pyridinium p-toluenesulfonate. A mild and efficient catalyst for the tetrahydropyranylation of alcohols, The Journal of Organic Chemistry 42(23) (1977) 3772-3774.
[4] H.J. Ringold, E. Batres, O. Mancera, G. Rosenkranz, Steroids. LXXXII.1 Synthesis of 4-Halo Hormone Analogs, The Journal of Organic Chemistry 21(12) (1956) 1432-1435.
[5] K. Chen, C. Liu, L. Deng, G. Xu, A practical Delta 1-dehydrogenation of Delta 4-3-keto-steroids with DDQ in the presence of TBDMSCl at room temperature, Steroids 75(7) (2010) 513-6.
[6] A. van Oeveren, M. Motamedi, N.S. Mani, K.B. Marschke, F.J. Lopez, W.T. Schrader, A. Negro-Vilar, L. Zhi, Discovery of 6-N,N-bis(2,2,2-trifluoroethyl)amino- 4-trifluoromethylquinolin-2(1H)-one as a novel selective androgen receptor modulator, Journal of medicinal chemistry 49(21) (2006) 6143-6.
[7] M. Marull, O. Lefebvre, M. Schlosser, An Improved Access to 4-Trifluoromethyl-2(1H)-quinolinones: The "Watering Protocol", 2004(1) (2004) 54-63.
[8] L. Zhi, SELECTIVE ANDROGEN RECEPTOR MODULATORS (SARMS) AND USES THEREOF, PCT International Application, WO/2009/082437 (2009).

3.2. *In vivo* assessment of disturbances of corticosteroid homeostasis

Alterations in circulating steroid levels can be the result of direct effects on adrenal steroidogenesis, impaired peripheral steroid metabolism or altered feedback mechanism. EDCs can interfere at all three levels and this needs to be taken into consideration in safety assessments.

The HPA axis plays a fundamental role in maintaining steroid homeostasis by regulating glucocorticoid hormone synthesis in the adrenal gland. Glucocorticoids are produced in the adrenal cortex in response to ACTH secretion by the anterior pituitary gland, which in turn is stimulated by corticotrophin-releasing hormone (CRH) and arginine vasopressin released from the hypothalamic paraventricular nucleus in a circadian and pulsatile manner [50, 51]. Glucocorticoid hormone levels themselves provide a negative feedback signal in order to control their own synthesis by inhibiting CRH and ACTH secretion [50-53]. For example, elevated glucocorticoid levels cause a reduction in plasma ACTH concentrations as a consequence of negative feedback regulation followed by a decrease in adrenal glucocorticoid production. In case of reduced levels of active glucocorticoids, for instance through inhibition of CYP11B1 or 11β-hydroxysteroid dehydrogenase type 1 (11β-HSD1), or in course of GR resistance, i.e. in the presence of antagonists or desensitization by phosphorylation, ACTH levels increase due to less negative feedback regulation at the pituitary and thus lead to an increase in the production of adrenal glucocorticoids.

In peripheral tissues, local glucocorticoid hormone action is regulated by 11β-HSD1 and 11β-HSD2 [54, 55]. These enzymes catalyze the interconversion of biologically inactive cortisone and active cortisol and determine the intracellular concentrations of active glucocorticoids. 11β-HSD1 mediates the reactivation of inactive glucocorticoids, thereby allowing that intracellular concentrations of active glucocorticoids not only depend on circulating active hormone levels but can utilize the freely circulating pool of inactive 11-ketoglucocorticoids. This tissue-specific activation leads to pre-receptor regulation of the GR [54, 56]. Inhibition of 11β-HSD1 is assumed to have beneficial effects in glucocorticoid-excess-related diseases including type 2 diabetes mellitus, osteoporosis, glaucoma and wound healing [57-63]. Whereas 11β-HSD1 is ubiquitously expressed, 11β-HSD2 inactivates glucocorticoids mainly in the kidney, colon and placenta. In the placenta, 11β-HSD2 protects the fetus from the approximately tenfold higher maternal cortisol levels and, consequently, impairment of its function is related to a reduction in fetal growth and a predisposition to future cardio-metabolic diseases [64-66]. In the kidney and colon, 11β-HSD2 renders specificity for aldosterone to the MR, since aldosterone and cortisol exhibit similar binding affinities for this receptor and circulating cortisol concentrations are about 100- to 1000-fold higher than those of aldosterone [67, 68]. Loss-of-function mutations in the gene encoding 11β-HSD2 cause the syndrome of apparent mineralocorticoid excess (AME) characterized by hypertension, hypokalemia, low plasma renin and aldosterone levels [64, 69].

Disruption of both peripheral metabolism and feedback-mediated HPA axis regulation are associated with metabolic and cardiovascular diseases, impaired immune system and depressive disorders [11, 51, 55]. The purpose of this part of the thesis was to assess xenobiotic-induced disturbances of corticosteroid action resulting from dysregulated feedback of the HPA axis and altered peripheral corticosteroid metabolism. Targeted analysis of corticosteroids and androgens in human serum and urine samples was performed and steroid metabolite ratios were evaluated to gain initial mechanistic information.

The published article 'Effects of lisdexamfetamine on plasma steroid concentrations compared with D-amphetamine in healthy subjects: A randomized, double-blind, placebo-controlled study' [70] (see chapter 3.2.1) describes the detection of changes in circulating steroids in plasma samples from healthy human subjects treated with placebo, D-amphetamine or lisdexamfetamine. Lisdexamfetamine is a slow release form of D-amphetamine covalently linked to the amino acid L-lysine and is used for the treatment of attention deficit hyperactivity disorder (ADHD) in patients (children older than six years and adults) not responding to methylphenidate (Ritalin®) [71-74]. Furthermore, plasma levels of ACTH as well as D-amphetamine concentrations were measured to identify altered HPA axis regulation and compare pharmacokinetic profiles of D-amphetamine and lisdexamfetamine, respectively.

Additionally, a comprehensive analysis of blood and urine steroid profiles was performed in samples from two case studies in which patients received posaconazole, an azole antifungal drug to treat systemic fungal infections [75]. Steroid metabolites and their ratios, which serve as indicators of endocrine disruption, were assessed to provide initial insight into the mechanism of posaconazole-induced hypertension and hypokalemia. The resulting data were published in the case report 'Posaconazole-induced hypertension due to inhibition of 11β-hydroxylase and 11β-hydroxysteroid dehydrogenase 2' [75], see chapter 3.2.2.

3.2.1 Published article:

Effects of lisdexamfetamine on plasma steroid concentrations compared with D-amphetamine in healthy subjects: A randomized, double-blind, placebo-controlled study

Petra Strajhar[a,1], Patrick Vizeli[b,1], Melanie Patt[a], Patrick C. Dolder[b], Denise V. Kratschmar[a], Matthias E. Liechti[b], Alex Odermatt[a], J Steroid Biochem Mol Biol. 2019 Feb;186:212-225.

[1]These authors contributed equally to the study.

[a]Division of Molecular and Systems Toxicology, Department of Pharmaceutical Sciences, University of Basel, Basel, Switzerland

[b]Division of Clinical Pharmacology and Toxicology, Department of Biomedicine and Department of Clinical Research, University Hospital Basel and University of Basel, Basel, Switzerland

Contribution:

Contributed to sample preparation, steroid quantification, analysis of the data and to the writing of the manuscript as well as created the graphical abstract.

Journal of Steroid Biochemistry and Molecular Biology 186 (2019) 212–225

Contents lists available at ScienceDirect

Journal of Steroid Biochemistry and Molecular Biology

journal homepage: www.elsevier.com/locate/jsbmb

Effects of lisdexamfetamine on plasma steroid concentrations compared with D-amphetamine in healthy subjects: A randomized, double-blind, placebo-controlled study

Petra Strajhar[a,1], Patrick Vizeli[b,1], Melanie Patt[a], Patrick C. Dolder[b], Denise V. Kratschmar[a], Matthias E. Liechti[b,**], Alex Odermatt[a,*]

[a] Division of Molecular and Systems Toxicology, Department of Pharmaceutical Sciences, University of Basel, Basel, Switzerland
[b] Division of Clinical Pharmacology and Toxicology, Department of Biomedicine and Department of Clinical Research, University Hospital Basel and University of Basel, Basel, Switzerland

ARTICLE INFO

Keywords:
Amphetamine
Lisdexamfetamine
Psychostimulant
Glucocorticoid
Attention-deficit/hyperactivity disorder

ABSTRACT

The novel D-amphetamine prodrug lisdexamfetamine is applied to treat attention-deficit/hyperactivity disorder (ADHD). D-Amphetamine releases dopamine and norepinephrine and stimulates the hypothalamic-pituitary-adrenal (HPA) axis, which may contribute to its reinforcing effects and risk of abuse. However, no data is currently available on the effects of lisdexamfetamine on circulating steroids. This randomized, double-blind, placebo-controlled, cross-over study evaluated the effects of equimolar doses of D-amphetamine (40 mg) and lisdexamfetamine (100 mg) and placebo on circulating steroids in 24 healthy subjects. Plasma steroid and D-amphetamine levels were determined up to 24 h. Delayed increase and peak levels of plasma D-amphetamine concentrations were observed following lisdexamfetamine treatment compared with D-amphetamine administration, however the maximal concentrations and total exposure (area under the curve [AUC]) were similar. Lisdexamfetamine and D-amphetamine significantly enhanced plasma levels of adrenocorticotropic hormone, glucocorticoids (cortisol, cortisone, corticosterone, 11-dehydrocorticosterone, and 11-deoxycortisol), androgens (dehydroepiandrosterone, dehydroepiandrosterone sulfate, and Δ4-androstene-3,17-dione [androstenedione]), and progesterone (only in men) compared with placebo. Steroid concentration-time curves were shifted to later time points due to a non-significantly later onset following lisdexamfetamine administration than after D-amphetamine, however maximal plasma steroid concentrations and AUCs did not differ between the active treatments. None of the active treatments altered plasma levels of the mineralocorticoids aldosterone and 11-deoxycorticosterone or the androgen testosterone compared with placebo. The effects of the amphetamines on glucocorticoid production were similar to those that were previously reported for methylphenidate (60 mg) but weaker than those for the serotonin releaser 3,4-methylenedioxymethamphetamine (MDMA; 125 mg) or direct serotonin receptor agonist lysergic acid diethylamide (LSD; 0.2 mg). Lisdexamfetamine produced comparable HPA axis activation and had similar pharmacokinetics than D-amphetamine, except for a delayed time of onset. Thus, serotonin (MDMA, LSD) may more effectively stimulate the HPA axis than dopamine and norepinephrine (D-amphetamine).

1. Introduction

Lisdexamfetamine is a prodrug of D-amphetamine [1,2], and both are applied to treat attention-deficit/hyperactivity disorder (ADHD), similar to methylphenidate. In addition to their use as medications, amphetamines and methylphenidate are also misused as recreational drugs or neuroenhancers to induce euphoria or stay awake [3–5]. Lisdexamfetamine is thought to be gradually converted to D-amphetamine in the circulation following oral administration [6], leading to a prolonged pharmacokinetic profile with a proposed low peak but sustained

* Corresponding author at: Division of Molecular and Systems Toxicology, Department of Pharmaceutical Sciences, University of Basel, Klingelbergstrasse 50, Basel, CH-4056, Switzerland.
** Corresponding author at: Division of Clinical Pharmacology and Toxicology, University Hospital Basel, Schanzenstrasse 55, Basel, CH-4056, Switzerland.
E-mail addresses: matthias.liechti@usb.ch (M.E. Liechti), alex.odermatt@unibas.ch (A. Odermatt).
[1] These authors contributed equally to the study.

https://doi.org/10.1016/j.jsbmb.2018.10.016
Received 10 October 2018; Received in revised form 18 October 2018; Accepted 24 October 2018
Available online 28 October 2018

plasma amphetamine levels [7]. Delayed effects on dopamine (DA) release, decreased euphoric effects, and a possibly lower risk of misuse were reported to be linked with a prolonged pharmacokinetic profile [7–9]. Indeed, in rats, a lower peak plasma amphetamine concentration (C_{max}) was observed following lisdexamfetamine treatment, along with a gradually enhanced and sustained dopamine efflux and considerably decreased locomotor activity compared with D-amphetamine [10]. In humans, administration of 100 mg lisdexamfetamine resulted in decreased subjective "drug liking" compared with an equivalent dose of 40 mg D-amphetamine in one study, although other subjective effects including euphoria and stimulation did not differ between the two drugs [7]. Moreover, in a recent study of the pharmacokinetics and pharmacodynamics of lisdexamfetamine and D-amphetamine, we found no difference between the two drugs in the maximal plasma concentrations of amphetamine or any of their subjective effects [11].

The goal of this study was to investigate the effects of lisdexamfetamine and D-amphetamine compared with placebo and each other on circulating steroids. Amphetamines and methylphenidate enhance subjective mood, concentration, and wakefulness but also act as acute pharmacological stressors that stimulate the hypothalamic-pituitary-adrenal (HPA) axis to elevate concentrations of circulating stress hormones, including adrenocorticotropic hormone (ACTH), cortisol, epinephrine, and norepinephrine (NE) [12–16]. However, the effects of lisdexamfetamine on the HPA axis are unknown. In the US in 2010, lisdexamfetamine was the third-most prescribed drug for ADHD in pediatrics patients [17]. Additionally, more lisdexamfetamine misuse cases have been reported to poison centres in the US between 2007 and 2012, resulting in a higher number of cases associated with lisdexamfetamine compared to extended-release D-amphetamine [18]. Because, disturbances of HPA axis function, e.g. the glucocorticoid circadian rhythm, can lead to learning, memory and behavioral deficits, mood disorders such as depression, impaired immune system, and development of metabolic syndrome [19–23], information on the effects of lisdexamfetamine on HPA axis function is of interest. It is also unknown whether lisdexamfetamine produces less HPA axis activation than D-amphetamine based on its reportedly prolonged kinetic characteristics [7–9]. Animal studies indicate that HPA axis stimulation may be associated with a greater risk of drug abuse. Specifically, rats that exhibit greater HPA axis reactivity or were administered corticosterone more likely self-administered D-amphetamine [24]. These observations suggest that lisdexamfetamine may have a lower risk of oral abuse compared with D-amphetamine because of a slowed raise in circulating D-amphetamine levels and consequently a lower HPA response. Therefore, we directly compared plasma ACTH and steroid concentrations after administration of equivalent and relatively high doses of D-amphetamine and lisdexamfetamine. The pharmacokinetic, subjective, and cardiovascular effects have been reported in detail elsewhere [11] and selected effects are also shown here. The primary hypothesis of this investigation was that lisdexamfetamine would produce a lower C_{max} and longer time to C_{max} (T_{max}) for both D-amphetamine and plasma steroids compared with immediate-release D-amphetamine. Equimolar doses of lisdexamfetamine and D-amphetamine were expected to result in equivalent areas under the plasma concentration-time curve (AUCs) for D-amphetamine and steroids, confirming the use of equivalent doses.

The present study used relatively high lisdexamfetamine and D-amphetamine doses. D-Amphetamine at low oral doses of 10–20 mg has been repeatedly shown to increase plasma and saliva cortisol concentrations [16,25–31], with no effect on plasma cortisol levels [32]. Few studies used higher doses of D-amphetamine that would possibly better reflect stimulant misuse. One study reported an increase in plasma cortisol levels compared with baseline after 34 mg D-amphetamine [33]. However, this previous study did not include a placebo control condition. Therefore, the present study evaluated the impact of relatively high D-amphetamine (40 mg) and lisdexamfetamine (100 mg) doses as well as placebo primarily on plasma concentrations of cortisol and secondarily also on other circulating steroids and ACTH.

Both amphetamine and methylphenidate enhance DA and NE neurotransmission [34]. D-amphetamine releases DA and NE from presynaptic terminals and inhibits their reuptake [35]. Methylphenidate only inhibits their reuptake without inducing transporter-mediated release [36]. Although methylphenidate stimulates DA and NE systems similarly to D-amphetamine, methylphenidate produced only moderate stimulating effects on the HPA axis [13,15]. Specifically, single low oral doses of 10–20 mg methylphenidate had no significant effect on plasma cortisol concentrations compared with placebo [29]. A single intermediate oral dose of 40 mg methylphenidate only moderately increased plasma cortisol levels [14]. A high dose of 60 mg methylphenidate non-significantly enhanced plasma levels of cortisol, cortisone, corticosterone, and 11-dehydrocorticosterone compared with placebo [13,15]. Interestingly, a relatively high dose of 60 mg methylphenidate produced at least similar subjective "drug liking" to 30 mg D-amphetamine [15,37], indicating that methylphenidate may induce lower HPA axis stimulation than D-amphetamine at doses producing similar subjective drug liking. This view is supported by a study that directly compared plasma cortisol concentrations after low 10–20 mg doses of both D-amphetamine and methylphenidate [29], but higher doses of both drugs have not been directly or indirectly compared. Therefore, this study also indirectly compared the effects of a high dose of 40 mg D-amphetamine with a high dose of 60 mg methylphenidate that was previously tested in the same laboratory in a similar healthy population using the same clinical and analytical methods [13]. Based on previous data [13,15,29], the hypothesis was that D-amphetamine would produce greater HPA axis activation than methylphenidate.

A final goal of this investigation was to address the role of different monoamine neurotransmitters in regulating HPA activity. D-amphetamine releases both DA and NE and may release cortisol mainly via NE [38]. In contrast, the amphetamine derivative 3,4-methylenedioxymethamphetamine (MDMA) mainly releases serotonin (5-hydroxytryptamine [5-HT]) and NE [35,39,40]. Therefore, MDMA and D-amphetamine may be useful as pharmacological modulators to study the impact of 5-HT *vs*. DA release on HPA axis stimulation. Accordingly, we indirectly compared the effects of D-amphetamine on plasma steroid concentrations with those after 125 mg oral MDMA that was previously tested in the same laboratory using the same clinical and analytical methods [13]. To further study the role of 5-HT *vs*. DA and NE release in psychoactive substance-induced HPA axis stimulation in humans, we also compared the effects of D-amphetamine with similar historical data [41] on the direct 5-HT receptor agonist lysergic acid diethylamide (LSD) [42]. We hypothesized that MDMA and LSD would result in a more pronounced raise in cortisol levels than D-amphetamine in humans. This would indicate a more prominent role for 5-HT compared with DA and NE in stimulating the main human glucocorticoid cortisol by psychoactive substances and further establish cortisol as a marker of acute serotonergic activity [41,43].

2. Materials and methods

2.1. Study design

The clinical trial protocol (Protocol S1) and the CONSORT checklist (Checklist S1) are available as supporting information. The CONSORT flowchart is depicted in Fig. 1. This was a double-blind (subjects and study personnel), placebo-controlled, cross-over study comprising three experimental test days (D-amphetamine, lisdexamfetamine, and placebo). The treatment sequence was randomly selected from four blocks of all possible six sequences and all treatments were counterbalanced, with at least 7 days of washout period between the sessions. The study was approved by the Ethics Committee northwest/central Switzerland (EKNZ) and Swiss Agency for Therapeutic Products (Swissmedic) and performed according to the guidelines of the Declaration of Helsinki and International Conference on Harmonization in Good Clinical Practice. The study was registered at ClinicalTrials.gov

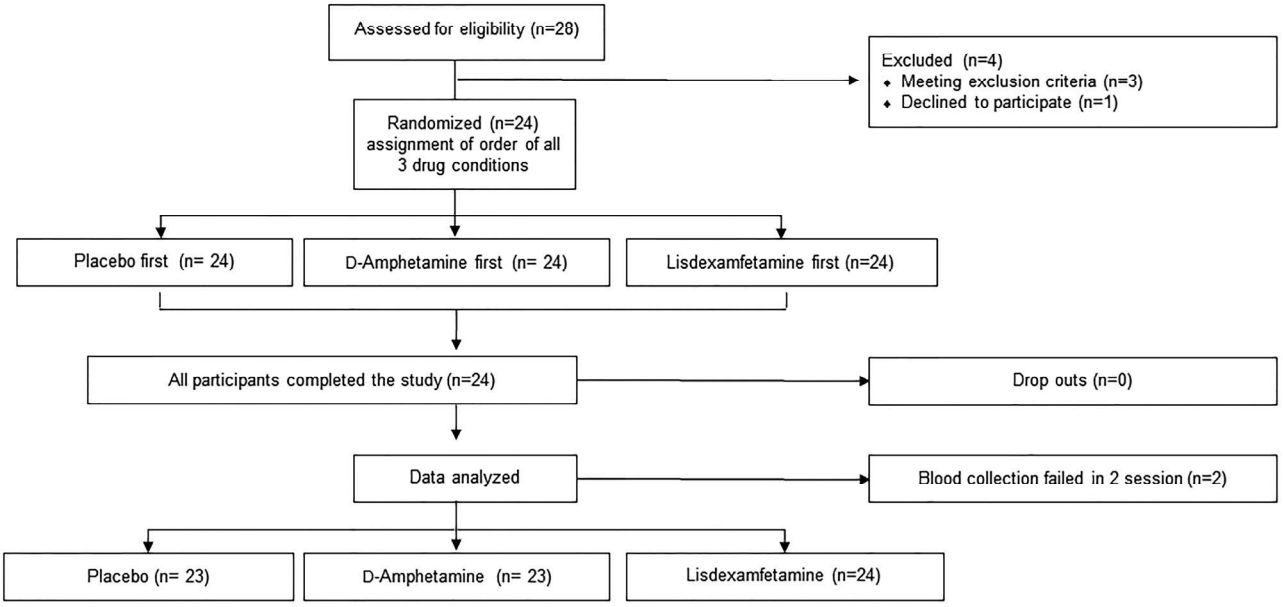

Fig. 1. CONSORT flowchart. The treatment sequence was randomly selected from four blocks of all possible six sequences and all treatments were counterbalanced.

(NCT02668926), and prior their participation all subjects provided written informed consent.

2.2. Participants

The study included 24 healthy subjects (12 men and 12 women; mean age ± SD: 25.3 ± 3.0 years; range: 21–34 years). The treatment order was allocated by drawing from blocks of six different balanced drug treatment sequences by a pharmacist of the University Hospital Basel who was not involved in the study. The codes were stored in a sealed envelope until the end of the study. The sample-size estimation indicated inclusion of a minimum of 15 subjects in order to detect a meaningful difference of 20% in C_{max} levels between D-amphetamine and lisdexamfetamine with more than 80% power applying a within-subjects study design. The inclusion criteria were age between 18 and 45 years, body mass index between 18 and 27 kg/m^2, and birth control for women. The exclusion criteria were chronic or acute medical conditions, such as clinically relevant abnormalities on physical exam, laboratory values, or electrocardiography, personal and family (first-degree relative) history of psychotic or major affective disorder, lifetime prevalence of illicit drug use > 5 times (with the exception of tetrahydrocannabinol), illicit drug use within the last 2 months, pregnancy, regular use of medications, smoking (> 10 cigarettes/day), and alcohol consumption (> 10/week). The subjects were requested not to consume excessive amounts of alcohol between test sessions and not to drink caffeine-containing liquids after midnight prior to the study day. Urine drug tests were performed at study inclusion and prior to each test session using TRIAGE 8 (Biosite, San Diego, CA, USA).

2.3. Drugs

Lisdexamfetamine dimesylate (100 mg salt; Opopharma, Rümlang, Switzerland) and D-amphetamine sulfate (40.3 mg salt; Hänseler, Herisau, Switzerland), both corresponding to 29.6 mg D-amphetamine, as well as placebo (mannitol) were prepared as gelatin capsules, followed by randomization by the University Hospital Basel's pharmacy according to Good Manufacturing Practice. The recommended doses of lisdexamfetamine for ADHD treatment are between 30–70 mg/day, at a starting dose of 30 mg A relatively high dose of 100 mg lisdexamfetamine, above the upper recommended daily dose of 70 mg, was chosen in order to induce greater subjective drug liking and mimic misuse, and for reaching plasma levels after a single dose that are similar to those obtained after repeated administration of 70 mg when steady state is reached.

2.4. Study procedures

Before the test session, abstinence from drug abuse was verified based on urine analysis, and in women a pregnancy test was performed. The test session started at 8:00 AM by placing an indwelling intravenous catheter in an antecubital vein for collecting blood. At 9:00 AM, lisdexamfetamine, D-amphetamine, or placebo was administered orally (a single dose). The subjects were resting during the whole test session in hospital beds in a calm standard hospital room. They obtained a standardized lunch and dinner at 11:30 AM and 6:30 PM, respectively. Blood samples were collected in lithium heparin tubes 1 h prior to and 0, 0.5, 1, 1.5, 2, 2.5, 3, 3.5, 4, 5, 6, 8, 10, 12, and 24 h after drug administration in order to analyze plasma hormone and D-amphetamine concentrations. The blood samples were immediately centrifuged, followed by storage of plasma at −20 °C. For the determination of ACTH concentrations, blood samples were drawn into ethylenediaminetetraacetic acid-containing tubes 1 h before and 3.5 h after drug administration. The test session ended at 9:00 PM, and the subjects went home. They returned the next day at 9:00 AM to draw the final 24 h blood sample. Subjective, autonomic, and adverse responses were also assessed and have been reported in detail elsewhere [11].

2.5. Steroid quantification in plasma

The following plasma steroid hormones with the corresponding lower limit of quantification (LLOQ; values in brackets) were determined using a previously published ultra-high performance liquid chromatography-tandem mass spectrometry (UHPLC-MS/MS) method [41] with minor modifications: cortisol [1.95 nM], cortisone [1.95 nM], corticosterone [0.98 nM], 11-dehydrocorticosterone [0.98 nM], 11-deoxycorticosterone [0.78 nM], aldosterone [0.2 nM], dehydroepiandrosterone (DHEA) [3.91 nM], DHEA sulfate (DHEAS) [19.53 nM], Δ4-androstene-3,17-dione (androstenedione) [0.78 nM], testosterone [0.39 nM], 11-deoxycortisol [0.78 nM], progesterone [0.05 nM], androsterone [3.91 nM], and 17α-hydroxyprogesterone [0.78 nM]. The accuracy, determined for all analytes at three different concentrations, was between 85% and 115% with a coefficient of variation < 15%, and

the recovery of control samples was 80–120%. The details of the applied method and its validation were reported previously [41]. Briefly, after protein precipitation, plasma samples that were spiked with deuterium-labeled aldosterone, corticosterone, androstenedione, androsterone, and testosterone as internal standards were solid-phase extracted. After evaporation and reconstitution in methanol, steroid separation and quantification was performed on an Agilent 1290 UPLC device connected to an Agilent 6490 triple quadrupole mass spectrometer containing a jet-stream electrospray ionization interface. A reverse-phase column (Waters Acquity UPLC BEH C18, 1.7 µm, 2.1 × 150 mm) was used to separate steroids. Data acquisition and analysis was performed using Mass Hunter software (Agilent Technologies).

2.6. Quantification of adrenocorticotropic hormone in human plasma samples

ACTH was determined by a chemiluminescent immunometric assay (Immulite 2000 ACTH; Siemens, Erlangen, Germany).

2.7. D-Amphetamine quantification in plasma samples

Plasma D-amphetamine concentrations were quantified by UHPLC-MS/MS (for details see Supplementary Material S1 File). The method had a lower limit of detection (LOD) of 0.26 ng/ml and LLOQ of 0.78 ng/ml for D-amphetamine and was validated over the range of 0.78 to 200 ng/ml for D-amphetamine. Plasma D-amphetamine concentrations were primarily measured to confirm the use of bioequivalent lisdexamfetamine and D-amphetamine doses with regard to total D-amphetamine exposure and to assess D-amphetamine-steroid response relationships. The comprehensive pharmacokinetic data from this study have been reported elsewhere [11].

2.8. Subjective effects

Time-dependent subjective drug effects were assessed by repeatedly applying Visual Analog Scales (VASs). The VASs "drug liking", “good drug effects”, “drug high”, and “stimulated” were presented as 100 mm horizontal lines (0 to +100), marked from "not at all" on the left to "extremely" on the right. The VASs were assessed 1 h before and 0, 0.5, 1, 1.5, 2, 2.5, 3, 3.5, 4, 5, 6, 7, 8, 9, 10, 11, 12, and 24 h after drug administration.

2.9. Statistical analyses

C_{max}, E_{max}, and T_{max} were derived directly from the observed data. The time to reach 10% of C_{max} (T_{onset}) and areas under the concentration-time curve from time 0 to 12 h (AUC_{12}) were calculated applying the linear trapezoidal method in Phoenix WinNonlin 6.4 software (Pharsight, St. Louis, MO). The statistical significance was analyzed using Statistica 12 software (StatSoft, Tulsa, OK, USA) and the computing environment R (R Development Core Team, 2017, Vienna, Austria). Kinetic parameters and subjective effect ratings (E_{max}) were compared using repeated-measures analysis of variance (ANOVA), with drug (D-amphetamine, lisdexamfetamine, and placebo) as the within-subjects factor, followed by the Tukey *post hoc* test. Means of the effect sizes are displayed with confidence intervals of 95%. P-Values of the multiple ANOVAs were Bonferroni-adjusted for the 14 different hormones tested. Additionally, sex differences were assessed by adding sex as a between-subjects factor in addition to drug in complementary ANOVAs. Furthermore, supplementary ANOVAs with order as additional factor were performed to exclude treatment order effects (absence of drug × order interactions). Plasma amphetamine concentration-effect relationships were studied by plotting endocrine responses as a difference from time-matched placebo against the plasma amphetamine concentration for each time point. Selected peak endocrine effects of D-amphetamine and lisdexamfetamine were calculated as differences from placebo and then compared with the effects of 60 mg methylphenidate [13], 125 mg MDMA [13], and 200 µg LSD [41] (also as placebo-corrected responses) using ANOVA, with drug as the between-subjects (between-studies) factor, followed by the Tukey *post hoc* test. The data for methylphenidate, MDMA, and LSD were obtained from previous identical studies in healthy subjects in the same laboratory. The use of placebo-corrected values accounted for between-subject differences in baseline steroid levels and circadian within-subject changes.

3. Results

Blood could not be drawn from one subject in the D-amphetamine and from one subject in the placebo condition. Therefore, complete datasets were available for D-amphetamine, placebo, and lisdexamfetamine for 23, 23, and 24 subjects, respectively.

3.1. Plasma amphetamine levels after administration of D-amphetamine and lisdexamfetamine and subjective effects

Following administration of D-amphetamine and lisdexamfetamine, identical plasma amphetamine concentration-time curves were obtained, with the exception of a significantly delayed T_{onset} and T_{max} upon lisdexamfetamine administration compared with D-amphetamine treatment (Fig. 2, Table 1). The C_{max} and AUC_{12} values were similar (Table 1). Fig. 2 presents subjective drug effects over time. The effects in "drug liking", “good drug effect”, “drug high”, and “stimulated” between lisdexamfetamine and D-amphetamine in comparison with placebo (Table 1, Fig. 2) did not increase differently. The subjective drug effect-time curves were shifted to the right (Fig. 2) as evidenced by a significantly delayed time to onset and time to maximal effect values following lisdexamfetamine administration than with D-amphetamine (Table 1), reflecting the pharmacokinetics of the two drugs. Importantly, E_{max} values were not different between lisdexamfetamine and D-amphetamine (Table 1). The pharmacokinetics and additional pharmacodynamic effects are described in more detail elsewhere [11].

3.2. Effects of D-amphetamine and lisdexamfetamine on plasma steroid and adrenocorticotropic hormone concentrations

The impact of D-amphetamine, lisdexamfetamine, and placebo on plasma steroid hormone concentrations is shown in Figs. 3 and 4. Table 1 shows the corresponding T_{max}, C_{max}, and AUC values, with comparative statistics.

Sex steroid levels were different between males and females when sex was added as additional factor to the ANOVAs (effects of sex: $F_{1,20} = 5.34$, $p = 0.032$; 184, $p < 0.001$; 3.21, $p = 0.088$;, and 61.7, $p < 0.001$, for androstenedione, testosterone, progesterone, and testosterone + androstenedione, respectively) but sex did not moderate the drug effects (no relevant sex × drug interactions [Supplementary Table S1]). Therefore, ANOVAs were conducted and results shown for each sex separately for androstenedione, testosterone, progesterone, and testosterone + androstenedione.

Both active treatments significantly and similarly enhanced the plasma levels of the glucocorticoids cortisol, cortisone, corticosterone, 11-dehydrocorticosterone, and 11-deoxycortisol compared with placebo (Fig. 3A–E, Table 1). Elevated glucocorticoid production was reflected by significant increases in the sums of active and inactive glucocorticoids (i.e., cortisol + cortisone, corticosterone + 11-dehydrocorticosterone; Table 1) and all glucocorticoids measured (data not shown). The cortisol/cortisone and corticosterone/11-dehydrocorticosterone ratios also increased (Table 1). The pharmacokinetic parameters, such as C_{max}, T_{max}, and AUC_{12}, and the shape of the concentration-time curves for corticosteroids were practically identical following D-amphetamine and lisdexamfetamine administration (Fig. 3,

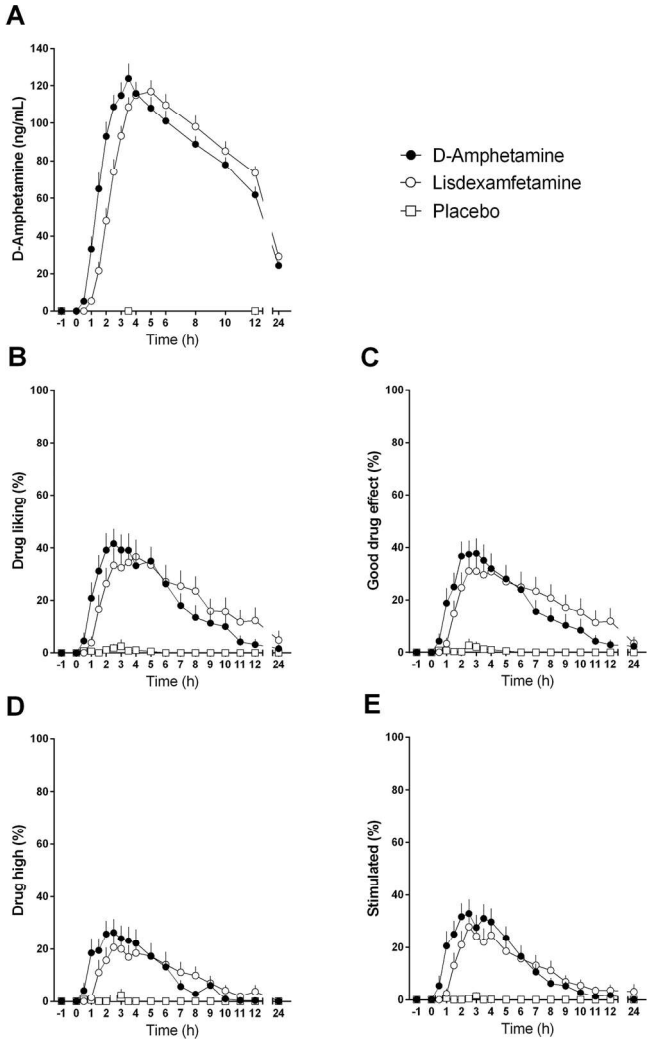

Fig. 2. Lisdexamfetamine administration causes delayed onset but similar maximal values and curve shapes for plasma amphetamine levels and subjective drug effects compared with D-amphetamine. Subjects were given D-amphetamine, lisdexamfetamine, or placebo at t = 0 h. Values for amphetamine concentrations (A) are mean ± SEM of 23, 24, and 23 subjects after administration of D-amphetamine, lisdexamfetamine and placebo. The subjective effects "drug liking" (B), "good drug effect" (C), "drug high" (D), and "stimulated" (E) are expressed as the mean ± SEM in 24 subjects.

Table 1). The mineralocorticoids aldosterone (Fig. 3F) and 11-deoxycorticosteone (data not shown) and the progestogen 17α-hydroxyprogesterone (Fig. 4C) were unaltered by lisdexamfetamine and D-amphetamine compared with placebo. One exception was plasma progesterone concentrations in men, in which greater C_{max} and AUC values were found compared with placebo (Table 1, Supplementary Fig. S1). Progesterone in women was not significantly altered, although a trend toward an increase was observed (Supplementary Fig. S1). The plasma concentrations of DHEA, DHEAS, and androstenedione (Fig. 4A, B, D, E) were significantly increased by the two active drugs compared with placebo. However, lisdexamfetamine and D-amphetamine had no effect on C_{max} and AUC values for the sum of androstenedione + testosterone neither in women nor in men. Moreover, lisdexamfetamine and D-amphetamine did not affect the concentrations of testosterone and the androgen degradation metabolite androsterone (Table 1). The plasma concentrations of 11-deoxycorticosterone were above the LOD but below the LLOQ; therefore, the quantification of this steroid was not validly possible.

Plasma concentrations of ACTH are shown in Fig. 5. A main effect of drug was found at the 3.5 h time point ($F_{2,40} = 33.83, p < 0.001$), and both active drugs resulted in higher plasma ACTH concentrations compared with placebo at 3.5 h (both $p < 0.001$). There were no relevant order × treatment interactions in the ANOVAs, indicating the absence of confounding by treatment order as expected based on the counter-balanced design (Supplementary Table S1).

3.3. Relationship between plasma amphetamine and steroid concentrations after D-amphetamine and lisdexamfetamine administration

Selected drug exposure-steroid concentration response relationships are depicted in Supplementary Fig. S2. Clockwise hysteresis was observed, indicating acute pharmacological tolerance.

3.4. Peak endocrine effects following D-amphetamine and lisdexamfetamine administration compared with other prototypical substances

The peak endocrine effects of D-amphetamine, lisdexamfetamine, methylphenidate, MDMA, and LSD are shown in Table 2. The drug effects are presented as within-subject changes from placebo (placebo-corrected responses). D-amphetamine, lisdexamfetamine, and methylphenidate produced comparable increases in cortisol. D-amphetamine increased cortisone and 11-dehydrocorticosterone to greater levels than methylphenidate. MDMA induced higher peak concentrations of cortisol, lower levels of cortisone, but still higher cortisol + cortisone levels than D-amphetamine. LSD produced much higher peak concentrations of cortisol and corticosterone than D-amphetamine, but in contrast to MDMA, the levels of cortisone and 11-dehydrocorticosterone resembled those that were observed after D-amphetamine administration.

4. Discussion

The key finding of this work was that the novel ADHD treatment lisdexamfetamine produced similar HPA axis stimulation and plasma steroid concentration-time curves as the classic immediate-release D-amphetamine. These findings did not support the hypothesis of the study, in which we expected to observe a smaller and more prolonged endocrine response to lisdexamfetamine compared with D-amphetamine. The reason for the identical endocrine responses of the two amphetamine formulations was the unexpected finding of similar peak amphetamine concentrations after lisdexamfetamine and D-amphetamine administration. Lisdexamfetamine had a significantly longer onset and thus also T_{max} but otherwise a very similar plasma amphetamine concentration-time curve shape compared with D-amphetamine. D-Amphetamine administration 1 h later would likely have produced a pharmacokinetic profile that was almost identical to lisdexamfetamine. The steroid concentration-time curves were shifted to the right (delayed in time), similar to the plasma amphetamine concentration-time curve upon lisdexamfetamine administration compared with D-amphetamine, but this effect did not reach statistical significance for any of the steroid concentration T_{max} values.

Unexpectedly, the present study found similar C_{max} values for amphetamine and all of the steroids at equivalent doses of lisdexamfetamine and D-amphetamine, which is in contrast to the limited preclinical [10] and clinical [7,8] data that were used to generate the present study hypotheses. Specifically, a previous study in rats found a lower C_{max} for amphetamine following lisdexamfetamine treatment compared with D-amphetamine administration [10], in contrast to the present human data. An initial pharmacokinetic study in humans (referred to in [7]) reportedly found a delayed T_{max} and decreased C_{max} for plasma amphetamine after lisdexamfetamine administration compared with immediate-release D-amphetamine. However, these data have not been published. The present relatively large study clearly showed comparable C_{max} values for amphetamine following treatment with both lisdexamfetamine and D-amphetamine, with equal AUC values, thus demonstrating the equivalence of the drug doses and formulations

Table 1
Kinetic parameters of plasma steroids and amphetamine after D-amphetamine, lisdexamfetamine, or placebo.

		D-Amphetamine	Lisdexamfetamine	Placebo	Main effect of drug ($^{a,b,c}F_{2,42}$)	p value (non-corrected)	p value Bonferroni adjusted	Lisdexamfetamine - D-Amphetamine Mean (CI. low, CI. High)	p value	Placebo - D-Amphetamine Mean (CI. low, CI. High)	p value	Placebo - Lisdexamfetamine Mean (CI. low, CI. High)	p value
Amphetamine	T_{onset}	0.8 ± 0.1	1.4 ± 0.1		33.86	< 0.001		0.57 (0.37, 0.78)					
	T_{max}	3.2 ± 0.2	4.4 ± 0.2		16.47	< 0.001		1.0 (0.51, 1.58)					
	C_{max}	134 ± 7	128 ± 5		0.88	NS		-3.0 (-13, 7.2)					
	AUC_{12}	1014 ± 47	983 ± 42		0.66	NS		-7.4 (-56, 42)					
Subjective effects													
Drug liking	T_{onset}	0.9 ± 0.1	1.6 ± 0.2		11.1	0.0035							
	T_{max}	2.7 ± 0.4	4.5 ± 0.5		6.66	0.04							
	E_{max}	51.2 ± 5.8	48.0 ± 6.9	3.7 ± 2.6	38.8	< 0.001		-3.2 (-17, 11)	NS	-48 (-62, -33)	< 0.001	-44 (-58, -44)	< 0.001
	AUC_{12}	251 ± 43	260 ± 52	5.2 ± 4.3	17.8	< 0.001		9.0 (-105, 122)	NS	-246 (-359, -132)	< 0.001	-255 (-368, -255)	< 0.001
Good drug effect	T_{onset}	0.9 ± 0.1	1.5 ± 0.1		8.3	0.0092							
	T_{max}	2.8 ± 0.3	4.4 ± 0.5		7.46	0.013							
	E_{max}	48.5 ± 5.6	41.8 ± 6.5	4.0 ± 2.5	30.2	< 0.001		-4.4 (-18, 9.6)	NS	-42 (-56, -28)	< 0.001	-38 (-52, -38)	< 0.001
	AUC_{12}	226 ± 42	236 ± 51	5.4 ± 4.4	14.8	< 0.001		9.6 (-103, 122)	NS	-221 (-333, -108)	< 0.001	-230 (-343, -230)	< 0.001
Drug high	T_{onset}	1.0 ± 0.1	1.9 ± 0.3		8.19	0.01							
	T_{max}	2.4 ± 0.2	3.6 ± 0.4		7.04	0.016							
	E_{max}	35.5 ± 5.6	29.3 ± 6.2	3.3 ± 2.6	16.8	< 0.001		-6.2 (-20, 7.7)	NS	-32 (-46, -18)	< 0.001	-26 (-40, -26)	< 0.001
	AUC_{12}	134 ± 30	125 ± 33	2.5 ± 1.9	10.3	< 0.001		-8.8 (-84, 67)	NS	-131 (-207, -56)	< 0.001	-123 (-198, -123)	< 0.001
Stimulated	T_{onset}	1.0 ± 0.1	1.8 ± 0.3		6.19	0.022							
	T_{max}	2.3 ± 0.2	4.4 ± 1.0		5.88	0.025							
	E_{max}	43.8 ± 5.7	38.0 ± 6.8	2.4 ± 1.7	26	< 0.001		-5.8 (-20, 8.8)	NS	-41 (-56, -27)	< 0.001	-36 (-50, -36)	< 0.001
	AUC_{12}	178 ± 30	152 ± 35	1.7 ± 1.1	16.1	< 0.001		-26 (-105, 52)	NS	-176 (-255, -98)	< 0.001	-150 (-228, -150)	< 0.001
Glucocorticoids													
Cortisol	T_{max}	2.72 ± 0.29	3.17 ± 0.41	1.20 ± 0.41	7.54	0.0016	0.022	0.59 (-0.69, 1.9)	NS	-1.5 (-2.8, -0.19)	0.019	-2.1 (-3.4, -2.1)	< 0.001
	C_{max}	534 ± 28.9	519 ± 24.9	417 ± 35.2	17.5	< 0.001	< 0.001	-26 (-80, 27)	NS	-128 (-181, -74)	< 0.001	-102 (-155, -102)	< 0.001
	AUC_{12}	4116 ± 286	4207 ± 287	2621 ± 252	62.2	< 0.001	< 0.001	-56 (-414, 301)	NS	-1501 (-1858, -1143)	< 0.001	-1444 (-1801, -1444)	< 0.001
Cortisone	T_{max}	4.39 ± 0.3	4.67 ± 0.3	2.80 ± 0.5	6.86	0.0026	0.037	0.32 (-0.91, 1.5)	NS	-1.5 (-2.7, -0.27)	0.012	-1.8 (-3.0, -1.8)	0.0015
	C_{max}	80.6 ± 4.2	82.8 ± 4.3	58.0 ± 3.0	36.3	< 0.001	< 0.001	0.50 (-7.1, 8.1)	NS	-24 (-31, -16)	< 0.001	-24 (-32, -24)	< 0.001
	AUC_{12}	707 ± 35.2	739 ± 35.5	503 ± 26.4	47.1	< 0.001	< 0.001	19 (-41, 78)	NS	-203 (-262, -144)	< 0.001	-222 (-281, -222)	< 0.001
Corticosterone	T_{max}	2.59 ± 0.47	3.0 ± 0.38	2.24 ± 0.5	1.15	NS	NS	0.59 (-0.75, 1.9)	NS	-0.25 (-1.6, 1.1)	NS	-0.84 (-2.2, -0.84)	NS
	C_{max}	22.6 ± 2.6	20.1 ± 2.0	11.6 ± 1.4	15.8	< 0.001	< 0.001	-2.3 (-7.4, 2.8)	NS	-12 (-17, -6.5)	< 0.001	-9.2 (-14, -9.2)	< 0.001
	AUC_{12}	85.1 ± 6.2	83.1 ± 6.0	36.6 ± 3.2	62.7	< 0.001	< 0.001	-3.0 (-14, 8.4)	NS	-49 (-60, -37)	< 0.001	-46 (-57, -46)	< 0.001
11-Dehydro-	T_{max}	2.96 ± 0.48	2.88 ± 0.38	2.46 ± 0.55	0.4	NS	NS	0.07 (-1.3, 1.4)	NS	-0.41 (-1.8, 0.95)	NS	-0.48 (-1.8, -0.48)	NS
corticosterone	C_{max}	8.93 ± 0.86	8.82 ± 0.64	5.43 ± 0.53	23.5	< 0.001	< 0.001	-0.13 (-1.6, 1.4)	NS	-3.8 (-5.3, -2.3)	< 0.001	-3.7 (-5.2, -3.7)	< 0.001
	AUC_{12}	51.4 ± 4.0	53.7 ± 3.2	28.8 ± 2.2	65.7	< 0.001	< 0.001	1.6 (-4.1, 7.2)	NS	-23 (-29, -17)	< 0.001	-25 (-30, -25)	< 0.001
Cortisol +	T_{max}	2.93 ± 0.3	3.65 ± 0.38	1.20 ± 0.41	9.85	< 0.001	0.0043	0.61 (-0.66, 1.9)	NS	-1.7 (-3.0, -0.44)	0.0046	-2.3 (-3.6, -2.3)	< 0.001
cortisone	C_{max}	601 ± 31	583 ± 26.5	469 ± 36	20.3	< 0.001	< 0.001	-29 (-85, 27)	NS	-144 (-200, -88)	< 0.001	-115 (-171, -115)	< 0.001
	AUC_{12}	4824 ± 299	4945 ± 307	3124 ± 266	67.9	< 0.001	< 0.001	-38 (-429, 354)	NS	-1704 (-2095, -1312)	< 0.001	-1666 (-2057, -1666)	< 0.001

(*continued on next page*)

Table 1 (*continued*)

		D-Amphetamine	Lisdexamfetamine	Placebo	Main effect of drug ($^{a,b,c}F_{2,42}$)	p value (non-corrected)	p value Bonferroni adjusted	Lisdexamfetamine - D-Amphetamine Mean (CI. low, CI. High)	p value	Placebo - D-Amphetamine Mean (CI. low, CI. High)	p value	Placebo - Lisdexamfetamine Mean (CI. low, CI. High)	p value
Ratio	T_{max}	1.83 ± 0.44	3.10 ± 0.61	2.02 ± 0.63	2.79	0.073	NS	1.5 (-0.06, 3.0)	0.064	0.32 (-1.2, 1.9)	NS	-1.2 (-2.7, -1.2)	NS
cortisol/cortisone	C_{max}	9.42 ± 0.57	9.25 ± 0.49	8.81 ± 0.72	0.66	NS	NS	-0.31 (-1.7, 1.0)	NS	-0.66 (-2.0, 0.69)	NS	-0.35 (-1.7, -0.35)	NS
	AUC_{12}	72.3 ± 5.1	69.8 ± 4.0	61.5 ± 5.2	9.93	< 0.001	0.0041	-3.9 (-10, 2.4)	NS	-12 (-18, -5.4)	< 0.001	-7.8 (-14, -7.8)	0.0097
Corticosterone +	T_{max}	2.59 ± 0.47	3.0 ± 0.36	2.37 ± 0.54	0.99	NS	NS	0.59 (-0.67, 1.8)	NS	-0.11 (-1.4, 1.1)	NS	-0.70 (-2.0, -0.70)	NS
11-dehydro-	C_{max}	31.2 ± 3.3	28.5 ± 2.6	16.9 ± 1.9	18	< 0.001	< 0.001	-2.5 (-8.9, 3.9)	NS	-15 (-22, -8.8)	< 0.001	-13 (-19, -13)	< 0.001
corticosterone	AUC_{12}	136 ± 9.5	137.0 ± 8.6	65.3 ± 5.0	74.8	< 0.001	< 0.001	-1.2 (-17, 15)	NS	-72 (-87, -56)	< 0.001	-70 (-86, -70)	< 0.001
ratio	T_{max}	2.59 ± 0.44	2.98 ± 0.43	2.39 ± 0.56	0.28	NS	NS	0.36 (-1.2, 2.0)	NS	-0.14 (-1.7, 1.5)	NS	-0.50 (-2.1, -0.50)	NS
corticosterone/11-	C_{max}	3.01 ± 0.24	2.73 ± 0.14	2.24 ± 0.14	7.48	0.0017	0.023	-0.29 (-0.75, 0.18)	NS	-0.76 (-1.2, -0.29)	< 0.001	-0.47 (-0.94, -0.47)	0.045
dehydrocorticosterone	AUC_{12}	18.7 ± 1.1	17.3 ± 0.93	13.9 ± 1.03	18.1	< 0.001	< 0.001	-1.5 (-3.5, 0.43)	NS	-4.9 (-6.8, -2.9)	< 0.001	-3.4 (-5.3, -3.4)	< 0.001
11-Deoxycortisol	T_{max}	3.02 ± 0.29	3.83 ± 0.32	4.22 ± 0.67	1.99	NS	NS	0.77 (-0.76, 2.3)	NS	1.3 (-0.23, 2.8)	NS	0.52 (-1.0, 0.52)	NS
	C_{max}	2.70 ± 0.17	2.68 ± 0.17	1.60 ± 0.14	35.3	< 0.001	< 0.001	-0.02 (-0.39, 0.34)	NS	-1.1 (-1.5, -0.78)	< 0.001	-1.1 (-1.5, -1.1)	< 0.001
	AUC_{12}	17.7 ± 1.08	18.1 ± 1.2	11.0 ± 1.2	46.3	< 0.001	< 0.001	0.27 (-1.7, 2.2)	NS	-6.8 (-8.8, -4.9)	< 0.001	-7.1 (-9.1, -7.1)	< 0.001
Mineralocorticoids													
Aldosterone	T_{max}	4.11 ± 0.84	3.88 ± 0.73	3.43 ± 0.67	0.03	NS	NS	-0.11 (-2.4, 2.2)	NS	-0.25 (-2.5, 2.0)	NS	-0.14 (-2.4, -0.14)	NS
	C_{max}	0.31 ± 0.03	0.34 ± 0.03	0.31 ± 0.03	1.42	NS	NS	0.01 (-0.01, 0.03)	NS	-0.01 (-0.03, 0.01)	NS	-0.02 (-0.04, -0.02)	NS
	AUC_{12}	3.06 ± 0.2	3.19 ± 0.21	3.12 ± 0.24	1.76	NS	NS	0.12 (-0.03, 0.28)	NS	0.06 (-0.09, 0.22)	NS	-0.06 (-0.22, -0.06)	NS
11-Deoxy-	T_{max}	3.43 ± 0.44	3.85 ± 0.48	2.98 ± 0.65	0.56	NS	NS	0.16 (-1.6, 1.9)	NS	-0.59 (-2.3, 1.2)	NS	-0.75 (-2.5, -0.75)	NS
corticosterone	C_{max}	0.53 ± 0.08	0.57 ± 0.07	0.49 ± 0.07	2.29	NS	NS	0.04 (-0.03, 0.11)	NS	-0.02 (-0.09, 0.05)	NS	-0.06 (-0.13, -0.06)	0.088
	AUC_{12}	5.84 ± 0.88	6.10 ± 0.87	5.45 ± 0.86	1.66	NS	NS	0.34 (-0.25, 0.94)	NS	-0.10 (-0.69, 0.50)	NS	-0.44 (-1.0, -0.44)	NS
Androgens													
DHEA	T_{max}	3.50 ± 0.53	4.88 ± 0.53	3.76 ± 0.7	1.58	NS	NS	1.2 (-0.74, 3.2)	NS	-0.11 (-2.1, 1.8)	NS	-1.3 (-3.3, -1.3)	NS
	C_{max}	80.9 ± 7.0	78.5 ± 6.0	57.1 ± 5.3	8.77	< 0.001	0.0092	-0.95 (-16, 14)	NS	-24 (-39, -8.7)	< 0.001	-23 (-38, -23)	0.0013
	AUC_{12}	609 ± 41.1	608 ± 43.0	455 ± 36.9	20.2	< 0.001	< 0.001	13 (-51, 77)	NS	-143 (-207, -79)	< 0.001	-156 (-220, -156)	< 0.001
DHEAS	T_{max}	5.40 ± 0.68	5.80 ± 0.58	4.50 ± 0.64	0.94	NS	NS	0.45 (-1.6, 2.5)	NS	-0.73 (-2.8, 1.3)	NS	-1.2 (-3.2, -1.2)	NS
	C_{max}	13764 ± 1397	14452 ± 1307	11896 ± 1280	11.8	< 0.001	0.0012	855 (-522, 2232)	NS	-1932 (-3310, -555)	0.003	-2787 (-4165, -2787)	< 0.001
	AUC_{12}	129057 ± 15047	136822 ± 12643	113005 ± 13334	7.05	0.0023	0.032	8277 (-7361, 23915)	NS	-16339 (-31977, -701)	0.038	-24616 (-40254, -24616)	< 0.001

(*continued on next page*)

Table 1 (*continued*)

		D-Amphetamine	Lisdexamfetamine	Placebo	Main effect of drug ($^{a,b,c}F_{2,42}$)	p value (non-corrected)	p value Bonferroni adjusted	Lisdexamfetamine - D-Amphetamine Mean (CI. low, CI. High)	p value	Placebo - D-Amphetamine Mean (CI. low, CI. High)	p value	Placebo - Lisdexamfetamine Mean (CI. low, CI. High)	p value
Androsterone	T_{max}	4.93 ± 0.89	5.08 ± 0.79	4.74 ± 0.76	0.14	NS	NS	-0.61 (-3.3, 2.1)	NS	-0.30 (-3.0, 2.4)	NS	0.32 (-2.4, 0.32)	NS
	C_{max}	6.93 ± 0.44	6.25 ± 0.46	6.42 ± 0.58	0.12	NS	NS	-0.20 (-1.2, 0.80)	NS	-0.04 (-1.0, 0.96)	NS	0.16 (-0.83, 0.16)	NS
	AUC_{12}	46.6 ± 3.6	44.1 ± 3.5	43.3 ± 4.5	0.21	NS	NS	0.82 (-4.3, 6.0)	NS	-0.61 (-5.8, 4.5)	NS	-1.4 (-6.6, -1.4)	NS
Androstenedione	T_{max}	3.36 ± 0.52	5.13 ± 0.58	2.23 ± 0.81	5.03	0.018	NS	2.0 (-0.23, 4.1)	0.092	-0.95 (-3.1, 1.2)	NS	-2.9 (-5.1, -2.9)	0.0053
in women	C_{max}	3.63 ± 0.40	3.46 ± 0.23	2.59 ± 0.24	11.6	< 0.001	0.0082	-0.20 (-0.78, 0.38)	NS	-1.1 (-1.7, -0.53)	< 0.001	-0.91 (-1.5, -0.91)	< 0.001
	AUC_{12}	31.5 ± 3.4	31.2 ± 2.1	23.6 ± 2.1	8.07	0.0032	0.044	-0.96 (-6.7, 4.8)	NS	-8.9 (-15, -3.2)	< 0.001	-8.0 (-14, -8.0)	0.0032
Androstenedione	T_{max}	3.46 ± 0.57	3.96 ± 0.51	2.83 ± 0.82	0.76	NS	NS	0.50 (-1.6, 2.6)	NS	-0.63 (-2.8, 1.5)	NS	-1.1 (-3.3, -1.1)	NS
in men	C_{max}	2.68 ± 0.18	2.52 ± 0.18	2.14 ± 0.19	8.42	0.0019	0.027	-0.16 (-0.47, 0.15)	NS	-0.53 (-0.84, -0.22)	< 0.001	-0.37 (-0.69, -0.37)	0.014
	AUC_{12}	22.3 ± 1.2	23.0 ± 1.6	18.7 ± 1.8	8.66	0.0017	0.023	0.64 (-1.9, 3.2)	NS	-3.6 (-6.2, -1.0)	0.0031	-4.2 (-6.8, -4.2)	< 0.001
Testosterone	T_{max}	3.32 ± 0.96	6.25 ± 0.83	3.64 ± 1.05	2.36	NS	NS	2.6 (-0.60, 5.7)	NS	0.05 (-3.1, 3.2)	NS	-2.5 (-5.6, -2.5)	NS
in women	C_{max}	0.88 ± 0.1	0.88 ± 0.1	0.87 ± 0.14	0.15	NS	NS	0.01 (-0.26, 0.28)	NS	0.06 (-0.21, 0.33)	NS	0.05 (-0.22, 0.05)	NS
	AUC_{12}	9.25 ± 1.1	9.59 ± 1.2	8.14 ± 0.98	0.77	NS	NS	0.50 (-1.2, 2.2)	NS	-0.42 (-2.2, 1.3)	NS	-0.92 (-2.7, -0.92)	NS
Testosterone	T_{max}	4.21 ± 1.0	4.75 ± 0.66	3.50 ± 0.79	0.64	NS	NS	0.54 (-2.1, 3.1)	NS	-0.71 (-3.3, 1.9)	NS	-1.3 (-3.9, -1.3)	NS
in men	C_{max}	6.23 ± 0.40	6.17 ± 0.4	5.69 ± 0.37	1.46	NS	NS	-0.06 (-0.87, 0.74)	NS	-0.54 (-1.3, 0.27)	NS	-0.47 (-1.3, -0.47)	NS
	AUC_{12}	62.0 ± 4.3	62.0 ± 3.8	57.0 ± 3.6	1.59	NS	NS	0.00 (-7.7, 7.7)	NS	-5.1 (-13, 2.6)	NS	-5.1 (-13, -5.1)	NS
Testosterone +	T_{max}	3.41 ± 0.52	5.13 ± 0.58	2.50 ± 0.78	4.14	0.033	NS	1.9 (-0.29, 4.1)	NS	-0.70 (-2.9, 1.5)	NS	-2.6 (-4.8, -2.6)	0.015
androstenedione	C_{max}	4.45 ± 0.39	4.30 ± 0.22	3.40 ± 0.28	7.74	0.0038	0.053	-0.15 (-0.82, 0.53)	NS	-1.0 (-1.7, -0.37)	< 0.001	-0.90 (-1.6, -0.90)	0.0051
in women	AUC_{12}	40.8 ± 3.5	40.8 ± 2.2	31.7 ± 2.4	6.83	0.0062	0.087	-0.46 (-7.2, 6.2)	NS	-9.4 (-16, -2.7)	0.0032	-8.9 (-16, -8.9)	0.0052
Testosterone +	T_{max}	4.38 ± 0.96	4.13 ± 0.62	3.04 ± 0.69	0.84	NS	NS	-0.25 (-2.8, 2.3)	NS	-1.3 (-3.9, 1.2)	NS	-1.1 (-3.6, -1.1)	NS
androstenedione	C_{max}	8.50 ± 0.48	8.54 ± 0.48	7.62 ± 0.51	2.86	0.079	NS	0.05 (-0.97, 1.1)	NS	-0.87 (-1.9, 0.14)	NS	-0.92 (-1.9, -0.92)	0.086
in men	AUC_{12}	84.4 ± 4.7	85.0 ± 4.7	75.7 ± 4.7	3.19	0.061	NS	0.64 (-9.0, 10)	NS	-8.7 (-18, 0.99)	0.089	-9.3 (-19, -9.3)	0.061
Progestins													
Progesterone	T_{max}	5.73 ± 1.3	6.54 ± 0.98	4.73 ± 1.4	0.15	NS	NS	0.45 (-4.0, 4.9)	NS	-0.60 (-5.1, 3.9)	NS	-1.1 (-5.5, -1.1)	NS
in women	C_{max}	3.38 ± 2.4	4.95 ± 3.2	1.94 ± 1.1	0.76	NS	NS	2.2 (-5.0, 9.3)	NS	-1.6 (-8.8, 5.6)	NS	-3.8 (-11, -3.8)	NS
	AUC_{12}	31.8 ± 24.4	41.6 ± 26.7	17.4 ± 11.7	0.57	NS	NS	14 (-52, 81)	NS	-16 (-83, 51)	NS	-30 (-97, -30)	NS

(*continued on next page*)

Table 1 (*continued*)

		D-Amphetamine	Lisdexamfetamine	Placebo	Main effect of drug ($^{a,b,c}F_{2,42}$)	p value (non-corrected)	p value Bonferroni adjusted	Lisdexamfetamine - D-Amphetamine Mean (CI. low, CI. High)	p value	Placebo - D-Amphetamine Mean (CI. low, CI. High)	p value	Placebo - Lisdexamfetamine Mean (CI. low, CI. High)	p value
Progesterone	T_{max}	3.25 ± 0.40	3.42 ± 0.6	4.75 ± 0.94	1.53	NS	NS	0.17 (-2.0, 2.4)	NS	1.5 (-0.70, 3.7)	NS	1.3 (-0.87, 1.3)	NS
in men	C_{max}	0.52 ± 0.06	0.50 ± 0.06	0.39 ± 0.06	13.7	< 0.001	0.0019	-0.02 (-0.08, 0.04)	NS	-0.13 (-0.19, -0.06)	< 0.001	-0.11 (-0.17, -0.11)	< 0.001
	AUC_{12}	4.34 ± 0.64	4.47 ± 0.64	3.84 ± 0.68	13.9	< 0.001	0.0018	0.13 (-0.16, 0.43)	NS	-0.50 (-0.79, -0.20)	< 0.001	-0.63 (-0.93, -0.63)	< 0.001
17α-Hydroxy-	T_{max}	4.20 ± 0.58	4.27 ± 0.35	4.24 ± 0.79	0.02	NS	NS	0.00 (-2.0, 2.0)	NS	0.14 (-1.9, 2.2)	NS	0.14 (-1.9, 0.14)	NS
progesterone	C_{max}	4.01 ± 0.47	3.72 ± 0.46	2.91 ± 0.58	2.97	0.062	NS	-0.19 (-1.3, 0.96)	NS	-1.1 (-2.3, 0.03)	0.059	-0.93 (-2.1, -0.93)	NS
	AUC_{12}	31.2 ± 3.8	30.8 ± 4.0	24.5 ± 5.0	1.63	NS	NS	0.48 (-9.9, 11)	NS	-6.7 (-17, 3.7)	NS	-7.2 (-18, -7.2)	NS

Values for amphetamine and steroids are mean ± SEM in 23, 24 and 23 subjects after administration of D-amphetamine, lisdexamfetamine and placebo, respectively. Values for the subjective effects are from 24 subjects (mean ± SEM). CI, Confidence Interval 95%; T_{onset}, time to reach 10% of C_{max} (h); C_{max}, peak plasma concentration (nM); E_{max}, maximal effect on the Visual Analog Scale (%max); NS, not significant (p value > 0.1); T_{max}, time to reach C_{max} (h); AUC_{12}, area under the concentration–time curve to 12 h (ng × h/mL and nM × h and for amphetamine and steroids, respectively); DHEA, dehydroepiandrosterone; DHEAS, dehydroepiandrosterone sulfate; [a]for amphetamine $F_{1,22}$; [b]Subjective effects: $T_{onset/max}$: $F_{1,20}$, E_{max} and AUC_{12}: $F_{2,46}$; [c]only women $F_{2,18}$ or only men $F_{2,22}$. There were no significant differences in the steroid plasma concentrations between D-amphetamine and lisdexamfetamine.

used (Fig. 2, Table 1, see also [11]). Additionally, in the present study, the subjective and cardiovascular responses to lisdexamfetamine and D-amphetamine did not differ as also reported in detail elsewhere [11]. In contrast, another study in chronic stimulant users found that 100 mg lisdexamfetamine induced lower ratings of subjective "drug liking" than 40 mg D-amphetamine [7]. However, ratings of euphoria, amphetamine-like effects, and stimulant effects did not differ between the two treatments [7]. Altogether, the present findings reveal nearly identical pharmacokinetics and pharmacodynamics of a high dose of the recently marketed drug lisdexamfetamine and an equimolar dose of the classic immediate-release D-amphetamine that was given 1 h later. These results indicate a delay of the onset of the raise in circulating amphetamine levels, without altering the slope or maximal amphetamine concentrations. Therefore, lisdexamfetamine unlikely has prolonged clinical effects (aside from the later onset) or a lower abuse potential than the immediate-release D-amphetamine when used orally (unless the delayed onset is considered to reduce immediate rewarding effects). A lower risk of oral misuse may be expected with a slow elevation of plasma D-amphetamine concentrations and its associated effects, but this was clearly not the case, at least not at the doses tested in this study. In contrast, extended-release amphetamines may have a lower and delayed C_{max} compared with lisdexamfetamine [44]. Parenteral misuse of lisdexamfetamine produced effects that were comparable to oral use [45,46], suggesting an intranasal and intravenous abuse-deterrent property of lisdexamfetamine compared with D-amphetamine.

The effects of lisdexamfetamine on the HPA axis have not been previously studied. In this study, the impact of lisdexamfetamine and D-amphetamine on HPA axis activation was similar. Both amphetamines increased the concentrations of the active glucocorticoids cortisol and corticosterone and their respective inactive metabolite and precursor cortisone and 11-dehydrocorticosterone, which has been similarly reported for lower doses of D-amphetamine [16,25,26,28–31,47]. The mineralocorticoids aldosterone and 11-deoxycorticosterone were unaltered by lisdexamfetamine or D-amphetamine, in contrast to increases that were found after MDMA administration [13]. Plasma concentrations of the adrenal androgen precursors DHEA, DHEAS, and androstenedione increased, whereas testosterone and its degradation product androsterone were unaltered by the two D-amphetamine formulations. Plasma progesterone levels increased compared with placebo in men. In women, the absolute increase appeared to be larger but did not reach significance because of high interindividual variability (Supplementary Fig. S1).

In this study, we statistically compared the endocrine effects of D-amphetamine with other psychoactive substances that were tested in previous separate studies in our laboratory in healthy subjects under similar conditions [13,41]. In contrast to our hypothesis, D-amphetamine and lisdexamfetamine produced effects on plasma cortisol and corticosterone concentrations that were comparable to methylphenidate. Although the effects of methylphenidate on these active corticosteroids did not reach significance compared with placebo in our previous smaller study [13], the respective effects of D-amphetamine that were significant compared with placebo in this study were not significantly greater than those of methylphenidate. However, D-amphetamine produced greater cortisone and 11-dehydrocorticosterone levels than methylphenidate. Nevertheless, the present study indicates that the overall effects of D-amphetamine, lisdexamfetamine, and methylphenidate on plasma steroids at equivalent psychostimulant doses [37] are largely congruent.

Norepinephrine, DA, and 5-HT have all been implicated in mediating HPA axis stimulation [41,48]. However, the relative contribution of these monoamines to psychotropic-induced HPA axis stimulation in humans is unclear [48]. D-amphetamine may release cortisol mainly via NE [38]. Specifically, D-amphetamine more potently interacts with the NE transporter compared with the DA and 5-HT transporters, and it has a very low potency at the 5-HT transporter [35]. Additionally, the

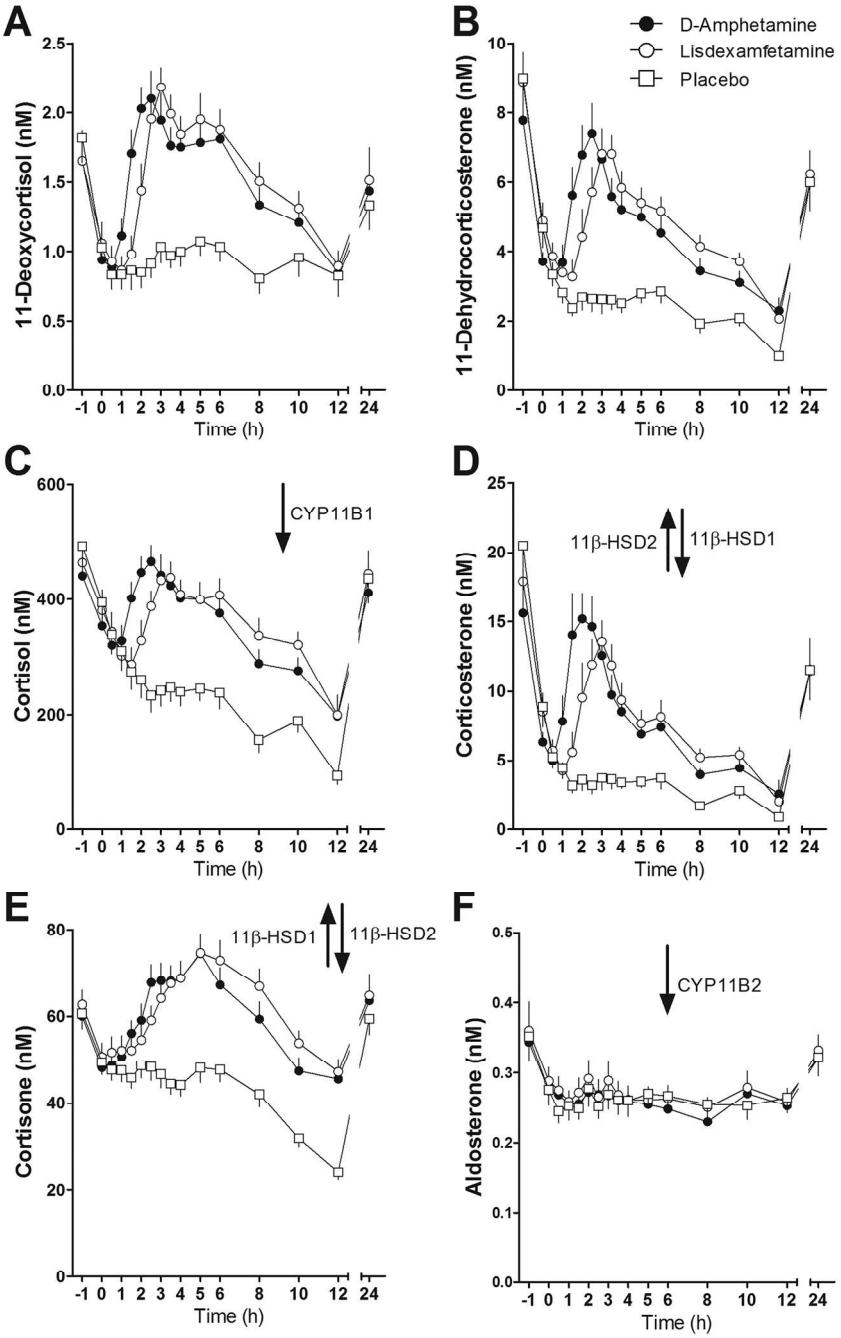

Fig. 3. Lisdexamfetamine administration results in delayed onset but similar increase and curve shapes of plasma glucocorticoid levels compared with D-amphetamine. Plasma concentrations of glucocorticoids and mineralocorticoids (11-deoxycortisol (A), 11-dehydrocorticosterone (B), cortisol (C), corticosterone (D), cortisone (E), and aldosterone (F)), following administration of D-amphetamine, lisdexamfetamine, and placebo, were quantified by UHPLC-MS/MS. Values are mean ± SEM in 23, 24, and 23 subjects, respectively. CYP, cytochrome P450; HSD, hydroxysteroid dehydrogenase.

effects of D-amphetamine and methamphetamine on plasma corticosteroids were blocked by α-adrenergic receptor antagonists [49] but not DA receptor antagonists [50]. Purely or predominantly serotonergic substances strongly stimulate the HPA axis [32,41,43]. In this study, we also statistically compared the effects of D-amphetamine with similar historical data on MDMA and LSD that were obtained in the same laboratory using the same clinical and analytical methods [13,41]. Compared with D-amphetamine and methylphenidate (which stimulate NE and DA), MDMA and LSD (which mainly stimulate 5-HT) produced greater increases in plasma concentrations of the biologically active glucocorticoids cortisol and corticosterone. Additionally, the MDMA-induced elevation of plasma cortisol was shown to be mediated by the release of 5-HT but not DA [51,52]. These findings support the view that 5-HT activation primarily or more strongly increases plasma cortisol compared with activation of the DA or NE systems [13,41,43].

We found other differential effects of the substances studied herein on HPA axis stimulation. Notably, compared with D-amphetamine, MDMA-induced increases in cortisol and corticosterone were paralleled by relatively smaller changes in the respective 11β-hydroxysteroid dehydrogenase 2 (11β-HSD2)-formed metabolite and precursor cortisone and 11-dehydrocorticosterone, indicating impairments in 11β-HSD2 activity that were caused by inhibition or saturation at elevated substrate concentrations by MDMA. In contrast, the LSD-induced increases in cortisol and corticosterone were significantly higher compared with

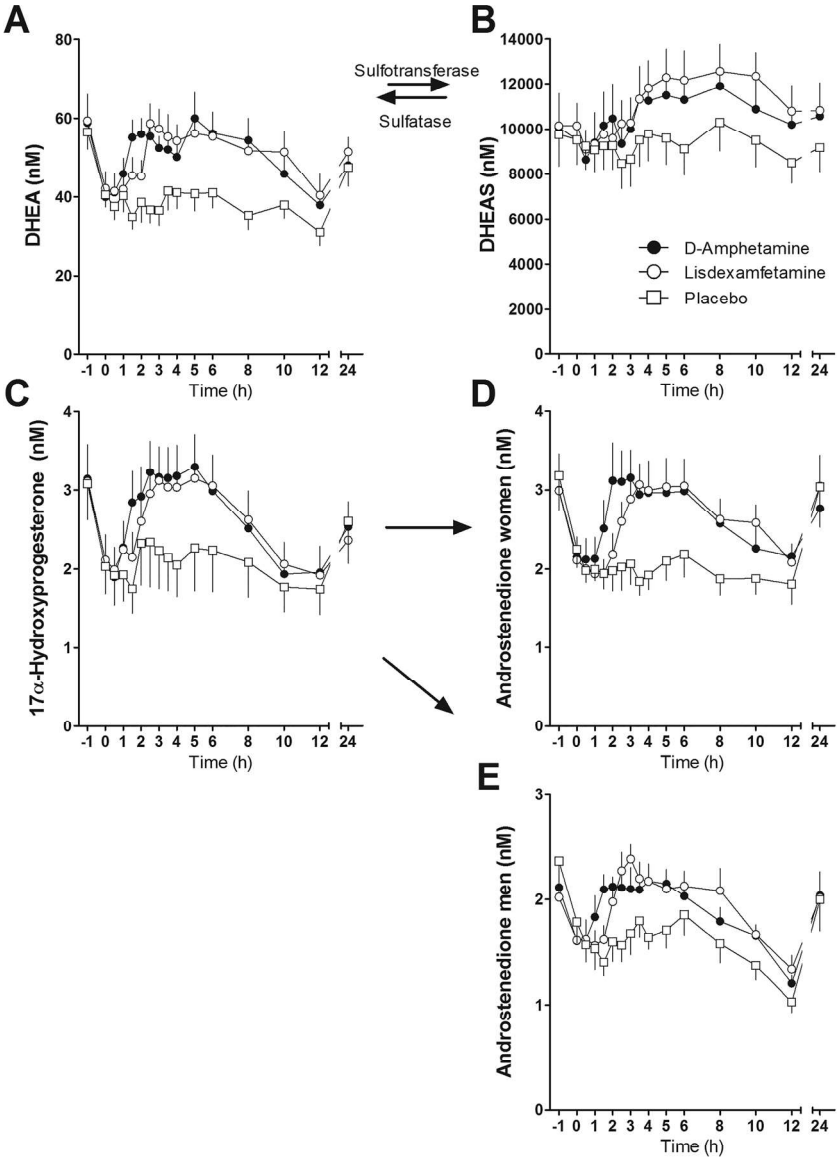

Fig. 4. D-amphetamine and lisdexamfetamine enhance plasma concentrations of adrenal androgens. The plasma concentrations of dehydroepiandrosterone (DHEA) (A), dehydroepiandrosterone sulfate (DHEAS) (B), 17α-hydroxyprogesterone (C), and androstenedione in women (D) and men (E), following administration of D-amphetamine and lisdexamfetamine compared with placebo, were quantified by UHPLC-MS/MS. The data in men represent the mean ± SEM in 12 subjects. The data in women represent the mean ± SEM in 11, 12, and 11 subjects, following administration of D-amphetamine, lisdexamfetamine, and placebo, respectively.

D-amphetamine, whereas the inactive metabolites cortisone and 11-dehydrocorticosterone induced comparable increases as those after D-amphetamine administration. Both the 5-HT releaser MDMA and 5-HT receptor agonist LSD [42] increased the sum of cortisol + cortisone more than D-amphetamine, indicating greater glucocorticoid production. This finding further supports the critical role of 5-HT in HPA axis stimulation by psychoactive substances and supports the use of cortisol as a marker of acute 5-HT activation [13,41,43].

In the present study, the endocrine response to both D-amphetamine formulations showed moderate acute tolerance, reflected by clockwise hysteresis of the amphetamine *vs.* cortisol or corticosterone concentration plots and as reported previously for the subjective response to D-amphetamine [53]. Plasma corticosterone levels normalized more rapidly than D-amphetamine disappeared from plasma (Supplementary Fig. S2). The characteristics of these hysteresis curves were similar after lisdexamfetamine and D-amphetamine administration, thus pointing towards the similarity of these two formulations in humans, in contrast to previous animal data on the pharmacokinetic-pharmacodynamic relationship [10]. Even more pronounced acute tolerance to the cortisol and corticosterone responses was previously reported for the amphetamine derivative MDMA [13,41] but not for the direct receptor agonist LSD [41]. The effects of lisdexamfetamine and D-amphetamine on plasma concentrations of cortisol and corticosterone lasted 10–12 h in the present study, whilst the effects of MDMA lasted only 4–6 h. These findings may reflect the somewhat longer half-live of D-amphetamine compared with MDMA (11 h *vs.* 8 h, respectively) [54,55] and likely also more pronounced acute tolerance to the effects of MDMA compared with D-amphetamine.

Activation of the HPA axis by amphetamines may be clinically relevant. This activation reflects a pharmacological stress response and has been shown to include increases in other endocrine markers of stress, including copeptin, oxytocin, epinephrine, and NE in the case of MDMA [13,15,40,56,57]. In recreational settings, MDMA increased plasma cortisol levels by up to 800% [58]. These marked endocrine responses that are induced by psychostimulants may affect mood, energy metabolism, sleep, and immune function [12,59]. For example, D-amphetamine, methylphenidate, and MDMA increased natural killer cells in plasma, reflecting activation of innate immune function

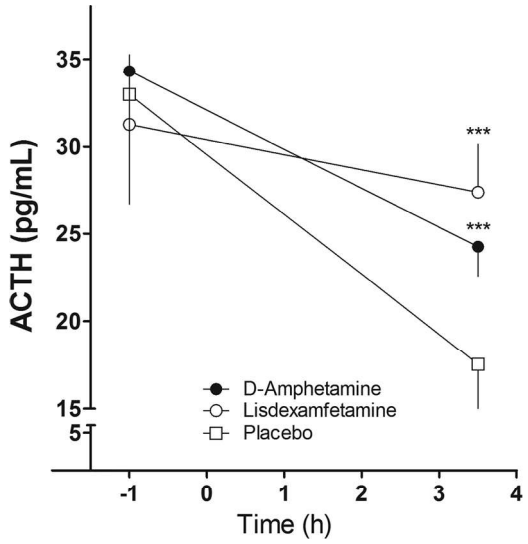

Fig. 5. D-amphetamine and lisdexamfetamine administration result in increased plasma ACTH concentrations. Plasma ACTH concentrations were measured 1 h before and 3.5 h after administration of D-amphetamine, lisdexamfetamine or placebo. Data represent mean ± SEM. ***$p < 0.001$, compared with placebo.

[12,60]. Increases in plasma epinephrine concentrations after methylphenidate and MDMA administration were associated with acute increases in circulating natural killer cells [12]. Increases in plasma cortisol following MDMA administration correlated with MDMA's cardiovascular effects and subjective "drug liking" [61]. Steroids may contribute to the mood-enhancing effects of psychostimulants [61–64], enhance the rewarding and reinforcing effects of drugs [24], and increase the risk of misuse. Furthermore, the disruption of circadian rhythms, including steroid secretion, has been associated with impairments in immune function, metabolic disturbances, eating and mood disorders, and cancer progression [65]. Several studies suggest that the chronic misuse of amphetamines interferes with HPA axis function and its circadian rhythms [66–68]. The effects of different chronic stimulant medications on cortisol levels in patients are unclear [69]. Some studies reported elevated morning or bedtime cortisol levels during treatment with methylphenidate and atomoxetine [70], transient increases in cortisol levels during methylphenidate treatment with normalization over 6 months [71], or no effect of methylphenidate [72]. Comparable data on the effects of chronic lisdexamfetamine and D-amphetamine administration on cortisol levels are lacking. Tolerance to subjective effects and cardio-stimulation has been observed after chronic lisdexamfetamine use [73–75]. However, whether and to what extent tolerance develops to the neuroendocrine effects of chronic use of these D-amphetamine formulations and the time-course of such tolerance remain to be determined.

A limitation of the present study is the use of only single and relatively high doses of lisdexamfetamine and D-amphetamine. The single dose of 100 mg lisdexamfetamine was above the maximal therapeutic dose for the treatment of ADHD of 70 mg. However, the single dose of 100 mg lisdexamfetamine mimics the misuse of lisdexamfetamine and produces plasma D-amphetamine concentrations that were comparable to those of repeated daily administration of 70 mg lisdexamfetamine when steady state is reached. Furthermore, plasma exposure to D-amphetamine would be higher in children compared to adults after the administration of the same dose of lisdexamfetamine [76]. Nevertheless, we cannot rule out possible differences in the pharmacokinetics and endocrine effects of lisdexamfetamine and D-amphetamine when they are administered at lower or higher doses than those used in this study. Additionally, we studied only acute administration. Repeated lisdexamfetamine administration may result in tolerance to its endocrine effects, which has been reported for subjective effects with chronic use [73–75]. Furthermore, the statistical comparisons between the effects of D-amphetamine, methylphenidate, MDMA, and LSD relied on data from different studies within the same laboratory, and thus such comparisons were indirect and not within the same study and subjects. Thus, we cannot exclude that the differences are due to differences between studies rather than drugs. This part of the study was also limited by the use of only one dose for all of the substances.

5. Conclusion

Lisdexamfetamine and an immediate-release D-amphetamine formulation produced similar peak plasma concentrations of active D-amphetamine and HPA axis stimulation in healthy subjects, suggesting similar pharmacokinetic, endocrine, and likely oral abuse-related properties. Moderate acute pharmacological tolerance to the endocrine response to lisdexamfetamine and D-amphetamine was observed. Whether chronic tolerance develops to the endocrine response of amphetamines requires further study. Comparable HPA axis activation was induced by the noradrenergic/dopaminergic substances lisdexamfetamine, D-amphetamine, and methylphenidate, whereas the serotonergic substances MDMA and LSD induced significantly greater HPA axis activation, supporting a predominant role for 5-HT in HPA axis stimulation by psychoactive substances.

Conflicts of interest

The authors declare that they have no conflicts of interest

Acknowledgments

The authors acknowledge the assistance of Toya Caluori, Raoul Dürig, Florian Hirt, and Felix Hammann for study management and Michael Arends for text editing. This study was supported by the Swiss Centre of Applied Human Toxicology (to AO) and the Swiss National Science Foundation (31003A-179400 to AO and 320030-170249 to MEL). The funders had no role in study design, data collection and

Table 2
Peak effects of D-amphetamine, lisdexamfetamine, methylphenidate, MDMA, and LSD on plasma glucocorticoids.

	D-Amphetamine 40 mg (N = 22)	Lisdexamfetamine 100 mg (N = 23)	Methylphenidate 60 mg (N = 16)[a]	MDMA 125 mg (N = 16)[a]	LSD 200 µg (N = 16)[b]	$F_{4,88}$	p value
Cortisol	314.5 ± 25.7	298.5 ± 17.4	275.7 ± 48.1	513.1 ± 51.9**	690.1 ± 54.3***	20.4	< 0.001
Cortisone	38.0 ± 3.3	39.0 ± 3.1	18.1 ± 3.4***	16.4 ± 3.3***	37.5 ± 4.1	10.5	< 0.001
Cortisol + cortisone	337.8 ± 27.9	323.5 ± 19.5	288.8 ± 49.1	520.3 ± 54.0*	721.4 ± 55.6***	19.3	< 0.001
Corticosterone	19.5 ± 2.7	16.4 ± 2.0	8.9 ± 2.5	27.6 ± 2.4	34.9 ± 3.8**	12.4	< 0.001
11-Dehydrocorticosterone	6.5 ± 0.8	6.1 ± 0.6	1.9 ± 0.4***	4.3 ± 0.4	6.0 ± 0.9	7.68	< 0.001
Corticosterone + 11-dehydrocorticosterone	26.0 ± 3.4	22.0 ± 2.6	10.3 ± 2.9**	31.6 ± 2.5	40.5 ± 4.6*	10.4	< 0.001

Values are mean ± SEM of the peak differences from placebo. *P < 0.05, **P < 0.01, ***P < 0.001 Tukey post hoc test compared with D-amphetamine. MDMA, 3,4-methylenedioxymethamphetamine or ecstasy; LSD, lysergic acid diethylamide. Data were adjusted from [a]Seibert et al. 2014 and [b]Strajhar et al. 2016.

analysis, decision to publish, or preparation of the manuscript.

Appendix A. Supplementary data

Supplementary material related to this article can be found, in the online version, at doi:https://doi.org/10.1016/j.jsbmb.2018.10.016.

References

[1] S.M. Krishnan, J.G. Stark, Multiple daily-dose pharmacokinetics of lisdexamfetamine dimesylate in healthy adult volunteers, Curr. Med. Res. Opin. 24 (1) (2008) 33–40.

[2] S.M. Krishnan, M. Pennick, J.G. Stark, Metabolism, distribution and elimination of lisdexamfetamine dimesylate: open-label, single-centre, phase I study in healthy adult volunteers, Clin. Drug Investig. 28 (12) (2008) 745–755.

[3] L.D. Johnston, P.M. O'Malley, J.G. Bachmann, J.E. Schulenberg, R.A. Miech, Monitoring the Future: National Survey Results on Drug Use, 1975–2013: Volume 2, College Students and Adults Ages 19-55, Institute for Social Research, University of Michigan, Ann Arbor, 2014.

[4] E. Liakoni, M.P. Schaub, L.J. Maier, G.V. Glauser, M.E. Liechti, The use of prescription drugs, recreational drugs, and "soft enhancers" for cognitive enhancement among Swiss secondary school students, PLoS One 10 (10) (2015) e0141289.

[5] L.J. Maier, E. Liakoni, J. Schildmann, M.P. Schaub, M.E. Liechti, Swiss university students' attitudes toward pharmacological cognitive enhancement, PLoS One 10 (12) (2015) e0144402.

[6] M. Pennick, Absorption of lisdexamfetamine dimesylate and its enzymatic conversion to d-amphetamine, Neuropsychiatr. Dis. Treat. 6 (2010) 317–327.

[7] D.R. Jasinski, S. Krishnan, Abuse liability and safety of oral lisdexamfetamine dimesylate in individuals with a history of stimulant abuse, J. Psychopharmacol. 23 (4) (2009) 419–427.

[8] D.J. Heal, S.L. Smith, J. Gosden, D.J. Nutt, Amphetamine, past and present—a pharmacological and clinical perspective, J. Psychopharmacol. 27 (6) (2013) 479–496.

[9] D.R. Coghill, B. Caballero, S. Sorooshian, R. Civil, A systematic review of the safety of lisdexamfetamine dimesylate, CNS Drugs 28 (6) (2014) 497–511.

[10] H.L. Rowley, R. Kulkarni, J. Gosden, R. Brammer, D. Hackett, D.J. Heal, Lisdexamfetamine and immediate release d-amfetamine - differences in pharmacokinetic/pharmacodynamic relationships revealed by striatal microdialysis in freely-moving rats with simultaneous determination of plasma drug concentrations and locomotor activity, Neuropharmacology 63 (6) (2012) 1064–1074.

[11] P.C. Dolder, P. Strajhar, P. Vizeli, F. Hammann, A. Odermatt, M.E. Liechti, Pharmacokinetics and pharmacodynamics of lisdexamfetamine compared with D-amphetamine in healthy subjects, Front. Pharmacol. 8 (2017) 617.

[12] M.B. Bigler, S.B. Egli, C.M. Hysek, G. Hoenger, L. Schmied, F.S. Baldin, F.A. Marquardsen, M. Recher, M.E. Liechti, C. Hess, C.T. Berger, Stress-induced in vivo recruitment of human cytotoxic natural killer cells favors subsets with distinct receptor profiles and associates with increased epinephrine levels, PLoS One 10 (12) (2015) e0145635.

[13] J. Seibert, C.M. Hysek, C.A. Penno, Y. Schmid, D.V. Kratschmar, M.E. Liechti, A. Odermatt, Acute effects of 3,4-methylenedioxymethamphetamine and methylphenidate on circulating steroid levels in healthy subjects, Neuroendocrinology 100 (2014) 17–25.

[14] Y. Schmid, C.M. Hysek, L.D. Simmler, M.J. Crockett, B.B. Quednow, M.E. Liechti, Differential effects of MDMA and methylphenidate on social cognition, J. Psychopharmacol. 28 (2014) 847–856.

[15] C.M. Hysek, L.D. Simmler, N. Schillinger, N. Meyer, Y. Schmid, M. Donzelli, E. Grouzmann, M.E. Liechti, Pharmacokinetic and pharmacodynamic effects of methylphenidate and MDMA administered alone and in combination, Int. J. Neuropsychopharmacol. 17 (2014) 371–381.

[16] G.M. Besser, P.W. Butler, J. Landon, L. Rees, Influence of amphetamines on plasma corticosteroid and growth hormone levels in man, Br. Med. J. 4 (5682) (1969) 528–530.

[17] G. Chai, L. Governale, A.W. McMahon, J.P. Trinidad, J. Staffa, D. Murphy, Trends of outpatient prescription drug utilization in US children, 2002–2010, Pediatrics 130 (1) (2012) 23–31.

[18] M.E. Kaland, W. Klein-Schwartz, Comparison of lisdexamfetamine and dextroamphetamine exposures reported to U.S. poison centers, Clin. Toxicol. (Phila.) 53 (5) (2015) 477–485.

[19] S. Chung, G.H. Son, K. Kim, Circadian rhythm of adrenal glucocorticoid: its regulation and clinical implications, Biochim. Biophys. Acta 1812 (5) (2011) 581–591.

[20] T. Damstra, S. Barlow, A. Bergman, R. Kavlock, G. Van Der Kraak, Global Assessment of the State-of-the-Science of Endocrine Disruptors, International Programme on Chemical Safety, WHO Publication No. WHO/PCS/EDC/02.2, World Health Organization, Geneva, Switzerland, 2002.

[21] X. Du, T.Y. Pang, Is dysregulation of the HPA-axis a core pathophysiology mediating co-morbid depression in neurodegenerative diseases? Front. Psychiatry 6 (2015) 32.

[22] L. Fu, C.C. Lee, The circadian clock: pacemaker and tumour suppressor, Nat. Rev. Cancer 3 (5) (2003) 350–361.

[23] T. Ota, J.M. Fustin, H. Yamada, M. Doi, H. Okamura, Circadian clock signals in the adrenal cortex, Mol. Cell. Endocrinol. 349 (1) (2012) 30–37.

[24] P.V. Piazza, S. Maccari, J.M. Deminiere, M. Le Moal, P. Mormede, H. Simon, Corticosterone levels determine individual vulnerability to amphetamine self-administration, Proc. Natl. Acad. Sci. U. S. A. 88 (6) (1991) 2088–2092.

[25] T.L. White, A.J. Justice, H. de Wit, Differential subjective effects of D-amphetamine by gender, hormone levels and menstrual cycle phase, Pharmacol. Biochem. Behav. 73 (4) (2002) 729–741.

[26] R.G. Dos Santos, M. Valle, J.C. Bouso, J.F. Nomdedeu, J. Rodriguez-Espinosa, E.H. McIlhenny, S.A. Barker, M.J. Barbanoj, J. Riba, Autonomic, neuroendocrine, and immunological effects of ayahuasca: a comparative study with d-amphetamine, J. Clin. Psychopharmacol. 31 (6) (2011) 717–726.

[27] M. Sofuoglu, J. Poling, K. Hill, T. Kosten, Atomoxetine attenuates dextroamphetamine effects in humans, Am. J. Drug Alcohol Abuse 35 (6) (2009) 412–416.

[28] T.L. White, D.C. Lott, H. de Wit, Personality and the subjective effects of acute amphetamine in healthy volunteers, Neuropsychopharmacology 31 (5) (2006) 1064–1074.

[29] W.A. Brown, D.P. Corriveau, M.H. Ebert, Acute psychologic and neuroendocrine effects of dextroamphetamine and methylphenidate, Psychopharmacology (Berl.) 58 (2) (1978) 189–195.

[30] P.W. Butler, G.M. Besser, H. Steinberg, Changes in plasma cortisol induced by dexamphetamine and chlordiazepoxide given alone and in combination in man, J. Endocrinol. 40 (3) (1968) 391–392.

[31] D. Jacobs, T. Silverstone, L. Rees, The neuroendocrine response to oral dextroamphetamine in normal subjects, Int. Clin. Psychopharmacol. 4 (2) (1989) 135–147.

[32] M. Tancer, C.E. Johanson, Reinforcing, subjective, and physiological effects of MDMA in humans: a comparison with d-amphetamine and mCPP, Drug Alcohol Depend. 72 (1) (2003) 33–44.

[33] T.A. Grady, A. Broocks, S.K. Canter, T.A. Pigott, B. Dubbert, J.L. Hill, D.L. Murphy, Biological and behavioral responses to D-amphetamine, alone and in combination with the serotonin3 receptor antagonist ondansetron, in healthy volunteers, Psychiatry Res. 64 (1) (1996) 1–10.

[34] B.E. Schmeichel, C.W. Berridge, Neurocircuitry underlying the preferential sensitivity of prefrontal catecholamines to low-dose psychostimulants, Neuropsychopharmacology 38 (2013) 1079–1084.

[35] L. Simmler, T. Buser, M. Donzelli, Y. Schramm, L.H. Dieu, J. Huwyler, S. Chaboz, M. Hoener, M.E. Liechti, Pharmacological characterization of designer cathinones in vitro, Br. J. Pharmacol. 168 (2) (2013) 458–470.

[36] L.D. Simmler, A. Rickli, Y. Schramm, M.C. Hoener, M.E. Liechti, Pharmacological profiles of aminoindanes, piperazines, and pipradrol derivatives, Biochem. Pharmacol. 88 (2) (2014) 237–244.

[37] W.R. Martin, J.W. Sloan, J.D. Sapira, D.R. Jasinski, Physiologic, subjective, and behavioral effects of amphetamine, methamphetamine, ephedrine, phenmetrazine, and methylphenidate in man, Clin. Pharmacol. Ther. 12 (2) (1971) 245–258.

[38] S. Feldman, N. Conforti, J. Weidenfeld, Limbic pathways and hypothalamic neurotransmitters mediating adrenocortical responses to neural stimuli, Neurosci. Biobehav. Rev. 19 (2) (1995) 235–240.

[39] C.M. Hysek, L.D. Simmler, V. Nicola, N. Vischer, M. Donzelli, S. Krähenbühl, E. Grouzmann, M.C. Hoener, M.E. Liechti, Duloxetine inhibits effects of MDMA ("ecstasy") in vitro and in humans in a randomized placebo-controlled laboratory study, PLoS One 7 (2012) e36476.

[40] C.M. Hysek, L.D. Simmler, M. Ineichen, E. Grouzmann, M.C. Hoener, R. Brenneisen, J. Huwyler, M.E. Liechti, The norepinephrine transporter inhibitor reboxetine reduces stimulant effects of MDMA ("ecstasy") in humans, Clin. Pharmacol. Ther. 90 (2) (2011) 246–255.

[41] P. Strajhar, Y. Schmid, E. Liakoni, P.C. Dolder, K.M. Rentsch, D.V. Kratschmar, A. Odermatt, M.E. Liechti, Acute effects of lysergic acid diethylamide on circulating steroid levels in healthy subjects, J. Neuroendocrinol. 28 (3) (2016) 12374.

[42] A. Rickli, O.D. Moning, M.C. Hoener, M.E. Liechti, Receptor interaction profiles of novel psychoactive tryptamines compared with classic hallucinogens, Eur. Neuropsychopharmacol. 26 (8) (2016) 1327–1337.

[43] E. Seifritz, P. Baumann, M.J. Muller, O. Annen, M. Amey, U. Hemmeter, M. Hatzinger, F. Chardon, E. Holsboer-Trachsler, Neuroendocrine effects of a 20-mg citalopram infusion in healthy males: a placebo-controlled evaluation of citalopram as 5-HT function probe, Neuropsychopharmacology 14 (4) (1996) 253–263.

[44] J. Biederman, S.W. Boellner, A. Childress, F.A. Lopez, S. Krishnan, Y. Zhang, Lisdexamfetamine dimesylate and mixed amphetamine salts extended-release in children with ADHD: a double-blind, placebo-controlled, crossover analog classroom study, Biol. Psychiatry 62 (9) (2007) 970–976.

[45] D.R. Jasinski, S. Krishnan, Human pharmacology of intravenous lisdexamfetamine dimesylate: abuse liability in adult stimulant abusers, J. Psychopharmacol. 23 (4) (2009) 410–418.

[46] J.C. Ermer, K. Dennis, M.B. Haffey, W.J. Doll, E.P. Sandefer, M. Buckwalter, R.C. Page, B. Diehl, P.T. Martin, Intranasal versus oral administration of lisdexamfetamine dimesylate: a randomized, open-label, two-period, crossover, single-dose, single-centre pharmacokinetic study in healthy adult men, Clin. Drug Investig. 31 (6) (2011) 357–370.

[47] M. Sofuoglu, A.J. Waters, M. Mooney, T. Kosten, Riluzole and D-amphetamine interactions in humans, Prog. Neuropsychopharmacol. Biol. Psychiatry 32 (1) (2008) 16–22.

[48] V. Locatelli, E. Bresciani, L. Tamiazzo, A. Torsello, Central nervous system-acting drugs influencing hypothalamic-pituitary-adrenal axis function, Endocr. Dev. 17 (2010) 108–120.

[49] G.M. Besser, P.W. Butler, J.G. Ratcliffe, L. Rees, P. Young, Release by amphetamine in man of growth hormone and corticosteroids: the effects of thymoxamine and propranolol, Br. J. Pharmacol. 39 (1) (1970) 196P–197P.

[50] J.I. Nurnberger Jr., S. Simmons-Alling, L. Kessler, S. Jimerson, J. Schreiber, E. Hollander, C.A. Tamminga, N.S. Nadi, D.S. Goldstein, E.S. Gershon, Separate mechanisms for behavioral, cardiovascular, and hormonal responses to

dextroamphetamine in man, Psychopharmacology (Berl.) 84 (2) (1984) 200–204.
[51] C.M. Hysek, G. Domes, M.E. Liechti, MDMA enhances "mind reading" of positive emotions and impairs "mind reading" of negative emotions, Psychopharmacology (Berl.) 222 (2012) 293–302.
[52] Y. Schmid, A. Rickli, A. Schaffner, U. Duthaler, E. Grouzmann, C.M. Hysek, M.E. Liechti, Interactions between bupropion and 3,4-methylenedioxymethamphetamine in healthy subjects, J. Pharmacol. Exp. Ther. 353 (1) (2015) 102–111.
[53] L.H. Brauer, J. Ambre, H. De Wit, Acute tolerance to subjective but not cardiovascular effects of d-amphetamine in normal, healthy men, J. Clin. Psychopharmacol. 16 (1) (1996) 72–76.
[54] Y. Schmid, P. Vizeli, C.M. Hysek, K. Prestin, H.E. Meyer Zu, M.E. Schwabedissen, Liechti, CYP2D6 function moderates the pharmacokinetics and pharmacodynamics of 3,4-methylene-dioxymethamphetamine in a controlled study in healthy individuals, Pharmacogenet. Genom. 26 (8) (2016) 397–401.
[55] J. Ermer, R. Homolka, P. Martin, M. Buckwalter, J. Purkayastha, B. Roesch, Lisdexamfetamine dimesylate: linear dose-proportionality, low intersubject and intrasubject variability, and safety in an open-label single-dose pharmacokinetic study in healthy adult volunteers, J. Clin. Pharmacol. 50 (9) (2010) 1001–1010.
[56] C.M. Hysek, Y. Schmid, L.D. Simmler, G. Domes, M. Heinrichs, C. Eisenegger, K.H. Preller, B.B. Quednow, M.E. Liechti, MDMA enhances emotional empathy and prosocial behavior, Soc. Cogn. Affect. Neurosci. 9 (2014) 1645–1652.
[57] L.D. Simmler, C.M. Hysek, M.E. Liechti, Sex differences in the effects of MDMA (ecstasy) on plasma copeptin in healthy subjects, J. Clin. Endocrinol. Metab. 96 (2011) 2844–2850.
[58] A. Parrott, J. Lock, L. Adnum, J. Thome, MDMA can increase cortisol levels by 800% in dance clubbers, J. Psychopharmacol. 27 (1) (2013) 113–114.
[59] A.C. Parrott, Cortisol and 3,4-methylenedioxymethamphetamine: neurohormonal aspects of bioenergetic stress in ecstasy users, Neuropsychobiology 60 (3–4) (2009) 148–158.
[60] R. Pacifici, P. Zuccaro, C. Hernandez Lopez, S. Pichini, S. Di Carlo, M. Farre, P.N. Roset, J. Ortuno, J. Segura, R.L. Torre, Acute effects of 3,4-methylenedioxymethamphetamine alone and in combination with ethanol on the immune system in humans, J. Pharmacol. Exp. Ther. 296 (1) (2001) 207–215.
[61] D.S. Harris, M. Baggott, J.H. Mendelson, J.E. Mendelson, R.T. Jones, Subjective and hormonal effects of 3,4-methylenedioxymethamphetamine (MDMA) in humans, Psychopharmacology (Berl.) 162 (4) (2002) 396–405.
[62] D.S. Harris, V.I. Reus, O.M. Wolkowitz, J.E. Mendelson, R.T. Jones, Altering cortisol level does not change the pleasurable effects of methamphetamine in humans, Neuropsychopharmacology 28 (9) (2003) 1677–1684.
[63] J.H. Mendelson, N.K. Mello, M.B. Sholar, A.J. Siegel, N. Mutschler, J. Halpern, Temporal concordance of cocaine effects on mood states and neuroendocrine hormones, Psychoneuroendocrinology 27 (1–2) (2002) 71–82.
[64] N.K. Mello, I.M. Knudson, M. Kelly, P.A. Fivel, J.H. Mendelson, Effects of progesterone and testosterone on cocaine self-administration and cocaine discrimination by female rhesus monkeys, Neuropsychopharmacology 36 (11) (2011) 2187–2199.
[65] N. Nader, G.P. Chrousos, T. Kino, Interactions of the circadian CLOCK system and the HPA axis, Trends Endocrinol. Metab. 21 (5) (2010) 277–286.
[66] A.C. Parrott, C. Montgomery, M.A. Wetherell, L.A. Downey, C. Stough, A.B. Scholey, MDMA, cortisol, and heightened stress in recreational ecstasy users, Behav. Pharmacol. 25 (5-6) (2014) 458–472.
[67] V.G. Frokjaer, D. Erritzoe, K.K. Holst, K.S. Madsen, P.M. Fisher, J. Madsen, C. Svarer, G.M. Knudsen, In abstinent MDMA users the cortisol awakening response is off-set but associated with prefrontal serotonin transporter binding as in non-users, Int. J. Neuropsychopharmacol. 17 (8) (2014) 1119–1128.
[68] G. King, D. Alicata, C. Cloak, L. Chang, Psychiatric symptoms and HPA axis function in adolescent methamphetamine users, J. Neuroimmune Pharmacol. 5 (4) (2010) 582–591.
[69] S. Lurie, A. O'Quinn, Neuroendocrine responses to methylphenidate and d-amphetamine: applications to attention-deficit disorder, J. Neuropsychiatry Clin. Neurosci. 3 (1) (1991) 41–50.
[70] Y.H. Chen, X.X. Lin, H. Chen, Y.Y. Liu, G.X. Lin, L.X. Wei, Y.L. Hong, The change of the cortisol levels in children with ADHD treated by methylphenidate or atomoxetine, J. Psychiatr. Res. 46 (3) (2012) 415–416.
[71] L.J. Wang, Y.S. Huang, C.C. Hsiao, C.K. Chen, The trend in morning levels of salivary cortisol in children with ADHD during 6 months of methylphenidate treatment, J. Atten. Disord. 21 (3) (2017) 254–261.
[72] R. Maayan, R. Yoran-Hegesh, R. Strous, A. Nechmad, E. Averbuch, A. Weizman, B. Spivak, Three-month treatment course of methylphenidate increases plasma levels of dehydroepiandrosterone (DHEA) and dehydroepiandrosterone-sulfate (DHEA-S) in attention deficit hyperactivity disorder, Neuropsychobiology 48 (3) (2003) 111–115.
[73] C. Steer, J. Froelich, C.A. Soutullo, M. Johnson, M. Shaw, Lisdexamfetamine dimesylate: a new therapeutic option for attention-deficit hyperactivity disorder, CNS Drugs 26 (8) (2012) 691–705.
[74] R.L. Findling, A.C. Childress, A.J. Cutler, M. Gasior, M. Hamdani, M.C. Ferreira-Cornwell, L. Squires, Efficacy and safety of lisdexamfetamine dimesylate in adolescents with attention-deficit/hyperactivity disorder, J. Am. Acad. Child Adolesc. Psychiatry 50 (4) (2011) 395–405.
[75] L.A. Adler, D. Goodman, R. Weisler, M. Hamdani, T. Roth, Effect of lisdexamfetamine dimesylate on sleep in adults with attention-deficit/hyperactivity disorder, Behav. Brain Funct. 5 (2009) 34.
[76] J.C. Ermer, M. Pennick, G. Frick, Lisdexamfetamine dimesylate: prodrug delivery, amphetamine exposure and duration of efficacy, Clin. Drug Investig. 36 (5) (2016) 341–356.

Supplementary data

Acute effects of D-amphetamine and lisdexamfetamine on plasma steroid concentrations in healthy subjects

Petra Strajhar, Patrick Vizeli, Melanie Patt, Patrick C. Dolder, Denise V. Kratschmar, Matthias E. Liechti, and Alex Odermatt

1. Quantification of D-amphetamine in human plasma samples

1.1. Chemicals and reagents

HPLC-grade purity methanol and formic acid were purchased from Sigma-Aldrich (St. Louis, MO) or Biosolve (Dieuze, France). Distilled water was deionized using a MilliQ water purification system (Millipore, USA). Solutions of **D**-amphetamine hydrochloride and **D**-amphetamine-D_3 sulfate >99.9% were obtained from Lipomed (Arlesheim, Switzerland). All other chemicals were purchased from Sigma-Aldrich (St. Louis, MO), and of the highest grade available.

1.2. Instrumentation and analytical conditions

Analytical instruments: Ultra-High pressure liquid chromatography-tandem mass spectrometry (UHPLC-MS/MS) using a Agilent 1290 UHPLC instrument equipped with a binary solvent delivery system, an auto sampler (at 4°C), and a column oven, coupled to an Agilent 6490 triple quadrupole mass spectrometer equipped with a jet stream electrospray ionization interface (AJS-ESI) (Agilent Technologies, Basel, Switzerland) was used to determine **D**-amphetamine and **D**-amphetamine-D_3.

Liquid chromatography: The chromatographic separation was performed on a Waters Acquity UPLC BEH C18, 1.7 µm, 2.1×150 mm, column (Waters, Wexford, Ireland) at column temperature of 65ºC. The mobile phase was water-methanol-formic acid (41/59/0.1; v/v/v) and the flow rate was set at 0.45 mL/min. The analysis time was 1.5 min. A methanol in water (75/25 v/v) mixture was used as needle and needle-seat flushing solvent for 10 s after sample aspiration. Samples were stored until analysis in the auto sampler (maintained at 4°C). The injection volume was 3 µL per sample. Under these conditions, **D**-amphetamine and **D**-amphetamine-D_3 showed a retention time of 0.8 min.

Mass spectrometry: Characteristic precursor ions and their corresponding product ions for multiple reaction monitoring (MRM) were defined by using the compound optimizer software module included within the Mass Hunter Workstation software (Agilent Technologies, California, USA). **D**-amphetamine and **D**-amphetamine-D_3 (internal standard) were quantified using the corresponding mass transitions (**D**-amphetamine *m/z* 136.1→91.0 (16 V, Dwell 100 ms), *m/z* 136.1→119 (12 V, Dwell 100 ms) and **D**-amphetamine-D_3 *m/z* 139.1→94.0 (16 V, Dwell 10 ms)). The AJS-ESI source conditions were optimized using the integrated source optimizer tool and set in the positive ion mode as following: Nitrogen gas temperature (290°C), gas flow (14 L/min), nebulizer (20 psi), sheath gas temperature (300 °C), sheath gas flow (11 L/min), capillary voltage (3000 V), and nozzle voltage (1500 V) (Agilent Technologies, California, USA, B.08.00/Build 8.0.8023.0).

Data analysis: The Mass Hunter Workstation Acquisition software Version B.08.00/Build 8.0.8023.0 and MassHunter Workstation Software Quantitative Analysis Version B.07.01 /Build 7.1.524.0, respectively (Agilent Technologies, California, USA) was used for data acquisition and subsequent data analysis.

Standard solutions: **D**-amphetamine hydrochloride (1 mg free base /1 mL methanol) and **D**-amphetamine-D_3 sulfate (0.1 mg free base /1 mL methanol) solutions were bought as reference standards. Stock solutions in methanol containing 10 µL/mL **D**-amphetamine or **D**-amphetamine-D_3 were prepared and stored at -20ºC.

Sample preparation: To 100 µL of sample, calibrator or quality control, 20 µL of a **D**-amphetamine-D_3 internal standard solution (0.25 µg/mL), and 500 µL ethyl acetate for liquid–liquid extraction was added. The samples were shortly vortexed, vigorously mixed on a rotating mixer for 5 min, and centrifuged for 10 min at 16,000 x g at 4°C. The upper ethyl acetate layer (350 µL) was transferred into fresh vials and evaporated to dryness under nitrogen. Afterwards the samples were reconstituted in 50 µL methanol (10 min, 1300 rpm, 4°C, thermoshaker) and transferred into new glass vials.

Chromatographic performance: Ten-point calibration curves over the range of 0.78 to 200 ng/mL for ***D***-amphetamine were generated by a zero sample and nine calibrators in human plasma. The coefficient of determination (R^2) was 0.99 and at least 75% of all calibrators have to be valid.

Specificity: Human plasma samples without the addition of **D**-amphetamine and **D**-amphetamine-D_3 were processed and injected into the UHPLC–MS/MS within an analytical run. The peak areas evaluated in the blank samples were not allowed to exceed 20% of the mean LLOQ peak area.

Recovery: By comparing the mean peak areas of extracted with those of unextracted samples (100% recovery) the absolute recovery was determined. The **D**-amphetamine recoveries were 101.7%, 102.2%, and 100.3% at concentrations of 1.66, 12.5, and 100 ng/mL.

Limit of detection (LLOD) and limit of quantification (LLOQ): Lower limit of detection (LLOD) and lower limit of quantification (LLOQ) were assessed by analyzing decreasing amounts of **D**-amphetamine in human plasma and were calculated as the concentration giving peaks with a signal-to-noise ratio of ≥ 5 and ≥ 10, respectively. The LLOQ was decided as the lowest concentration on the calibration curve which fulfilled the criteria of imprecision below 20%, and inaccuracy within ±20%. The method had a LLOD of 0.26 ng/mL, respectively a LLOQ of 0.78 ng/mL for **D**-amphetamine.

Reproducibility: Five replicates of quality controls (QCs) at the concentration of 1.66, 12.5, and 100 ng/mL were processed and injected into the UHPLC–MS/MS. To ensure the reproducibility, these sets of QCs were tested within validation runs. In each run, intra-run imprecision (% coefficient of variation; CV%) of each QC series had to be below 15% (20% at the LLOQ) and intra-run inaccuracy (% relative error of measurement; RE%) had to be within ±15% of the nominal values (±20% at the LLOQ). The intra-day precision was less than 8.8% and the accuracy ranged from −12.5 to 14.9% throughout all QC concentrations.

Stability: The stability of **D**-amphetamine in human plasma was assessed using QC at the concentrations of 1.66, 12.5, and 100 ng/ml. The samples were reanalyzed after kept at different

storage conditions. The determined auto sampler stability (QC stored at 4°C for 24 h), as well as the short-term stability (storage of QC samples at −20°C for 1-week) were within ±15% of the nominal values.

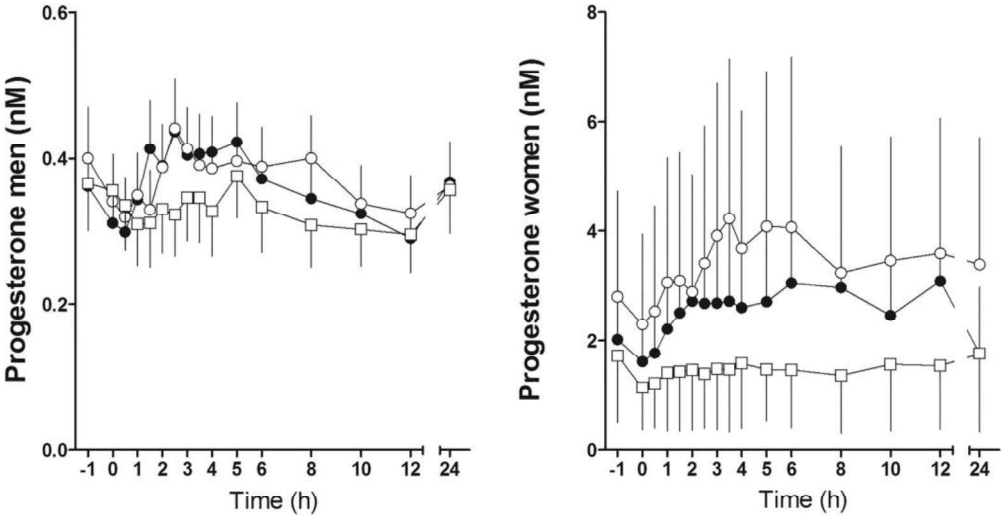

S1 Fig. Plasma concentrations of progesterone. Data in men represent mean and SEM in 12 subjects, whereas data in women represent mean and SEM in 11, 12, and 11 subjects following administration of D-amphetamine, lisdexamfetamine, and placebo, respectively.

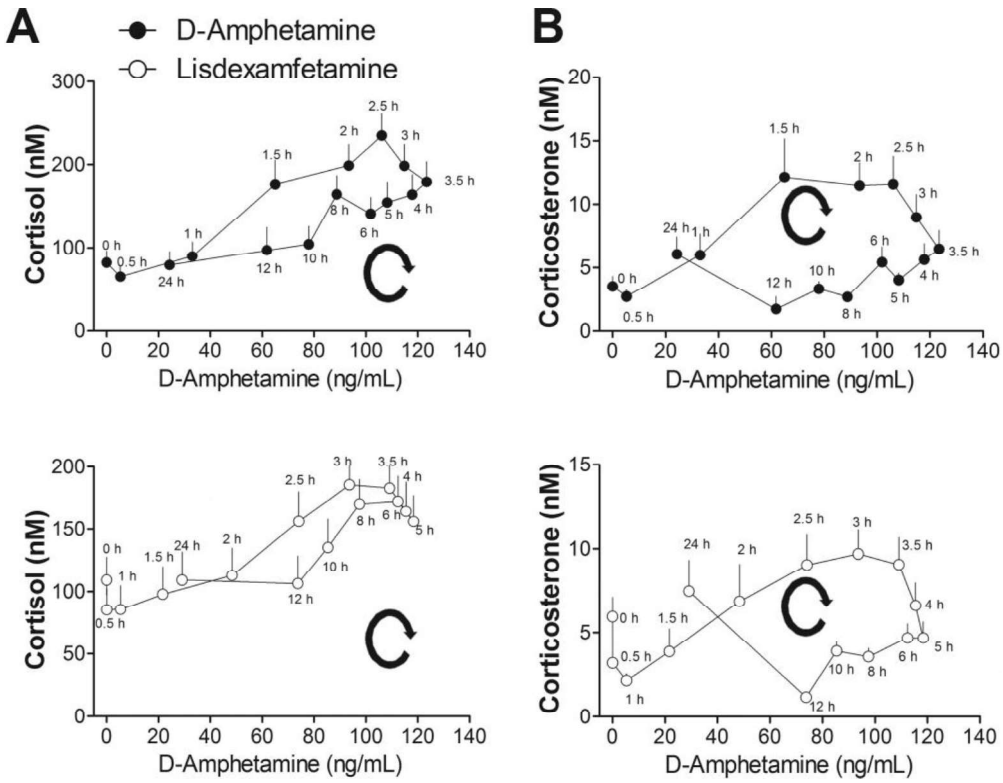

S2 Fig. D-amphetamine and lisdexamfetamine result in comparable acute pharmacological tolerance to the endocrine response of amphetamine. Drug-induced changes in plasma concentrations of cortisol (A) and corticosterone (B) are plotted against D-amphetamine concentrations over time (hysteresis curves) after administration of lisdexamfetamine and D-amphetamine in 24 and 23 subjects, respectively. The endocrine response represents the difference from placebo calculated for each time point to account for circadian changes in hormone levels. Lisdexamfetamine and D-amphetamine were administered at t = 0. The time of sampling is noted next to each point. The clockwise hysteresis indicates acute pharmacological tolerance to the endocrine response of amphetamine which was comparable after administration of the two formulations. Data are mean ± SEM.

S1 Table. Interaction analysis of plasma steroids and subjective effects after D-amphetamine, lisdexamfetamine, or placebo with sex and treatment order.

			D-Amphetamine	Lisdexamfetamine	Placebo	Interaction effect of drug x treatment order($^{a,b,c}F_{10,32}$)	*p* value	Interaction effect of drug x sex($^{c,d}F_{2,40}$)	*p* value
Amphetamine		T_{onset}	0.8 ± 0.1	1.4 ± 0.1		0.06	NS	0.72	NS
		T_{max}	3.2 ± 0.2	4.4 ± 0.2		1.47	NS	2.37	NS
		C_{max}	134 ± 7	128 ± 5		0.12	NS	0.24	NS
		AUC_{12}	1014 ± 47	983 ± 42		0.21	NS	0.23	NS
Subjective effects	Drug liking	T_{onset}	0.9 ± 0.1	1.6 ± 0.2		3.16	0.092	0.89	NS
		T_{max}	2.7 ± 0.4	4.5 ± 0.5		3.58	0.074	0.36	NS
		E_{max}	51.2 ± 5.8	48.0 ± 6.9	3.7 ± 2.6	1.36	NS	0.85	NS
		AUC_{12}	251 ± 43	260 ± 52	5.2 ± 4.3	1.05	NS	0.48	NS
	Good drug effect	T_{onset}	0.9±0.1	1.5±0.1		5.28	0.033	0.57	NS
		T_{max}	2.8±0.3	4.4±0.5		0.04	NS	0.39	NS
		E_{max}	48.5±5.6	41.8±6.5	4.0±2.5	1.32	NS	0.49	NS
		AUC_{12}	226±42	236±51	5.4±4.4	1.07	NS	0.29	NS
	Drug high	T_{onset}	1.0±0.1	1.9±0.3		0.01	NS	2.32	NS
		T_{max}	2.4±0.2	3.6±0.4		0.41	NS	0.48	NS
		E_{max}	35.5±5.6	29.3±6.2	3.3±2.6	1.99	0.065	1.61	NS
		AUC_{12}	134±30	125±33	2.5±1.9	1.05	NS	1.43	NS
	Stimulated	T_{onset}	1.0±0.1	1.8±0.3		0.01	NS	1.21	NS
		T_{max}	2.3±0.2	4.4±1.0		0.07	NS	0.91	NS
		E_{max}	43.8±5.7	38.0±6.8	2.4±1.7	1.55	NS	0.41	NS
		AUC_{12}	178±30	152±35	1.7±1.1	0.69	NS	1.25	NS
Glucocorticoids	Cortisol	T_{max}	2.72 ± 0.29	3.17 ± 0.41	1.20 ± 0.41	1.88	0.085	0.74	NS
		C_{max}	534 ± 28.9	519 ± 24.9	417 ± 35.2	1.03	NS	1.65	NS
		AUC_{12}	4116 ± 286	4207 ± 287	2621 ± 252	1.82	0.097	0.33	NS
	Cortisone	T_{max}	4.39 ± 0.3	4.67 ± 0.3	2.80 ± 0.5	3.85	0.0017	0.67	NS
		C_{max}	80.6 ± 4.2	82.8 ± 4.3	58.0 ± 3.0	0.81	NS	3.56	0.038
		AUC_{12}	707 ± 35.2	739 ± 35.5	503 ± 26.4	0.86	NS	2.82	0.072

	Corticosterone	T_{max}	2.59 ± 0.47	3.0 ± 0.38	2.24 ± 0.5	0.3	NS	4.91	0.012
		C_{max}	22.6 ± 2.6	20.1 ± 2.0	11.6 ± 1.4	0.48	NS	1.93	NS
		AUC_{12}	85.1 ± 6.2	83.1 ± 6.0	36.6 ± 3.2	0.84	NS	0.15	NS
	11-Dehydro-	T_{max}	2.96 ± 0.48	2.88 ± 0.38	2.46 ± 0.55	1	NS	3.54	0.038
	corticosterone	C_{max}	8.93 ± 0.86	8.82 ± 0.64	5.43 ± 0.53	0.4	NS	0.14	NS
		AUC_{12}	51.4 ± 4.0	53.7 ± 3.2	28.8 ± 2.2	0.77	NS	0.23	NS
	Cortisol +	T_{max}	2.93 ± 0.3	3.65 ± 0.38	1.20 ± 0.41	1.86	0.089	0.72	NS
	cortisone	C_{max}	601 ± 31	583 ± 26.5	469 ± 36	1.14	NS	1.13	NS
		AUC_{12}	4824 ± 299	4945 ± 307	3124 ± 266	1.91	0.081	0.47	NS
	Ratio	T_{max}	1.83 ± 0.44	3.10 ± 0.61	2.02 ± 0.63	0.76	NS	0.76	NS
	cortisol/cortisone	C_{max}	9.42 ± 0.57	9.25 ± 0.49	8.81 ± 0.72	0.86	NS	7.48	0.0017
		AUC_{12}	72.3 ± 5.1	69.8 ± 4.0	61.5 ± 5.2	0.53	NS	4.22	0.022
	Corticosterone +	T_{max}	2.59 ± 0.47	3.0 ± 0.36	2.37 ± 0.54	0.32	NS	5	0.012
	11-dehydro-	C_{max}	31.2 ± 3.3	28.5 ± 2.6	16.9 ± 1.9	0.37	NS	1.42	NS
	corticosterone	AUC_{12}	136 ± 9.5	137.0 ± 8.6	65.3 ± 5.0	0.82	NS	0.1	NS
	ratio	T_{max}	2.59 ± 0.44	2.98 ± 0.43	2.39 ± 0.56	0.79	NS	0.48	NS
	corticosterone/11-	C_{max}	3.01 ± 0.24	2.73 ± 0.14	2.24 ± 0.14	1.48	NS	1.65	NS
	dehydrocorticosterone	AUC_{12}	18.7 ± 1.1	17.3 ± 0.93	13.9 ± 1.03	0.84	NS	0.25	NS
	11-Deoxycortisol	T_{max}	3.02 ± 0.29	3.83 ± 0.32	4.22 ± 0.67	1.02	NS	2.13	NS
		C_{max}	2.70 ± 0.17	2.68 ± 0.17	1.60 ± 0.14	0.65	NS	1.24	NS
		AUC_{12}	17.7 ± 1.08	18.1 ± 1.2	11.0 ± 1.2	1.24	NS	0.72	NS
Mineralocorticoids	Aldosterone	T_{max}	4.11 ± 0.84	3.88 ± 0.73	3.43 ± 0.67	1.05	NS	0.58	NS
		C_{max}	0.31 ± 0.03	0.34 ± 0.03	0.31 ± 0.03	0.77	NS	0.56	NS
		AUC_{12}	3.06 ± 0.2	3.19 ± 0.21	3.12 ± 0.24	1.14	NS	1.29	NS
	11-Deoxy-	T_{max}	3.43 ± 0.44	3.85 ± 0.48	2.98 ± 0.65	0.55	NS	0.49	NS
	corticosterone	C_{max}	0.53 ± 0.08	0.57 ± 0.07	0.49 ± 0.07	0.73	NS	0.52	NS
		AUC_{12}	5.84 ± 0.88	6.10 ± 0.87	5.45 ± 0.86	0.91	NS	1	NS
Androgens	DHEA	T_{max}	3.50 ± 0.53	4.88 ± 0.53	3.76 ± 0.7	0.61	NS	1.52	NS
		C_{max}	80.9 ± 7.0	78.5 ± 6.0	57.1 ± 5.3	1.88	0.086	0.47	NS

		AUC_{12}	609 ± 41.1	608 ± 43.0	455 ± 36.9	0.94	NS	1.86	NS
	DHEAS	T_{max}	5.40 ± 0.68	5.80 ± 0.58	4.50 ± 0.64	1.46	NS	2.7	0.079
		C_{max}	13764 ± 1397	14452 ± 1307	11896 ± 1280	1.58	NS	0.49	NS
		AUC_{12}	129057 ± 15047	136822 ± 12643	113005 ± 13334	1.38	NS	1.4	NS
	Androsterone	T_{max}	4.93 ± 0.89	5.08 ± 0.79	4.74 ± 0.76	1.82	0.098	0.29	NS
		C_{max}	6.93 ± 0.44	6.25 ± 0.46	6.42 ± 0.58	0.97	NS	1.26	NS
		AUC_{12}	46.6 ± 3.6	44.1 ± 3.5	43.3 ± 4.5	0.59	NS	1.82	NS
	Androstenedione	T_{max}	3.36 ± 0.52	5.13 ± 0.58	2.23 ± 0.81	1.56	NS		
	in women	C_{max}	3.63 ± 0.40	3.46 ± 0.23	2.59 ± 0.24	0.17	NS		
		AUC_{12}	31.5 ± 3.4	31.2 ± 2.1	23.6 ± 2.1	0.27	NS		
	Androstenedione	T_{max}	3.46 ± 0.57	3.96 ± 0.51	2.83 ± 0.82	0.74	NS		
	in men	C_{max}	2.68 ± 0.18	2.52 ± 0.18	2.14 ± 0.19	0.88	NS		
		AUC_{12}	22.3 ± 1.2	23.0 ± 1.6	18.7 ± 1.8	0.49	NS		
	Testosterone	T_{max}	3.32 ± 0.96	6.25 ± 0.83	3.64 ± 1.05	0.7	NS		
	in women	C_{max}	0.88 ± 0.1	0.88 ± 0.1	0.87 ± 0.14	0.77	NS		
		AUC_{12}	9.25 ± 1.1	9.59 ± 1.2	8.14 ± 0.98	0.48	NS		
	Testosterone	T_{max}	4.21 ± 1.0	4.75 ± 0.66	3.50 ± 0.79	0.73	NS		
	in men	C_{max}	6.23 ± 0.40	6.17 ± 0.4	5.69 ± 0.37	0.7	NS		
		AUC_{12}	62.0 ± 4.3	62.0 ± 3.8	57.0 ± 3.6	0.49	NS		
	Testosterone +	T_{max}	3.41 ± 0.52	5.13 ± 0.58	2.50 ± 0.78	1.28	NS		
	androstenedione	C_{max}	4.45 ± 0.39	4.30 ± 0.22	3.40 ± 0.28	0.31	NS		
	in women	AUC_{12}	40.8 ± 3.5	40.8 ± 2.2	31.7 ± 2.4	0.26	NS		
	Testosterone +	T_{max}	4.38 ± 0.96	4.13 ± 0.62	3.04 ± 0.69	0.68	NS		
	androstenedione	C_{max}	8.50 ± 0.48	8.54 ± 0.48	7.62 ± 0.51	0.51	NS		
	in men	AUC_{12}	84.4 ± 4.7	85.0 ± 4.7	75.7 ± 4.7	0.43	NS		
Progestins	Progesterone	T_{max}	5.73 ± 1.3	6.54 ± 0.98	4.73 ± 1.4	1.69	NS		
	in women	C_{max}	3.38 ± 2.4	4.95 ± 3.2	1.94 ± 1.1	0.71	NS		
		AUC_{12}	31.8 ± 24.4	41.6 ± 26.7	17.4 ± 11.7	0.82	NS		
	Progesterone	T_{max}	3.25 ± 0.40	3.42 ± 0.6	4.75 ± 0.94	0.44	NS		
	in men	C_{max}	0.52 ± 0.06	0.50 ± 0.06	0.39 ± 0.06	0.82	NS		

	AUC_{12}	4.34 ± 0.64	4.47 ± 0.64	3.84 ± 0.68	0.6	NS		
17α-Hydroxy-	T_{max}	4.20 ± 0.58	4.27 ± 0.35	4.24 ± 0.79	2.08	0.057	0.71	NS
progesterone	C_{max}	4.01 ± 0.47	3.72 ± 0.46	2.91 ± 0.58	0.92	NS	0.17	NS
	AUC_{12}	31.2 ± 3.8	30.8 ± 4.0	24.5 ± 5.0	0.95	NS	0.3	NS

S1 Table. Interaction analysis of plasma steroids and subjective effects after D-amphetamine, lisdexamfetamine, or placebo with sex and treatment order. Values for amphetamine and steroids are mean ± SEM in 23, 24 and 23 subjects after administration of D-amphetamine, lisdexamfetamine and placebo. Values for the subjective effects are from 24 subjects (mean ± SEM). T_{onset}, time to reach 10% of C_{max} (h); C_{max}, peak plasma concentration (nM); E_{max}, maximal effect on the Visual Analog Scale (%max); NS, not significant; T_{max}, time to reach C_{max} (h); AUC_{12}, area under the concentration–time curve to 12 h (ng×h/mL and nM×h and for amphetamine and steroids, respectively); DHEA, dehydroepiandrosterone; DHEAS, dehydroepiandrosterone sulfate; [a]for subjective effects $T_{onset/max}$: $F_{1,19}$, E_{max} and AUC_{12}: $F_{10,36}$; [b]only women $F_{10,8}$ or only men $F_{10,12}$; [c]for amphetamine $F_{1,21}$; [d]for subjective effects: $T_{onset/max}$: $F_{1,19}$, E_{max} and AUC_{12}: $F_{2,44}$. There were no significant differences in the steroid plasma concentrations between D-amphetamine and lisdexamfetamine.

3.2.2 Published article:

Posaconazole-induced hypertension due to inhibition of 11β-hydroxylase and 11β-hydroxysteroid dehydrogenase 2

George R. Thompson III[1], Katharina R. Beck[2], Melanie Patt[2], Denise V. Kratschmar[2], Alex Odermatt[2], J Endocr Soc. 2019 Jun 6;3(7):1361-1366.

[1]Department of Internal Medicine, Division of Infectious Diseases and the Department of Medical Microbiology and Immunology, University of California Davis Medical Center, Davis, California 95616

[2]Swiss Centre for Applied Human Toxicology and Division of Molecular and Systems Toxicology, Department of Pharmaceutical Sciences, University of Basel, 4056 Basel, Switzerland

Contribution:

Quantified and analyzed steroid hormones in plasma samples and contributed to the writing of the manuscript.

ISSN 2472-1972

Posaconazole-Induced Hypertension Due to Inhibition of 11β-Hydroxylase and 11β-Hydroxysteroid Dehydrogenase 2

George R. Thompson III,[1] Katharina R. Beck,[2] Melanie Patt,[2] Denise V. Kratschmar,[2] and Alex Odermatt[2]

[1]Department of Internal Medicine, Division of Infectious Diseases and the Department of Medical Microbiology and Immunology, University of California Davis Medical Center, Davis, California 95616; and [2]Swiss Centre for Applied Human Toxicology and Division of Molecular and Systems Toxicology, Department of Pharmaceutical Sciences, University of Basel, 4056 Basel, Switzerland

ORCiD numbers: 0000-0002-6820-2712 (A. Odermatt).

We describe two cases of hypertension and hypokalemia due to mineralocorticoid excess caused by posaconazole treatment of coccidioidomycosis and rhinocerebral mucormycosis infections, respectively. Clinical laboratory evaluations, including a comprehensive analysis of blood and urine steroid profiles, revealed low renin and aldosterone and indicated as the underlying mechanism primarily a block of 11β-hydroxylase activity in patient 1, whereas patient 2 displayed weaker 11β-hydroxylase but more pronounced 11β-hydroxysteroid dehydrogenase 2 inhibition. The results show that both previously suggested mechanisms must be considered and emphasize significant interindividual differences in the contribution of each enzyme to the observed mineralocorticoid excess phenotype. The mineralocorticoid symptoms of patient 1 resolved after replacement of posaconazole therapy by isavoconazole, and posaconazole dosage de-escalation ameliorated the effects in patient 2. By providing a thorough analysis of the patients' blood and urine steroid metabolites, this report adds further evidence for two individually pronounced mechanisms of posaconazole-induced hypertension and hypokalemia. The elucidation of the factors responsible for the individual phenotype warrants further research.

Freeform/Key Words: posaconazole, hypertension, 11β-hydroxylase, 11β-hydroxysteroid dehydrogenase, mineralocorticoid excess, hypokalemia

1. Case Reports

Recent case reports describing posaconazole-induced mineralocorticoid excess suggested two distinct mechanisms promoting the observed hypertension and hypokalemia: inhibition of the adrenal enzyme 11β-hydroxylase [1, 2] or the peripheral cortisol metabolizing 11β-hydroxysteroid dehydrogenase 2 (11β-HSD2) [2–5]. The majority of these studies did not evaluate the patient's steroid profile in blood and urine, allowing only a limited understanding of the relative contribution of the two enzymes leading to the drug-induced hypertension and hypokalemia. Therefore, we conducted a detailed analysis of blood and urine steroid metabolites for the two presented cases to address this issue.

Abbreviations: 11β-HSD2, 11β-hydroxysteroid dehydrogenase 2; 11-DHC, 11-dehydrocorticosterone; 11-DOC, 11-deoxycorticosterone; UHPLC-MS/MS, ultra-high-performance liquid chromatography–tandem mass spectrometry.

Received 18 May 2019
Accepted 31 May 2019
First Published Online 6 June 2019

Case Report
July 2019 | Vol. 3, Iss. 7
doi: 10.1210/js.2019-00189 | Journal of the Endocrine Society | 1361–1366

2. Patient 1

A 54-year-old man with no past medical history presented with fever, chills, cough, and weight loss. His initial examination, vital signs (blood pressure 127/90 mm Hg), and chemistry and laboratory values (chem 10 test, liver function profile) were normal with the exception of positive serologic testing for coccidioidomycosis. Therefore, he was placed on fluconazole 600 mg daily. However, over the next 6 weeks he developed nausea and cheilitis and xerosis that were attributed to fluconazole therapy, and he was transitioned to posaconazole 300 mg daily. His systemic and respiratory symptoms improved; however, he developed new-onset hypertension (163/94 mm Hg) and hypokalemia (3.1 mmol/L) 8 weeks after starting posaconazole therapy. Besides posaconazole, he received only pantoprazole.

Because of suspected posaconazole-induced mineralocorticoid excess, an initial clinical laboratory evaluation was obtained, revealing very low renin (0.2 ng/mL/h) and undetectable aldosterone values (<3.0 ng/dL) but elevated concentrations of estradiol (49 pg/mL) and 11-deoxycortisol (320 ng/dL) and a posaconazole serum blood concentration of 3.1 μg/mL. Serum electrolyte concentrations were normal with the exception of continued hypokalemia (3.0 mmol/L). Treatment was continued and serum was obtained again 4 weeks later, with posaconazole levels of 2.7 μg/mL at that time. To gain closer insight into the mechanism of the posaconazole-induced mineralocorticoid excess, a comprehensive serum (Table 1) and urinary (Table 2) steroid analysis was performed with ultra-high-performance liquid chromatography–tandem mass spectrometry (UHPLC-MS/MS). The results confirmed serum aldosterone concentrations below the limit of detection, low corticosterone (42 ng/dL) and androstenedione (45 ng/dL) concentrations, and moderately elevated concentrations of 11-deoxycortisol (216 ng/dL) (Table 1), suggesting inhibition of 11β-hydroxylase. Normal serum levels were detected for cortisol (7.4 μg/dL), cortisone (1.65 μg/dL), 11-dehydrocorticosterone (11-DHC) (36 ng/dL), 11-deoxycorticosterone (11-DOC) (8.3 ng/dL), 17-hydroxyprogesterone [17-OH progesterone (102 ng/dL)], testosterone (242 ng/dL), and androstenedione (46 ng/dL).

Analysis of 24-hour urine revealed undetectable levels of aldosterone and very low tetrahydroaldosterone (4.95 μg/24 h) but normal concentrations of cortisol (111 μg/24 h), cortisone (113 μg/24 h), and their tetrahydro-metabolites (Table 2). Importantly, urinary 11-deoxycortisol (1.99 μg/24 h) and 11-DOC (2.96 μg/24 h) were markedly elevated, supporting an inhibition of 11β-hydroxylase. 17-OH progesterone (2.11 μg/24 h) was slightly elevated, and androgen metabolites were normal or low. Creatinine from the 24-hour urine collection was 61 mg/dL, and total creatinine 1552 mg.

Table 1. Detailed Analysis of Steroids in Blood From Posaconazole-Treated Patients

Steroid	Patient 1	Patient 2	Reference Range
Aldosterone, ng/dL	nd	nd	2.0–18
Cortisol (F), μg/dL	7.4	5.2	5.0–25
Cortisone (E), μg/dL	1.65	0.19[a]	1.0–3.5
F/E	4.5	27[b]	2–8
Corticosterone (B), ng/dL	42[a]	54[a]	62–1600
11-DHC (A), ng/dL	36	6.5	nr
B/A	1.16	8.3	nr
11-deoxycortisol, ng/dL	216[b]	186[b]	<158
11-DOC, ng/dL	8.3	3.2	2.0–19
Testosterone, ng/dL	242	32[a]	200–1070
Androstenedione, ng/dL	46	3.8[a]	30–250
17-OH progesterone, ng/dL	101	36	5–250

Steroids were quantified in a serum sample and a whole blood sample from patient 1 and patient 2, respectively. Samples were collected at 8 AM and analyzed by UHPLC-MS/MS [6]. Reference ranges are for men, age 20–50, samples taken between 8 and 10 AM, supine position [7, 8].
Abbreviations: nd, below lower limit of detection; nr, not reported.
[a]Below normal range.
[b]Above normal range.

Table 2. Comprehensive Analysis of Steroids in Urine From Posaconazole-Treated Patients

	Patient 1		Patient 2		Range
Steroid	**24-h Urine (μg/24 h)**	**24-h Urine Normalized to CRT × 10^{-6}**	**Spot Urine (ng/mL)**	**Spot Urine Normalized to CRT × 10^{-6}**	**24-h Urine (μg/24 h)**
Cortisol (F)	111	71	57	60	35–168
Cortisone (E)	113	73	29.5	31[a]	92–366
F/E	0.98[b]		1.95[b]		0.28–0.85
a-THF	626[a]	403	612	644[a]	796–2456
b-THF	1647	1061	1214	1277	942–2800
a-THE	69	44	22.1	23[a]	62–752
b-THE	2569	1655	516	543[a]	1365–5788
sumTHF/sumTHE	0.86		[b] 3.39		0.66–1.44
Corticosterone (B)	6.35[b]	4.1	2.21	2.33	0.2–4.8
11-DHC (A)	12.4	8.0	3.11	3.27[a]	6–40
B/A	0.51		0.71		nr
b-THB	348[b]	224	392	413	40–326
a-THB	370	238	119	126	86–588
b-THA	220[b]	142	21.8	23	3–65
a-THA	58[b]	37	24.1	25	2–29
sumTHB/sumTHA	2.58		11.1		
11-Deoxycortisol	1.99[b]	1.28	1.24	1.31[b]	<0.5
11-Deoxy-corticosterone	2.96[b]	1.91	1.37	1.44[b]	0.1–0.5
Aldosterone	nd[a]	nd	nd	nd[a]	2.3–21
TH-aldo	4.95[a]	3.19	nd		6–79
18-OH-F	23[a]	15	2.74	2.88[a]	51–515
18-OH-corticosterone	9.87[b]	6.4	1.30	1.37	1.5–6.5
a-Cortolone	1489	959	263	276[a]	333–1667
b-Cortolone	976	629	185	194	249–1049
b-Cortol	579[b]	373	256	270	70–336
Testosterone	6.87	4.4	0.56	0.59[a]	3–47
Androstenedione	19.9[a]	12.8	2.62	2.76[a]	50–220
Etiocholanolone	1406	906	192	202	430–3300
Androsterone	1315	847	271	285	320–5400
17-OH-progesterone	2.11[b]	1.4	1.40	1.47	0.2–1.5
11-Keto-etiocholanolone	315	203	nd	nd[a]	79–1026
11b-OH-etiocholanolone	864	557	39	41[a]	18–1034
11b-OH-androsterone	113[a]	73	26	27[a]	500–1733
Progesterone	2.62[a]	1.69	1.47	1.55	nr
Dehydroepiandrosterone	9.46[a]	6.1	1.54	1.62[a]	21–2710
Creatinine	0.61 mg/mL		0.95 mg/mL		0.63–2.50 g/24 h

Steroids were quantified in a 24-h urine sample and a spot urine sample from patient 1 and patient 2, respectively, by UHPLC-MS/MS. Total urine volume: 2550 mL. Reference ranges are for men, age 20–50 [8–10].
Abbreviations: 11-DHC, 11-dehydrocorticosterone; CRT, creatinine; E, cortisone; F, cortisol; nd, below lower limit of detection; nr, not reported; OH, hydroxy; TH-aldo, tetrahydroaldosterone; THA, tetrahydro-11-dehydrocorticosterone; THB, tetrahydrocorticosterone; THE, tetrahydrocortisone; THF, tetrahydrocortisol.
[a]Below normal range.
[b]Above normal range.

Posaconazole therapy was discontinued, and isavuconazole (186 mg daily) was initiated. On follow-up 6 weeks later, the patient's hypertension and hypokalemia had resolved (134/92 mm Hg and 4.3 mmol/L, respectively).

3. Patient 2

A 73-year-old man with a past medical history of multiple myeloma presented 3 months after initiation of dexamethasone and chemotherapy. He complained of left eye swelling and pain of 1 week's duration and was found on MRI to have maxillary sinus thickening with erosion and

inflammation of the surrounding structures, including the orbit. He immediately underwent surgical evaluation and received a diagnosis of rhinocerebral mucormycosis (*Rhizopus* spp identified on cultures and histopathology of the resected tissue). He underwent left orbital exenteration and maxillectomy and was treated with liposomal amphotericin B and micafungin for 21 days. He was thereafter transitioned to oral posaconazole 300 mg daily and discharged after 72 hours of observation and repeated surgical intervention showing no further evidence of infection.

Upon outpatient follow-up, ~9 weeks later, he was noted to have new onset of hypertension (blood pressure 154/69 mm Hg) and hypokalemia (3.3 mmol/L). All other vital signs were within normal limits. Besides posaconazole, this patient received filgrastim, sitagliptin, pantoprazole, and oxycodone. Physical examination found postoperative changes, left facial numbness, and no signs of ongoing infection. Laboratory evaluation revealed low renin (0.36 ng/mL/h), undetectable aldosterone (<2 ng/dL), and elevated 11-deoxycortisol (406 ng/dL) concentrations and a serum osmolality of 292 mOsm/kg, indicating mineralocorticoid excess due to posaconazole-dependent inhibition of 11β-hydroxylase. Furthermore, serum posaconazole levels were high (5.0 μg/mL), and estradiol concentrations were below the limit of detection (<15 pg/mL). Urine analyses at this time revealed spot osmolality of 292 mOsm/kg and potassium of 23.9 mmol/L, confirming a transtubular potassium gradient of 7.24.

The patient's posaconazole dosage was then reduced to 200 mg/d. However, after 4 weeks of this treatment, renin and aldosterone levels were found to be further dramatically decreased (<0.1 ng/mL/h and <2 ng/dL, respectively), and posaconazole concentrations were still elevated (3.3 μg/mL) but lower compared with the last visit, and estradiol levels stayed comparably low (<15 pg/mL). Again, further comprehensive blood steroid analyses were performed and revealed normal concentrations of cortisol (5.2 μg/dL) and 11-DOC (3.2 ng/dL), low levels of corticosterone (54 ng/dL), and clearly decreased levels of cortisone (0.19 μg/dL) and 11-DHC (6.5 ng/dL) (Table 1). 11-Deoxycortisol levels (186 ng/dL) were confirmed to be slightly elevated. However, cortisol to cortisone (27) and corticosterone to 11-DHC ratios (8.4) were markedly increased, indicating potent inhibition of 11β-HSD2. Testosterone and androstenedione were very low, whereas 17-OH progesterone was normal.

Analysis of spot urine revealed elevated ratios of cortisol to cortisone (1.95) and their tetrahydro-metabolites (3.39), supporting 11β-HSD2 inhibition (Table 2). Aldosterone and tetrahydroaldosterone were not detectable, whereas a qualitative analysis after normalization to creatinine suggested elevated levels of 11-deoxycortisol and 11-DOC, supporting partial inhibition of 11β-hydroxylase. Spot urine creatinine was 95 mg/dL.

Subsequently, his daily posaconazole dosage was lowered to 100 mg, and 3 weeks later his serum posaconazole level had further decreased to 1.68 μg/mL, his blood pressure had normalized to 130/76 mm Hg, and his potassium normalized at 4.4 mmol/L. The patient declined further laboratory evaluation due to the expense.

4. Discussion

The occurrence of hypertension and hypokalemia as adverse effects of posaconazole treatment has been reported in market authorization studies [6]. Nevertheless, only recently have several case studies addressed the mechanism underlying the symptoms of mineralocorticoid excess in more detail, with some debate about the predominantly affected enzyme [1, 2, 4, 5, 12–14]. Whereas some reports proposed 11β-HSD2 to be the cause of apparent mineralocorticoid excess [4, 5], others suggested 11β-hydroxylase to be responsible for the observed phenotype [1].

The detailed analyses of blood and urine steroids in the two presented cases allowed us to unravel the relative contribution of the two enzymes to the posaconazole-induced low-renin, low-aldosterone hypertension and hypokalemia. The elevated 11-deoxycortisol and 11-DOC concentrations along with normal or only slightly elevated ratios of cortisol to cortisone and their tetrahydro-metabolites indicate inhibition of CYP11B1 (and CYP11B2) as the predominant cause in patient 1, with weak or negligible inhibition of 11β-HSD2. In contrast, the markedly elevated ratios of active to inactive glucocorticoids, in both blood and urine, indicate

pronounced inhibition of 11β-HSD2 in patient 2. Additionally, the moderately increased 11-deoxycortisol revealed that CYP11B1 (and CYP11B2) was at least partially inhibited.

Patients with mineralocorticoid excess phenotype were found to generally exhibit high serum posaconazole concentrations (>2.5 μg/mL). The factors responsible for the increased serum levels and for the differential inhibition of CYP11B1/2 and 11β-HSD2 are not fully understood. The interindividual differences for the enzymatic inhibition may be explained by different distribution volumes limiting the concentrations of posaconazole reached in the adrenals, necessary to inhibit 11β-hydroxylase, compared with those in the kidney or colon, important for 11β-HSD2 inhibition.

Posaconazole is metabolized mainly by glucuronidation via UGT1A4 and a potent inhibitor of CYP3A4 and a substrate/inhibitor of the P-glycoprotein efflux transporter [15–17]. Thus, comedication must be carefully monitored. Regarding the two presented cases, comedication was unlikely to be a contributing factor to the onset of hypertension. Both patients received the proton pump inhibitor pantoprazole, which increases gastric pH, thereby potentially reducing the adsorption of posaconazole upon oral intake. No interactions with posaconazole are known for filgrastim and sitagliptin. A reduced metabolism of oxycodone by CYP3A4 might have been occurred, however, promoting opioid-dependent adverse effects rather than the mineralocorticoid excess. Furthermore, the bioavailability of posaconazole may be increased by reduced binding to serum albumin (>98% under normal conditions) in situations of severe inflammation or reduced liver and kidney function [18] or by genetic polymorphisms in metabolism (UGT1A4) and transport (P-glycoprotein) or altered expression of these proteins.

The two cases emphasize detailed blood and urine steroid analyses (especially quantification of aldosterone, tetrahydroaldosterone, cortisol, cortisone, their tetrahydrometabolites, 11-DOC, and 11-deoxycortisol) to unravel the underlying mechanism of the posaconazole-induced hypertension and hypokalemia. Two distinct mechanisms (*i.e.,* inhibition of 11β-hydroxylase and 11β-HSD2) were found to be responsible for posaconazole-induced pseudohyperaldosteronism, with significant interindividual differences. Careful consideration of comedications affecting the pharmacokinetics and pharmacodynamics is warranted. In addition, further research on the impact of susceptibility factors such as polymorphisms in genes encoding for proteins involved in metabolism or transport of posaconazole is needed.

Acknowledgments

The institutional review board of the University of California, Davis School of Medicine approved this study.

Financial Support: This work was supported by a grant from the Swiss Centre for Applied Human Toxicology (to A.O.).

Correspondence: Alex Odermatt, PhD, Division of Molecular and Systems Toxicology, Department of Pharmaceutical Sciences, University of Basel, Basel, Switzerland. E-mail: alex.odermatt@unibas.ch.

Disclosure Summary: The authors have nothing to disclose.

Data Availability: All data generated or analyzed during this study are included in this published article or in the data repositories listed in References.

References and Notes

1. Barton K, Bavis TK, Marshall B, Elward A, White NH. Posaconazole-induced hypertension and hypokalemia due to inhibition of the 11β-hydroxylase enzyme. *Clin Kidney J*. 2018;**11**(5):1–3.
2. Boughton C, Taylor D, Ghataore L, Taylor N, Whitelaw BC. Mineralocorticoid hypertension and hypokalaemia induced by posaconazole. *Endocrinol Diabetes Metab Case Rep*. 2018;**2018**(1).
3. Beck KR, Bächler M, Vuorinen A, Wagner S, Akram M, Griesser U, Temml V, Klusonova P, Yamaguchi H, Schuster D, Odermatt A. Inhibition of 11β-hydroxysteroid dehydrogenase 2 by the fungicides itraconazole and posaconazole. *Biochem Pharmacol*. 2017;**130**:93–103.

4. Kuriakose K, Nesbitt WJ, Greene M, Harris B. Posaconazole-induced pseudohyperaldosteronism. *Antimicrob Agents Chemother*. 2018;**62**(5):e02130-17.
5. Thompson GR III, Chang D, Wittenberg RR, McHardy I, Semrad A. In vivo 11β-hydroxysteroid dehydrogenase inhibition in posaconazole-induced hypertension and hypokalemia. *Antimicrob Agents Chemother*. 2017;**61**(8):e00760-17.
6. Strajhar P, Vizeli P, Patt M, Dolder PC, Kratschmar DV, Liechti ME, Odermatt A. Effects of lisdexamfetamine on plasma steroid concentrations compared with d-amphetamine in healthy subjects: A randomized, double-blind, placebo-controlled study. *J Steroid Biochem Mol Biol*. 2019;**186**:212–225.
7. Kratz A, Ferraro M, Sluss PM, Lewandrowski KB. Case records of the Massachusetts General Hospital. Weekly clinicopathological exercises. Laboratory reference values. *N Engl J Med*. 2004;**351**(15): 1548–1563.
8. Nakamoto JM, Mason PW, Quest Diagnostics, eds. *Endocrinology: Test Selection and Interpretation. The Quest Diagnostics Manual*. Fifth Edition. Chantilly, VA: Quest Diagnostics Nichols Institute; 2012.
9. Matos V, van Melle G, Boulat O, Markert M, Bachmann C, Guignard JP. Urinary phosphate/creatinine, calcium/creatinine, and magnesium/creatinine ratios in a healthy pediatric population. *J Pediatr*. 1997; **131**(2):252–257.
10. Marcos J, Renau N, Casals G, Segura J, Ventura R, Pozo OJ. Investigation of endogenous corticosteroids profiles in human urine based on liquid chromatography tandem mass spectrometry. *Anal Chim Acta*. 2014;**812**:92–104.
11. MSD Merck Sharp & Dohme AG. NOXAFIL (posaconazole) prescribing information. Available at: https://www.accessdata.fda.gov/drugsatfda_docs/label/2015/022003s018s020,0205053s002s004,0205596s001s003lbl.pdf. Accessed June 27, 2019.
12. Mahmood M, Abu Saleh O, Sohail MR. Hypokalemia and hypertension associated with supratherapeutic posaconazole levels. *Antimicrob Agents Chemother*. 2017;**61**(4):e00019-17.
13. Martino J, Fisher BT, Bosse KR, Bagatell R. Suspected posaconazole toxicity in a pediatric oncology patient. *Pediatr Blood Cancer*. 2015;**62**(9):1682.
14. Wassermann T, Reimer EK, McKinnon M, Stock W. Refractory hypokalemia from syndrome of apparent mineralocorticoid excess on low-dose posaconazole. *Antimicrob Agents Chemother*. 2018;**62**(7): e02605-17.
15. Saad AH, DePestel DD, Carver PL. Factors influencing the magnitude and clinical significance of drug interactions between azole antifungals and select immunosuppressants. *Pharmacotherapy*. 2006; **26**(12):1730–1744.
16. Wexler D, Courtney R, Richards W, Banfield C, Lim J, Laughlin M. Effect of posaconazole on cytochrome P450 enzymes: a randomized, open-label, two-way crossover study. *Eur J Pharm Sci*. 2004; **21**(5):645–653.
17. Ghosal A, Hapangama N, Yuan Y, Achanfuo-Yeboah J, Iannucci R, Chowdhury S, Alton K, Patrick JE, Zbaida S. Identification of human UDP-glucuronosyltransferase enzyme(s) responsible for the glucuronidation of posaconazole (Noxafil). *Drug Metab Dispos*. 2004;**32**(2):267–271.
18. Li Y, Theuretzbacher U, Clancy CJ, Nguyen MH, Derendorf H. Pharmacokinetic/pharmacodynamic profile of posaconazole. *Clin Pharmacokinet*. 2010;**49**(6):379–396.

3.3. Discussion

There is an increasing interest worldwide in the identification and characterization of potential EDCs [76]. Regarding the large number of chemicals required to be thoroughly tested, new discovery and assessment strategies including improved *in silico* and *in vitro* assays are needed to facilitate the prioritization of chemicals for further toxicological investigations. To address this issue, the present thesis represents a proof-of-concept for the application of pharmacophore-based virtual screening and molecular modeling combined with biological evaluation in H295R cells to characterize potential EDCs interfering with corticosteroid synthesis.

Pharmacophore models can be generated based on chemical properties of active compounds and are extremely useful in filtering promising compounds out of large databases in the course of virtual screening in order to prioritize chemicals for biological evaluation [37]. Additionally, molecular docking calculations can be applied to predict possible binding modes of a specific molecule to the target. The predictive power of a virtual screen highly relies on the quality of the data underlying the model. Thus, it is essential to continuously refine an existing molecular model with new biological data, as it was done in the present thesis (described in the published article 'Identification of the fungicide epoxiconazole by virtual screening and biological assessment as inhibitor of human 11β-hydroxylase and aldosterone synthase' [49], in chapter 3.1.2). In toxicological applications, pharmacophore models are often less restrictive in order to identify all possible hazardous chemicals, although this has the disadvantage of receiving more false positive virtual hits. Another limitation of the virtual screening assessment is that chemical databases are not fully representative and only few databases containing environmental chemicals, food additives or cosmetics are available [37]. In this regard, extending existing databases with newly identified metabolites would be highly useful for future screening approaches. In addition, individual virtual hits can be obtained by applying different computational programs, even if the same protein structure and chemical library are employed. This emphasizes to use multiple computational programs and validated models in parallel and merge their hit lists [77]. Nevertheless, pharmacophore-based virtual screening is a useful tool to identify potential EDCs, provided that it is used in combination with biological testing rather than as an isolated technique [37].

Importantly, the results obtained from computational approaches need to be accurately validated by suitable *in vitro* assays. In cell-free systems including purified protein or cell lysates expressing the protein of interest at a low background environment, the test compound has direct access to its target, which is crucial to verify virtual hits. Intact cell systems are not suited to exclude inactive compounds or classify active hits according to their activity, since the availability of a compound at the target site depends on the expression of transport proteins, intracellular binding proteins and metabolizing enzymes in intact cells [37, 78, 79].

However, valuable information on potential disturbances at the cellular level, including alterations in hormone production and conversion, as well as on the regulation of downstream signaling, can be gained from cell-based steroidogenesis assays, assuming that the test compound reaches the cellular target. Moreover, cell-based models not only allow the identification of potential EDCs, but can also provide first mechanistic information about their mode-of-action. The results obtained from cell-based *in vitro* assays can indicate a potential toxicological concern, implying that further investigations including *in vivo* studies may be necessary. Furthermore, *in vitro* testing systems have become increasingly important, since the principles of 3Rs (Replacement, Reduction and Refinement) have been developed and embedded in the legislation of many countries as well as the animal testing ban on cosmetics has been implemented in the EU [80-82]. However, limitations of each testing system need to be considered during data interpretation in order to correctly interpret the results obtained and to draw correct conclusions.

This thesis focused on the improvement of the H295R steroidogenesis assay, OECD test guideline No. 456, in order to assess interferences of potential EDCs with adrenal steroidogenesis and concluded that it is a valuable *in vitro* tool for an initial search for substances causing adrenocortical toxicity. The H295R steroidogenesis assay is an appropriate model to identify chemicals potentially disrupting the production of adrenal steroids and is designed to use the H295R cell line in its basal state [41, 83]. In their basal state, adrenal H295R cells synthesize rather moderate levels of corticosteroids and adrenal androgens, thus facilitating the detection of chemicals inducing steroid hormone production (as demonstrated in the published article 'Steroid profiling in H295R cells to identify chemicals potentially disrupting the production of adrenal steroids' [48], see chapter 3.1.1). The present thesis suggests to use H295R cells not only in their basal state but also under stimulated conditions. Although the time point of adding a steroidogenic inducer might be of debate, the application of activated cells (by pre-incubation or simultaneous addition of a stimulus) is more favorable to detect inhibitory effects of test compounds at different steps of steroidogenic pathways.

Torcetrapib is a cholesteryl ester transfer protein (CETP) inhibitor markedly increasing aldosterone and cortisol production by inducing the expression of CYP11B1 and CYP11B2. The mechanism leading to increased steroidogenesis and aldosterone production is still not fully understood but assumed to involve an activation of voltage-gated L-type Ca^{2+} channels [25, 26]. The subsequently increased intracellular calcium concentrations result in an activation of the calcium-binding protein calmodulin (CaM) and its protein kinase (CaMK), leading to an induction of the transcription of CYP11B [84, 85]. Thus, torcetrapib was used as an appropriate stimulus for CYP11B upregulation and secretion of corticosteroids in H295R cells in order to study the effects of potential CYP11B inhibitors. This facilitates the further characterization of selected virtual hits predicted to inhibit CYP11B, as it was demonstrated in the present thesis for epoxiconazole (more details are presented in the published

article ‘Identification of the fungicide epoxiconazole by virtual screening and biological assessment as inhibitor of human 11β-hydroxylase and aldosterone synthase’ [49], in chapter 3.1.2). Torcetrapib-stimulation of H295R cells was associated with higher hormone production, most obvious for aldosterone, for which an approximately 14-fold increase was observed compared to cells under basal conditions ([49], Supplementary Fig. S4, herein under chapter 3.1.2).

Moreover, instead of stimulating only corticosteroid production, forskolin can be used to additionally increase adrenal androgen synthesis ensuring a more general stimulation of adrenal steroidogenesis and allowing testing for inhibitory effects of compounds without previous knowledge of a potential mode-of-action. Forskolin is a diterpenoid mimicking the effects of ACTH by the activation of adenylyl cyclase [86]. This leads to enhanced cAMP levels in adrenal cells and thus stimulates steroidogenic enzymes and increases steroid production. Therefore, forskolin was used as a suitable inducer of steroidogenesis in H295R cells (the results are described in the submitted manuscript ‘Profiling of anabolic androgenic steroids and selective androgen receptor modulators for interference with adrenal steroidogenesis’, see chapter 3.1.3), which are insensitive to ACTH due to low expression levels of ACTH receptors [87]. Under forskolin-stimulated conditions, expression levels of steroidogenic enzymes differ from those under basal conditions, with specific enzymes being upregulated when cells are activated (presented in more detail in the published article ‘Steroid profiling in H295R cells to identify chemicals potentially disrupting the production of adrenal steroids’ [48], in chapter 3.1.1). Changes in enzyme expression levels can result in altered steroid metabolite concentrations and thus in a shift of steroid flux, which should be considered when comparing inhibitory effects of test compounds. Furthermore, the steroidogenic transcript profile in forskolin-induced H295R cells resembles more closely the gene expression pattern in the adult adrenal gland [88]. For this purpose, forskolin-stimulated H295R cells constitute a useful tool for studying inhibitory effects on adrenal steroidogenesis.

Besides ACTH, angiotensin II and potassium are further primary regulators of adrenal steroid hormone synthesis. H295R cells respond to angiotensin II and potassium by increased expression of CYP11B2 and aldosterone production [89-91]. Alternative systems for studies directed toward ACTH action might include transgenic technologies overexpressing ACTH receptors in the H295R cell line and primary cultures of adrenocortical cells or mouse adrenal cell lines such as Y-1, ATC1 and ATC7, which are responsive to ACTH [92-94]. However, the most prominent issues of primary adrenal cells as *in vitro* models are their short lifespan and potential contaminations with non-steroidogenic cells. Additionally, while cells of rodent origin do not produce cortisol and adrenal androgens resulting from a lack of 17α-hydroxylase (CYP17A1) expression, cells from different human donors exhibit considerable variability [43]. Thus, established cell lines from adrenocortical carcinomas have several benefits for testing chemically-induced disturbances of adrenal steroidogenesis.

The exposure of H295R cells to steroidogenic inducers or inhibitors appears to selectively influence the production of certain steroid hormone groups and thereby mimic zone-specific steroid expression profiles [43]. Chemicals with known mode-of-action that stimulate or inhibit a specific steroidogenic enzyme can be used to obtain zone-specific cell models. For instance, treatment of H295R cells with angiotensin II or potassium in combination with abiraterone, a CYP17A1 inhibitor, would enhance aldosterone production and block the synthesis of glucocorticoids and adrenal androgens, resembling the steroid pattern of the *zona glomerulosa* [48, 95]. In the study 'Profiling of anabolic androgenic steroids and selective androgen receptor modulators for interference with adrenal steroidogenesis' (manuscript submitted, see chapter 3.1.3), clostebol was found to decrease mineralocorticoid and cortisol levels but to increase adrenal androgens, suggesting CYP21A2 dysfunction and thus reflecting the phenotype of *zona reticularis*.

Another important improvement in the usage of the H295R cell system was the inclusion of a medium control sample at the beginning of the experiment, since batch-to-batch variability in the amount of steroids contributed by the Nu-serum might lead to misinterpretation of changes in hormone levels (described in more detail in the published article 'Steroid profiling in H295R cells to identify chemicals potentially disrupting the production of adrenal steroids' [48], see chapter 3.1.1).

Furthermore, to include reference compounds with a known mode-of-action not only allows the detection of alterations in the testing system but contributes to initially classify the effects of test compounds [48]. For instance, etomidate, an imidazole derivative and potent CYP11B inhibitor, could be used as a suitable reference control for inhibited corticosteroid production. At a high concentration of 1 µM, etomidate completely blocked steroidogenesis indicating the inhibition of the upstream side-chain cleavage enzyme (CYP11A1), as described in the published article 'Identification of the fungicide epoxiconazole by virtual screening and biological assessment as inhibitor of human 11β-hydroxylase and aldosterone synthase' [49] - chapter 3.1.2, while at lower concentrations etomidate was found to predominantly inhibit CYP11B1 [96].

Equally important is to apply an appropriate analytical method, i.e. liquid or gas chromatography-tandem mass spectrometry measurements (LC-MS/MS; GC-MS/MS) instead of antibody-based approaches, to ensure a specific quantification of individual steroids (details are listed in the published article 'Steroid profiling in H295R cells to identify chemicals potentially disrupting the production of adrenal steroids' [48], see chapter 3.1.1).

In addition, as exemplified with epoxiconazole ('Identification of the fungicide epoxiconazole by virtual screening and biological assessment as inhibitor of human 11β-hydroxylase and aldosterone synthase' [49], see chapter 3.1.2), the simultaneous quantification of major adrenal steroids provided preliminary information about the concentration-dependent mechanistic details of compound-

mediated disruption of steroidogenesis. Moreover, the quantification of a panel of adrenal steroids allowed to group compounds according to their steroid-interfering effects (as presented in more detail in the submitted manuscript 'Profiling of anabolic androgenic steroids and selective androgen receptor modulators for interference with adrenal steroidogenesis', see chapter 3.1.3). To gain even further mechanistic information, the analytical method applied herein should be extended by additional analytes such as 11β-hydroxylase-dependent adrenal androgen and progestin metabolites (11β-hydroxytestosterone, 11β-hydroxyandrostenedione, 11β-hydroxyprogesterone), reflecting CYP11B activity [97-99].

Furthermore, the H295R steroidogenesis assay should be combined with gene and protein expression analysis, enzyme activity analysis as well as investigations of signaling pathways. Several studies have shown that different signaling pathways including PKB/Akt, MEK/MAPK/ERK, Wnt/beta-catenin and JNK signal transduction pathways are present in the H295R cell line and can be studied to explain possible effects on steroidogenesis [100-104]. Interestingly, the impact of glucocorticoid-, androgen- and estrogen receptor-mediated effects on the regulation of steroid hormone synthesis have been examined using H295R cells, demonstrating its ability to serve as a useful model to study receptor-mediated mechanisms [105-107]. Additionally, also the MR is assumed to be effectively expressed in the H295R cell line [108]. Whether the activation of these steroid receptors in the adrenocortical cells represents a feedback mechanism for the control of steroid output remains an interesting issue to be addressed. Regarding the analysis of underlying mechanisms, time course investigations considering more than one time point (48 h) are needed to elaborate chemically-induced time-dependent variations in gene and protein expression during steroid synthesis.

Nevertheless, the refined H295R steroidogenesis assay described in this thesis constitutes a unique bioassay system, allowing the identification and characterization of chemicals potentially disrupting corticosteroid action and providing a first mechanistic insight into the mode-of-action. Furthermore, cortisol and aldosterone secretion as endpoints are currently lacking in any regulatory endocrine disruption strategy and the extension of glucocorticoid and mineralocorticoid endpoints into validation programs would lead to the recognition of the adrenal gland as a particularly vulnerable target for endocrine disruption [15].

The endocrine disruptive effects of certain chemicals on adrenal function depend on the concentrations reached *in vivo* at the target site. In functional assays, chemicals are often tested at high but sub-cytotoxic concentrations that might not be of toxicological relevance. For example, at high concentrations, compounds may affect enzymes and receptors with low affinities and thereby causing functional effects that are not toxicological relevant in real exposure scenarios. Currently, there are no comprehensive data available defining the relevant concentrations of epoxiconazole

found in humans upon occupational or environmental exposures. Thus, the toxicological relevance of the *in vitro* results needs to be further investigated and might be especially relevant in occupational exposure situations [109-111]. However, clinically used antifungal drugs of the same class such as itraconazole (Sporanox®) and posaconazole (Noxafil®), two triazole agents widely prescribed to treat certain fungal infections, need to be considered for CYP11B inhibition. Clinical evidence for inhibition of CYP11B by posaconazole was found in our recent case report describing two cases of apparent mineralocorticoid excess (AME) secondary to posaconazole treatment (more details are presented in the published case article 'Posaconazole-induced hypertension due to inhibition of 11β-hydroxylase and 11β-hydroxysteroid dehydrogenase 2' [75], chapter 3.2.2). Further *in vitro* screening for inhibition of individual CYPs including CYP11B1, CYP11B2 and CYP17A1 by these and other frequently used antifungals such as fluconazole, voriconazole and isavuconazole (used orally), miconazole and econazole (used topically), as well as tebuconazole and propiconazole (used agriculturally) would be of great value to assess their endocrine disruptive potential. For epoxiconazole, only direct effects on CYP11B inhibition were investigated, but the azole fungicides should also be tested for their capacity to interfere with mRNA and protein expression levels of the individual CYPs.

Although it is doubtful whether concentrations of epoxiconazole can be reached to inhibit CYP11B enzymes *in vivo*, the endocrine disrupting potential of epoxiconazole as a part of environmental mixtures should be carefully taken into account when estimating human exposures of EDCs.

Moreover, further studies addressing the combined effects of exposure to mixtures would complement our risk assessment of anabolic androgenic steroids (AAS) (described in the submitted manuscript 'Profiling of anabolic androgenic steroids and selective androgen receptor modulators for interference with adrenal steroidogenesis', in chapter 3.1.3). AAS abusers are known to consume several AAS simultaneously and combine other drugs in an attempt to counterbalance the side effects and thereby possibly potentiate other risk factors. Analgesics, antidepressants, diuretics (to lose weight and mask the presence of other substances) and anti-estrogens such as tamoxifen (to prevent gynecomastia) represent only a few examples [112-114].

Chemicals are usually tested for their endocrine disrupting potential as individual substances and the ability of several chemicals in combination to cause a cocktail effect constitutes a neglected topic of investigation. Nowadays, an individual is surrounded by a large number of chemicals and their combined exposure might lead to additive or synergistic effects, even if individual substances in the mixture are below their respective safety levels. For example, mixtures of equimolar concentrations of different azole fungicides could be investigated for their additive endocrine disrupting effects on CYP11B. Assuming additivity, the effects of the pesticides in combination would already occur at lower concentrations than those of the individual compounds. Another interesting question would be whether a mixture of different pesticides might lower cortisol levels not only by inhibiting CYP11B1

but also by suppressing GR sensitivity through a synergistic mechanism. Combination effects and synergistic interactions of chemicals in mixtures are becoming increasingly important and there are a few studies evaluating the cocktail effects of EDCs predominantly on the production of sex steroid hormones [115, 116].

The lifelong environmental exposures, including lifestyle factors, are defined as exposome and should be considered in the comprehensive EDC safety assessment [117]. Although sophisticated 'omics' technologies are currently being developed [118, 119], studying the entire exposome might be challenging, since an individual's exposome is highly variable and also dynamic throughout life. A key challenge will be to distinguish between individual and temporal variances and changes that lead to health impairments.

An important limitation of the H295R steroidogenesis assay is that it does not allow to study the effects of chemicals acting at the level of HPA axis regulation. The HPA axis is a highly complex system involving positive and negative feedback influences between the hypothalamus, pituitary and adrenal gland, providing several potential targets for endocrine disruptors. Interestingly, only a limited number of assays, allowing to evaluate chemicals potentially interfering with the HPA axis, are currently established and there are no assays specific to the HPA axis that have been approved by the regulators [120-122]. Concerning complex steroidogenic responses, co-culture models have been developed to study the impact of potentially hazardous chemicals on steroidogenesis. Thus, the co-culture of H295R and BeWo cells was applied to investigate the effects of EDCs on steroidogenic interactions between placenta and fetus during pregnancy [123-126], while the H295R/MCF-7 co-culture was used to test herbal menopausal supplements on ER-dependent breast cancer cell proliferation [127]. In order to evaluate the feedback effects of EDCs on ACTH secretion, an interesting option would be to design a co-culture model of mouse adrenal ATC7 cells responding to ACTH [94] in combination with mouse pituitary corticotropic AtT-20 cells able to secrete ACTH [128]. Alternatively, it could be advantageous to create an HPA-axis-on-a-chip. Organs-on-chips are microfluidic networks with 3D tissue engineered models that represent a specific human organ, including lung, liver, kidney, gut, uterus, brain, blood-brain-barrier, heart, pancreas, primarily used for drug discovery but also for toxicological studies [129-135]. These devices can also be combined to build a "body-on-a-chip" or "human-on-a-chip" in order to simulate interactions between multiple organs [129, 131]. Unfortunately, to date no adrenal-on-a-chip is available.

In this regard, *in vivo* studies are still unavoidable. Analysis of blood and urine samples of humans treated with pharmaceuticals interfering with corticosteroid action as well as the assessment of ratios of suitable metabolites were addressed in the corresponding part of this thesis (described in more detail in the two published articles in chapter 3.2.1 'Effects of lisdexamfetamine on plasma steroid concentrations compared with D-amphetamine in healthy subjects: A randomized, double-blind,

placebo-controlled study' [70] and chapter 3.2.2 'Posaconazole-induced hypertension due to inhibition of 11β-hydroxylase and 11β-hydroxysteroid dehydrogenase 2' [75], respectively).

After administration of lisdexamfetamine or D-amphetamine, plasma levels of ACTH, glucocorticoids and the adrenal androgens DHEA and androstenedione were markedly elevated, suggesting a stimulation of the HPA axis, possibly mediated by adrenergic receptors rather than dopaminergic or serotonergic receptors (discussed in more detail in the published article 'Effects of lisdexamfetamine on plasma steroid concentrations compared with D-amphetamine in healthy subjects: A randomized, double-blind, placebo-controlled study' [70], in chapter 3.2.1). However, lisdexamfetamine- or D-amphetamine-induced HPA axis stimulation was observed after a single supra-therapeutic dose in healthy subjects. Since ADHD treatment regimens consider chronic daily administration of lisdexamfetamine, it is unclear what impact this would actually have on the HPA axis function and its recovery after drug cessation [73, 74]. In rats, the repeated amphetamine administration led to reduced corticosterone and ACTH levels, indicating a desensitization and adaption of the HPA axis over time [136], and withdrawal from amphetamine has been linked to elevated states of anxiety and depression [137]. Moreover, analysis of glucocorticoid metabolites in 24-hour urine collections would support the lisdexamfetamine- or D-amphetamine-induced increase in plasma glucocorticoid levels by providing integrated measures of steroid production and avoiding the precise timing of blood samples in relation to the circadian rhythm of adrenal activity. In addition, spot urine samples might be sufficient to determine hormonal imbalances regarding subjects with highly deranged steroid hormone production.

A thorough analysis of blood and urine steroid profiles, as performed in the published case study 'Posaconazole-induced hypertension due to inhibition of 11β-hydroxylase and 11β-hydroxysteroid dehydrogenase 2' [75] - chapter 3.2.2, allows to define suitable metabolites, and ratios thereof can serve as markers for disturbances, potentially providing initial diagnostic information. For example, inhibition of 11β-HSD2, the enzyme responsible for cortisol inactivation, does not result in increased plasma cortisol levels but elevated ratios of 11β-hydroxyglucocorticoids (cortisol, corticosterone) to 11-ketoglucocorticoids (cortisone, 11-dehydrocorticosterone) and their tetrahydro metabolites [75, 138]. Furthermore, CYP11B1 inhibition might lead to enhanced levels of mineralocorticoids and adrenal androgens rather than altered plasma cortisol concentrations, potentially contributing to mineralocorticoid-dependent hypertension (further details can be found in the published case article 'Posaconazole-induced hypertension due to inhibition of 11β-hydroxylase and 11β-hydroxysteroid dehydrogenase 2' [75], in chapter 3.2.2). Recently, two cases of posaconazole-induced hypertension and hypokalemia with 10-20-fold increased 11-DOC and 11-deoxycortisol levels compared to the upper limit of the normal range have been described, indicating a prominent inhibition of CYP11B1 by posaconazole [139, 140]. Also, serum concentrations of androstenedione and 17α-

hydroxyprogesterone were elevated in these two cases, assuming normal CYP17A1 function. Increased levels of 11-deoxycortisol and an elevated cortisol/cortisone ratio were found for another patient treated with posaconazole, supporting inhibition of CYP11B1/2 [141]. A fourth case study reported moderately increased 11-deoxycortisol and 17α-hydroxyprogesterone levels, along with a markedly elevated cortisol/cortisone ratio, but normal 11-DOC and androgen levels, providing evidence for inhibition of 11β-HSD2 and, in addition, at least partial CYP11B1 inhibition [142]. Since these studies only partially analyzed the steroid profiles in serum and/or urine samples of patients treated with this azole, insufficient information was obtained to completely unravel the underlying mechanism of posaconazole-induced pseudohyperaldosteronism. After their synthesis, steroid hormones are subjected to peripheral metabolism including inactivation and hepatic conjugation with sulfate or glucuronic acid to facilitate their excretion in the urine. Thus, detection of disturbances of steroid hormone levels in blood samples might be challenging and extended steroid metabolite analysis of blood and urinary profiles, as it was done in the present study for posaconazole, are often essential to gain a thorough and accurate understanding of the mechanism underlying the disturbances. Two cases of mineralocorticoid-dependent hypertension and hypokalemia caused by posaconazole have been reported, presenting predominant CYP11B1 and CYP11B2 inhibition in one patient and predominant inhibition of 11β-HSD2 in the other, demonstrating the inter-individual differences in the mechanism underlying posaconazole-induced hypertension and hypokalemia (results are presented in the published case report 'Posaconazole-induced hypertension due to inhibition of 11β-hydroxylase and 11β-hydroxysteroid dehydrogenase 2' [75], see chapter 3.2.2). Interestingly, there are two case studies describing hypertension, hypokalemia, lowered renin and aldosterone levels following treatment with itraconazole, another widely used triazole antifungal drug assumed to preferably inhibit 11β-HSD2 [143, 144]. Although it is difficult to determine which enzyme is involved, itraconazole is supposed to preferably inhibit 11β-HSD2, resulting in cortisol-dependent activation of the MR, whereas posaconazole might exhibit a dual inhibition mechanism but preferably affects CYP11B1, indicating 11-DOC-mediated MR activation. In all case studies, plasma drug concentrations reached higher levels than the therapeutic concentration range and reducing the drug dose as well as substituting with fluconazole and voriconazole resolved the mineralocorticoid symptoms [145], thus emphasizing therapeutic options.

In conclusion, computational tools including pharmacophore-based virtual screening and molecular modeling in combination with biological tests such as the refined H295R steroidogenesis assay described in this thesis, constitute a useful approach for the evaluation of potential endocrine disruptors interfering with adrenal steroidogenesis and provide initial mechanistic information. Further detailed characterization of potential EDCs requires additional *in vitro* experimentation and finally *in vivo* studies to achieve a more comprehensive risk assessment.

4. Glucocorticoid Receptor Modulation

Corticosteroids play a vital role in the regulation of essential physiological processes including energy metabolism, cell growth and differentiation, immune and inflammatory responses, brain function, as well as electrolyte and fluid balance. Impairment of corticosteroid homeostasis has been associated with many pathological conditions such as metabolic and cardiovascular diseases, immune disorders, osteoporosis, cancer and depressive disorders [146-149]. Despite their important function and the fact that their impaired action can have various health consequences, only limited information is available on the potential disruption of corticosteroid hormone action by xenobiotics.

Glucocorticoids and mineralocorticoids exert their effects predominantly through binding to their respective receptors. The GR is an intracellular receptor protein belonging to the nuclear receptor superfamily and is ubiquitously expressed in almost all human tissues and organs [150, 151]. This receptor undergoes alternative splicing in exon 9, generating two highly homologous protein isoforms, GRα and GRβ. GRα mediates diverse actions of glucocorticoids by functioning as a ligand-dependent transcription factor, while GRβ does not bind glucocorticoids and diminishes the transcriptional activity of GRα [152-154]. Further splice variants of yet unknown physiological functions have been identified as isoforms GRγ, GR-A and GR-P [155, 156]. Additional GR isoforms can be generated by starting translation from an alternative initiation site located further downstream of the classical ATG start codon in the mRNA, a process known as alternative translation initiation. At least eight translational isoforms are formed from mRNA transcripts of GRα and GRβ, respectively. They exhibit cell type-specific expression patterns and regulate specificity and sensitivity to glucocorticoids in various tissues [157, 158].

This thesis focused on GRα, which will be referred to as GR. Upon binding to cortisol, GR shuttles between the cytoplasm and the nucleus and modulates directly or indirectly (through protein-protein interactions) the transcription of glucocorticoid-responsive genes in either a positive or negative manner [149, 159]. The cellular response to glucocorticoids is highly dynamic and depends on GR binding capacity and sensitivity to glucocorticoids, intracellular GR location, receptor degradation and recycling, and interaction with other proteins. The GR is associated with multiple proteins and factors including other transcription factors and chromatin modifiers that affect binding to the promoter region and alter the nucleosomal structure of DNA. This creates a complex gene regulatory network that controls gene expression [160-162]. The active GR complex modulates the transcriptional regulation of GR target genes contributing to the cell-type- and tissue-specific action of glucocorticoids. Finally, post-translational modifications including phosphorylation, acetylation, methylation, SUMOylation and ubiquitination of these proteins further increase GR diversity [162-165]. Thus, glucocorticoid hormone action involves several levels and xenobiotic-induced disturbances might

occur through different mechanisms at various stages of hormone action [12] (see Fig. 2 for an overview of the important steps involved in glucocorticoid homeostasis).

Xenobiotics might interfere with glucocorticoid responses not only by acting via direct binding to the ligand binding pocket of the GR, but also by binding to allosteric sites, disrupting protein-protein interactions or altering post-translational modifications and thus, may contribute to immune disorders, cancer and metabolic disturbances [12, 166, 167]. Further elucidation of the signaling pathways involved in GR function and the underlying mechanisms is of fundamental importance to understand potential interferences of xenobiotics with glucocorticoid action. Identifying new factors that regulate the GR and investigating how they modulate the cellular response to glucocorticoids, as well as improving the knowledge of the functions of GR associated proteins, could support the development of novel strategies for detecting chemicals disrupting glucocorticoid action.

The present thesis assessed the impact of the protein phosphatase PP1α on GR function by applying HEK-293 cells expressing recombinant human GR and PP1α as well as A549 human lung adenocarcinoma cells expressing these proteins endogenously. PP1α is a serine/threonine-specific phosphatase and among others regulates the expression and the activity of other steroid receptors [168-170]. Furthermore, first insights into the mechanism underlying the PP1α-dependent effect on GR stimulation were provided, revealing altered levels of phosphorylated GR at Ser211 and suggesting the involvement of glycogen synthase kinase 3 (GSK-3). Further details are reported in the manuscript 'Protein phosphatase 1 alpha enhances glucocorticoid receptor activity by a mechanism involving phosphorylation of serine-211' – chapter 4.1.

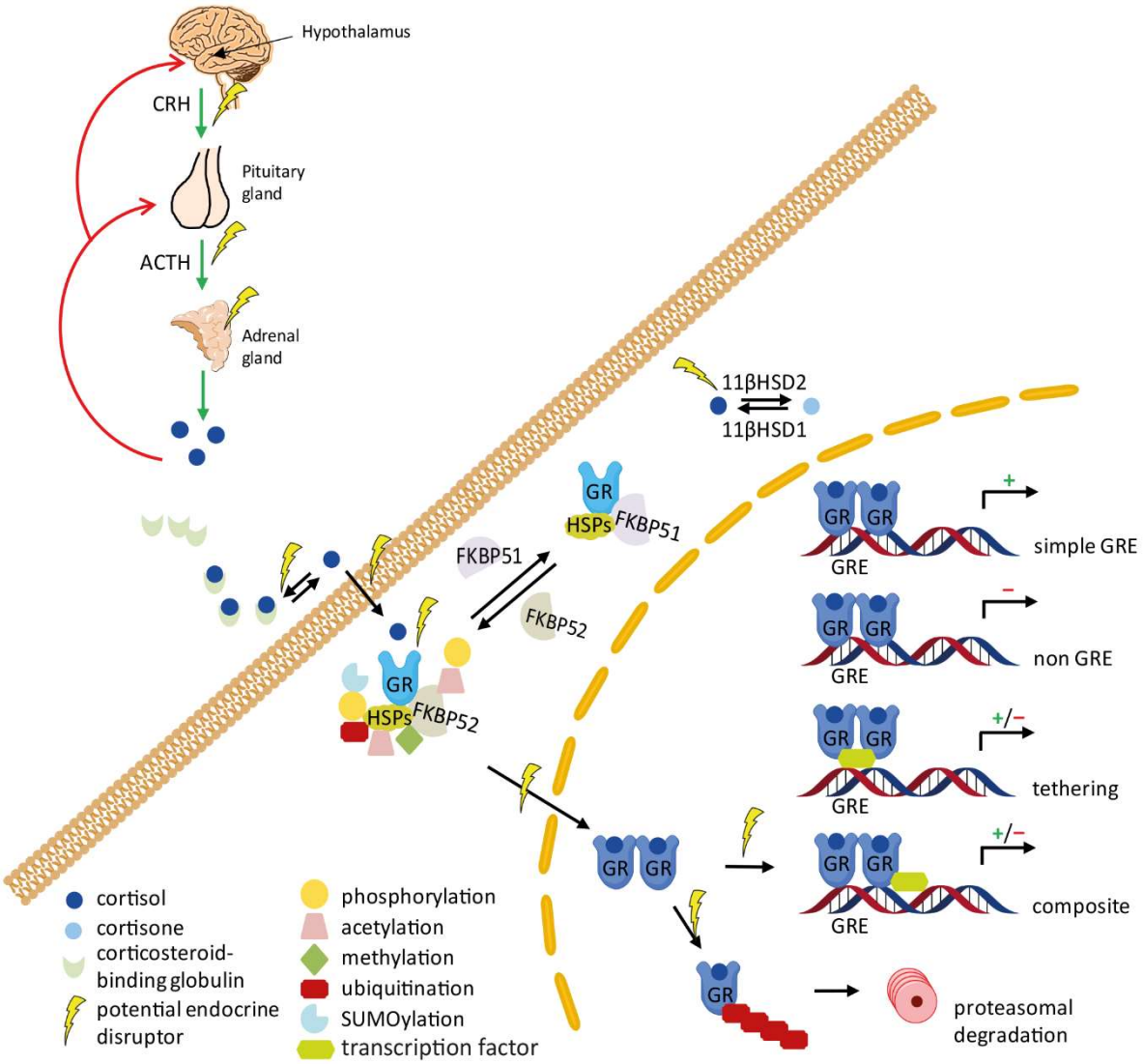

Figure 2. Schematic illustration of the important steps involved in glucocorticoid homeostasis. Xenobiotics might interfere at different steps in the cascade with glucocorticoid hormone action, potentially leading to altered glucocorticoid responses and contributing to various diseases. Possible targets are the HPA-axis, adrenal steroidogenesis, binding capacity of serum proteins, cellular uptake, intracellular metabolism by 11β-HSD, activation of GR, function of GR-associated proteins, GR complex nuclear translocation, binding to GR-responsive elements in the promoter region of target genes, receptor degradation as well as degradation and excretion of glucocorticoid hormones.

4.1. Manuscript in preparation (data complete):

Protein phosphatase 1 alpha enhances glucocorticoid receptor activity by a mechanism involving phosphorylation of serine-211

Melanie Patt[1,2], Joël Gysi[2], Nourdine Faresse[3], John A. Cidlowski[4], Alex Odermatt[1,2]

[1]Swiss Centre for Applied Human Toxicology (SCAHT), University of Basel, Missionsstrasse 64, 4055 Basel, Switzerland

[2]Division of Molecular and Systems Toxicology, Department of Pharmaceutical Sciences, University of Basel, Klingelbergstrasse 50, 4056 Basel, Switzerland

[3]DIVA Expertise, 31100 Toulouse, France

[4]Signal Transduction Laboratory, NIEHS, National Institutes of Health, Department of Health and Human Services, Research Triangle Park, North Carolina 27709.

Contribution:

Performed all experiments, analyzed data, wrote the manuscript.

Protein phosphatase 1 alpha enhances glucocorticoid receptor activity by a mechanism involving phosphorylation of serine-211

Melanie Patt[1,2], Joël Gysi[2], Nourdine Faresse[3], John A. Cidlowski[4], Alex Odermatt[1,2*]

[1]Swiss Centre for Applied Human Toxicology (SCAHT), University of Basel, Missionsstrasse 64, 4055 Basel, Switzerland.

[2]Division of Molecular and Systems Toxicology, Department of Pharmaceutical Sciences, University of Basel, Klingelbergstrasse 50, 4056 Basel, Switzerland. MP: melanie.patt@unibas.ch; JG: joel.gysi@gmx.ch; AO: alex.odermatt@unibas.ch.

[3]DIVA Expertise, 31100 Toulouse, France. NF: nourdine.faresse@diva-expertise.com.

[4]Signal Transduction Laboratory, NIEHS, National Institutes of Health, Department of Health and Human Services, Research Triangle Park, North Carolina 27709. JAC: cidlows1@niehs.nih.gov.

*Address of correspondence: Dr. Alex Odermatt, Swiss Centre for Applied Human Toxicology and Division of Molecular and Systems Toxicology, Department of Pharmaceutical Sciences, University of Basel, Klingelbergstrasse 50, 4056 Basel, Switzerland.

Alex.Odermatt@unibas.ch; Phone: + 41 61 207 1530

Abstract

By acting as a ligand-dependent transcription factor the glucocorticoid receptor (GR) mediates the actions of glucocorticoids and regulates many physiological processes. An impaired regulation of glucocorticoid action has been associated with numerous disorders. Thus, the elucidation of underlying signaling pathways is essential to understand mechanisms of disrupted glucocorticoid function and contribution to diseases. This study found increased GR transcriptional activity upon overexpression of protein phosphatase 1 alpha (PP1α) in HEK-293 cells and decreased expression levels of GR-responsive genes following PP1α knockdown. Mechanistic investigations revealed reduced phosphorylation of GR-Ser211 following PP1α silencing and provided evidence for an involvement of glycogen synthase kinase 3 (GSK-3). Thus, the present study identified PP1α as a novel post-translational activator of GR signaling, suggesting that disruption of PP1α function could lead to impaired glucocorticoid action and thereby contribute to diseases.

Keywords

Glucocorticoid receptor; protein phosphatase 1 alpha; glycogen synthase kinase 3; phosphorylation; signaling.

1. Introduction

Glucocorticoids (GC) are steroid hormones naturally produced and secreted by the adrenal gland in order to maintain body homeostasis. They act highly tissue-specifically and affect almost every organ in the human body by regulating energy homeostasis (carbohydrates, lipids, proteins), bone metabolism, cell growth and differentiation, apoptosis, stress and immune responses, as well as brain function [1-6]. GC are essential for life and dysregulation of their signaling is involved in numerous disorders including metabolic and cardiovascular diseases, asthma and chronic obstructive pulmonary disease (COPD), mood and cognitive disorders, immune diseases and cancer. Because of their anti-inflammatory, immunosuppressive and pro-apoptotic effects, synthetic GC are amongst the most widely prescribed drugs for the treatment of inflammation, autoimmune disorders and cancer.

GC exert their effects by binding to the glucocorticoid receptor (GR), a ligand-dependent transcription factor belonging to the nuclear receptor superfamily. The GR consists of an N-terminal transactivation domain (NTD), a DNA binding domain (DBD) and a C-terminal ligand binding domain (LBD) [7]. The NTD contains a transcriptional activation function domain (AF-1) responsible for post-translational modifications and protein-protein interactions. In the absence of ligand, the GR is sequestered in the cytoplasm in a heat-shock protein 90 (HSP-90)-chaperone complex. Ligand binding induces conformational changes that allow the release of the cytosolic GR from the HSP-90-chaperone complex, followed by receptor dimerization and translocation into the nucleus. The hormone-activated GR binds then to specific palindromic DNA sequences in the promoter regions of target genes (glucocorticoid response elements, GREs) and regulates their transcription. Induction or suppression of target gene transcription can occur, depending on the cell type, promoter context and cofactor recruitment. Upon prolonged exposure to GC, the GR is

subjected to degradation by the ubiquitin-proteasomal pathway, resulting in termination of the transcriptional response [8-14].

In addition to ligand binding, cross-talk with other signaling pathways can modulate GR activity by post-translational modifications, including phosphorylation, ubiquitination, and SUMOylation [8, 15-18]. GR phosphorylation affects its interaction with coregulators, subcellular localization, DNA binding and protein stability. Phosphorylation is paramount in receptor regulation and highly cell-, tissue-, species- and promoter-specific and the vast diversity of kinases and phosphatases mediates the high variety of cellular responses to GC [7, 19]. Various kinases, including cyclin-dependent kinases (CDKs), p38 mitogen activated protein kinases (MAPKs), c-Jun N-terminal kinases (JNKs), extracellular signal-regulated kinases (ERKs), protein kinase B (Akt), and glycogen synthase kinase 3 (GSK-3) were shown to modulate GR activity by phosphorylation at several sites, including serine residues 134, 203, 211, 226 and 404 [9, 20-29].

GR function is also regulated by numerous phosphatases. Recent studies emphasized the importance of protein phosphatases in regulating GR and contributing to the cytokine-induced GC insensitivity seen in patients with severe asthma [30-32]. Protein phosphatase 2A (PP2A) was found to dephosphorylate JNK, resulting in decreased GR-Ser226 phosphorylation and enhanced GR nuclear translocation, while protein phosphatase 5 (PP5) was proposed to negatively regulate GR activity by direct dephosphorylation of GR-Ser211. Protein phosphatase 1 alpha (PP1α) has been shown to control the expression and activity of several steroid receptors, including the mineralocorticoid receptor (MR), the androgen receptor (AR) and the estrogen receptor-α (ER) [33-35]. PP1α was found to bind to the LBD of these steroid receptors, thereby stabilizing their expression by dephosphorylation and inactivation of the E3 ubiquitin-ligase mouse double minute 2 (MDM2). In contrast to PP2A and PP5, it remained unclear whether PP1α also regulates GR function. In rat fibroblasts, the subcellular distribution of the GR was influenced by inhibiting

activities of PP1 and PP2A using okadaic acid, a potent but unspecific inhibitor of PP1 (IC_{50} = 15-20 nM) and PP2A (IC_{50} = 0.1 nM) [20, 36-38]. The PP1 holoenzyme is a serine/threonine-specific phosphoprotein phosphatase consisting of a catalytic subunit (PP1c) and multiple regulatory subunits. PP1c has four isoforms PP1α, PP1β, and the splice variants PP1γ_1 and PP1γ_2, encoded by three different genes PPP1CA, PPP1CB and PPP1CC. These isoforms share a high level of sequence homology and are ubiquitously expressed, except of PP1γ_2, which is restricted to the testis [39-41].

The present study evaluated the impact of PP1α on GR function by performing a reporter gene assay in HEK-293 cells expressing recombinant human GRα and PP1α. To investigate the endogenous effect of PP1α on GR activity, the expression of GC-induced genes was followed after knockdown of PP1α in A549 human lung carcinoma cells. Furthermore, to assess whether PP1α regulates GR through dephosphorylation of MDM2, as shown for the related steroid receptors, or by a direct mechanism similarly to PP2A and PP5, the pathways underlying the PP1α-mediated effect on GR stimulation were assessed in A549 cells after silencing of PP1α.

2. Materials and methods

2.1. *Chemicals and reagents*

Cortisol (CAS Nr. 50-23-7) was purchased from Steraloids (Newport, RI). Inhibitors of JNK (SP600125, CAS Nr. 129-56-6), p38 MAPK (SB203580, CAS Nr. 152121-47-6), Akt1/2 kinase (CAS Nr. 612847-09-3), MEK1/2 (PD98059, CAS Nr. 167869-21-8), and GSK-3 (CHIR99021, CAS Nr. 252917-06-9) were obtained from Sigma-Aldrich (Buchs SG, Switzerland). Stock solutions (10 mM) were prepared in dimethyl sulfoxide (DMSO, CAS Nr. 67-68-5; AppliChem, Darmstadt, Germany).

2.2. *Cell culture and treatments*

Human embryonic kidney-293 (HEK-293) cells and A549 human alveolar carcinoma cells were obtained from ATCC (Manassa, VA, USA). Cell culture media were purchased from Sigma-Aldrich. HEK-293 cells were cultured in Dulbecco's modified Eagle medium (DMEM) supplemented with 10% fetal bovine serum, 4.5 g/L glucose, 100 U/mL penicillin/streptomycin, 2 mM L-glutamine, 10 mM HEPES, pH 7.4, and 10% MEM non-essential amino acid solution. A549 cells were grown in Kaighn's Modification of Ham's F-12 medium (F-12K medium) completed with 10% fetal bovine serum and 100 U/mL penicillin/streptomycin.

Lipofectamine RNAiMax (Thermo Fisher Scientific, Waltham, MA, USA) was used for small interfering RNA (siRNA) delivery. Cells (150'000/6-well) were reverse transfected with 100 pmol siRNA against PP1α and/or 50 pmol siRNA against GSK-3 and 3.75 µL lipofectamine reagent for 64-66 h. The target sequences recognized by the siRNAs are: mock (scrambled) 5′-UGGUUUACAUGUUUUCUGA-3′, PPP1CA (PP1α) 5'-CAAGAGACGCUACAACAUC-3' (both from Microsynth AG, Balgach, Switzerland); GSK3A (L-003009-00-0005) 5'-UCACAAGCUUUAACUGAGA-3', 5'-GAAGGUGACCACAGUCGUA-3', 5'-GAGUUCAAGUUCCCUCAGA-3', 5'-CUGGACCACUGCAAUAUUG-3' and GSK3B (L-003010-00-0005) 5'-GAUCAUUUGGUGUGGUAUA-3', 5'-GCUAGAUCACUGUAACAUA-3', 5'-GUUCCGAAGUUUAGCCUAU-3', 5'-GCACCAGAGUUGAUCUUUG-3' (all from Dharmacon ON-TARGET plus SMART POOL; Dharmacon, Lafayette, CO, USA).

To determine effects of PP1α knockdown on endogenous GC-induced transcripts, A549 cells were cultured in steroid-free medium for 16-18 h prior to incubation with increasing concentrations of cortisol (18.75 nM - 1200 nM) or vehicle (DMSO) for 4 h. To study effects of kinase inhibitors on PP1α-dependent downregulation of GC-induced genes, A549 cells were treated with indicated inhibitors (10 µM, except for GSK-3 inhibitor (5 µM)) in serum-free medium for 16-18 h prior to

incubation with cortisol (500 nM) or vehicle (DMSO) for another 4 h. Following treatments, total RNA was isolated and quantitative polymerase chain reaction performed to quantify *GILZ* (glucocorticoid-induced leucine zipper) and *IGFBP1* (insulin-like growth factor binding protein 1). Cellular fractionation and phosphorylation of GR was assessed by pre-incubating the cells with steroid-free medium overnight following treatment of cortisol for another 1 h prior to cell lysis. Cellular fractionation experiments in HEK-293 and A549 cells were performed using 50 nM and 500 nM cortisol, respectively. GR phosphorylation in A549 cells was analyzed in the presence of 10 nM and 50 nM cortisol.

In all cell treatments, the final concentration of DMSO did not exceed 0.05%.

2.3. *GR-dependent reporter gene assay*

HEK-293 cells (100,000 cells/well) were seeded in poly-L-lysine coated 24-well plates, incubated for 24 h and co-transfected by calcium phosphate precipitation with the reporter gene TAT3- TATA luciferase (0.375 µg/well), pCMV-Renilla constitutive luciferase transfection control (0.03 µg/well) and the indicated plasmids coding for human GRα, Flag-PP1α and Myc-MDM2 (at a ratio of 1:4:4). Empty vector pcDNA3.1 was supplemented to equalize the total amount of DNA in the transfection. After 4 h, cells were washed with phosphate-buffered saline (PBS) and incubated in DMEM for another 18 h. Cells were then adapted to charcoal-treated DMEM (cDMEM) for 2 h. Cells were exposed 24 h post-transfection to DMSO control or cortisol (0.1 – 100 nM), followed by incubation for another 24 h. Cells were then lysed in passive lysis buffer (Promega, Madison, WI, USA) and fire fly and Renilla luciferase activity were determined according to the Dual-Luciferase® reporter assay kit (Promega, Madison, WI, USA) using a SpectraMax-L luminometer (Molecular Devices, Devon, UK).

2.4. *RNA isolation and quantitative polymerase chain reaction (qPCR)*

For isolation of total RNA, the RNeasy Mini Kit (QIAGEN, Hilden, Germany) was applied on a QIAcube extraction robot (QIAGEN) according to the manufacturers' instructions. The extracted RNA was treated with the RapidOut DNA Removal Kit (Thermo Fisher Scientific) and complementary DNA (cDNA) was subsequently synthesized using the GoScript Reverse Transcription System (Promega) following the manufacturer's protocol. Quantitative RT-PCR comprising 40 cycles of 95°C for 10 s, 60°C for 15 s, followed by a final extension at 72°C for 20 s, and a dissociation curve (72°C to 95°C) was performed in technical triplicate for each sample in the Rotor-Gene Q (QIAGEN) by using KAPA SYBR Fast qPCR Master Mix (2X) Kit (KAPA Biosystems, Woburn, MA, USA). For relative quantification, expression levels were normalized to those of the endogenous control gene PPIA according to the comparative $2^{-\Delta Ct}$ method [42]. Sequences of oligonucleotide primers are listed in Table 1.

Gene name	**Forward primers (5'-3')**	**Reverse primers (5'-3')**
PPIA	CATCTGCACTGCCAAGACTGA	TGCAATCCAGCTAGGCATG
GILZ	ACAAGATCGAACAGGCCATG	TTGCCAGGGTCTTCAACAG
IGFBP1	CCATGTCACCAACATCAAAAA	TCGTAGAGAGTTTAGCCAAGGC

Table 1. Sequences of gene-specific primers used for qPCR.

2.5. *Western blot analysis*

Upon treatment, cells were washed in PBS and lysed for 30 min on ice in RIPA buffer (Sigma-Aldrich) containing protease inhibitor cocktail (Roche, Rotkreuz, Switzerland). After centrifugation (16'000 × g, 15 min, 4°C), the supernatant was analyzed using a Pierce® biocinchonic acid protein assay kit (Thermo Fisher Scientific). Laemmli solubilization buffer (LSB) (60 mM Tris–HCl, 10% glycerol, 2% (w/v) sodium dodecyl sulfate, 0.01% bromophenol blue, pH 6.8) supplemented with 5% β-mercaptoethanol (Promega) was added and samples were

boiled for 3 min. Total protein (20 µg) of whole-cell extracts was resolved on 8% or 12% bis-acrylamide gels by sodium dodecyl sulfate-polyacrylamide gel electrophoresis (SDS-PAGE). All proteins were transferred to Immun-Blot® polyvinylidene difluoride (PVDF) membranes (Bio-Rad Laboratories, Hercules, CA, USA), which were subsequently blocked with 5% defatted milk in Tris-buffered saline (20 mM Tris buffer (pH 7.6), 150 mM NaCl) containing 0.1% Tween-20 (TBS-T) for 1 h. Membranes were incubated with the indicated primary antibodies in blocking solution overnight at 4 °C. After washing with TBS-T, the membranes were probed with horseradish peroxidase-conjugated goat anti-mouse secondary antibody (A0168) or goat anti-rabbit secondary antibody (A0545; both 1:10'000, from Sigma-Aldrich) for 1 h at room temperature. Visualization and detection of the protein bands was performed on a Fujifilm ImageQuant™ LAS-4000 (GE Healthcare, Glattbrugg, Switzerland) using the Immobilon Western Chemiluminescent HRP substrate kit (Merck, Kenilworth, NJ, USA). Quantitation of at least two independent experiments was done by using NIH ImageJ software and densitometry values were corrected for loading differences by normalization to those of β-actin or cyclophilin A (peptidylprolyl isomerase A, PPIA) house-keeping control.

The following primary antibodies were used: Anti-GR antibody (1:2'000; sc-1003), anti-PP1α antibody (1:5'000; sc-271762), and anti-β-actin (1:10'000; sc-47778; all from Santa Cruz Biotechnology, Dallas, TX, USA); anti-pSer134 GR antibody (1:2'000; 85060), anti-pSer211 GR antibody (1:2'000; 4161), anti-pSer226 GR antibody (1:10'000; 97285), and anti-GSK-3 antibody (1:5'000; 5676; all from Cell Signaling Technology, Danvers, MA, USA); anti-pSer203 GR antibody (1:2'000; orb127112; Biorbyt Ltd., Cambridge, United Kingdom); anti-Flag antibody (1:2'000; MA1-91878; Thermo Fisher Scientific), anti-pSer404 GR antibody (1:1'000; described earlier [27]), anti-PPIA (1:10'000, ab41684; Abcam Inc, Cambridge, United Kingdom).

2.6. *Cellular fractionation*

Treated cells were washed with PBS, scraped from culture dishes on ice and centrifuged at 500 × g for 5 min at 4°C. Cell pellets were resuspended in ice-cold lysis buffer (10 mM HEPES, 1.5 mM $MgCl_2$, 10 mM KCl, pH 7.6) supplemented with protease inhibitor cocktail (Roche) and 1 mM dithiothreitol (DTT, AppliChem). After incubation for 15 min, cells were permeabilized with 0.57% IGEPAL CA-630 (Sigma-Aldrich), vortexed vigorously for 10 s and centrifuged at 8'000 × g for 5 min at 4°C. The supernatant was collected as cytosolic fraction and clarified by centrifugation (16'000 × g, 5 min, 4°C) following protein quantification. After removing the cytosolic fraction, the pellet was washed twice with PBS, centrifuged (800 × g, 5 min, 4°C) and the supernatant discarded. The pellet was resuspended in extraction buffer (20 mM HEPES, 1.5 mM $MgCl_2$, 0.42 M NaCl, 0.2 mM EDTA, 25% (v/v) glycerol, pH 7.9) supplemented with protease inhibitor cocktail (Roche) and 1 mM DTT for 20 min at 4°C and 1'400 rotations/min on an orbital shaker (Thermomixer, Vaudaux-Eppendorf, Buchs, Switzerland). The homogenate was centrifuged at 21'000 × g for 5 min at 4°C and the supernatant removed as nuclear fraction, followed by protein quantification. Nuclear and cytoplasmic fractions were electrophoretically separated and blotted to PVDF membranes. Membranes were probed with anti-β-actin or anti-α-tubulin (1:10'000; GTX628802; GeneTex, Irvine, CA, USA) antibodies as cytoplasmic markers and anti-HDAC1 antibody (1:5'000; 5356; Cell Signaling Technology) as nuclear marker.

2.7. *Co-immunoprecipitation*

For co-immunoprecipitation experiments using Pierce™ NHS-Activated Agarose Slurry (Thermo Scientific), anti-GR antibody (sc-1003, Santa Cruz Biotechnology) was immobilized on beads according to the manufacturer's protocol. Cells suspended in lysis buffer [43] and proteins (1000 µg) were immunoprecipitated with antibody-coupled beads overnight at 4°C. As a control of

antigen-antibody binding specificity, lysates were incubated with rabbit IgG antibody (sc-2027, Santa Cruz Biotechnology). After elution of the precipitated protein, Western blot analysis was performed.

Co-immunoprecipitation with Pierce™ Protein A/G Plus Agarose (Thermo Scientific) was performed as described previously [44]. Briefly, 1000 µg of whole-cell extract proteins were incubated with anti-GR antibody (3660, Cell Signaling Technology) or anti-PP1α antibody (sc-271762, Santa Cruz Biotechnology) overnight at 4°C. Rabbit IgG antibody (12-370, Merck, Darmstadt, Germany) or mouse IgG antibody (sc-2025, Santa Cruz Biotechnology) was used as a control of non-antigen specific binding. Beads were added to each sample for another 3 h at 4°C. The beads were washed twice with Co-IP buffer (50 mM Tris buffer, pH 7.6), 150 mM NaCl, 1% NP-40, 10% glycerol, 5 mM $MgCl_2$) containing protease inhibitor cocktail and 1 mM phenylmethanesulfonyl fluoride (PMSF; AppliChem) and twice with PBS. After eluting, the proteins from the beads by adding LSB supplemented with 5% β-mercaptoethanol and heating for 5 min at 99°C, they were subjected to Western blot analysis.

2.8. *Statistical analysis*

Statistical evaluation was conducted in GraphPad Prism version 5.0. Statistical significance of differences between treatments was calculated using an unpaired two-tailed Student's *t* test or one-way ANOVA followed by Tukey's multiple comparisons test to adjust the false discovery rate. Values represent mean ± SD and levels of significance are: $*P < 0.05$, $**P < 0.01$, $***P < 0.001$, $****P < 0.0001$.

3. Results

3.1. *PP1α stimulates GR activity independently of MDM2*

Although PP1α was found to enhance the activity of AR and MR through a mechanism involving MDM2-dependent control of receptor protein stability [33, 34], it remained unclear whether PP1α would stimulate GR activity and if so by which mechanism. To investigate the effect of PP1α on GR activity, HEK-293 cells were transiently transfected with human GR, PP1α and a GR-dependent luciferase reporter gene (Fig. 1A). An excess of PP1α over GR expression plasmid of 4:1 optimally stimulated GR-dependent luciferase reporter activity. Co-transfection with PP1α significantly increased the basal as well as the cortisol-dependent GR activity. PP1α increased GR activity by a cortisol concentration-dependent manner (Fig. 1B). In PP1α-overexpressed cells, the maximal GR transcriptional activity was observed when cells were treated with 3.7 nM cortisol, resulting in a 7-fold increase in GR-mediated luciferase activity compared with cells expressing GR alone. In the absence of PP1α, maximal GR activity was detected in the presence of 30 nM cortisol. PP1α overexpression significantly affected the affinity of GR for cortisol ($EC_{50\ GR}$ = 5.9 ± 2.8 nM; $EC_{50\ GR+PP1\alpha}$ = 1.4 ± 0.1 nM; *P* value = 0.01).

Since the effects of PP1α on MR and AR were assumed to be mediated by inhibition of MDM2-dependent receptor degradation [33, 34], the impact of MDM2 on GR activity was assessed in HEK-293 cells expressing the respective recombinant proteins. Although MDM2 overexpression led to decreased GR-mediated reporter gene activity, PP1α-dependent stimulation of GR transactivation could not be prevented, neither under basal (Fig. 1C) nor under cortisol-stimulated (Fig. 1D) conditions. In the basal state, PP1α enhanced the GR transactivation in the absence of MDM2 4.5-fold and in its presence 4-fold. Similarly, in the presence of 100 nM cortisol PP1α stimulated GR activity about 2-fold.

Furthermore, to test whether PP1α alters the translocation of cytosolic GR into the nucleus, nuclear and cytosolic fractions of HEK-293 cells transfected with GR in the absence or presence of PP1α were analyzed by Western blotting (Fig. 1E and 1F). As expected, cortisol treatment induced nuclear translocation of GR; however, PP1α overexpression significantly enhanced GR translocation by about 3 times, when the cells were treated with cortisol (Fig. 1F).

3.2. *PP1α knockdown decreases GR-dependent gene transcription in A549 cells*

In order to support the stimulatory influence of PP1α on GR activity that was observed in the HEK-293 overexpression model, A549 human alveolar carcinoma cells endogenously expressing PP1α and GR were applied. PP1α was downregulated using siRNA, followed by detection of GR protein by Western blot analysis. PP1α protein was efficiently down regulated (Fig. 2A and 2B), but without significantly affecting GR protein expression (Fig. 2A and 2C). Next, cytosolic and nuclear fractionation of A549 cells transfected with PP1α siRNA was conducted (Fig. 2D and 2E), whereby no significant alterations of cytosolic and nuclear GR protein amounts could be detected. These data suggest that PP1α-dependent GR activation is independent of the receptor stability and unlikely mediated through MDM2.

Furthermore, co-immunoprecipitation assays using A549 cell lysates were performed according to two different protocols in order to determine whether PP1α and the GR interact directly. Although pull-down experiments were performed once with an antibody against GR (Suppl. Fig. 1A and 1B) and once with an antibody against PP1α (Suppl. Fig. 1C and 1D), there was no evidence for a physical interaction between PP1α and GR both, in the absence (Suppl. Fig. 1A and 1C) and presence (Suppl. Fig. 1B and 1D) of cortisol.

Importantly, the cortisol-induced expression of the endogenous GR-responsive genes insulin-like growth factor binding protein 1 (*IGFBP1*) and glucocorticoid-induced leucine zipper (*GILZ*) was

significantly downregulated, in a concentration-dependent manner, in PP1α siRNA transfected cells compared to mock siRNA transfected cells (Fig. 2F and 2G).

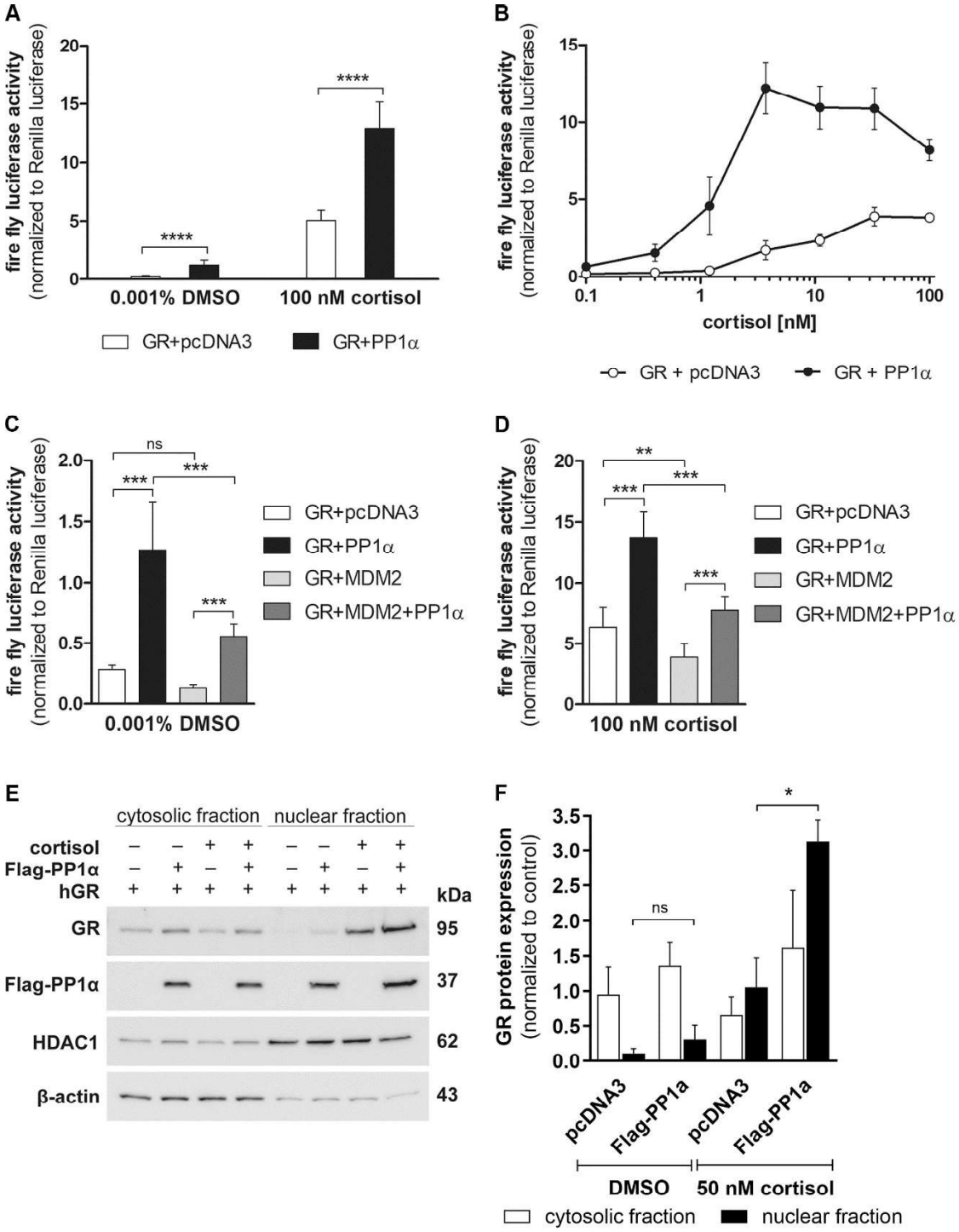

Fig. 1. Effect of PP1α overexpression on GR activity and nuclear translocation. (A, B, C and D) HEK-293 cells were transiently transfected with plasmids coding for GR with or without PP1α, a luciferase reporter gene and a Renilla luciferase transfection control. Empty vector pcDNA3.1

was supplemented to equalize the total amount of DNA in the transfection. After 24 h of transfection, cells were incubated with vehicle or 100 nM cortisol (A) or increasing concentrations of cortisol (B) for another 24 h. The luciferase reporter activity was normalized to the internal Renilla control. (C and D) Same as (A) but with co-transfection of MDM2. Data represent mean ± SD from at least two independent experiments, each performed in triplicate, ****$P < 0.0001$, ***$P < 0.001$, ** $P < 0.01$, *ns* not significant. (E and F) HEK-293 cells were transfected with GR, with and without PP1α for 24 h, incubated overnight in charcoal-treated medium and then exposed to vehicle or 50 nM cortisol for 1 h. Cytosolic and nuclear fractions were analyzed by Western blot using antibodies against GR and the Flag-tag on PP1α. As controls, the fractions were reprobed with anti-β-actin (cytosolic) and anti-HDAC1 (nuclear) antibodies. A representative blot (E) and analysis of band density (F) from two independent experiments are shown. Values are depicted as mean ± SD, *$P < 0.05$, *ns* not significant.

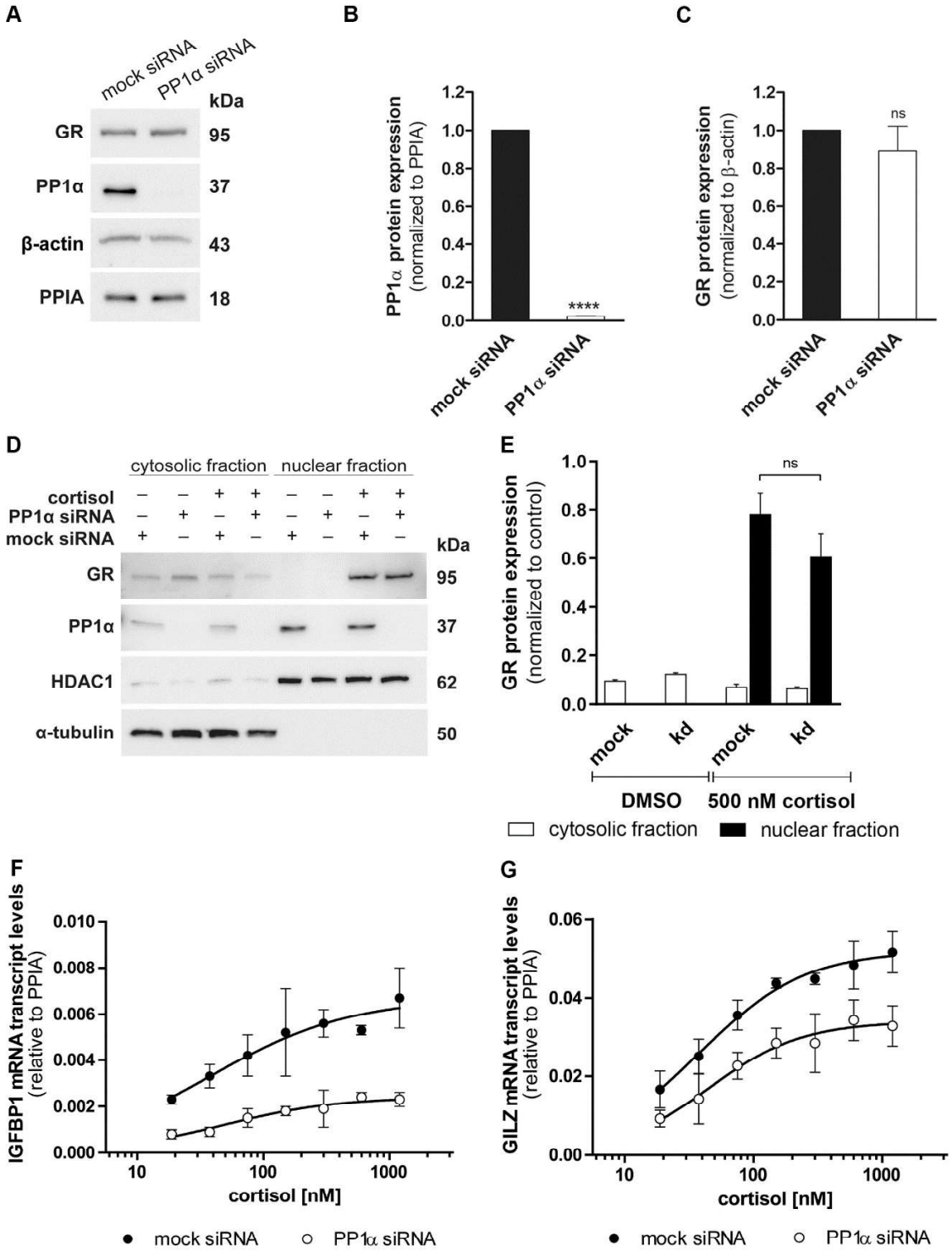

Fig. 2. Impact of PP1α knockdown on endogenous GR protein expression, translocation and GC-induced transcripts. (A, B and C) Western blot analysis for protein expression of GR and PP1α was performed after mock or PP1α knockdown in A549 cells. A representative blot (A) and

densitometry analysis of PP1α (B) and GR (C) from three independent experiments are shown. Data are normalized to mock siRNA samples (mean ± SD, ****$P < 0.0001$, *ns* not significant). (D and E) A549 cells were transfected with siRNA against PP1α for 48 h, incubated in serum-free medium for overnight and treated with vehicle or 500 nM cortisol for 1 h. Western blot analysis for cytosolic and nuclear fractions was performed using antibodies against GR and PP1α. As controls, the fractions were reprobed with anti-α-tubulin (cytosolic) and anti-HDAC1 (nuclear) antibodies. A representative blot (D) and analysis of band density (E) from two independent experiments are shown. Values are presented as mean ± SD, *ns* not significant. (F and G) At 48 h after knockdown of PP1α, A549 cells were cultured in steroid-free medium overnight prior to incubation with vehicle or increasing concentrations of cortisol (18.75 nM – 1200 nM) for 4 h. Cortisol-induced transcription of the GR-responsive genes *IGFBP1* (F) and *GILZ* (G) was measured by RT-PCR in technical triplicate for each sample. Data are represented as $2^{-\Delta Ct}$ means ± SD from three independent experiments.

3.3. *PP1α knockdown results in reduced GR-Ser211 phosphorylation*

Since PP1α stimulated the activity of the GR but did not seem to influence its stability nor directly interact with the receptor, this study assessed whether altered phosphorylation at five well-characterized sites on GR, namely serine residues 134, 203, 211, 226 and 404, may affect the transcriptional response to GC. For this purpose, A549 cells were transfected with siRNA against PP1α, treated with 10 nM or 50 nM cortisol for 1 h, prior to cell lysis and Western blot analysis using phospho-specific and total anti-GR antibodies was performed to determine the serine residues influenced (Fig. 3A). Silencing of PP1α did not affect GR phosphorylation of serine residues 134, 203, 226 or 404, but reduced the phosphorylation status of Ser211 in a GC-independent manner (Fig. 3B). Influences on the phosphorylation of Ser404 were also tested and

although the antibody signal was very weak, there was no evidence for altered phosphorylation (Suppl. Fig. 2).

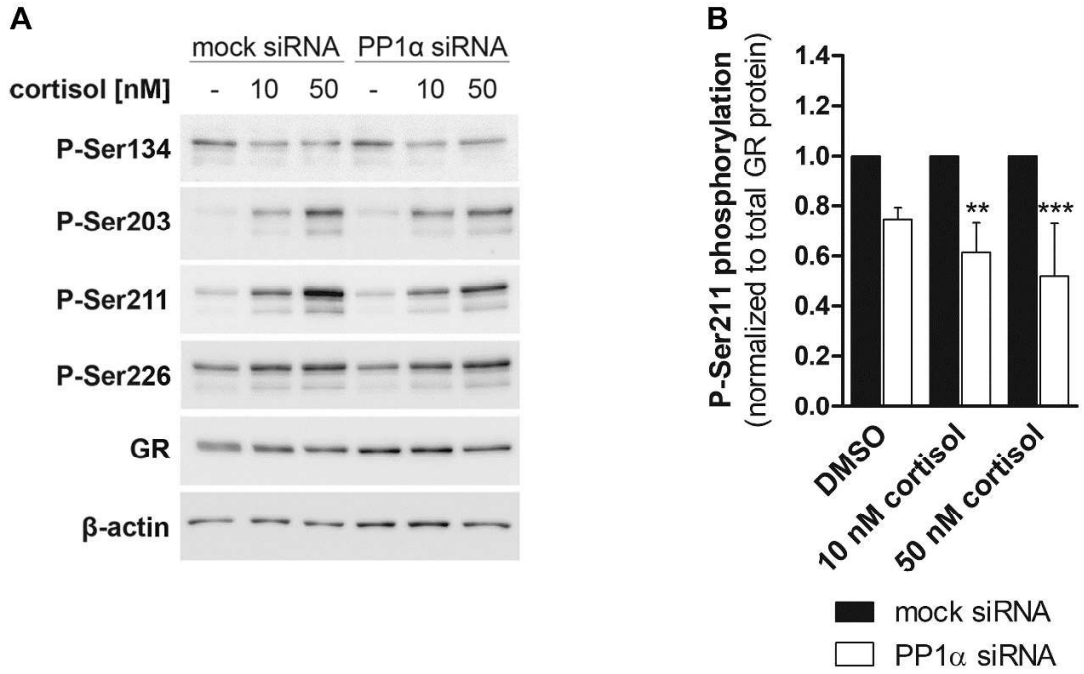

Fig. 3. Effect of PP1α knockdown on GR phosphorylation. A549 cells were transfected with mock or anti-PP1α siRNA for 48 h, incubated in serum-free medium for 16-18 h, treated with vehicle or cortisol (10 nM and 50 nM cortisol) for 1 h, followed by cell lysis and Western blot analysis. A representative Western blot image (A) and densitometry values (B) are presented. Levels of phosphorylated Ser211 from three independent experiments were normalized to total GR levels and are depicted as values normalized to mock siRNA control (mean ± SD, $^{**}P < 0.01$, $^{***}P < 0.001$).

3.4. *Impact of various kinase inhibitors on the PP1α-mediated effect on GR-induced transcripts*

Next, in an attempt to start to understand the mechanism underlying the influence of PP1α on GR-Ser211 phosphorylation, A549 cells treated with mock or anti-PP1α siRNA were exposed to inhibitors of several known kinases. The mRNA expression levels of the two GR-responsive genes

IGFBP1 and *GILZ* were then measured in order to identify the kinase(s) involved in the PP1α-dependent GR stimulation. In both, the basal and cortisol-activated state, a significant decrease in the *GILZ* and *IGFBP1* mRNA expression was observed in cells transfected with siRNA against PP1α compared to mock siRNA treated cells (Fig. 4A-D). This effect of PP1α knockdown was retained when the cells were exposed to inhibitors of p38, MEK1/2, JNK and Akt1/2. In contrast, the PP1α-mediated effect on both genes was reversed by treatment with the GSK-3 inhibitor, indicating an involvement of GSK-3 in the PP1α-dependent GR stimulation.

3.5. Inhibition or knockdown of GSK-3 abrogates the PP1α-dependent effect on GR-Ser211 phosphorylation

To assess whether pharmacological inhibition of GSK-3 can diminish the PP1α-dependent effect on GR-Ser211 phosphorylation, A549 cells were treated with GSK-3 inhibitor, followed by Western blot analysis. In mock siRNA transfected cells, GSK-3 inhibition partially abrogated the phosphorylation of GR-Ser211, reducing the phosphorylation level to that observed in PP1α siRNA treated cells (Fig. 5A and 5B). To further support a role for GSK-3 and exclude an off-target effect of the GSK-3 kinase inhibitor as well as to examine the involved GSK-3 isoform, isoform-specific anti-GSK-3 siRNAs were applied (Fig. 5C and 5D). Whereas silencing of either GSK-3α or GSK-3β both diminished the effect of PP1α but did not result in a complete reversal, the combination of both siRNAs completely abrogated the PP1α influence on GR-Ser211 phosphorylation. These results imply that GSK-3 inhibition could prevent the effect of PP1α on Ser211 phosphorylation.

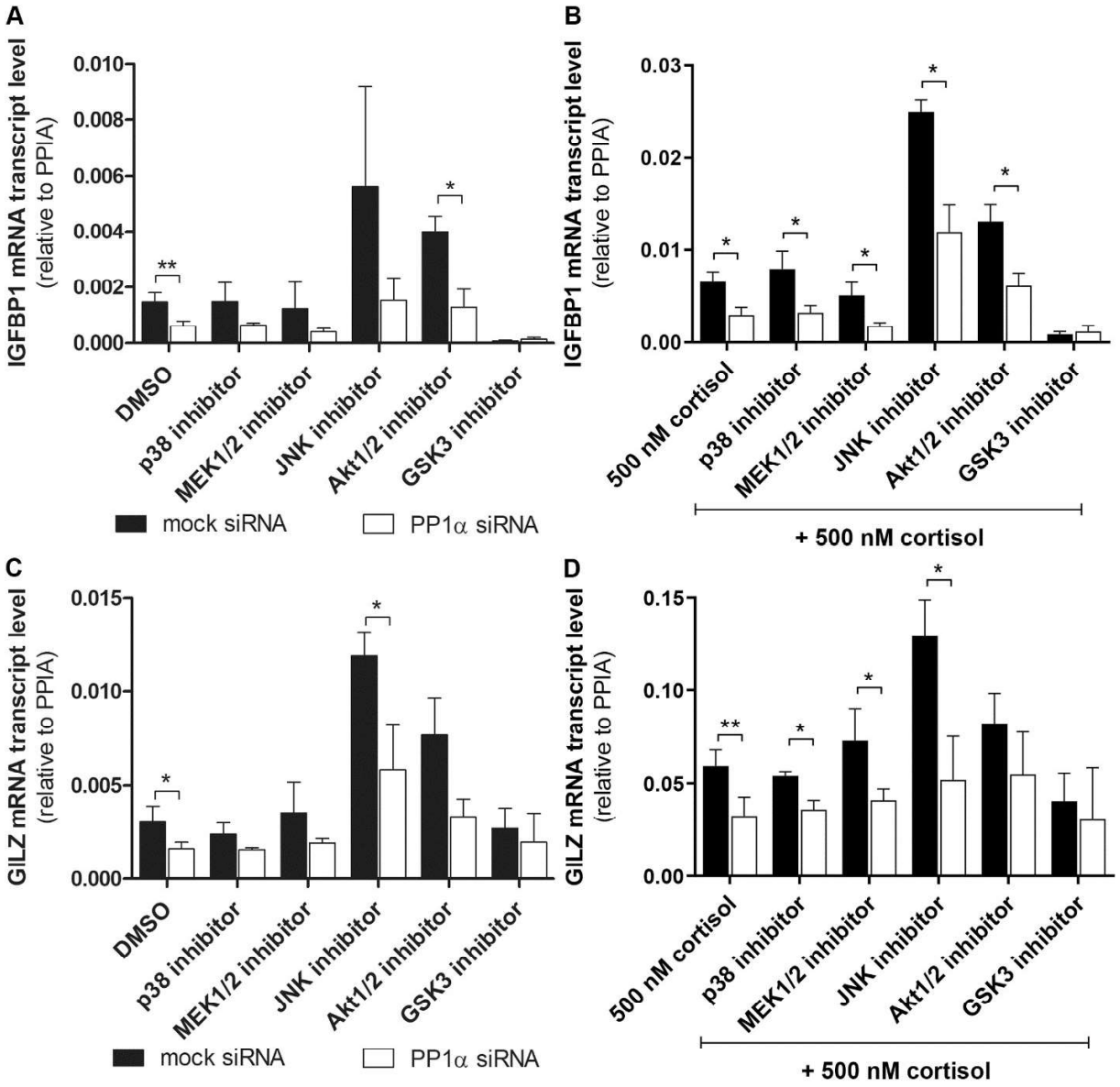

Fig. 4. Effect of various kinase inhibitors on PP1α-dependent effect on GR-induced transcripts. A549 cells were transfected with mock or anti-PP1α siRNA for 48 h, incubated overnight with indicated inhibitors (10 μM; except for GSK-3 inhibitor, 5 μM) in serum-free medium prior to further incubation with vehicle (A and C) or 500 nM cortisol (B and D) for another 4 h. Expression levels of GR-responsive genes *IGFBP1* (A and B) and *GILZ* (C and D) were analyzed by RT-PCR in technical triplicate for each sample. Values are presented as $2^{-\Delta Ct}$ means ± SD from at least two independent experiments, $^{**}P < 0.01$, $^{*}P < 0.05$.

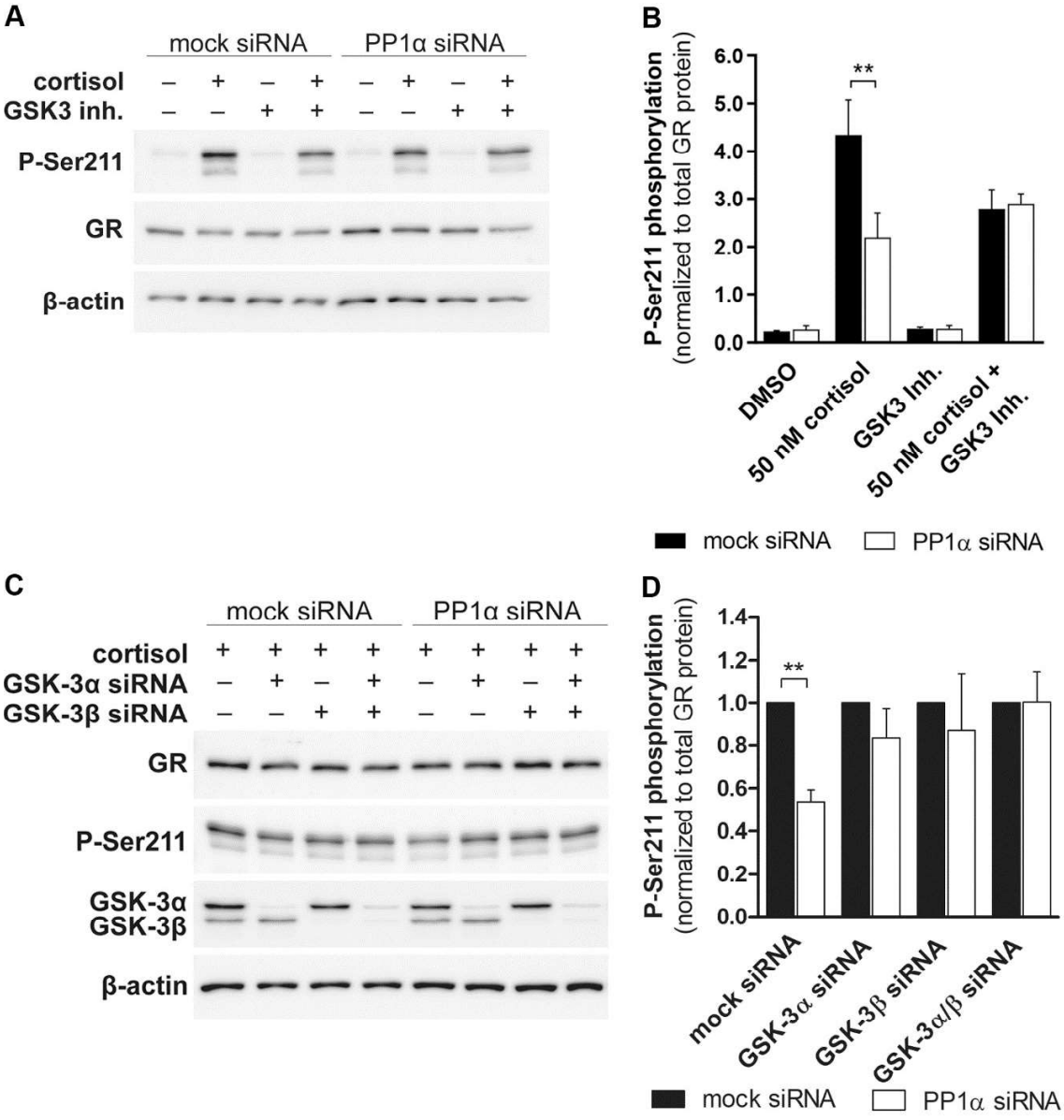

Fig. 5. Effect of GSK-3 on PP1α-mediated impact on GR-Ser211 phosphorylation. (A and B) After treatment with mock or anti-PP1α siRNA, A549 cells were incubated overnight with 5 μM GSK-3 inhibitor in serum-free medium prior to further incubation with vehicle or 50 nM cortisol for another 1 h. Western blot analysis for expression of total GR protein and Ser211 phosphorylation was performed. A representative blot (A) and densitometry values of Ser211 phosphorylation (B) from two independent experiments normalized to total GR are shown (mean ± SD, $^{**}P < 0.01$). (C and D) A549 cells were co-transfected with siRNA against PP1α and/or

GSK-3α and/or GSK-3β for 48 h, incubated overnight in serum-free medium prior to treatment with 50 nM cortisol for another 1 h. Western blotting for expression of total GR protein and Ser211 phosphorylation was conducted. A representative blot (C) and densitometry analysis of Ser211 phosphorylation (D) from three independent experiments normalized to total GR is presented as values normalized to mock siRNA control (mean ± SD, $^{**}P < 0.01$).

4. Discussion

The cell- and tissue-specific sensitivity towards GC plays a pivotal role in the fine-tuned regulation of physiological functions as well as for the response to pharmacological doses in the treatment of pathological conditions. Phosphorylation at multiple sites belongs to the most important mechanisms allowing a rapid modulation of the sensitivity of the GR towards GC. The basal and ligand-stimulated phosphorylation of the GR is regulated by various kinases and phosphatases, and an impaired phosphorylation can result in hypersensitivity or resistance to GC, thereby contributing to diseases [9, 20-32].

The current study assessed whether PP1α can stimulate GR function and tested two different hypotheses: First, that PP1α regulates GR activity through inactivation of MDM2 by dephosphorylating it at Ser166, thereby reducing the MDM2-mediated ubiquitination of GR and the subsequent proteasomal degradation of the receptor, as shown for the MR and AR [33, 34]; and second, that PP1α directly dephosphorylates the GR at a particular site to relieve functional repression as demonstrated for PP2 and PP5 [30-32].

The results revealed a stimulating effect of PP1α on GR activity in HEK-293 cells overexpressing recombinant proteins and a GR-dependent luciferase reporter (Fig. 1A and 1B), as well as in A549 cells expressing endogenous GR and PP1α levels by PP1α silencing and assessment of the expression of the GC-target genes *IGFBP1* and *GILZ* (Fig. 2F and 2G). MDM2 has been shown to

control the expression of several steroid receptors including the GR [10]. In line with previous observations, co-transfection with MDM2 in HEK-293 cells was found to decrease GR transcriptional activity, both in the basal and cortisol-activated state. However, MDM2 overexpression could not prevent the PP1α-mediated GR activation, with similar relative increases of GR activity in the absence or presence of MDM2, indicating that PP1α stimulates GR activity independent of MDM2. Moreover, knockdown of PP1α in A549 cells revealed reduced GR-dependent gene expression but did not result in decreased GR protein expression levels, further supporting that PP1α-dependent GR stimulation is independent of MDM2 modulated receptor stability and differs from the mechanism observed for MR and AR [33, 34].

Furthermore, proximity ligation assays suggested an interaction between PP1α and MR, and immunoprecipitation analysis indicated that PP1α interacts with the LBD of the AR [33, 34]. In this study, co-immunoprecipitation assays failed to detect a direct interaction between GR and PP1α, further favoring a different mechanism compared to MR and AR.

To achieve its transcriptional activity, nuclear translocation of GR is required to translocate to the nucleus. Nuclear and cytosolic fractionation of HEK-293 cells overexpressing recombinant GR and PP1α resulted in a slight but significant increase in nuclear receptor protein when PP1α was overexpressed (Fig. 1E and 1F). In contrast, the amount of GR in the nuclear fraction did not alter after PP1α silencing in A549 cells expressing endogenous receptor levels (Fig. 2D and 2E). This difference in the nuclear import of the GR between the two cell lines might derive from the presence or absence of receptor-associated co-regulators. Furthermore, it should be noted that while overexpressed PP1α in HEK-293 cells is equally distributed between cytoplasm and nucleus, endogenous PP1α in A549 cells is mainly located in the nucleus. This suggests that subcellular localization less likely is a major factor contributing to the PP1α-dependent GR activation.

The site-specific phosphorylation of GR regulates its transcriptional activity [7, 19]. Earlier studies reported that phosphorylation of GR-Ser211 enhances the activity of the receptor, whereas phosphorylation of serine residues 134, 203, 226 and 404 is associated with reduced GR function [21-25, 27, 28, 45-48]. Thus, this study explored whether PP1α-dependent GR stimulation was due to an altered phosphorylation of GR at specific serine residues known to be critical for its activity. The data obtained demonstrated that the level of GR-Ser211 phosphorylation significantly decreased after PP1α silencing (Fig. 3A and 3B) whereas all other phosphorylation sites tested were unaffected. Since phosphorylation of GR-Ser211 is essential for receptor activity, a reduced phosphorylation of this specific residue implicates a decreased transcriptional activity, which was supported by the diminished expression of GC-inducible genes in A549 cells upon PP1α knockdown (Fig. 2F and 2G). The involvement of GR-Ser211 phosphorylation supports the assumption that altered subcellular trafficking is a mechanism less likely contributing to the PP1α-dependent GR activation. Earlier findings have shown that mutation of murine GR at Ser220, the phosphorylation site equivalent to human Ser211, did not affect hormone-dependent nuclear translocation [9]. The fact that PP1α altered the phosphorylation state of GR-Ser211, and bearing in mind that PP1α is a protein phosphatase, indicates an indirect effect of PP1α on GR, involving another protein.

The present study addressed whether PP1α might dephosphorylate a specific kinase, which in turn is activated, thereby phosphorylating GR at Ser211. Treatment of A549 cells with different inhibitors of known kinases indicated an involvement of GSK-3 in the PP1α-dependent regulation of GC-responsive genes (Fig. 4). Inhibition of GSK-3 prevented the PP1α-mediated difference in the expression levels of *GILZ* and completely abolished the effects on *IGFBP1*. *IGFBP1* contains a thymine-rich insulin response element (TIRE) in its promotor region which requires GSK-3 to be active for gene transcription [49], providing an explanation for the repression of *IGFBP1* gene

expression upon treatment of cells with GSK-3 inhibitor. To assess the role of GSK-3 in the PP1α-dependent effect on GR function, Western blot analysis was performed to determine GR-Ser211 phosphorylation levels. Treatment of A549 cells with GSK-3 inhibitor (Fig. 5A and 5B) and siRNA against GSK-3α/β (Fig. 5C and 5D) resulted in a diminished GR-Ser211 phosphorylation and an abrogated PP1α-mediated effect. Specific knockdown of either GSK-3α or GSK-3β partially abolished the PP1α-dependent effect, suggesting that the isoforms might compensate for each other and both are involved in the stimulatory effects of PP1α on GR activity.

GSK-3 is a serine/threonine protein kinase encoded by two genes GSK3A and GSK3B. The closely related isoforms α and β are highly homologous in their catalytic domains but differ significantly in the N- and C-terminal regions [50, 51], suggesting that they could be differentially regulated. However, both proteins are similarly modified at the N-terminal region: phosphorylation of Ser21 on GSK-3α and Ser9 on GSK-3β [52, 53]. PP1α is a known activator of GSK-3β by dephosphorylation of Ser9 [54, 55], and was shown to be engaged in a positive feedback loop with its inhibitor-2 and GSK-3β. GSK-3β can phosphorylate inhibitor-2 of PP1α at Thr72, resulting in PP1α activation, which in turn dephosphorylates and further stimulates GSK-3β [55, 56]. It is also assumed that PP1α can dephosphorylate the inhibitory Ser21 on GSK-3α [56, 57]. GSK-3 was originally identified as a protein capable of regulating glycogen synthase in order to inhibit glycogen synthesis [58] and since then has been described to phosphorylate a wide variety of substrates being involved in many cellular processes, including glucose metabolism, cell differentiation and apoptosis [59-61]. In addition, GSK-3 was found to interact with the GR. In the absence of a ligand, GSK-3α is supposed to be sequestered to the GR and dissociates from it upon exposure to GC [57]. So far, most studies focused on the β-isoform of GSK-3. Inhibition of GSK-3β was reported to suppress GR reporter gene activity and reduce mRNA expression levels of *GILZ*, implying that GSK-3β has a positive role in GR stimulation [62]. However, GSK-3β was

also proposed to phosphorylate GR-Ser404 and thereby decreasing its function [27]. Further studies are required to clarify the role of GSK-3 in GR regulation, considering cell type-specific differences. Furthermore, most of the GSK-3 substrates need to be primed by pre-phosphorylation at a specific serine-proline site prior to recognition by GSK-3 [63]. Up to now, such a priming site for GSK-3 within the GR has not been described. Signaling pathways are complex involving a number of components that can cross-talk with other signal transduction pathways. Further research needs to address whether GSK-3 is directly responsible for the PP1α-dependent phosphorylation of GR-Ser211 or whether the observed effect is mediated indirectly through another coregulator. Additionally, it cannot be excluded that GSK-3 dephosphorylation by PP1α is indirect and mediated by a PP1α regulatory protein.

Moreover, the physiological relevance of PP1α-mediated GR signaling needs to be examined. PP1α has been reported to be involved in the progression of several disease states, including memory loss, type II diabetes and cancer [64-66]. PP1α is assumed to suppress learning and memory and acts as a potential mediator of cognitive decline during ageing [67]. Excessive GSK-3 activity has been associated with neurodegenerative and psychiatric disorders, and GSK-3 inhibitors as well as GR antagonists are discussed as new potential treatments of Alzheimer's disease [68-70]. In addition, aberrant GC action and excessive activity of GSK-3 have been linked with obesity and type II diabetes [71, 72], and regulatory subunits of PP1 have been associated with insulin resistance [73, 74]. Finally, chronic GC treatment can lead to reduced sensitivity or even resistance in specific cell-types or tissues and underlying mechanisms have been mainly attributed to the impaired GR signaling pathway [75, 76]. Due to the ability of PP1α to enhance GR activity, one could speculate that cells with impaired PP1α function have an altered response to GC. Further elucidation of post-translational modification of GR is essential to understand mechanisms of aberrant GC action potentially leading to GC insensitivity.

In this study, PP1α was identified as novel regulator of GR, enhancing its activity but not affecting the expression of the receptor, both under basal and ligand-dependent conditions. Furthermore, the results provided a first insight into the molecular mechanism, proposing GR-Ser211 to be modulated through involvement of GSK-3. Thus, PP1α constitutes a new component of the GR signaling pathway, suggesting that impaired activity of PP1α in specific situations could alter GC action and contribute to diseases.

Conflicts of Interest

MP, JG and AO declare no conflict of interest.

JC…

NF…

Acknowledgements

This work was supported by the Swiss Centre for Applied Human Toxicology (SCAHT).

References

[1] M.J. Garabedian, C.A. Harris, F. Jeanneteau, Glucocorticoid receptor action in metabolic and neuronal function, F1000Res 6 (2017) 1208.

[2] R.A. Quax, L. Manenschijn, J.W. Koper, J.M. Hazes, S.W. Lamberts, E.F. van Rossum, R.A. Feelders, Glucocorticoid sensitivity in health and disease, Nat Rev Endocrinol 9(11) (2013) 670-86.

[3] K.L. Gross, J.A. Cidlowski, Tissue-specific glucocorticoid action: a family affair, Trends Endocrinol Metab 19(9) (2008) 331-9.

[4] M. Ahmad, Y. Hachemi, K. Paxian, F. Mengele, M. Koenen, J. Tuckermann, A Jack of All Trades: Impact of Glucocorticoids on Cellular Cross-Talk in Osteoimmunology, Front Immunol 10 (2019) 2460.

[5] A. Blum, E. Maser, Enzymology and molecular biology of glucocorticoid metabolism in humans, Progress in nucleic acid research and molecular biology 75 (2003) 173-216.

[6] J.C. Buckingham, Glucocorticoids: exemplars of multi-tasking, British journal of pharmacology 147 Suppl 1 (2006) S258-68.

[7] J. Zhou, J.A. Cidlowski, The human glucocorticoid receptor: one gene, multiple proteins and diverse responses, Steroids 70(5-7) (2005) 407-17.

[8] A.D. Wallace, J.A. Cidlowski, Proteasome-mediated glucocorticoid receptor degradation restricts transcriptional signaling by glucocorticoids, The Journal of biological chemistry 276(46) (2001) 42714-21.

[9] J.C. Webster, C.M. Jewell, J.E. Bodwell, A. Munck, M. Sar, J.A. Cidlowski, Mouse glucocorticoid receptor phosphorylation status influences multiple functions of the receptor protein, The Journal of biological chemistry 272(14) (1997) 9287-93.

[10] S. Sengupta, B. Wasylyk, Ligand-dependent interaction of the glucocorticoid receptor with p53 enhances their degradation by Hdm2, Genes & development 15(18) (2001) 2367-80.

[11] H.K. Kinyamu, T.K. Archer, Estrogen receptor-dependent proteasomal degradation of the glucocorticoid receptor is coupled to an increase in mdm2 protein expression, Molecular and cellular biology 23(16) (2003) 5867-81.

[12] P. Connell, C.A. Ballinger, J. Jiang, Y. Wu, L.J. Thompson, J. Hohfeld, C. Patterson, The co-chaperone CHIP regulates protein triage decisions mediated by heat-shock proteins, Nature cell biology 3(1) (2001) 93-6.

[13] M.D. Galigniana, J.M. Harrell, P.R. Housley, C. Patterson, S.K. Fisher, W.B. Pratt, Retrograde transport of the glucocorticoid receptor in neurites requires dynamic assembly of complexes with the protein chaperone hsp90 and is linked to the CHIP component of the machinery for proteasomal degradation, Brain research. Molecular brain research 123(1-2) (2004) 27-36.
[14] X. Wang, D.B. DeFranco, Alternative effects of the ubiquitin-proteasome pathway on glucocorticoid receptor down-regulation and transactivation are mediated by CHIP, an E3 ligase, Molecular endocrinology (Baltimore, Md.) 19(6) (2005) 1474-82.
[15] A.M.S. Garza, S.H. Khan, R. Kumar, Site-specific phosphorylation induces functionally active conformation in the intrinsically disordered N-terminal activation function (AF1) domain of the glucocorticoid receptor, Molecular and cellular biology 30(1) (2010) 220-230.
[16] H. Faus, B. Haendler, Post-translational modifications of steroid receptors, Biomedicine & pharmacotherapy = Biomedecine & pharmacotherapie 60(9) (2006) 520-8.
[17] N. Ismaili, M.J. Garabedian, Modulation of glucocorticoid receptor function via phosphorylation, Annals of the New York Academy of Sciences 1024 (2004) 86-101.
[18] Y. Le Drean, N. Mincheneau, P. Le Goff, D. Michel, Potentiation of glucocorticoid receptor transcriptional activity by sumoylation, Endocrinology 143(9) (2002) 3482-9.
[19] A.J. Galliher-Beckley, J.A. Cidlowski, Emerging roles of glucocorticoid receptor phosphorylation in modulating glucocorticoid hormone action in health and disease, IUBMB life 61(10) (2009) 979-86.
[20] D.B. DeFranco, M. Qi, K.C. Borror, M.J. Garabedian, D.L. Brautigan, Protein phosphatase types 1 and/or 2A regulate nucleocytoplasmic shuttling of glucocorticoid receptors, Molecular endocrinology (Baltimore, Md.) 5(9) (1991) 1215-28.
[21] M.D. Krstic, I. Rogatsky, K.R. Yamamoto, M.J. Garabedian, Mitogen-activated and cyclin-dependent protein kinases selectively and differentially modulate transcriptional enhancement by the glucocorticoid receptor, Molecular and cellular biology 17(7) (1997) 3947-54.
[22] T. Kino, T. Ichijo, N.D. Amin, S. Kesavapany, Y. Wang, N. Kim, S. Rao, A. Player, Y.L. Zheng, M.J. Garabedian, E. Kawasaki, H.C. Pant, G.P. Chrousos, Cyclin-dependent kinase 5 differentially regulates the transcriptional activity of the glucocorticoid receptor through phosphorylation: clinical implications for the nervous system response to glucocorticoids and stress, Molecular endocrinology (Baltimore, Md.) 21(7) (2007) 1552-68.

[23] I. Rogatsky, S.K. Logan, M.J. Garabedian, Antagonism of glucocorticoid receptor transcriptional activation by the c-Jun N-terminal kinase, Proceedings of the National Academy of Sciences of the United States of America 95(5) (1998) 2050-5.
[24] A.J. Galliher-Beckley, J.G. Williams, J.A. Cidlowski, Ligand-independent phosphorylation of the glucocorticoid receptor integrates cellular stress pathways with nuclear receptor signaling, Molecular and cellular biology 31(23) (2011) 4663-75.
[25] T. Habib, A. Sadoun, N. Nader, S. Suzuki, W. Liu, P.V. Jithesh, T. Kino, AKT1 has dual actions on the glucocorticoid receptor by cooperating with 14-3-3, Molecular and cellular endocrinology 439 (2017) 431-443.
[26] M. Itoh, M. Adachi, H. Yasui, M. Takekawa, H. Tanaka, K. Imai, Nuclear export of glucocorticoid receptor is enhanced by c-Jun N-terminal kinase-mediated phosphorylation, Molecular endocrinology (Baltimore, Md.) 16(10) (2002) 2382-92.
[27] A.J. Galliher-Beckley, J.G. Williams, J.B. Collins, J.A. Cidlowski, Glycogen synthase kinase 3beta-mediated serine phosphorylation of the human glucocorticoid receptor redirects gene expression profiles, Molecular and cellular biology 28(24) (2008) 7309-22.
[28] A.L. Miller, M.S. Webb, A.J. Copik, Y. Wang, B.H. Johnson, R. Kumar, E.B. Thompson, p38 Mitogen-activated protein kinase (MAPK) is a key mediator in glucocorticoid-induced apoptosis of lymphoid cells: correlation between p38 MAPK activation and site-specific phosphorylation of the human glucocorticoid receptor at serine 211, Molecular endocrinology (Baltimore, Md.) 19(6) (2005) 1569-83.
[29] I. Rogatsky, C.L. Waase, M.J. Garabedian, Phosphorylation and inhibition of rat glucocorticoid receptor transcriptional activation by glycogen synthase kinase-3 (GSK-3). Species-specific differences between human and rat glucocorticoid receptor signaling as revealed through GSK-3 phosphorylation, The Journal of biological chemistry 273(23) (1998) 14315-21.
[30] Y. Kobayashi, N. Mercado, P.J. Barnes, K. Ito, Defects of protein phosphatase 2A causes corticosteroid insensitivity in severe asthma, PLoS One 6(12) (2011) e27627-e27627.
[31] B. Bouazza, K. Krytska, M. Debba-Pavard, Y. Amrani, R.E. Honkanen, J. Tran, O. Tliba, Cytokines alter glucocorticoid receptor phosphorylation in airway cells: role of phosphatases, American journal of respiratory cell and molecular biology 47(4) (2012) 464-73.
[32] K. Pazdrak, C. Straub, R. Maroto, S. Stafford, W.I. White, W.J. Calhoun, A. Kurosky, Cytokine-Induced Glucocorticoid Resistance from Eosinophil Activation: Protein Phosphatase 5

Modulation of Glucocorticoid Receptor Phosphorylation and Signaling, Journal of immunology (Baltimore, Md. : 1950) 197(10) (2016) 3782-3791.
[33] S. Nagarajan, T. Vohra, J. Loffing, N. Faresse, Protein Phosphatase 1alpha enhances renal aldosterone signaling via mineralocorticoid receptor stabilization, Molecular and cellular endocrinology 450 (2017) 74-82.
[34] X. Liu, W. Han, S. Gulla, N.I. Simon, Y. Gao, C. Cai, H. Yang, X. Zhang, J. Liu, S.P. Balk, S. Chen, Protein phosphatase 1 suppresses androgen receptor ubiquitylation and degradation, Oncotarget 7(2) (2016) 1754-64.
[35] A. Bollig, L. Xu, A. Thakur, J. Wu, T.H. Kuo, J.D. Liao, Regulation of intracellular calcium release and PP1alpha in a mechanism for 4-hydroxytamoxifen-induced cytotoxicity, Molecular and cellular biochemistry 305(1-2) (2007) 45-54.
[36] P. Cohen, S. Klumpp, D.L. Schelling, An improved procedure for identifying and quantitating protein phosphatases in mammalian tissues, FEBS letters 250(2) (1989) 596-600.
[37] C. Bialojan, A. Takai, Inhibitory effect of a marine-sponge toxin, okadaic acid, on protein phosphatases. Specificity and kinetics, The Biochemical journal 256(1) (1988) 283-90.
[38] J.P. Somers, D.B. DeFranco, Effects of okadaic acid, a protein phosphatase inhibitor, on glucocorticoid receptor-mediated enhancement, Molecular endocrinology (Baltimore, Md.) 6(1) (1992) 26-34.
[39] H. Ceulemans, M. Bollen, Functional diversity of protein phosphatase-1, a cellular economizer and reset button, Physiological reviews 84(1) (2004) 1-39.
[40] P.T. Cohen, Protein phosphatase 1--targeted in many directions, Journal of cell science 115(Pt 2) (2002) 241-56.
[41] G.B.G. Moorhead, L. Trinkle-Mulcahy, A. Ulke-Lemée, Emerging roles of nuclear protein phosphatases, Nature Reviews Molecular Cell Biology 8 (2007) 234.
[42] K.J. Livak, T.D. Schmittgen, Analysis of relative gene expression data using real-time quantitative PCR and the 2(-Delta Delta C(T)) Method, Methods (San Diego, Calif.) 25(4) (2001) 402-8.
[43] A.G. Atanasov, L.G. Nashev, L. Gelman, B. Legeza, R. Sack, R. Portmann, A. Odermatt, Direct protein-protein interaction of 11beta-hydroxysteroid dehydrogenase type 1 and hexose-6-phosphate dehydrogenase in the endoplasmic reticulum lumen, Biochimica et biophysica acta 1783(8) (2008) 1536-43.

[44] M.G. Petrillo, R.H. Oakley, J.A. Cidlowski, beta-Arrestin-1 inhibits glucocorticoid receptor turnover and alters glucocorticoid signaling, The Journal of biological chemistry 294(29) (2019) 11225-11239.
[45] Z. Wang, J. Frederick, M.J. Garabedian, Deciphering the phosphorylation "code" of the glucocorticoid receptor in vivo, The Journal of biological chemistry 277(29) (2002) 26573-80.
[46] S. Takabe, K. Mochizuki, T. Goda, De-phosphorylation of GR at Ser203 in nuclei associates with GR nuclear translocation and GLUT5 gene expression in Caco-2 cells, Archives of biochemistry and biophysics 475(1) (2008) 1-6.
[47] W. Chen, T. Dang, R.D. Blind, Z. Wang, C.N. Cavasotto, A.B. Hittelman, I. Rogatsky, S.K. Logan, M.J. Garabedian, Glucocorticoid receptor phosphorylation differentially affects target gene expression, Molecular endocrinology (Baltimore, Md.) 22(8) (2008) 1754-66.
[48] A.L. Miller, A.S. Garza, B.H. Johnson, E.B. Thompson, Pathway interactions between MAPKs, mTOR, PKA, and the glucocorticoid receptor in lymphoid cells, Cancer cell international 7 (2007) 3.
[49] D. Finlay, S. Patel, L.M. Dickson, N. Shpiro, R. Marquez, C.J. Rhodes, C. Sutherland, Glycogen synthase kinase-3 regulates IGFBP-1 gene transcription through the thymine-rich insulin response element, BMC Mol Biol 5 (2004) 15-15.
[50] J.R. Woodgett, Molecular cloning and expression of glycogen synthase kinase-3/factor A, The EMBO journal 9(8) (1990) 2431-8.
[51] J.R. Woodgett, cDNA cloning and properties of glycogen synthase kinase-3, Methods in enzymology 200 (1991) 564-77.
[52] C. Sutherland, P. Cohen, The alpha-isoform of glycogen synthase kinase-3 from rabbit skeletal muscle is inactivated by p70 S6 kinase or MAP kinase-activated protein kinase-1 in vitro, FEBS letters 338(1) (1994) 37-42.
[53] C. Sutherland, I.A. Leighton, P. Cohen, Inactivation of glycogen synthase kinase-3 beta by phosphorylation: new kinase connections in insulin and growth-factor signalling, The Biochemical journal 296 (Pt 1) (1993) 15-9.
[54] G. Morfini, G. Szebenyi, H. Brown, H.C. Pant, G. Pigino, S. DeBoer, U. Beffert, S.T. Brady, A novel CDK5-dependent pathway for regulating GSK3 activity and kinesin-driven motility in neurons, The EMBO journal 23(11) (2004) 2235-45.
[55] E. Szatmari, A. Habas, P. Yang, J.J. Zheng, T. Hagg, M. Hetman, A positive feedback loop between glycogen synthase kinase 3beta and protein phosphatase 1 after stimulation of NR2B

NMDA receptors in forebrain neurons, The Journal of biological chemistry 280(45) (2005) 37526-35.
[56] F. Zhang, C.J. Phiel, L. Spece, N. Gurvich, P.S. Klein, Inhibitory phosphorylation of glycogen synthase kinase-3 (GSK-3) in response to lithium. Evidence for autoregulation of GSK-3, The Journal of biological chemistry 278(35) (2003) 33067-77.
[57] R. Spokoini, S. Kfir-Erenfeld, E. Yefenof, R.V. Sionov, Glycogen synthase kinase-3 plays a central role in mediating glucocorticoid-induced apoptosis, Molecular endocrinology (Baltimore, Md.) 24(6) (2010) 1136-50.
[58] N. Embi, D.B. Rylatt, P. Cohen, Glycogen synthase kinase-3 from rabbit skeletal muscle. Separation from cyclic-AMP-dependent protein kinase and phosphorylase kinase, European journal of biochemistry 107(2) (1980) 519-27.
[59] A. Ali, K.P. Hoeflich, J.R. Woodgett, Glycogen synthase kinase-3: properties, functions, and regulation, Chemical reviews 101(8) (2001) 2527-40.
[60] J.E. Forde, T.C. Dale, Glycogen synthase kinase 3: a key regulator of cellular fate, Cellular and molecular life sciences : CMLS 64(15) (2007) 1930-44.
[61] M.P. Soutar, W.Y. Kim, R. Williamson, M. Peggie, C.J. Hastie, H. McLauchlan, W.D. Snider, P.R. Gordon-Weeks, C. Sutherland, Evidence that glycogen synthase kinase-3 isoforms have distinct substrate preference in the brain, Journal of neurochemistry 115(4) (2010) 974-83.
[62] C. Rubio-Patiño, C.M. Palmeri, A. Pérez-Perarnau, A.M. Cosialls, C. Moncunill-Massaguer, D.M. González-Gironès, L. Pons-Hernández, J.M. López, F. Ventura, J. Gil, G. Pons, D. Iglesias-Serret, Glycogen synthase kinase-3β is involved in ligand-dependent activation of transcription and cellular localization of the glucocorticoid receptor, Molecular endocrinology (Baltimore, Md.) 26(9) (2012) 1508-1520.
[63] A.J. Harwood, Regulation of GSK-3: a cellular multiprocessor, Cell 105(7) (2001) 821-4.
[64] J. Figueiredo, E.S.O.A. da Cruz, M. Fardilha, Protein phosphatase 1 and its complexes in carcinogenesis, Current cancer drug targets 14(1) (2014) 2-29.
[65] J. Ladha, S. Donakonda, S. Agrawal, B. Thota, M.R. Srividya, S. Sridevi, A. Arivazhagan, K. Thennarasu, A. Balasubramaniam, B.A. Chandramouli, A.S. Hegde, P. Kondaiah, K. Somasundaram, V. Santosh, S.M. Rao, Glioblastoma-specific protein interaction network identifies PP1A and CSK21 as connecting molecules between cell cycle-associated genes, Cancer research 70(16) (2010) 6437-47.

[66] A.H. Shastry, B. Thota, M.R. Srividya, A. Arivazhagan, V. Santosh, Nuclear Protein Phosphatase 1 alpha (PP1A) Expression is Associated with Poor Prognosis in p53 Expressing Glioblastomas, Pathology oncology research : POR 22(2) (2016) 287-92.
[67] D. Genoux, U. Haditsch, M. Knobloch, A. Michalon, D. Storm, I.M. Mansuy, Protein phosphatase 1 is a molecular constraint on learning and memory, Nature 418(6901) (2002) 970-5.
[68] D. Muyllaert, A. Kremer, T. Jaworski, P. Borghgraef, H. Devijver, S. Croes, I. Dewachter, F. Van Leuven, Glycogen synthase kinase-3beta, or a link between amyloid and tau pathology?, Genes, brain, and behavior 7 Suppl 1 (2008) 57-66.
[69] A. Martinez, D.I. Perez, GSK-3 inhibitors: a ray of hope for the treatment of Alzheimer's disease?, Journal of Alzheimer's disease : JAD 15(2) (2008) 181-91.
[70] G. Canet, N. Chevallier, V. Perrier, C. Desrumaux, L. Givalois, Targeting Glucocorticoid Receptors: A New Avenue for Alzheimer’s Disease Therapy, in: S. Singh, N. Joshi (Eds.), Pathology, Prevention and Therapeutics of Neurodegenerative Disease, Springer Singapore, Singapore, 2019, pp. 173-183.
[71] A.J. Rose, A. Vegiopoulos, S. Herzig, Role of glucocorticoids and the glucocorticoid receptor in metabolism: insights from genetic manipulations, The Journal of steroid biochemistry and molecular biology 122(1-3) (2010) 10-20.
[72] E.J. Henriksen, B.B. Dokken, Role of glycogen synthase kinase-3 in insulin resistance and type 2 diabetes, Current drug targets 7(11) (2006) 1435-41.
[73] L. Ragolia, N. Begum, Protein phosphatase-1 and insulin action, Molecular and cellular biochemistry 182(1) (1998) 49-58.
[74] J. Xia, S.W. Scherer, P.T. Cohen, M. Majer, T. Xi, R.A. Norman, W.C. Knowler, C. Bogardus, M. Prochazka, A common variant in PPP1R3 associated with insulin resistance and type 2 diabetes, Diabetes 47(9) (1998) 1519-24.
[75] P.J. Barnes, Mechanisms and resistance in glucocorticoid control of inflammation, The Journal of steroid biochemistry and molecular biology 120(2-3) (2010) 76-85.
[76] N. Yang, D.W. Ray, L.C. Matthews, Current concepts in glucocorticoid resistance, Steroids 77(11) (2012) 1041-9.

Supplemental Figures

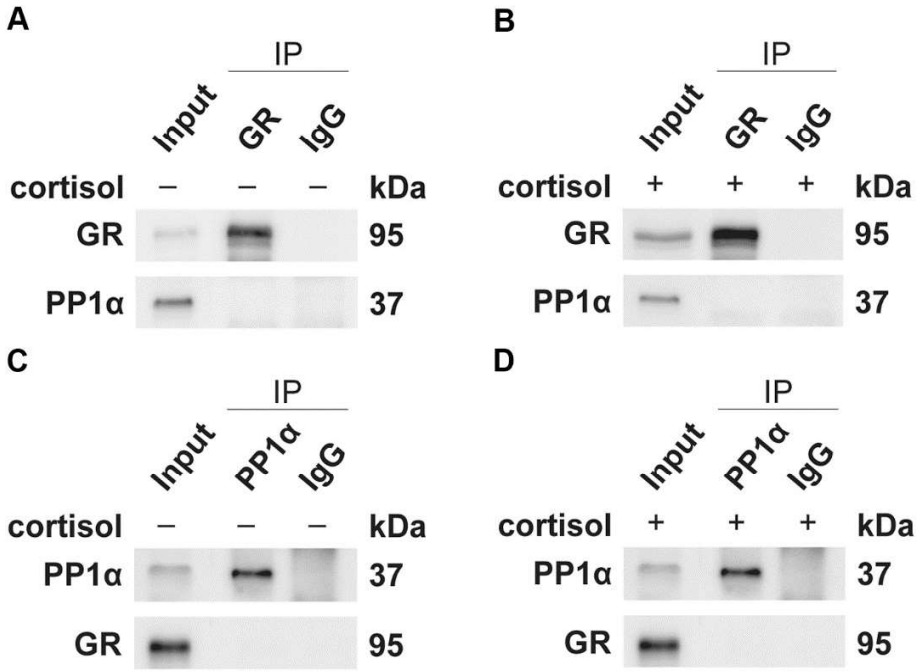

Suppl. Fig. 1. Co-immunoprecipitation of endogenous GR and PP1α. A549 cells endogenously expressing GR and PP1α were treated with (B and D) or without (A and C) 500 nM cortisol for 1 h. Cell lysates were then immunoprecipitated using an anti-GR antibody (A and B) or an anti-PP1α antibody (C and D) and immunoblots were probed with both, anti-GR and anti-PP1α antibodies.

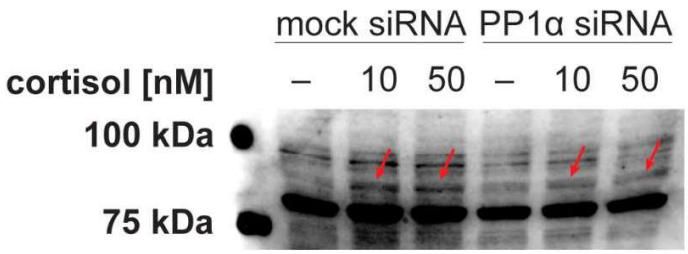

Suppl. Fig. 2. Effect of PP1α knockdown on phosphorylation of GR-Ser404. A549 cells were transfected with mock or anti-PP1α siRNA for 48 h, incubated in serum-free medium for 16-18 h and treated with vehicle or cortisol (10 nM and 50 nM cortisol) for another 1 h, followed by Western blot analysis using a phospho-specific anti-GR-Ser404 antibody. The corresponding band of Ser404 in cortisol-treated samples is indicated by an arrow.

4.2. Discussion

GR and MR are steroid receptors essential for maintaining body homeostasis and their function may be disrupted by exposure to xenobiotics. Indeed, there is a growing literature on chemicals potentially interfering with GR and MR action [12, 166, 167]. In addition to disturbing receptor activity, previous reports focused on EDCs potentially influencing the physiological effects of glucocorticoids and mineralocorticoids by affecting enzymes involved in the biosynthesis and pre-receptor regulation, but rarely investigated impacts on altered receptor function due to post-translational modifications.

The great majority of studies applied molecular modeling and/or biological evaluation to identify EDCs directly binding to corticosteroid receptors [12]. Ligand-receptor binding is mainly assessed by computational docking analysis and *in vitro* competitive binding assays using radio-isotope labeled ligands. Moreover, reporter gene transactivation assays have been developed as a high-throughput method for the analysis of receptor activities. In contrast to binding assays, transactivation assays can distinguish between agonistic and antagonistic effects of chemicals, which is required to assess the potential toxicity of a given compound. The evaluation of receptor activities is often performed with partial constructs containing only the ligand binding domain rather than using a full-length steroid receptor reporter system, potentially leading to biased results. Another possible readout for determining receptor activity is by analyzing changes in the expression level of hormone responsive genes.

Although the use of these *in silico* and *in vitro* techniques has led to the identification of a variety of chemicals that directly interfere with steroid receptors [12], EDCs affecting post-translational modifications and thereby altering receptor function might be missed.

For instance, withanolide A (WitA), a steroidal constituent of the Ashwagandha root, was proposed to act on GR, but molecular docking and GR binding assays could not detect any direct interference of WitA nor were there any effects observed on GR transactivation in HEK-293 cells [171]. However, WitA has been shown to induce neurite outgrowth in human neuroblastoma SH-SY5Y cells, similar to the GR antagonist mifepristone [171, 172]. Since a direct effect on the GR binding pocket is unlikely, WitA-dependent stimulation of neurite outgrowth might be mediated through inhibition of GR activity by phosphorylation of GR-Ser134 by PI3K/Akt or GR-Ser226 by ERK1/2, respectively, as it is the case upon blocking GR with mifepristone [173]. In fact, there is evidence that WitA induces the activation of PI3K/Akt and inhibition of JNK, ERK1/2 and p38 [174]. Withaferin A, another bioactive component of the Ashwagandha root, has also been shown to activate Akt and ERK [175]. Therefore, further research should investigate post-translational modifications of GR as potential targets for the WitA-dependent induction of neurite outgrowth.

The flame retardant tetrabromobisphenol A (TBBPA) represents another compound assumed to act on GR and for which no direct effects on GR function have been observed in GR transactivation and

binding assays as well as in molecular docking predictions [40]. Several studies reported that TBBPA may increase phosphorylation of Akt, ERK1/2, p38 and JNK [176-178], which might suppress GR function and thus may explain for the proposed inhibitory effects of TBBPA on GR activity, requiring further investigation.

The organotin dibutyltin (DBT), used as a stabilizer in the production of polyvinyl chloride plastic materials and constituting the main metabolite of the antifouling dye tributyltin (TBT), is reported to inhibit ligand binding to GR, its transcriptional activity and glucocorticoid-induced expression of phosphoenolpyruvate carboxykinase (PEPCK) [179]. Docking analysis revealed that DBT suppresses GR activation most likely by binding to an allosteric site. Besides allosteric inhibition, signaling pathways involved in receptor activation should be considered, since an alternative explanation might include post-translational modification of GR by PI3K/Akt, JNK or MAPK kinase pathways. Studies examining the ability of DBT to stimulate different kinases showed that PI3K/Akt, ERK1/2, p38 and JNK were activated upon exposure to DBT [180, 181]. This in turn might cause an inhibitory effect on GR activity, which warrants further investigation.

Phosphorylation plays an important role in enhancing or decreasing GR function, and receptor hypo- or hyperfunction may contribute to differential individual sensitivity towards the exposure to potential EDCs. Thus, protein kinases and phosphatases are key enzymes controlling GR activity and impairment of their function might support GR-associated diseases such as asthma, COPD, osteoporosis and metabolic disorders [182]. For example, increased activity of protein phosphatase 5 (PP5) resulted in dephosphorylation of GR-Ser211 that correlates with decreased transcriptional activity of the receptor and thus might promote corticosteroid insensitivity in patients with severe asthma [183, 184]. PP5 was identified as a major component of the GR-HSP-90-chaperone complex, which maintains the unliganded receptor in a transcriptionally inactive state [185, 186]. Besides, protein phosphatase 2A (PP2A) is supposed to increase GR nuclear translocation and corticosteroid sensitivity by dephosphorylation of GR-Ser226, mediated via dephosphorylation and inactivation of upstream JNK [187]. In peripheral blood mononuclear cells from severe asthma patients, PP2A expression and activity were significantly reduced compared with those in healthy subjects, while phosphorylation of GR-Ser226 and JNK were increased [188]. This is further evidence that protein phosphatases have an essential role in GR regulation and maintenance of glucocorticoid sensitivity.

Interestingly, a few studies attempted to restore glucocorticoid sensitivity by inhibiting p38 MAPK activity, particularly in inflammatory diseases. In corticosteroid-resistant asthma, elevated levels of inflammatory cytokines including IL-2 and IL-4 led to enhanced activation of the p38 MAPK pathway and reduced GR function [189]. Co-treatment with p38 inhibitors reversed glucocorticoid resistance and re-established the beneficial effects of glucocorticoids in asthma and COPD patients [189-191]. Microbial superantigens induced glucocorticoid resistance in T cells through activation of ERK1/2

pathways, resulting in increased GR phosphorylation and decreased nuclear translocation. This suppressed response to glucocorticoids could be restored by treatment with inhibitors of MEK and ERK [192]. In clones from the CEM line of childhood acute lymphoblastic leukemia (ALL) cells refractory to apoptosis upon glucocorticoid treatment, inhibition of JNK and ERK activity, stimulation of the cAMP/PKA pathway with forskolin as well as inhibition of mTOR with rapamycin reversed resistant cells to corticoid sensitivity by increasing phosphorylation of GR-Ser211 [193]. In another glucocorticoid-resistant clone of human CEM cells, co-treatment with anisomycin, a known agonist of p38-MAPK and JNK, led to an increase in apoptosis due to a remarkable activation of GR, p38 MAPK and JNK. All this could be prevented by the GR inhibitor mifepristone, indicating that GR might be an upstream activator of the p38-MAPK/JNK signaling pathway [194]. However, the interplay of GR and various kinases and phosphatases is complex and varies depending on cell type, the presence of interacting factors and the activity of other signaling pathways. Hence, the impact of phosphorylation of GR on diverse aspects of GR function and signaling is not yet fully understood.

In order to identify chemicals altering post-translational modifications of GR, it is crucial to further elucidate the signaling pathways upstream of GR and determine the corresponding membrane receptors and associated regulatory proteins. This might help to better understand the mechanisms of impaired glucocorticoid action. Thus, in this regard, the purpose of the present thesis was to study the influence of PP1α on GR function. Knockdown of PP1α was found to reduce GR activity by decreasing GR-Ser211 phosphorylation, probably by involvement of GSK-3 (further details are described in the manuscript 'Protein phosphatase 1 alpha enhances glucocorticoid receptor activity by a mechanism involving phosphorylation of serine-211', chapter 4.1). Considering the supposed stimulatory effect of PP1α on GR activity, it is likely that xenobiotic-induced impairment of PP1α function might lead to an aberrant glucocorticoid response and contribute to diseases involving the GR.

Several naturally occurring and life-threatening toxins are known to potently inhibit PP1 by blocking its function via binding to the catalytic subunit [195, 196]. These include tautomycin and calyculin A synthesized by soil bacteria and dinoflagellates, respectively [197-199], okadaic acid, a fatty acid polyether produced by marine dinoflagellates and being responsible for diarrheic shellfish poisoning in humans [200, 201], and microcystin, a cyclic heptapeptide secreted from cyanobacteria commonly found in fresh water blue-green algae [202, 203], which led to a WHO-recommended drinking water guidance value of 1 µg toxins/L [204]. Although tautomycin and okadaic acid differ structurally from microcystin and calyculin A, they are reported to bind to a common site of PP1, occlude the PP1 active site and extend into the PP1 hydrophobic groove [195]. Due to the ability of these toxins to potently inhibit both PP1 and PP2A, they have proven valuable in studying the functions of these protein phosphatases [196, 205].

PP1 is ubiquitously expressed and regulates an enormous variety of cellular processes by dephosphorylation of serine/threonine-phosphorylated protein substrates, including cell cycle progression, protein synthesis, transcription, splicing, calcium signaling, carbohydrate metabolism and muscle contraction [206, 207]. Despite its diverse functions, no studies have been conducted so far to identify xenobiotics potentially disrupting PP1 function. It is highly challenging to study PP1, since it acts pleiotropically as a holoenzyme consisting of one constant catalytic subunit (PP1c; existing in four isoforms PP1α, PP1β, PP1γ1 and PP1γ2) associated with variable regulatory subunits [206]. PP1c is specifically and tightly regulated by its interaction with more than 200 proteins that function as substrate-targeting subunits, location-targeting subunits or inhibitors, thereby determining substrate specificity, subcellular localization and catalytic activity of the holoenzyme. These regulatory subunits generate an astonishing diversity of holoenzymes by binding to PP1c through a specific motif including RVxF, SILK or MyPhoNE [207-209]. Inhibitors targeting PP1c such as the highly toxic natural compounds tautomycin, calyculin A, okadaic acid or microcystin cannot distinguish between different PP1 holoenzymes and, depending on the concentration, unselectively inhibit the activity of related protein phosphatases such as PP2A.

An attractive alternative approach for the development of PP1-selective modulators is targeting protein-protein interactions within the holoenzyme, either on PP1c or the regulatory subunit. For instance, targeting the RVxF-binding site on PP1 might inhibit PP1 by blocking the active site or activate PP1 by releasing the free PP1c [210]. In the search for new treatment strategies against HIV, a small molecule compound targeting the RVXF-binding cavity of PP1 was discovered by virtual screening using a structure-based pharmacophore model. This compound disrupted the interaction between the protein of interest and PP1, but did not affect the binding of PP1 to other regulatory subunits [211]. In analogy to the drug discovery process, this computational tool might be employed in toxicological studies to screen environmental databases for the identification of potential chemicals interfering with PP1. Recently, a molecular docking study has reported that several phytochemicals including apigenin and daidzein can bind to the PP1 hydrophobic groove, explaining their inhibitory effect on PP1c [212]. Therefore, it would be interesting to investigate the potential of these herbal compounds to interfere with the PP1α-dependent GR activity by using the lung A549 cell model (the established conditions are described in the manuscript 'Protein phosphatase 1 alpha enhances glucocorticoid receptor activity by a mechanism involving phosphorylation of serine-211', see chapter 4.1).

Furthermore, environmental factors assumed to contribute to glucocorticoid insensitivity such as cigarette smoke extract and diesel exhaust particles might be assessed for their ability to impair PP1α-mediated GR stimulation as a possible cause contributing to glucocorticoid resistance. Interestingly, cigarette smoke extract was found to significantly inhibit GSK-3β by increasing levels of inhibitory GSK-3β-Ser9 phosphorylation [213]. In addition, elevated levels of phosphorylated GSK-3β-Ser9 were

observed in alveolar macrophages, monocytes and bronchial epithelial cells of COPD patients and control smokers compared with non-smokers, implying a possible involvement of GSK-3β in glucocorticoid unresponsiveness in COPD [214]. Smoking also appeared to be the most important contributor to glucocorticoid resistance in patients suffering from glucocorticoid-resistant asthma [215]. Additionally, corticosteroid-refractory asthma has been associated with exposure to diesel exhaust particles (DEP) [216], although extracts of DEP have not altered GR transcriptional activity as evaluated by a GRE reporter gene assay [217]. This suggests that post-translational modifications of the GR may be involved in DEP-induced steroid insensitivity. Thus, the question arises whether smoking and/or DEP promote glucocorticoid insensitivity by potentially impairing PP1α function, which in turn might contribute to the inactivation of GSK-3 and GR. Further research is needed to address this issue, for example by using the established A549 cell model.

Also, it might be of interest to investigate the function of PP1α in a cell line that is resistant to glucocorticoids. Would it be possible to restore the glucocorticoid sensitivity of a resistant cell such as the aforementioned CEM cell line by overexpressing the recombinant PP1α? Instead of overexpression, treating the cells with a PP1-disrupting peptide would be a possibility to stimulate endogenous PP1 activity. It has been demonstrated that the proteolytically stable and cell-permeable peptide PDP-*Nal* specifically disrupts the interaction between PP1c and its endogenous inhibitor-2, which leads to the release of PP1c from the holoenzyme and thus to the activation of PP1 [218, 219]. If the responsible interactors and signaling pathways are present and glucocorticoid resistance is partly due to inactivation of PP1, the peptide-mediated activation of PP1 might lead to stimulation of GR and the reversal of glucocorticoid resistance in this cell line.

In contrast to xenobiotics directly interfering with the GR, little is known about chemically-induced disruption of signaling pathways upstream of GR. Importantly, GR signaling is not only based on ligand binding, and signaling pathways are highly complex and interconnected. Given the numerous proteins involved in signal transduction, unravelling cellular signaling networks remains a major challenge. Although considerable insight has been gained into the sophisticated regulation of GR function, it is of great importance to improve and extend the knowledge about existing and alternative signaling pathways that control GR activity. Understanding how these pathways intercommunicate and in which situations they can be considered as biologically relevant might not only permit to resolve the molecular mechanisms of glucocorticoid resistance, but also support the establishment of suitable *in silico* and *in vitro* approaches for the identification and characterization of xenobiotics potentially disturbing post-translational modifications of GR. There is increasing evidence for the occurrence of xenobiotics affecting GR and MR function, and potential disruption of corticosteroid hormone action should be considered for safety assessment of these chemicals [12, 166]. In contrast to the extensive information on xenobiotics interfering with androgen and estrogen responses, the identification of

corticosteroid disruptors is an emerging field of research. While phenotypic alterations caused by impaired AR and ER function are easier to recognize, changes in corticosteroid responses are more subtle in their expression and can contribute to diseases in the longer term, making them more challenging to detect and their cause more difficult to identify, but not less important.

5. Appendix

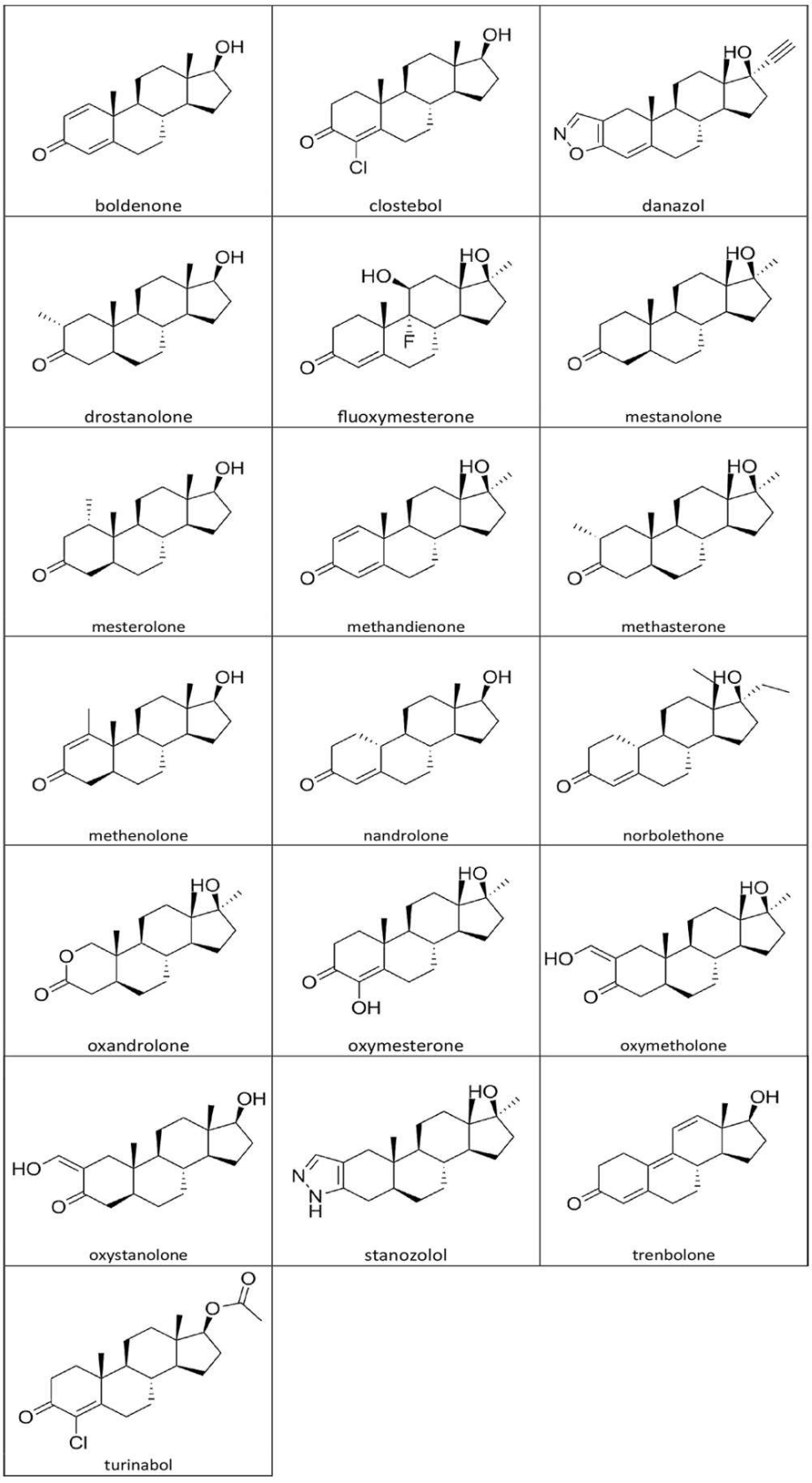

Figure A1. 2D-structures of anabolic androgenic steroids (AAS).

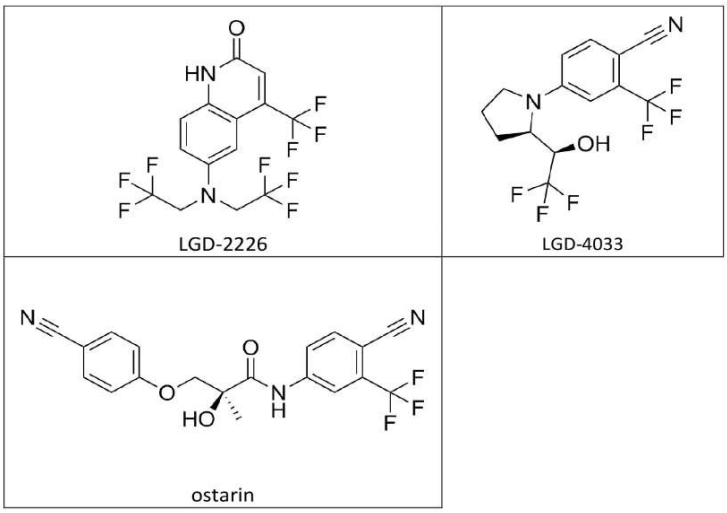

Figure A2. 2D-structures of selective androgen receptor modulators (SARMs).

6. Acknowledgement

I would like to thank Prof. Alex Odermatt for his enormous support, valuable and constructive recommendations, stimulating discussions and for giving me the unique opportunity to perform this thesis in his laboratory. I thank Prof. Jörg Huwyler and Prof. Michael Arand for co-advising my thesis and Prof. Stefan Krähenbühl for chairing my thesis committee. Further, I thank Prof. Serge Rudaz, Dr. Julien Boccard and Dr. Víctor González-Ruiz for their collaboration in the anabolic steroid project as well as Prof. Daniela Schuster and Dr. Muhammad Akram for their cooperation in the epoxiconazole project, without them this whole thesis would not have been possible. Additional thanks go to my master students Tobias Di Marco and Joël Gysi for their work and contribution of important data. Special thanks go to Dr. Katharina Beck for the many scientific discussions, her support and helpful project inputs. I also want to thank all members from the Molecular and Systems Toxicology group for their project suggestions, the discussions and the good time we had together. Finally, my sincere thanks go to my family and friends for their continuous support throughout my thesis.

7. References

[1] European Union, Registration, Evaluation, Authorization and Restriction of Chemicals (REACH) [Online] https://ec.europa.eu/growth/sectors/chemicals/reach/ [Accessed: October, 2019].
[2] U.S. Environmental Protection Agency (EPA), Endocrine Disruptor Screening Program (EDSP), [Online] https://www.epa.gov/endocrine-disruption/endocrine-disruptor-screening-program-edsp-overview [Accessed: October, 2019].
[3] U.S. Environmental Protection Agency (EPA), Toxicology in the 21st Century (Tox21) interagency collaboration program [Online] https://tox21.gov/ [Accessed: October, 2019].
[4] N.R. Council, Toxicity Testing in the 21st Century: A Vision and a Strategy, The National Academies Press, Washington, DC, 2007.
[5] U.S. Environmental Protection Agency (EPA), Toxicity Forecaster (ToxCast) [Online] https://www.epa.gov/chemical-research/toxicity-forecasting [Accessed: October, 2019].
[6] European Commission, Towards a comprehensive European Union framework on endocrine disruptors, [Online] https://ec.europa.eu/transparency/regdoc/rep/1/2018/EN/COM-2018-734-F1-EN-MAIN-PART-1.PDF [Accessed: October, 2019].
[7] Global Assessment of the State-of-the-Science of Endocrine Disruptors, International Programme on Chemical Safety, in: S. Damstra, A. Barlow, R.J. Bergman (Eds.), World Health Organization, Geneva, Switzerland, 2002 WHO publication no. WHO/PCS/EDC/02.2.
[8] F. Maqbool, S. Mostafalou, H. Bahadar, M. Abdollahi, Review of endocrine disorders associated with environmental toxicants and possible involved mechanisms, Life Sciences 145 (2016) 265-273.
[9] A. Bergman, J. Heindel, S. Jobling, K. Kidd, T. Zoeller, Geneva:UNEP/WHO, State-of-the-science of endocrine disrupting chemicals, 2012, [Online] https://www.who.int/ceh/publications/endocrine/en/ (2012) [Accessed: October, 2019].
[10] P.W. Harvey, D.J. Everett, C.J. Springall, Adrenal toxicology: a strategy for assessment of functional toxicity to the adrenal cortex and steroidogenesis, Journal of applied toxicology : JAT 27(2) (2007) 103-15.
[11] A. Odermatt, C. Gumy, A.G. Atanasov, A.A. Dzyakanchuk, Disruption of glucocorticoid action by environmental chemicals: Potential mechanisms and relevance, The Journal of steroid biochemistry and molecular biology 102(1) (2006) 222-231.
[12] J. Zhang, Y. Yang, W. Liu, D. Schlenk, J. Liu, Glucocorticoid and mineralocorticoid receptors and corticosteroid homeostasis are potential targets for endocrine-disrupting chemicals, Environment International 133 (2019) 105133.
[13] L.I. McKay, J.A. Cidlowski, Hormones of the Adrenal Cortex. In: Kufe DW, Pollock RE, Weichselbaum RR, et al., editors. Holland-Frei Cancer Medicine., Hamilton (ON): BC Decker 6th edition. (2003).
[14] P.W. Harvey, 11.13 - Toxic Responses of the Adrenal Cortex, in: C.A. McQueen (Ed.), Comprehensive Toxicology (Second Edition), Elsevier, Oxford, 2010, pp. 265-289.
[15] P.W. Harvey, Adrenocortical endocrine disruption, The Journal of steroid biochemistry and molecular biology 155 (2016) 199-206.
[16] W.E. Ribelin, The effects of drugs and chemicals upon the structure of the adrenal gland, Fundamental and Applied Toxicology 4(1) (1984) 105-119.
[17] W.L. Miller, R.J. Auchus, The molecular biology, biochemistry, and physiology of human steroidogenesis and its disorders, Endocrine reviews 32(1) (2011) 81-151.
[18] E. Melcescu, C.A. Koch, Syndromes of Mineralocorticoid Excess, in: C.A. Koch, G.P. Chrousos (Eds.), Endocrine Hypertension: Underlying Mechanisms and Therapy, Humana Press, Totowa, NJ, 2013, pp. 33-50.
[19] N. Strushkevich, A.A. Gilep, L. Shen, C.H. Arrowsmith, A.M. Edwards, S.A. Usanov, H.W. Park, Structural insights into aldosterone synthase substrate specificity and targeted inhibition, Molecular endocrinology (Baltimore, Md.) 27(2) (2013) 315-24.
[20] H. Globerman, A. Rosler, R. Theodor, M.I. New, P.C. White, An inherited defect in aldosterone biosynthesis caused by a mutation in or near the gene for steroid 11-hydroxylase, The New England journal of medicine 319(18) (1988) 1193-7.

[21] I.M. Ledingham, I. Watt, Influence of sedation on mortality in critically ill multiple trauma patients, Lancet (London, England) 1(8336) (1983) 1270.
[22] R.L. Wagner, P.F. White, P.B. Kan, M.H. Rosenthal, D. Feldman, Inhibition of adrenal steroidogenesis by the anesthetic etomidate, The New England journal of medicine 310(22) (1984) 1415-21.
[23] S. Hahner, A. Sturmer, M. Fassnacht, R.W. Hartmann, K. Schewe, S. Cochran, M. Zink, A. Schirbel, B. Allolio, Etomidate unmasks intraadrenal regulation of steroidogenesis and proliferation in adrenal cortical cell lines, Hormone and metabolic research = Hormon- und Stoffwechselforschung = Hormones et metabolisme 42(7) (2010) 528-34.
[24] P.J. Barter, M. Caulfield, M. Eriksson, S.M. Grundy, J.J. Kastelein, M. Komajda, J. Lopez-Sendon, L. Mosca, J.C. Tardif, D.D. Waters, C.L. Shear, J.H. Revkin, K.A. Buhr, M.R. Fisher, A.R. Tall, B. Brewer, Effects of torcetrapib in patients at high risk for coronary events, The New England journal of medicine 357(21) (2007) 2109-22.
[25] X. Hu, J.D. Dietz, C. Xia, D.R. Knight, W.T. Loging, A.H. Smith, H. Yuan, D.A. Perry, J. Keiser, Torcetrapib induces aldosterone and cortisol production by an intracellular calcium-mediated mechanism independently of cholesteryl ester transfer protein inhibition, Endocrinology 150(5) (2009) 2211-9.
[26] R.G. Clerc, A. Stauffer, F. Weibel, E. Hainaut, A. Perez, J.C. Hoflack, A. Benardeau, P. Pflieger, J.M. Garriz, J.W. Funder, A.M. Capponi, E.J. Niesor, Mechanisms underlying off-target effects of the cholesteryl ester transfer protein inhibitor torcetrapib involve L-type calcium channels, Journal of hypertension 28(8) (2010) 1676-86.
[27] W.L. Miller, MECHANISMS IN ENDOCRINOLOGY: Rare defects in adrenal steroidogenesis, European journal of endocrinology 179(3) (2018) R125-r141.
[28] T. Suzuki, H. Sasano, J. Takeyama, C. Kaneko, W.A. Freije, B.R. Carr, W.E. Rainey, Developmental changes in steroidogenic enzymes in human postnatal adrenal cortex: immunohistochemical studies, Clinical endocrinology 53(6) (2000) 739-47.
[29] L. Schiffer, L. Barnard, E.S. Baranowski, L.C. Gilligan, A.E. Taylor, W. Arlt, C.H.L. Shackleton, K.-H. Storbeck, Human steroid biosynthesis, metabolism and excretion are differentially reflected by serum and urine steroid metabolomes: A comprehensive review, The Journal of steroid biochemistry and molecular biology 194 (2019) 105439.
[30] Y. Tanrikulu, B. Krüger, E. Proschak, The holistic integration of virtual screening in drug discovery, Drug Discovery Today 18(7) (2013) 358-364.
[31] C.G. Wermuth, C.R. Ganellin, P. Lindberg, L.A. Mitscher, Glossary of terms used in medicinal chemistry (IUPAC Recommendations 1998), Pure and Applied Chemistry, 1998, p. 1129.
[32] A.R. Leach, V.J. Gillet, R.A. Lewis, R. Taylor, Three-Dimensional Pharmacophore Methods in Drug Discovery, Journal of medicinal chemistry 53(2) (2010) 539-558.
[33] G. Sliwoski, S. Kothiwale, J. Meiler, E.W. Lowe, Jr., Computational methods in drug discovery, Pharmacol Rev 66(1) (2013) 334-395.
[34] L.G. Nashev, D. Schuster, C. Laggner, S. Sodha, T. Langer, G. Wolber, A. Odermatt, The UV-filter benzophenone-1 inhibits 17beta-hydroxysteroid dehydrogenase type 3: Virtual screening as a strategy to identify potential endocrine disrupting chemicals, Biochemical pharmacology 79(8) (2010) 1189-99.
[35] L.G. Nashev, A. Vuorinen, L. Praxmarer, B. Chantong, D. Cereghetti, R. Winiger, D. Schuster, A. Odermatt, Virtual Screening as a Strategy for the Identification of Xenobiotics Disrupting Corticosteroid Action, PLOS ONE 7(10) (2012) e46958.
[36] K.R. Beck, M. Bachler, A. Vuorinen, S. Wagner, M. Akram, U. Griesser, V. Temml, P. Klusonova, H. Yamaguchi, D. Schuster, A. Odermatt, Inhibition of 11beta-hydroxysteroid dehydrogenase 2 by the fungicides itraconazole and posaconazole, Biochemical pharmacology 130 (2017) 93-103.
[37] K.R. Beck, T. Kaserer, D. Schuster, A. Odermatt, Virtual screening applications in short-chain dehydrogenase/reductase research, The Journal of steroid biochemistry and molecular biology 171 (2017) 157-177.
[38] M. Smiesko, A. Vedani, VirtualToxLab: Exploring the Toxic Potential of Rejuvenating Substances Found in Traditional Medicines, Methods in molecular biology (Clifton, N.J.) 1425 (2016) 121-37.

[39] A. Vedani, M. Dobler, M. Smiesko, VirtualToxLab - a platform for estimating the toxic potential of drugs, chemicals and natural products, Toxicol Appl Pharmacol 261(2) (2012) 142-53.
[40] K.R. Beck, T.J. Sommer, D. Schuster, A. Odermatt, Evaluation of tetrabromobisphenol A effects on human glucocorticoid and androgen receptors: A comparison of results from human- with yeast-based in vitro assays, Toxicology 370 (2016) 70-77.
[41] OECD, OECD guideline for the testing of chemicals. Test No. 456: H295R Steroidogenesis Assay, OECD Guidelines for the Testing of Chemicals, Section 4: Health Effects (2011).
[42] EPA, OPPTS 890.1550: Steroidogenesis (Human Cell Line – H295R), United States Environmental Protection Agency, (2009).
[43] T. Wang, W.E. Rainey, Human adrenocortical carcinoma cell lines, Mol Cell Endocrinol 351(1) (2012) 58-65.
[44] A. Odermatt, P. Strajhar, R.T. Engeli, Disruption of steroidogenesis: Cell models for mechanistic investigations and as screening tools, The Journal of steroid biochemistry and molecular biology 158 (2016) 9-21.
[45] A.F. Gazdar, H.K. Oie, C.H. Shackleton, T.R. Chen, T.J. Triche, C.E. Myers, G.P. Chrousos, M.F. Brennan, C.A. Stein, R.V. La Rocca, Establishment and characterization of a human adrenocortical carcinoma cell line that expresses multiple pathways of steroid biosynthesis, Cancer research 50(17) (1990) 5488-96.
[46] W.E. Rainey, I.M. Bird, C. Sawetawan, N.A. Hanley, J.L. McCarthy, E.A. McGee, R. Wester, J.I. Mason, Regulation of human adrenal carcinoma cell (NCI-H295) production of C19 steroids, The Journal of clinical endocrinology and metabolism 77(3) (1993) 731-7.
[47] M. Hecker, J.P. Giesy, Novel trends in endocrine disruptor testing: the H295R Steroidogenesis Assay for identification of inducers and inhibitors of hormone production, Analytical and bioanalytical chemistry 390(1) (2008) 287-91.
[48] P. Strajhar, D. Tonoli, F. Jeanneret, R.M. Imhof, V. Malagnino, M. Patt, D.V. Kratschmar, J. Boccard, S. Rudaz, A. Odermatt, Steroid profiling in H295R cells to identify chemicals potentially disrupting the production of adrenal steroids, Toxicology 381 (2017) 51-63.
[49] M. Akram, M. Patt, T. Kaserer, V. Temml, W. Waratchareeyakul, D.V. Kratschmar, J. Haupenthal, R.W. Hartmann, A. Odermatt, D. Schuster, Identification of the fungicide epoxiconazole by virtual screening and biological assessment as inhibitor of human 11beta-hydroxylase and aldosterone synthase, The Journal of steroid biochemistry and molecular biology (2019).
[50] N.C. Nicolaides, E. Charmandari, G.P. Chrousos, T. Kino, Circadian endocrine rhythms: the hypothalamic-pituitary-adrenal axis and its actions, Annals of the New York Academy of Sciences 1318 (2014) 71-80.
[51] N. Nader, G.P. Chrousos, T. Kino, Interactions of the circadian CLOCK system and the HPA axis, Trends in endocrinology and metabolism: TEM 21(5) (2010) 277-86.
[52] S. Chung, G.H. Son, K. Kim, Circadian rhythm of adrenal glucocorticoid: its regulation and clinical implications, Biochimica et biophysica acta 1812(5) (2011) 581-91.
[53] E.N. Kassi, G.P. Chrousos, The central CLOCK system and the stress axis in health and disease, Hormones (Athens, Greece) 12(2) (2013) 172-91.
[54] A. Odermatt, D.V. Kratschmar, Tissue-specific modulation of mineralocorticoid receptor function by 11beta-hydroxysteroid dehydrogenases: An overview, Mol Cell Endocrinol 350(2) (2012) 168-86.
[55] A. Blum, E. Maser, Enzymology and molecular biology of glucocorticoid metabolism in humans, Progress in nucleic acid research and molecular biology 75 (2003) 173-216.
[56] L.L. Gathercole, G.G. Lavery, S.A. Morgan, M.S. Cooper, A.J. Sinclair, J.W. Tomlinson, P.M. Stewart, 11β-Hydroxysteroid Dehydrogenase 1: Translational and Therapeutic Aspects, Endocrine reviews 34(4) (2013) 525-555.
[57] R. Ge, Y. Huang, G. Liang, X. Li, 11beta-hydroxysteroid dehydrogenase type 1 inhibitors as promising therapeutic drugs for diabetes: status and development, Current medicinal chemistry 17(5) (2010) 412-22.
[58] X. Li, J. Wang, Q. Yang, S. Shao, 11beta-Hydroxysteroid Dehydrogenase Type 1 in Obese Subjects With Type 2 Diabetes Mellitus, The American journal of the medical sciences 354(4) (2017) 408-414.

[59] J.S. Park, S.J. Bae, S.W. Choi, Y.H. Son, S.B. Park, S.D. Rhee, H.Y. Kim, W.H. Jung, S.K. Kang, J.H. Ahn, S.H. Kim, K.Y. Kim, A novel 11beta-HSD1 inhibitor improves diabesity and osteoblast differentiation, Journal of molecular endocrinology 52(2) (2014) 191-202.
[60] E.S. Ramli, F. Suhaimi, S.F. Asri, F. Ahmad, I.N. Soelaiman, Glycyrrhizic acid (GCA) as 11beta-hydroxysteroid dehydrogenase inhibitor exerts protective effect against glucocorticoid-induced osteoporosis, Journal of bone and mineral metabolism 31(3) (2013) 262-73.
[61] S. Rauz, E.A. Walker, C.H. Shackleton, M. Hewison, P.I. Murray, P.M. Stewart, Expression and putative role of 11 beta-hydroxysteroid dehydrogenase isozymes within the human eye, Investigative ophthalmology & visual science 42(9) (2001) 2037-42.
[62] S. Rauz, C.M. Cheung, P.J. Wood, M. Coca-Prados, E.A. Walker, P.I. Murray, P.M. Stewart, Inhibition of 11beta-hydroxysteroid dehydrogenase type 1 lowers intraocular pressure in patients with ocular hypertension, QJM : monthly journal of the Association of Physicians 96(7) (2003) 481-90.
[63] S. Boudon, M. Heidl, A. Vuorinen, E. Wandeler, R. Campiche, A. Odermatt, E. Jackson, Design, synthesis, and biological evaluation of novel selective peptide inhibitors of 11beta-hydroxysteroid dehydrogenase 1, Bioorganic & medicinal chemistry 26(18) (2018) 5128-5139.
[64] P.C. White, T. Mune, A.K. Agarwal, 11 beta-Hydroxysteroid dehydrogenase and the syndrome of apparent mineralocorticoid excess, Endocrine reviews 18(1) (1997) 135-56.
[65] M.J. Nyirenda, R.S. Lindsay, C.J. Kenyon, A. Burchell, J.R. Seckl, Glucocorticoid exposure in late gestation permanently programs rat hepatic phosphoenolpyruvate carboxykinase and glucocorticoid receptor expression and causes glucose intolerance in adult offspring, The Journal of clinical investigation 101(10) (1998) 2174-81.
[66] E.C. Cottrell, J.R. Seckl, M.C. Holmes, C.S. Wyrwoll, Foetal and placental 11beta-HSD2: a hub for developmental programming, Acta physiologica (Oxford, England) 210(2) (2014) 288-95.
[67] J.W. Funder, P.T. Pearce, R. Smith, A.I. Smith, Mineralocorticoid action: target tissue specificity is enzyme, not receptor, mediated, Science (New York, N.Y.) 242(4878) (1988) 583-5.
[68] C.R. Edwards, P.M. Stewart, D. Burt, L. Brett, M.A. McIntyre, W.S. Sutanto, E.R. de Kloet, C. Monder, Localisation of 11 beta-hydroxysteroid dehydrogenase--tissue specific protector of the mineralocorticoid receptor, Lancet (London, England) 2(8618) (1988) 986-9.
[69] T. Mune, F.M. Rogerson, H. Nikkila, A.K. Agarwal, P.C. White, Human hypertension caused by mutations in the kidney isozyme of 11 beta-hydroxysteroid dehydrogenase, Nature genetics 10(4) (1995) 394-9.
[70] P. Strajhar, P. Vizeli, M. Patt, P.C. Dolder, D.V. Kratschmar, M.E. Liechti, A. Odermatt, Effects of lisdexamfetamine on plasma steroid concentrations compared with d-amphetamine in healthy subjects: A randomized, double-blind, placebo-controlled study, The Journal of steroid biochemistry and molecular biology 186 (2019) 212-225.
[71] J. Sharman, M. Pennick, Lisdexamfetamine prodrug activation by peptidase-mediated hydrolysis in the cytosol of red blood cells, Neuropsychiatric disease and treatment 10 (2014) 2275-80.
[72] P.H. Hutson, M. Pennick, R. Secker, Preclinical pharmacokinetics, pharmacology and toxicology of lisdexamfetamine: a novel d-amphetamine pro-drug, Neuropharmacology 87 (2014) 41-50.
[73] Swissmedic, Arzneimittelinformation Elvanse, Schweizerisches Heilmittelinstitut, [Online] http://www.swissmedicinfo.ch/ [Accessed: October, 2019].
[74] US Food and Drug Administration, prescribing information Vyvanse, [Online] https://www.accessdata.fda.gov/drugsatfda_docs/label/2017/208510lbl.pdf [Accessed: October, 2019].
[75] G.R. Thompson, 3rd, K.R. Beck, M. Patt, D.V. Kratschmar, A. Odermatt, Posaconazole-Induced Hypertension Due to Inhibition of 11beta-Hydroxylase and 11beta-Hydroxysteroid Dehydrogenase 2, Journal of the Endocrine Society 3(7) (2019) 1361-1366.
[76] The International Panel on Chemical Pollution (IPCP), Overview Report I: Worldwide initiatives to identify endocrine disrupting chemicals (EDCs) and potential EDCs, [Online] https://wedocs.unep.org/bitstream/handle/20.500.11822/25633/EDC_report1.pdf?sequence=1&isAllowed=y [Accessed: October, 2019].
[77] A. Vuorinen, A. Odermatt, D. Schuster, In silico methods in the discovery of endocrine disrupting chemicals, The Journal of steroid biochemistry and molecular biology 137 (2013) 18-26.

[78] D.C. Fara, T.I. Oprea, E.R. Prossnitz, C.G. Bologa, B.S. Edwards, L.A. Sklar, Integration of virtual and physical screening, Drug Discovery Today: Technologies 3(4) (2006) 377-385.
[79] T. Kaserer, K.R. Beck, M. Akram, A. Odermatt, D. Schuster, Pharmacophore Models and Pharmacophore-Based Virtual Screening: Concepts and Applications Exemplified on Hydroxysteroid Dehydrogenases, Molecules (Basel, Switzerland) 20(12) (2015) 22799-832.
[80] W.M.S. Russell, The principles of humane experimental technique [by] W.M.S. Russell and R.L. Burch, Methuen, London, 1959.
[81] Directive 2010/63/EU of the European Parliament and of the Council of 22 September 2010 on the protection of animals used for scientific purposes, [Online] https://eur-lex.europa.eu/legal-content/EN/TXT/PDF/?uri=CELEX:02010L0063-20190626&from=EN [Accessed: October, 2019].
[82] Regulation (EC) No 1223/2009 of the European Parliament and of the Council of 30 November 2009 on cosmetic products, [Online] https://eur-lex.europa.eu/legal-content/EN/TXT/HTML/?uri=CELEX:32009R1223&from=EN#d1e1704-59-1 [Accessed: October, 2019].
[83] M. Hecker, J.L. Newsted, M.B. Murphy, E.B. Higley, P.D. Jones, R. Wu, J.P. Giesy, Human adrenocarcinoma (H295R) cells for rapid in vitro determination of effects on steroidogenesis: Hormone production, Toxicology and Applied Pharmacology 217(1) (2006) 114-124.
[84] A.G. Moraitis, W.E. Rainey, R.J. Auchus, Gene mutations that promote adrenal aldosterone production, sodium retention, and hypertension, The application of clinical genetics 7 (2013) 1-13.
[85] J.C. Condon, V. Pezzi, B.M. Drummond, S. Yin, W.E. Rainey, Calmodulin-dependent kinase I regulates adrenal cell expression of aldosterone synthase, Endocrinology 143(9) (2002) 3651-7.
[86] K.B. Seamon, W. Padgett, J.W. Daly, Forskolin: unique diterpene activator of adenylate cyclase in membranes and in intact cells, Proceedings of the National Academy of Sciences of the United States of America 78(6) (1981) 3363-7.
[87] K.G. Mountjoy, I.M. Bird, W.E. Rainey, R.D. Cone, ACTH induces up-regulation of ACTH receptor mRNA in mouse and human adrenocortical cell lines, Mol Cell Endocrinol 99(1) (1994) R17-R20.
[88] A. Oskarsson, E. Ullerås, K.E. Plant, J.P. Hinson, P.S. Goldfarb, Steroidogenic gene expression in H295R cells and the human adrenal gland: adrenotoxic effects of lindane in vitro, Journal of Applied Toxicology 26(6) (2006) 484-492.
[89] I.M. Bird, N.A. Hanley, R.A. Word, J.M. Mathis, J.L. McCarthy, J.I. Mason, W.E. Rainey, Human NCI-H295 adrenocortical carcinoma cells: A model for angiotensin-II-responsive aldosterone secretion, Endocrinology 133(4) (1993) 1555-1561.
[90] W.E. Rainey, I.M. Bird, J.I. Mason, The NCI-H295 cell line: a pluripotent model for human adrenocortical studies, Mol Cell Endocrinol 100(1) (1994) 45-50.
[91] U.D. Lichtenauer, I. Shapiro, A. Osswald, S. Meurer, A. Kulle, M. Reincke, F. Riepe, F. Beuschlein, Characterization of NCI-H295R cells as an in vitro model of hyperaldosteronism, Hormone and metabolic research = Hormon- und Stoffwechselforschung = Hormones et metabolisme 45(2) (2013) 124-9.
[92] W.E. Rainey, K. Saner, B.P. Schimmer, Adrenocortical cell lines, Mol Cell Endocrinol 228(1) (2004) 23-38.
[93] B. Ragazzon, A.-M. Lefrançois-Martinez, P. Val, I. Sahut-Barnola, C. Tournaire, C.l. Chambon, J.-L. Gachancard-Bouya, R.-J. Begue, G. Veyssière, A. Martinez, Adrenocorticotropin-Dependent Changes in SF-1/DAX-1 Ratio Influence Steroidogenic Genes Expression in a Novel Model of Glucocorticoid-Producing Adrenocortical Cell Lines Derived from Targeted Tumorigenesis, Endocrinology 147(4) (2006) 1805-1818.
[94] G. Hazell, G. Horn, S.L. Lightman, F. Spiga, Dynamics of ACTH-Mediated Regulation of Gene Transcription in ATC1 and ATC7 Adrenal Zona Fasciculata Cell Lines, Endocrinology 160(3) (2019) 587-604.
[95] J.C. Rijk, A.A. Peijnenburg, M.H. Blokland, A. Lommen, R.L. Hoogenboom, T.F. Bovee, Screening for modulatory effects on steroidogenesis using the human H295R adrenocortical cell line: a metabolomics approach, Chemical research in toxicology 25(8) (2012) 1720-31.
[96] M. Fassnacht, S. Hahner, F. Beuschlein, A. Klink, M. Reincke, B. Allolio, New mechanisms of adrenostatic compounds in a human adrenocortical cancer cell line, European journal of clinical investigation 30 Suppl 3 (2000) 76-82.

[97] T. du Toit, M.A. Stander, A.C. Swart, A high-throughput UPC(2)-MS/MS method for the separation and quantification of C19 and C21 steroids and their C11-oxy steroid metabolites in the classical, alternative, backdoor and 11OHA4 steroid pathways, Journal of chromatography. B, Analytical technologies in the biomedical and life sciences 1080 (2018) 71-81.
[98] L. Barnard, R. Gent, D. van Rooyen, A.C. Swart, Adrenal C11-oxy C21 steroids contribute to the C11-oxy C19 steroid pool via the backdoor pathway in the biosynthesis and metabolism of 21-deoxycortisol and 21-deoxycortisone, The Journal of steroid biochemistry and molecular biology 174 (2017) 86-95.
[99] D. van Rooyen, R. Gent, L. Barnard, A.C. Swart, The in vitro metabolism of 11beta-hydroxyprogesterone and 11-ketoprogesterone to 11-ketodihydrotestosterone in the backdoor pathway, The Journal of steroid biochemistry and molecular biology 178 (2018) 203-212.
[100] N. Marti, N. Bouchoucha, K.S. Sauter, C.E. Fluck, Resveratrol inhibits androgen production of human adrenocortical H295R cells by lowering CYP17 and CYP21 expression and activities, PLoS One 12(3) (2017) e0174224.
[101] S.S. Pereira, M.P. Monteiro, M.M. Costa, J. Ferreira, M.G. Alves, P.F. Oliveira, I. Jarak, D. Pignatelli, MAPK/ERK pathway inhibition is a promising treatment target for adrenocortical tumors, Journal of cellular biochemistry 120(1) (2019) 894-906.
[102] A.W. Krug, K. Vleugels, S. Schinner, V. Lamounier-Zepter, C.G. Ziegler, S.R. Bornstein, M. Ehrhart-Bornstein, Human adipocytes induce an ERK1/2 MAP kinases-mediated upregulation of steroidogenic acute regulatory protein (StAR) and an angiotensin II-sensitization in human adrenocortical cells, International journal of obesity (2005) 31(10) (2007) 1605-16.
[103] B. Rubin, C. Pilon, R. Pezzani, A. Rebellato, F. Fallo, The effects of mitotane and 1alpha,25-dihydroxyvitamin D3 on Wnt/beta-catenin signaling in human adrenocortical carcinoma cells, Journal of endocrinological investigation (2019).
[104] L. Wu, X. Huang, Y. Kuang, Z. Xing, X. Deng, Z. Luo, Thapsigargin induces apoptosis in adrenocortical carcinoma by activating endoplasmic reticulum stress and the JNK signaling pathway: an in vitro and in vivo study, Drug design, development and therapy 13 (2019) 2787-2798.
[105] L. Asser, S. Hescot, S. Viengchareun, B. Delemer, S. Trabado, M. Lombes, Autocrine positive regulatory feedback of glucocorticoid secretion: glucocorticoid receptor directly impacts H295R human adrenocortical cell function, Mol Cell Endocrinol 395(1-2) (2014) 1-9.
[106] C.N. Robitaille, P. Rivest, J.T. Sanderson, Antiandrogenic mechanisms of pesticides in human LNCaP prostate and H295R adrenocortical carcinoma cells, Toxicological sciences : an official journal of the Society of Toxicology 143(1) (2015) 126-35.
[107] D. Montanaro, M. Maggiolini, A.G. Recchia, R. Sirianni, S. Aquila, L. Barzon, F. Fallo, S. Ando, V. Pezzi, Antiestrogens upregulate estrogen receptor beta expression and inhibit adrenocortical H295R cell proliferation, Journal of molecular endocrinology 35(2) (2005) 245-56.
[108] O. Lesouhaitier, A. Chiappe, M.F. Rossier, Aldosterone increases T-type calcium currents in human adrenocarcinoma (H295R) cells by inducing channel expression, Endocrinology 142(10) (2001) 4320-30.
[109] J.E. Chambers, H. Greim, R.J. Kendall, H. Segner, R.M. Sharpe, G. Van Der Kraak, Human and ecological risk assessment of a crop protection chemical: a case study with the azole fungicide epoxiconazole, Critical reviews in toxicology 44(2) (2014) 176-210.
[110] U.S. Environmental Protection Agency (EPA), Pesticide Fact Sheet: Epoxiconazole, 2006, [Online] http://fluoridealert.org/wp-content/pesticides/epoxiconazole.epa.facts.aug.06.pdf [Accessed: October, 2019].
[111] E.F.S. Authority, Peer review of the pesticide risk assessment for the active substance epoxiconazole in light of confirmatory data submitted, EFSA Journal 13(6) (2015) 4123.
[112] A.B. Cadwallader, X. de la Torre, A. Tieri, F. Botrè, The abuse of diuretics as performance-enhancing drugs and masking agents in sport doping: pharmacology, toxicology and analysis, Br J Pharmacol 161(1) (2010) 1-16.
[113] P.C.A. Kam, M. Yarrow, Anabolic steroid abuse: physiological and anaesthetic considerations, Anaesthesia 60(7) (2005) 685-692.

[114] M.R. Graham, B. Davies, F.M. Grace, A. Kicman, J.S.J.S.M. Baker, Anabolic Steroid Use, 38(6) (2008) 505-525.
[115] M.B. Kjærstad, C. Taxvig, H.R. Andersen, C. Nellemann, Mixture effects of endocrine disrupting compounds in vitro, International Journal of Andrology 33(2) (2010) 425-433.
[116] F.K. Nielsen, C.H. Hansen, J.A. Fey, M. Hansen, B. Halling-Sorensen, E. Bjorklund, B. Styrishave, Mixture Effects of 3 Mechanistically Different Steroidogenic Disruptors (Prochloraz, Genistein, and Ketoconazole) in the H295R Cell Assay, International journal of toxicology 34(6) (2015) 534-42.
[117] C.P. Wild, Complementing the genome with an "exposome": the outstanding challenge of environmental exposure measurement in molecular epidemiology, Cancer epidemiology, biomarkers & prevention : a publication of the American Association for Cancer Research, cosponsored by the American Society of Preventive Oncology 14(8) (2005) 1847-50.
[118] M. Vrijheid, R. Slama, O. Robinson, L. Chatzi, M. Coen, P. van den Hazel, C. Thomsen, J. Wright, T.J. Athersuch, N. Avellana, X. Basagaña, C. Brochot, L. Bucchini, M. Bustamante, A. Carracedo, M. Casas, X. Estivill, L. Fairley, D. van Gent, J.R. Gonzalez, B. Granum, R. Gražulevičienė, K.B. Gutzkow, J. Julvez, H.C. Keun, M. Kogevinas, R.R.C. McEachan, H.M. Meltzer, E. Sabidó, P.E. Schwarze, V. Siroux, J. Sunyer, E.J. Want, F. Zeman, M.J. Nieuwenhuijsen, The human early-life exposome (HELIX): project rationale and design, Environ Health Perspect 122(6) (2014) 535-544.
[119] P. Vineis, M. Chadeau-Hyam, H. Gmuender, J. Gulliver, Z. Herceg, J. Kleinjans, M. Kogevinas, S. Kyrtopoulos, M. Nieuwenhuijsen, D.H. Phillips, N. Probst-Hensch, A. Scalbert, R. Vermeulen, C.P. Wild, E.X. Consortium, The exposome in practice: Design of the EXPOsOMICS project, Int J Hyg Environ Health 220(2 Pt A) (2017) 142-151.
[120] OECD, Detailed Review Paper on the State of the Science on Novel In Vitro and In Vivo Screening and Testing Methods and Endpoints for Evaluating Endocrine Disruptors, 2014.
[121] A.C. Gore, V.A. Chappell, S.E. Fenton, J.A. Flaws, A. Nadal, G.S. Prins, J. Toppari, R.T. Zoeller, EDC-2: The Endocrine Society's Second Scientific Statement on Endocrine-Disrupting Chemicals, Endocrine reviews 36(6) (2015) E1-E150.
[122] M.K. Manibusan, L.W. Touart, A comprehensive review of regulatory test methods for endocrine adverse health effects, Critical reviews in toxicology 47(6) (2017) 433-481.
[123] A.A. Hudon Thibeault, L. Laurent, S. Vo Duy, S. Sauve, P. Caron, C. Guillemette, J.T. Sanderson, C. Vaillancourt, Fluoxetine and its active metabolite norfluoxetine disrupt estrogen synthesis in a co-culture model of the feto-placental unit, Mol Cell Endocrinol 442 (2017) 32-39.
[124] E. Caron-Beaudoin, R. Viau, A.A. Hudon-Thibeault, C. Vaillancourt, J.T. Sanderson, The use of a unique co-culture model of fetoplacental steroidogenesis as a screening tool for endocrine disruptors: The effects of neonicotinoids on aromatase activity and hormone production, Toxicol Appl Pharmacol 332 (2017) 15-24.
[125] D. Yancu, T. Sanderson, Essential oils disrupt steroidogenesis in a feto-placental co-culture model, Reproductive toxicology (Elmsford, N.Y.) 90 (2019) 33-43.
[126] D. Yancu, C. Vaillancourt, J.T. Sanderson, Evaluating the effects on steroidogenesis of estragole and trans-anethole in a feto-placental co-culture model, Mol Cell Endocrinol 498 (2019) 110583.
[127] M.B. van Duursen, E.E. Smeets, J.C. Rijk, S.M. Nijmeijer, M. van den Berg, Phytoestrogens in menopausal supplements induce ER-dependent cell proliferation and overcome breast cancer treatment in an in vitro breast cancer model, Toxicol Appl Pharmacol 269(2) (2013) 132-40.
[128] M.D. Woods, M.J. Shipston, E.L. Mullens, F.A. Antoni, Pituitary corticotrope tumor (AtT20) cells as a model system for the study of early inhibition by glucocorticoids, Endocrinology 131(6) (1992) 2873-80.
[129] S. Cho, J.Y. Yoon, Organ-on-a-chip for assessing environmental toxicants, Current opinion in biotechnology 45 (2017) 34-42.
[130] K.-J. Jang, M.A. Otieno, J. Ronxhi, H.-K. Lim, L. Ewart, K.R. Kodella, D.B. Petropolis, G. Kulkarni, J.E. Rubins, D. Conegliano, J. Nawroth, D. Simic, W. Lam, M. Singer, E. Barale, B. Singh, M. Sonee, A.J. Streeter, C. Manthey, B. Jones, A. Srivastava, L.C. Andersson, D. Williams, H. Park, R. Barrile, J. Sliz, A. Herland, S. Haney, K. Karalis, D.E. Ingber, G.A. Hamilton, Reproducing human and cross-species drug toxicities using a Liver-Chip, Science Translational Medicine 11(517) (2019) eaax5516.

[131] H. Kimura, Y. Sakai, T. Fujii, Organ/body-on-a-chip based on microfluidic technology for drug discovery, Drug metabolism and pharmacokinetics 33(1) (2018) 43-48.
[132] M.A. Mofazzal Jahromi, A. Abdoli, M. Rahmanian, H. Bardania, M. Bayandori, S.M. Moosavi Basri, A. Kalbasi, A.R. Aref, M. Karimi, M.R. Hamblin, Microfluidic Brain-on-a-Chip: Perspectives for Mimicking Neural System Disorders, Molecular neurobiology 56(12) (2019) 8489-8512.
[133] S. Bang, S. Jeong, N. Choi, H.N. Kim, Brain-on-a-chip: A history of development and future perspective, Biomicrofluidics 13(5) (2019) 051301.
[134] K. Shik Mun, K. Arora, Y. Huang, F. Yang, S. Yarlagadda, Y. Ramananda, M. Abu-El-Haija, J.J. Palermo, B.N. Appakalai, J.D. Nathan, A.P. Naren, Patient-derived pancreas-on-a-chip to model cystic fibrosis-related disorders, Nature Communications 10(1) (2019) 3124.
[135] A.L. Glieberman, B.D. Pope, J.F. Zimmerman, Q. Liu, J.P. Ferrier, J.H.R. Kenty, A.M. Schrell, N. Mukhitov, K.L. Shores, A.B. Tepole, D.A. Melton, M.G. Roper, K.K. Parker, Synchronized stimulation and continuous insulin sensing in a microfluidic human Islet on a Chip designed for scalable manufacturing, Lab on a Chip 19(18) (2019) 2993-3010.
[136] H. Gagliano, R. Andero, A. Armario, R. Nadal, Repeated amphetamine administration in rats revealed consistency across days and a complete dissociation between locomotor and hypothalamic-pituitary-adrenal axis effects of the drug, Psychopharmacology 207(3) (2009) 447-59.
[137] J. Harro, Neuropsychiatric Adverse Effects of Amphetamine and Methamphetamine, International review of neurobiology 120 (2015) 179-204.
[138] A. Odermatt, B. Dick, P. Arnold, T. Zaehner, V. Plueschke, M.N. Deregibus, H. Repetto, B.M. Frey, F.J. Frey, P. Ferrari, A mutation in the cofactor-binding domain of 11beta-hydroxysteroid dehydrogenase type 2 associated with mineralocorticoid hypertension, J Clin Endocrinol Metab 86(3) (2001) 1247-52.
[139] K. Barton, T.K. Davis, B. Marshall, A. Elward, N.H. White, Posaconazole-induced hypertension and hypokalemia due to inhibition of the 11beta-hydroxylase enzyme, Clinical kidney journal 11(5) (2018) 691-693.
[140] C. Boughton, D. Taylor, L. Ghataore, N. Taylor, B.C. Whitelaw, Mineralocorticoid hypertension and hypokalaemia induced by posaconazole, Endocrinology, diabetes & metabolism case reports 2018 (2018).
[141] T. Wassermann, E.K. Reimer, M. McKinnon, W. Stock, Refractory Hypokalemia from Syndrome of Apparent Mineralocorticoid Excess on Low-Dose Posaconazole, Antimicrobial agents and chemotherapy 62(7) (2018).
[142] G.R. Thompson, 3rd, D. Chang, R.R. Wittenberg, I. McHardy, A. Semrad, In Vivo 11beta-Hydroxysteroid Dehydrogenase Inhibition in Posaconazole-Induced Hypertension and Hypokalemia, Antimicrobial agents and chemotherapy 61(8) (2017).
[143] T. Denolle, M. Azizi, C. Massart, M.C. Zennaro, [Itraconazole: a new drug-related cause of hypertension], Ann Cardiol Angeiol (Paris) 63(3) (2014) 213-5.
[144] W.J. Hoffmann, I. McHardy, G.R. Thompson, 3rd, Itraconazole induced hypertension and hypokalemia: Mechanistic evaluation, Mycoses 61(5) (2018) 337-339.
[145] K.R. Beck, G.R. Thompson, 3rd, A. Odermatt, Drug-induced endocrine blood pressure elevation, Pharmacological research (2019) 104311.
[146] M. Kadmiel, J.A. Cidlowski, Glucocorticoid receptor signaling in health and disease, Trends in pharmacological sciences 34(9) (2013) 518-30.
[147] J.C. Buckingham, Glucocorticoids: exemplars of multi-tasking, Br J Pharmacol 147 Suppl 1 (2006) S258-68.
[148] G.S. Ong, M.J. Young, Mineralocorticoid regulation of cell function: the role of rapid signalling and gene transcription pathways, Journal of molecular endocrinology 58(1) (2017) R33-r57.
[149] S. Ramamoorthy, J.A. Cidlowski, Corticosteroids: Mechanisms of Action in Health and Disease, Rheumatic diseases clinics of North America 42(1) (2016) 15-31, vii.
[150] M.A. Carson-Jurica, W.T. Schrader, B.W. O'Malley, Steroid receptor family: structure and functions, Endocrine reviews 11(2) (1990) 201-20.
[151] I.J. Encio, S.D. Detera-Wadleigh, The genomic structure of the human glucocorticoid receptor, The Journal of biological chemistry 266(11) (1991) 7182-8.

[152] R.H. Oakley, M. Sar, J.A. Cidlowski, The human glucocorticoid receptor beta isoform. Expression, biochemical properties, and putative function, The Journal of biological chemistry 271(16) (1996) 9550-9.
[153] R.H. Oakley, C.M. Jewell, M.R. Yudt, D.M. Bofetiado, J.A. Cidlowski, The dominant negative activity of the human glucocorticoid receptor beta isoform. Specificity and mechanisms of action, The Journal of biological chemistry 274(39) (1999) 27857-66.
[154] S.M. Hollenberg, C. Weinberger, E.S. Ong, G. Cerelli, A. Oro, R. Lebo, E.B. Thompson, M.G. Rosenfeld, R.M. Evans, Primary structure and expression of a functional human glucocorticoid receptor cDNA, Nature 318(6047) (1985) 635-41.
[155] P.A. Moalli, S. Pillay, N.L. Krett, S.T. Rosen, Alternatively spliced glucocorticoid receptor messenger RNAs in glucocorticoid-resistant human multiple myeloma cells, Cancer research 53(17) (1993) 3877-9.
[156] C. Beger, K. Gerdes, M. Lauten, W.J. Tissing, I. Fernandez-Munoz, M. Schrappe, K. Welte, Expression and structural analysis of glucocorticoid receptor isoform gamma in human leukaemia cells using an isoform-specific real-time polymerase chain reaction approach, British journal of haematology 122(2) (2003) 245-52.
[157] N.Z. Lu, J.A. Cidlowski, Translational regulatory mechanisms generate N-terminal glucocorticoid receptor isoforms with unique transcriptional target genes, Molecular cell 18(3) (2005) 331-42.
[158] J. Zhou, J.A. Cidlowski, The human glucocorticoid receptor: One gene, multiple proteins and diverse responses, Steroids 70(5) (2005) 407-417.
[159] R.H. Oakley, J.A. Cidlowski, The biology of the glucocorticoid receptor: new signaling mechanisms in health and disease, The Journal of allergy and clinical immunology 132(5) (2013) 1033-44.
[160] M.G. Rosenfeld, C.K. Glass, Coregulator codes of transcriptional regulation by nuclear receptors, The Journal of biological chemistry 276(40) (2001) 36865-8.
[161] S. John, P.J. Sabo, R.E. Thurman, M.H. Sung, S.C. Biddie, T.A. Johnson, G.L. Hager, J.A. Stamatoyannopoulos, Chromatin accessibility pre-determines glucocorticoid receptor binding patterns, Nature genetics 43(3) (2011) 264-8.
[162] J.R. Revollo, J.A. Cidlowski, Mechanisms generating diversity in glucocorticoid receptor signaling, Annals of the New York Academy of Sciences 1179 (2009) 167-78.
[163] S. Vandevyver, L. Dejager, C. Libert, Comprehensive Overview of the Structure and Regulation of the Glucocorticoid Receptor, Endocrine reviews 35(4) (2014) 671-693.
[164] G.P. Chrousos, T. Kino, Intracellular glucocorticoid signaling: a formerly simple system turns stochastic, Science's STKE : signal transduction knowledge environment 2005(304) (2005) pe48.
[165] D. Duma, C.M. Jewell, J.A. Cidlowski, Multiple glucocorticoid receptor isoforms and mechanisms of post-translational modification, The Journal of steroid biochemistry and molecular biology 102(1-5) (2006) 11-21.
[166] A. Odermatt, C. Gumy, Glucocorticoid and mineralocorticoid action: why should we consider influences by environmental chemicals?, Biochemical pharmacology 76(10) (2008) 1184-93.
[167] A. Odermatt, C. Gumy, Disruption of Glucocorticoid and Mineralocorticoid Receptor-Mediated Responses by Environmental Chemicals, CHIMIA International Journal for Chemistry 62(5) (2008) 335-339.
[168] X. Liu, W. Han, S. Gulla, N.I. Simon, Y. Gao, C. Cai, H. Yang, X. Zhang, J. Liu, S.P. Balk, S. Chen, Protein phosphatase 1 suppresses androgen receptor ubiquitylation and degradation, Oncotarget 7(2) (2016) 1754-64.
[169] S. Nagarajan, T. Vohra, J. Loffing, N. Faresse, Protein Phosphatase 1alpha enhances renal aldosterone signaling via mineralocorticoid receptor stabilization, Mol Cell Endocrinol 450 (2017) 74-82.
[170] A. Bollig, L. Xu, A. Thakur, J. Wu, T.H. Kuo, J.D. Liao, Regulation of intracellular calcium release and PP1alpha in a mechanism for 4-hydroxytamoxifen-induced cytotoxicity, Molecular and cellular biochemistry 305(1-2) (2007) 45-54.
[171] E.A. Crane, W. Heydenreuter, K.R. Beck, P. Strajhar, J. Vomacka, M. Smiesko, E. Mons, L. Barth, M. Neuburger, A. Vedani, A. Odermatt, S.A. Sieber, K. Gademann, Profiling withanolide A for therapeutic targets in neurodegenerative diseases, Bioorg Med Chem (2019).

[172] T. Kuboyama, C. Tohda, J. Zhao, N. Nakamura, M. Hattori, K. Komatsu, Axon- or dendrite-predominant outgrowth induced by constituents from Ashwagandha, Neuroreport 13(14) (2002) 1715-20.
[173] K. Terada, Y. Kojima, T. Watanabe, N. Izumo, K. Chiba, Y. Karube, Inhibition of nerve growth factor-induced neurite outgrowth from PC12 cells by dexamethasone: signaling pathways through the glucocorticoid receptor and phosphorylated Akt and ERK1/2, PLoS One 9(3) (2014) e93223.
[174] N.J. Dar, N.K. Satti, P. Dutt, A. Hamid, M. Ahmad, Attenuation of Glutamate-Induced Excitotoxicity by Withanolide-A in Neuron-Like Cells: Role for PI3K/Akt/MAPK Signaling Pathway, Molecular neurobiology 55(4) (2018) 2725-2739.
[175] Z. Yan, R. Guo, L. Gan, W.B. Lau, X. Cao, J. Zhao, X. Ma, T.A. Christopher, B.L. Lopez, Y. Wang, Withaferin A inhibits apoptosis via activated Akt-mediated inhibition of oxidative stress, Life Sci 211 (2018) 91-101.
[176] E.H. Han, J.H. Park, K.W. Kang, T.C. Jeong, H.S. Kim, H.G. Jeong, Risk assessment of tetrabromobisphenol A on cyclooxygenase-2 expression via MAP kinase/NF-kappaB/AP-1 signaling pathways in murine macrophages, Journal of toxicology and environmental health. Part A 72(21-22) (2009) 1431-8.
[177] A. Cato, L. Celada, E.C. Kibakaya, N. Simmons, M.M. Whalen, Brominated flame retardants, tetrabromobisphenol A and hexabromocyclododecane, activate mitogen-activated protein kinases (MAPKs) in human natural killer cells, Cell biology and toxicology 30(6) (2014) 345-60.
[178] G.H. Lee, S.W. Jin, S.J. Kim, T.H. Pham, J.H. Choi, H.G. Jeong, Tetrabromobisphenol A Induces MMP-9 Expression via NADPH Oxidase and the activation of ROS, MAPK, and Akt Pathways in Human Breast Cancer MCF-7 Cells, Toxicological research 35(1) (2019) 93-101.
[179] C. Gumy, C. Chandsawangbhuwana, A.A. Dzyakanchuk, D.V. Kratschmar, M.E. Baker, A. Odermatt, Dibutyltin disrupts glucocorticoid receptor function and impairs glucocorticoid-induced suppression of cytokine production, PLoS ONE 3(10) (2008) e3545.
[180] S.O. Odman-Ghazi, A. Abraha, E.T. Isom, M.M. Whalen, Dibutyltin activates MAP kinases in human natural killer cells, in vitro, Cell biology and toxicology 26(5) (2010) 469-79.
[181] B. Chantong, D.V. Kratschmar, A. Lister, A. Odermatt, Dibutyltin promotes oxidative stress and increases inflammatory mediators in BV-2 microglia cells, Toxicology letters 230(2) (2014) 177-87.
[182] A.J. Galliher-Beckley, J.A. Cidlowski, Emerging roles of glucocorticoid receptor phosphorylation in modulating glucocorticoid hormone action in health and disease, IUBMB life 61(10) (2009) 979-86.
[183] K. Pazdrak, C. Straub, R. Maroto, S. Stafford, W.I. White, W.J. Calhoun, A. Kurosky, Cytokine-Induced Glucocorticoid Resistance from Eosinophil Activation: Protein Phosphatase 5 Modulation of Glucocorticoid Receptor Phosphorylation and Signaling, Journal of immunology (Baltimore, Md. : 1950) 197(10) (2016) 3782-3791.
[184] B. Bouazza, K. Krytska, M. Debba-Pavard, Y. Amrani, R.E. Honkanen, J. Tran, O. Tliba, Cytokines alter glucocorticoid receptor phosphorylation in airway cells: role of phosphatases, American journal of respiratory cell and molecular biology 47(4) (2012) 464-73.
[185] A.M. Silverstein, M.D. Galigniana, M.S. Chen, J.K. Owens-Grillo, M. Chinkers, W.B. Pratt, Protein phosphatase 5 is a major component of glucocorticoid receptor.hsp90 complexes with properties of an FK506-binding immunophilin, The Journal of biological chemistry 272(26) (1997) 16224-30.
[186] M. Chinkers, Protein phosphatase 5 in signal transduction, Trends in endocrinology and metabolism: TEM 12(1) (2001) 28-32.
[187] B. Budziszewska, M. Szymanska, M. Leskiewicz, A. Basta-Kaim, L. Jaworska-Feil, M. Kubera, D. Jantas, W. Lason, The decrease in JNK- and p38-MAP kinase activity is accompanied by the enhancement of PP2A phosphate level in the brain of prenatally stressed rats, Journal of physiology and pharmacology : an official journal of the Polish Physiological Society 61(2) (2010) 207-15.
[188] Y. Kobayashi, N. Mercado, P.J. Barnes, K. Ito, Defects of protein phosphatase 2A causes corticosteroid insensitivity in severe asthma, PLoS One 6(12) (2011) e27627.
[189] E. Irusen, J.G. Matthews, A. Takahashi, P.J. Barnes, K.F. Chung, I.M. Adcock, p38 Mitogen-activated protein kinase-induced glucocorticoid receptor phosphorylation reduces its activity: role in steroid-insensitive asthma, The Journal of allergy and clinical immunology 109(4) (2002) 649-57.

[190] P. Bhavsar, M. Hew, N. Khorasani, A. Torrego, P.J. Barnes, I. Adcock, K.F. Chung, Relative corticosteroid insensitivity of alveolar macrophages in severe asthma compared with non-severe asthma, Thorax 63(9) (2008) 784-90.
[191] N. Khorasani, J. Baker, M. Johnson, K.F. Chung, P.K. Bhavsar, Reversal of corticosteroid insensitivity by p38 MAPK inhibition in peripheral blood mononuclear cells from COPD, International journal of chronic obstructive pulmonary disease 10 (2015) 283-91.
[192] L.B. Li, E. Goleva, C.F. Hall, L.S. Ou, D.Y. Leung, Superantigen-induced corticosteroid resistance of human T cells occurs through activation of the mitogen-activated protein kinase kinase/extracellular signal-regulated kinase (MEK-ERK) pathway, The Journal of allergy and clinical immunology 114(5) (2004) 1059-69.
[193] A.L. Miller, A.S. Garza, B.H. Johnson, E.B. Thompson, Pathway interactions between MAPKs, mTOR, PKA, and the glucocorticoid receptor in lymphoid cells, Cancer cell international 7 (2007) 3.
[194] Y. Liu, J. Ge, Q. Li, X. Guo, L. Gu, Z.G. Ma, X.H. Li, Y.P. Zhu, Low-dose anisomycin sensitizes glucocorticoid-resistant T-acute lymphoblastic leukemia CEM-C1 cells to dexamethasone-induced apoptosis through activation of glucocorticoid receptor and p38-MAPK/JNK, Leukemia & lymphoma 55(9) (2014) 2179-88.
[195] L. Zhang, Z. Zhang, F. Long, E.Y. Lee, Tyrosine-272 is involved in the inhibition of protein phosphatase-1 by multiple toxins, Biochemistry 35(5) (1996) 1606-11.
[196] J.E. Sheppeck, 2nd, C.M. Gauss, A.R. Chamberlin, Inhibition of the Ser-Thr phosphatases PP1 and PP2A by naturally occurring toxins, Bioorganic & medicinal chemistry 5(9) (1997) 1739-50.
[197] C. MacKintosh, S. Klumpp, Tautomycin from the bacterium Streptomyces verticillatus. Another potent and specific inhibitor of protein phosphatases 1 and 2A, FEBS letters 277(1-2) (1990) 137-40.
[198] M.S. Kelker, R. Page, W. Peti, Crystal structures of protein phosphatase-1 bound to nodularin-R and tautomycin: a novel scaffold for structure-based drug design of serine/threonine phosphatase inhibitors, Journal of molecular biology 385(1) (2009) 11-21.
[199] A. Kita, S. Matsunaga, A. Takai, H. Kataiwa, T. Wakimoto, N. Fusetani, M. Isobe, K. Miki, Crystal structure of the complex between calyculin A and the catalytic subunit of protein phosphatase 1, Structure (London, England : 1993) 10(5) (2002) 715-24.
[200] C. Bialojan, A. Takai, Inhibitory effect of a marine-sponge toxin, okadaic acid, on protein phosphatases. Specificity and kinetics, The Biochemical journal 256(1) (1988) 283-90.
[201] J.T. Maynes, K.S. Bateman, M.M. Cherney, A.K. Das, H.A. Luu, C.F. Holmes, M.N. James, Crystal structure of the tumor-promoter okadaic acid bound to protein phosphatase-1, The Journal of biological chemistry 276(47) (2001) 44078-82.
[202] R.W. MacKintosh, K.N. Dalby, D.G. Campbell, P.T. Cohen, P. Cohen, C. MacKintosh, The cyanobacterial toxin microcystin binds covalently to cysteine-273 on protein phosphatase 1, FEBS letters 371(3) (1995) 236-40.
[203] J. Goldberg, H.B. Huang, Y.G. Kwon, P. Greengard, A.C. Nairn, J. Kuriyan, Three-dimensional structure of the catalytic subunit of protein serine/threonine phosphatase-1, Nature 376(6543) (1995) 745-53.
[204] World Health Organization. (1999). Toxic cyanobacteria in water : a guide to their public health consequences, monitoring and management / edited by Ingrid Chorus and Jamie Bertram., [Online] https://apps.who.int/iris/bitstream/handle/10665/42827/0419239308_eng.pdf?sequence=1&isAllowed=y [Accessed: October, 2019].
[205] M. Swingle, L. Ni, R.E. Honkanen, Small-molecule inhibitors of ser/thr protein phosphatases: specificity, use and common forms of abuse, Methods in molecular biology (Clifton, N.J.) 365 (2007) 23-38.
[206] P.T. Cohen, Protein phosphatase 1--targeted in many directions, Journal of cell science 115(Pt 2) (2002) 241-56.
[207] H. Ceulemans, M. Bollen, Functional diversity of protein phosphatase-1, a cellular economizer and reset button, Physiological reviews 84(1) (2004) 1-39.
[208] M. Bollen, M. Beullens, Signaling by protein phosphatases in the nucleus, Trends in cell biology 12(3) (2002) 138-45.

[209] A. Hendrickx, M. Beullens, H. Ceulemans, T. Den Abt, A. Van Eynde, E. Nicolaescu, B. Lesage, M. Bollen, Docking motif-guided mapping of the interactome of protein phosphatase-1, Chemistry & biology 16(4) (2009) 365-71.
[210] M. Köhn, Miklós Bodanszky Award Lecture: Advances in the selective targeting of protein phosphatase-1 and phosphatase-2A with peptides, Journal of peptide science : an official publication of the European Peptide Society 23(10) (2017) 749-756.
[211] T. Ammosova, M. Platonov, V.R. Yedavalli, Y. Obukhov, V.R. Gordeuk, K.T. Jeang, D. Kovalskyy, S. Nekhai, Small molecules targeted to a non-catalytic "RVxF" binding site of protein phosphatase-1 inhibit HIV-1, PLoS One 7(6) (2012) e39481.
[212] P. Wongrattanakamon, P. Nimmanpipug, B. Sirithunyalug, C. Saenjum, S. Jiranusornkul, Molecular modeling investigation of the potential mechanism for phytochemical-induced skin collagen biosynthesis by inhibition of the protein phosphatase 1 holoenzyme, Molecular and cellular biochemistry 454(1-2) (2019) 45-56.
[213] D. Tian, M. Zhu, J. Li, Y. Ma, R. Wu, Cigarette smoke extract induces activation of beta-catenin/TCF signaling through inhibiting GSK3beta in human alveolar epithelial cell line, Toxicology letters 187(1) (2009) 58-62.
[214] A. Ngkelo, R.F. Hoffmann, A.L. Durham, J.A. Marwick, S.M. Brandenburg, H.G. de Bruin, M.R. Jonker, C. Rossios, E. Tsitsiou, G. Caramori, M. Contoli, P. Casolari, F. Monaco, F. Ando, G. Speciale, I. Kilty, K.F. Chung, A. Papi, M.A. Lindsay, N.H. Ten Hacken, M. van den Berge, W. Timens, P.J. Barnes, A.J. van Oosterhout, I.M. Adcock, P.A. Kirkham, I.H. Heijink, Glycogen synthase kinase-3beta modulation of glucocorticoid responsiveness in COPD, American journal of physiology. Lung cellular and molecular physiology 309(10) (2015) L1112-23.
[215] D. Reddy, F.F. Little, Glucocorticoid-resistant asthma: more than meets the eye, The Journal of asthma : official journal of the Association for the Care of Asthma 50(10) (2013) 1036-44.
[216] E.B. Brandt, G.K. Khurana Hershey, A combination of dexamethasone and anti-IL-17A treatment can alleviate diesel exhaust particle-induced steroid insensitive asthma, The Journal of allergy and clinical immunology 138(3) (2016) 924-928.e2.
[217] K. Pencikova, M. Ciganek, J. Neca, P. Illes, Z. Dvorak, J. Vondracek, M. Machala, Modulation of endocrine nuclear receptor activities by polyaromatic compounds present in fractionated extracts of diesel exhaust particles, The Science of the total environment 677 (2019) 626-636.
[218] J. Chatterjee, M. Beullens, R. Sukackaite, J. Qian, B. Lesage, D.J. Hart, M. Bollen, M. Kohn, Development of a peptide that selectively activates protein phosphatase-1 in living cells, Angewandte Chemie (International ed. in English) 51(40) (2012) 10054-9.
[219] Y. Wang, B. Hoermann, K. Pavic, M. Trebacz, P. Rios, M. Kohn, Interrogating PP1 Activity in the MAPK Pathway with Optimized PP1-Disrupting Peptides, Chembiochem : a European journal of chemical biology 20(1) (2019) 66-71.